Acknowledgements:

First of all, I would like to express my sincere gratitude to all the jury members for being a part of my project's evaluation and for taking the time to read this manuscript.

To my supervisor, Prof Ahmed JOUAITI, I am truly grateful for your support and patience throughout this study. Thank you for giving me the freedom to explore on my own, while also providing guidance when I needed it.

Prof Mohammed CHIGER, a co-supervisor with great expertise and high standards. Thank you for your valuable input, especially with the analytical chemistry (IR and NMR spectroscopy) section of this thesis.

My gratitude goes, in particular, to Professor Armando J. D. SILVESTRE, of the big opportunities, for the excellent scientific guidance, unconditional support and, above all, for all the trust they placed in me.

I would also like to acknowledge Dr. Fatima DUARTE help. Her assessment, comments, and suggestions in the biological activities approach were significant to improve the benchmark of this thesis.

Dr. Sónia Andreia Oliveira SANTOS I would like to offer special thanks for your availability, in particular for your precious help with the HPLC.

I would like to thank Dr. Patrícia Alexandra Bogango RAMOS for their tireless availability and numerous experimental tips on the GC-MS equipment. It has been a privilege to work with such a goal-driven and passionate researcher who enabled me to see the bigger picture at all times. It would have been impossible to complete this thesis without your guidance and persistent help.

Prof Mostafa KETATNI. Thank you for your interpretation of crystallography analysis of crystal structure is truly appreciated.

To the people who crossed my academic journey through Portugal abroad and research center of university Sultan Moulay Sliman whom, in one way or another, were important for my personal and social learning and development, I thank you for all the support and good times provided.

I would also like to say a huge thank you to all my family and for always teaching me the value of family unity and for all the unconditional support.

To my uncle Abdelaziz who always believed in me. Despite the enormous distance, he was always present when I was most needed and even when everything seemed lost they never doubted my abilities.

Last but not least, to my mother the foundations of my happiness, which has always supported and encouraged me to achieve my goals and dreams.

THANK YOU ALL…

Table of content

Table of content

Table of content

Table of content

Table of content

Table of content

Table of content

Notation

Abbreviations and symbols

ABTS – 2,2´-azinobis(3-ethylbenzothiazoline-6-sulfonic acid)

BC – breast cancer

BHA – butylated hydroxyanisole

BHT – butylated hydroxytoluene

^{13}C NMR–carbon-13 nuclear magnetic resonance

DPPH – 2,2-diphenyl-1-picrylhydrazyl

DCM – dichloromethane

DNA – deoxyribonucleic acid

dw – dry weight

ER – estrogen receptor

ESI – electrospray ionisation

FRAP – ferric reducing antioxidant power

FTIR – fourier Transform Infra Spectroscopy

GAE – gallic acid equivalent

GC – gas chromatography

HAT – hydrogen atom transfer

^{1}H NMR – proton nuclear magnetic resonance

HPLC – high-performance liquid chromatography

HSCCC – high-speed countercurrent chromatography

HT-UHPLC – high temperature-ultra HPLC

IC_{50} – inhibitory concentration at 50%

IR – Infrared spectroscopy

IS – Internal Standard

LPS – lipopolysaccharide

$[M]^{+\bullet}$ – molecular ion

$[M-H]^-$ – deprotonated molecular ion

MBCs – minimum bactericidal concentrations

MIC – minimum inhibitory concentration

MRSA – methicillin-resistant *Staphylococcus aureus*

MS – mass spectrometry

MSSA – Meticillin-Sensitive *Staphylococcus aureus*

MS^n – tandem MS

m/z – mass-to-charge ratio

NCEs – new chemical entities

NO – nitrite

NPs – natural products

NPD – natural products derivatives

ORAC – oxygen radical absorbance capacity

PCET – proton-coupled electron transfer

PCs – phenolic compounds

PTLC – preparative thin-layer chromatography

SPLET – proton-loss electron transfer

Rf – radio-frequency voltage

ROS – reactive oxygen species

RT – retention time

s – singlet

SET – single-electron transfer

t – triplet

TMS – trimethylsilyl

TMSOH – trimethylsilanol

TNBC – triple-negative breast cancer

TPC – total phenolic content

UHPLC– ultra high-performance liquid chromatography

UV– ultraviolet spectroscopy

LOD – limit of detection

LOQ – limit of quantification

Greek letters

λmax – wavelength at which ultraviolet/visible absorbance is maximum

δ – chemical shif

Part A

Chapter I

General introduction

Natural resources, namely plants and animals, have been used since ancient times by humans, mainly as a source of food and in the treatment of many diseases. Worldwide, plants are the main ingredients of medicines in most traditional systems of healing[1,2] and are the largest source of inspiration for several major pharmaceutical drugs.[2,3] Currently, the demand for herbal medicines continues,[1] and consequently, more plants are the target of new phytochemical studies, intending to know their chemical constituents and, mainly, discovering new biologically active products.[4,5] Natural products and their derivatives represent more than 50% of all drugs in clinical used in the world. It is also a fact that one-quarter of all medicinal prescriptions are formulations based on substances resulting from plants or plant-derived synthetic analogs.[6] Even though only, 5-15 percent of around 250,000 higher terrestrial plants in existence have been chemically and pharmacologically investigated systematically.[7]

Due to its privileged geographical position, Morocco has the most varied flora in the Mediterranean region and the richest in North Africa with about 4200 taxa, including 1282 subspecies of which 22% (879 taxa) are endemic.[8] Approximately 800 of the listed species are aromatic and medicinal plants.[9,10] This large number of vascular plants with a high percentage of endemic species classify Morocco in a privileged position among other Mediterranean countries.[8] *Zizyphus lotus* L. (*Z. lotus*, Rhamnaceae) and *Rubia tinctorum* L. (*R. tinctorum*, Rubiaceae) are among the endemic plants found in Morocco (e.g. Beni-Mellal). Both plant species are widely used by inhabitants in Beni-Mellal Region, which indicate their importance in traditional medicinal applications.

Z. lotus, also known as Jujube, is a deciduous shrub that belongs to the Rhamnaceae family.[11] Generally, it grows in arid or semi-arid countries, particularly in the Mediterranean region and southern European countries.[12] Several parts of *Z. lotus* have been used in traditional and ancestral medicine, both in North Africa and the Middle East, for the treatment of several pathologies, including liver complaints, obesity, urinary troubles, diabetes, skin infections, fever, diarrhea, insomnia, inflammation, and peptic ulcers.[13] Several biologically active molecules, in particular alkaloids[14–16] and saponins,[17,18] have been isolated from this plant. Hence, the presence of these molecules in *Z. lotus* extracts, along with phenolic compounds was supposed to be responsible for most of their beneficial effects.[19–22]

R. tinctorum, commonly known as "Madder", belonging to the flowering plant family Rubiaceae, which is native to the southern and southeastern Europe, in the Mediterranean area, and in central Asia.[23] The plant is traditionally used for the treatment of kidney stones,[24] urinary disorders,[25] and the treatment of inflammation.[26] Regarding the chemical studies of this plant, anthraquinones were isolated from this plant and were supposed to be in charge of its biological activities, namely anti-microbial, anti-fungal, hypotensive, analgesic, anti-malarial, anti-oxidant, anti-leukemic, and mutagenic proprieties.[24,27] Besides, the structure of anthraquinone is observed in some synthetic dyes and many naturally occurring substances, such as pigments, vitamins, and enzymes[27,28] and occupied an important place among the different classes of anti-tumor agents.[27]

Therefore, both species are nearly facing extinction by numerous factors including i) destruction of natural habitats, ii) cleaning of vegetation for agricultural expansion, and iii) climate change.[10] These factors lead to a serious decline in the number of medicinal plant species available, which in turn to loss of traditional medical knowledge associated with these plants, thus causing further reduction of their phytochemical studies. Wherefore, we describe

in the first step a detailed chemical characterization of extractable compounds from *Z. lotus* and their related pharmacological property while, the second step will be devoted to the purification of alizarin from *R. tinctorum*, which in turn will be used as a platform for the synthesis of new active derivatives. This would open several possibilities for the valorization of *Z. lotus* and *R. tinctorum* biomass, integrated into the cosmetics, food, and pharmaceutical industry, through the extraction of added-value bioactive compounds or functionalization of compounds known for their promising activities.

Objectives and outline of the thesis

The detailed study of the chemical composition of different morphological parts of *Z. lotus* is a key step towards the implementation of strategies for the identification of valuable components from these shrub species. Despite some information that has already been reported concerning the lipophilic and phenolic fractions of *Z. lotus*, a complete study, and mostly applying novel extraction and characterization techniques of identification have not yet been carried out. Besides, no study has been done so far concerning the biological activity of different extractable classes of *Z. lotus*, principally regarding the lipophilic fraction. Moreover, no study reported, so far, the inhibitory functions of the lipophilic components of *Z. lotus* in important signaling pathways, in what concerns to tumor cells proliferation.

Anthraquinones are the important members of the organic family which their scaffold is a promising platform for synthesis of active biological agents. Alizarin is widely found in roots of *R. tinctorum* and is known to display various pharmacological activities namely; anticancer properties. At the current knowledge, there is no previous study that described the incorporation of pyridine or dioxepine ring into the hydroxyl group of the alizarin moiety and the use of a DFT study to investigate its electronic structure proprieties.

In this context, several objectives were traced for this thesis:

- to determine the chemical composition of lipophilic and phenolic-rich fractions of seeds, pulp, leaves, and roots bark of wild *Z. lotus*, by employing, respectively gas chromatography-mass spectrometry (GC/MS) and high-performance liquid chromatography with UV detection coupled with mass spectrometry (HPLC/UV/MS^n;
- to evaluate the antioxidant activity of wild *Z. lotus* phenolic-rich extracts through an in vitro scavenging assay and ferric reducing power assay;
- to assess the in vitro inhibitory effects of lipophilic and phenolic-rich fractions of wild *Z. lotus* regarding the three cell lines such as MDA-MB-231 (triple-negative breast cancer), MCF-7 (breast cancer), and HepG2 (liver hepatocellular carcinoma);
- to study the suppressive actions of lipophilic and phenolic-rich extracts of wild *Z. lotus* on four bacteria, namely *Escherichia coli*, Methicillin-sensitive *Staphylococcus aureus*, Methicillin-resistant *Staphylococcus aureus*, and *Staphylococcus epidermidis.*
- to extract, purified, and characterized the alizarin from wild *R. tinctorum* and to be used as a platform to synthesis new bioactive derivatives.
- to evaluate the possible activity of alizarin derivatives using frontier molecular orbitals (FMOs) performed by Gaussian 09 software.
- to synthesis, and to study crystal structure, and Hirshfeld surface analysis of new alizarin derivatives (1,2-propylenedioxyanthraquinone).

The present thesis is thus organized in eight chapters.

In **Part A**, introduction and objectives of the thesis are indicated in the **Chapter I**.

The **Part B** is devoted to the chemical characterization of lipophilic and phenolic-rich extracts derived from wild *Z. lotus* and focused on the evaluation of their biological activities.

Chapter II reviews the most relevant literature data about the chemical composition of *Z. lotus* varieties, with more emphasis on extractable compounds, and the biological activity of their derived extracts, namely antioxidant, antitumor, and antibacterial properties.

Chapter III highlights the identification and quantification of seeds, pulp, leaves, and roots bark lipophilic extracts of *Z. lotus*, by applying gas chromatography-mass spectrometry.

Chapter IV addresses the identification and quantification of phenolic compounds in the several morphological parts of *Z. lotus*, by utilizing high-performance liquid chromatography-ultraviolet detection-mass spectrometry.

Chapter V describes the antioxidant activity of *Z. lotus* phenolic-rich extracts, by assessing the in vitro scavenging effect on 2,2-diphenyl-1-picrylhydrazyl free radicals, 2, 2'-azinobis (3-ethylbenzothiazoline-6-sulfonic acid) as well as ferric reducing antioxidant power. Comprehends the antibacterial activity of wild *Z. lotus* lipophilic and phenolic-rich extracts on the growth of four bacteria, namely Gram-negative: *Escherichia coli* and Gram-positive: Methicillin-sensitive *Staphylococcus aureus*, Methicillin-resistant *Staphylococcus aureus*, and *Staphylococcus epidermis*. The inhibitory effects of wild *Z. lotus* lipophilic and phenolic-rich extracts on MDA-MB-231, MCF-7, and HepG2 cellular viability were performed along with the downstream mechanisms involved in the MDA-MB-231 cellular inhibition of the most potent extract was further evaluated, in terms of other cellular assays. Also, the molecular signaling pathways were explored in what concerns to PI3K/Akt pathway.

Part C labels the reviews of the most relevant literature data about the chemical composition of *R. tinctorum*, with more emphasis on chemical structure, synthesis, and related biological activities of anthraquinones. Alizarin abundant natural 1,2-hydroxyanthraquinone was extracted and purified from the roots of wild *R. tinctorum*. A novel ligand series of pyridine fused alizarin was designed and synthesized whose potential activity was investigated by using a density functional theory DFT (B3LYP) method with the 6-311G+ (d, p) basis sets are indicated in **Chapter VI**.

Chapter VII 1,2-propylenedioxyanthraquinone derivative compounds were synthesized and their structure was confirmed by ^{1}H, ^{13}C NMR. The chemical structure was studied using single-crystal X-ray diffraction techniques along with Hirshfeld surface.

Finally, **Part D** comprises the most relevant conclusions obtained in this thesis, as well as suggestions for future work (**Chapter VIII**).

References

(1) Verma, S.; Singh, S. Vet. World **2008**, 1, 347–350.
(2) Newman, D. J.; Cragg, G. M.. J. Nat. Prod. **2012**, 75 (3), 311–335.
(3) Patwardhan, B.; Vaidya, A. D. B.;. Curr. Sci. **2004**, 86 (6), 789–799.
(4) Liebezeit, G. E. Senckenbergiana Maritima **2008**, 38 (1), 1–30.
(5) Nasir, B.; Fatima, H.; Ahmad, M. Austin J. Microbiol. **2015**, 1 (1), 1002.
(6) Aidi Wannes, W.; Marzouk, B. J. Acute Dis. **2016**, 5 (5), 357–363.
(7) Lahlou, M. Pharmacol. Pharm. **2013**, 4 (3), 17–31.
(8) Rankou, H.; Culham, A.; Jury, S. L.; Christenhusz, M. J. M. The Endemic Flora of Morocco; **2013**; Vol. 78.
(9) Bouiamrine, E. H.; Ibijbijen, J.; Nassiri, L.; El, C.; Bouiamrine, H.; Bachiri, L. J. Med. Plants Stud. **2017**, 5 (2), 123–128.
(10) Hamamouch, N. Med Aromat Plants **2017**, 9 (3), 349.
(11) Maraghni, M.; Gorai, M.; Neffati, M. S. South African J. Bot. **2010**, 76 (3), 453–459.
(12) Benammar, C.; Hichami, A.; Yessoufou, A.; Simonin, A. M.; Belarbi, M.; Allali, H.; Khan, N. A. BMC Complement. Altern. Med. **2010**, 10 (54), 1–9.
(13) Abdoul-Azize, S.; Bendahmane, M.; Hichami, A.; Dramane, G.; Simonin, A. M.; Benammar, C.; Sadou, H.; Akpona, S.; El Boustani, E. S.; Khan, N. A. Int. Immunopharmacol. **2013**, 15 (2), 364–371.
(14) Ghedira, K.; Chemli, R.; Richard, B.; Nwllard, J.; Men-olivier, L. L. E. **1993**, 32 (6), 1591–1594.
(15) Ghedira, K.; Chemli, R.; Caron, C.; Nuzilard, J. M.; Zeches, M.; Le Men-Olivier, L. Phytochemistry **1995**, 38 (3), 767–772.
(16) Le Crouéour, G.; Thépenier, P.; Richard, B.; Petermann, C.; Ghédira, K.; Zèches-Hanrot, M. Fitoterapia **2002**, 73 (1), 63–68.
(17) Renault, J.; Ghedira, K.; Thepenier, P.; Lavaud, C.; Zeches-hanrot, M.; Men-olivier, L. L. E. Phytochemistry **1997**, 44 (7), 1321–1327.
(18) Maciuk, A.; Lavaud, C.; Thépenier, P.; Jacquier, M. J.; Ghédira, K.; Zèches-Hanrot, M. J. Nat. Prod. **2004**, 67 (10), 1639–1643.
(19) Marmouzi, I.; Kharbach, M.; El, M.; Bouyahya, A.; Cherrah, Y.; Bouklouze, A.; Vander, Y.; El, M.; Faouzi, A. Ind. Crop. Prod. **2019**, 132, 134–139.
(20) Rached, W.; Barros, L.; Ziani, B. E. C.; Bennaceur, M.; Calhelha, R. C.; Heleno, S. A.; Alves, M. J.; Marouf, A.; Ferreira, I. C. F. R. Food Funct. **2019**, 10 (9), 5898–5909.
(21) Abdoul-Azize, S.; Bendahmane, M.; Hichami, A.; Dramane, G.; Simonin, A. M.; Benammar, C.; Sadou, H.; Akpona, S.; El Boustani, E. S.; Khan, N. A. Int. Immunopharmacol. **2013**, 15 (2), 364–371.
(22) Abdoul-Azize, S. J. Nutr. Metab. **2016**, 1–13.
(23) Nakanishi, F.; Nagasawa, Y.; Kabaya, Y.; Sekimoto, H.; Shimomura, K. Plant Physiol. Biochem. **2005**, 43 (10–11), 921–928.
(24) Lajkó, E.; Bányai, P.; Zámbó, Z.; Kursinszki, L.; Szőke, É.; Kőhidai, L. Cancer Cell Int. **2015**, 15 (1), 1–15.
(25) Some Traditional Herbal Medicines, Some Mycotoxins, Naphthalene and Styrene.; **2002**; Vol. 82.
(26) Sharifzadeh, M.; Ebadi, N.; Manayi, A.; Kamalinejad, M.; Rezaeizadeh, H.; Mirabzadeh, M.; Bonakdar Yazdi, B.; Khanavi, M. J. Med. Plants 2014, 13 (51), 62–70.
(27) Madje, B. R.; Shelke, K. F.; Sapkal, S. B.; Kakade, G. K.; Shingare, M. S. Green Chem. Lett. Rev. **2010**, 3 (4), 269–273.
(28) Thomson, R. . Naturally Occurring Quinones; Buttet-Worths: London; **1957**.

Part B

Chemical characterization and evaluation of biological activity of *Zizyphus lotus* extractable compounds

Chapter II

Bibliographic review of *Zizyphus lotus*

1. General considerations about *Zizyphus lotus*

1.1 Origin and Botany

Jujube is the common name of evergreen, deciduous shrub and trees of the buckthorn family, classified as the genus Zizyphus of the family Rhamnaceae, order Rhamnales and division Magnoliophyta that contain about 135–170 species worldwide.[1] The name of Zizyphus is related to the North African Coastal Arabic word zizoufo, the ancient Persian words zizfum or zizafun, and the ancient Greek word ziziphon, all of which were means a spiny shrub.[2] Usually, in Arabic, the fruits have the name of the tree, but in the case of genus Zizyphus, the tree is called Sedra and the fruit N'bag.[3]

Zizyphus jujuba (Mill.) and *Ziziphus mauritiana* (Lam.) are the most important jujube in terms of distribution and economic significance.[4] Recently, other Zizyphus species have been attracted much attention as a natural biomass resource. Among them, *Zizyphus lotus* (*Z. lotus* Lam.) which has been known since antiquity and it was even mentioned in the magic plants of the Odyssey. The story began when the consumption of its fruits saved a group of sailors (Ulysses with his companions) from the inevitable death when their ship crashed on the shores of the island of Lotophages. This incident remained a legend until 1784 when Desfontaine discovered this shrub near the desert in Tunisia called Djerba, which is the new name of Lotophages.[5,6]

At that time the botanical identification of this mysterious plant has given rise to many comments and controversy until the botanists Clusius, Bauhin, Shaw, and Desfontaines reached the same conclusion; which is, this shrub fruit belongs to the variety of jujube, and what is discovered by Desfontaines is the *Zizyphus lotus* Lam.[5] The Botanical description of *Z. lotus* is as follow:

Kingdom	Plantae-Plants
Subkingdom	Tracheobionta-Vascular plants
Division	Magnoliophyta-Flowering plants
Superdivision	Spermatophyta-Seed plants
Class	Magnoliopsida-Dicotyledons
Subclass	Rosidae
Order	Rhamnales
Family	Rhamnaceae-Buckthorn family
Genus	Ziziphus
Species	*Ziziphus lotus* Lam.

1.2 Morphological characteristics

Zizyphus lotus L. is an evergreen spiny shrub but sometimes attains the size of a small tree (1-2.5 m the high) (Fig 1, pic A) due to intensive grazing during the latter part of the dry

seasons.[3] This shrub is highly resistant to heat and drought and is divided into four parts: leaves, branches with leaves, branches, and stems (Fig 1).

The leaves are short, oval, and more or less elliptic with 1.2 to 1.9 mm in length and 4 to 9 mm in width. They are smooth and shiny on both sides and have three prominent longitudinal ribs starting from the petiole (Fig 1, pic B).[7,8] Leaves are falling in autumn and reappear by the end of the following spring, they are glabrous with a thin cuticle but the whole plant is filled with mucilage. The flowers are very visible and yellow with star-shaped sepals, small petals, and a bisexual superior ovary bloom in June (Fig 1, pic C). The fruits are ovoid-long, taken a shape and size of a beautiful olive with 0.8-1 cm in diameter. At first green and then yellow, it becomes dark red when ripe in October (Fig 1, pic D1-D2). It is usually two-seeded. However, it may be one-seeded if one of the two ovules aborts (Fig 1, pic E*). Seeds are circular (4-5 mm, diameter), the exocarp and the mesocarp form the edible (Fig 1, pic F).[8]

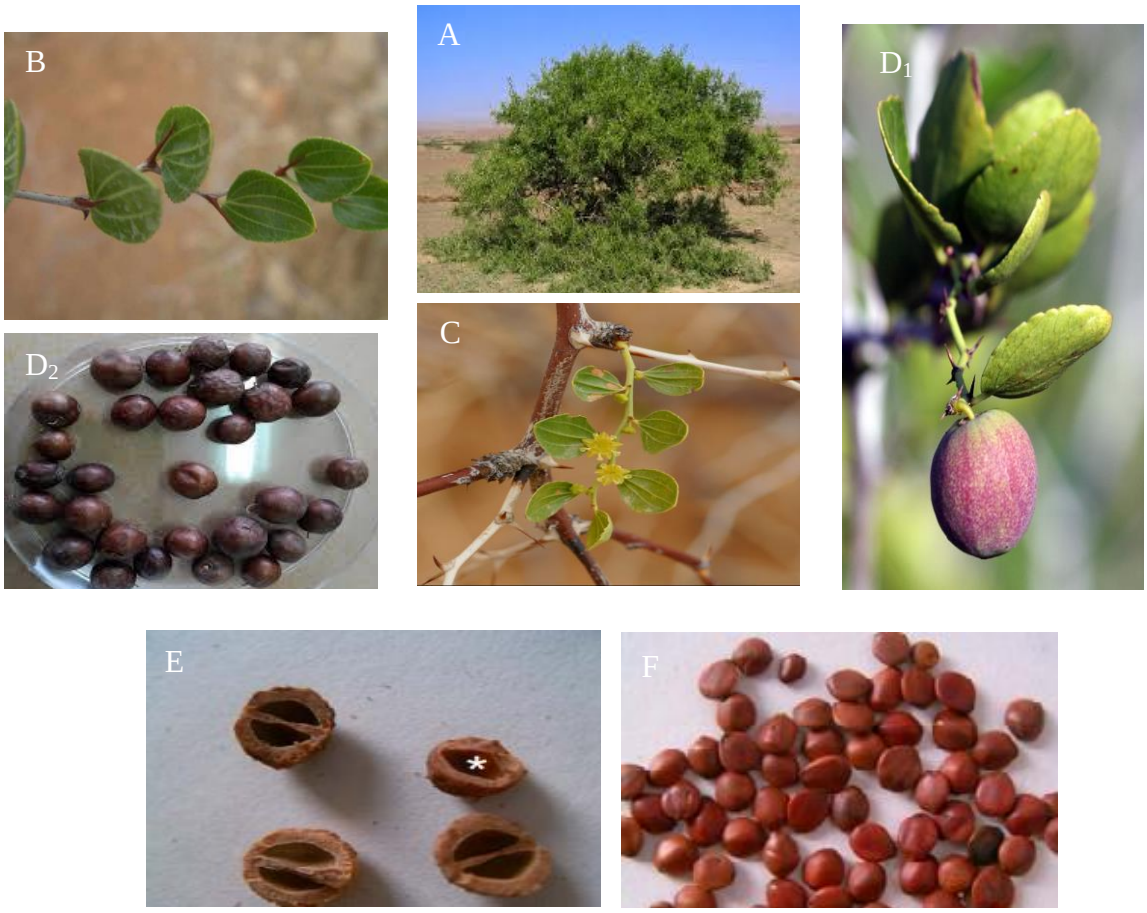

Figure 1: Different morphological parts of *Zizyphus lotus*.

1.3 Geographical distribution

Zizyphus lotus is a medicinal plant distributed in the Mediterranean region with a low penetration into the northern Sahara such as Morocco, Algeria, Tunisia, and Libya. It then reappears in Yemen, on the island of Socotra, in the Middle East like Palestine, Syria, Turkey. Although in Europe, has restricted to some semiarid areas in the southeast of Spain and the island of Sicily.[9] This shrub grows on all soils type such as limestones, siliceous, clayey, and

sandy, while generally supports small amounts of salt.[10] Z*izyphus lotus* is indigenous to Morocco, where its history of cultivation goes back over the old ages. It has been widely distributed in arid and semi-arid in plateau regions and along with the sandy riverbeds in the Saharan region.[11] Among the region of Morocco are Chaouia, Haouz, Zear, Rhamna, Middle Atlas, Gharb, Errachidia region, Souss, the coastal region of Safi in Sidi Ifni, the region of Khenifra, eastern Morocco, the Sahara and, the region of Oujda.[10]

1.4 Interest use of *Zizyphus lotus*

1.4.1 Traditional uses

The use of *Z. lotus* in traditional medicine was carried out according to the different parts of the plant. Leaves are applied as plasters to treat smallpox, measles, boils, abscesses. The ingestion of leaves decoction has been used as anti-diarrhea, anti-vomiting, and antiseptic urinary.[12] Moreover, the application of crushed leaves, relieve back pain,[12,13] and the powder of dried leaves mixed with carob (*Ceratonia siliqua*), nigella (*Nigella sativa*), and honey is widely used to treat gastralgia.[14] The fruit is not only appreciated as food, but also mixed with milk or water, to be used as labels to treat furuncles and abscess.[15] Besides, the decoction of fruits used as an emollient (throat irritations and bronchopulmonary), anti-ulcer and, against kidney stones. Root juice is used to treat ocular leukoma and infusion for vomiting. Moreover, the root bark is known for its anti-diabetic properties.[16] In North Africa and the Middle East the whole parts are used as convalescences (febrifuge and invigorating), sedative, diuretic, antidiabetic, antifever, antidiarrhea, antiinflammatory, alleviate stress and against insomnia, common colds, skin infections, weakness, liver complaints, urinary tract diseases, obesity, and hypoglycemia. Therefore, the wood ash, with vinegar, constitutes a local treatment of snake bites.[9,17]

1.4.2 Economy

The fruit of this shrub species was appreciated for both unprocessed consumptions, and for preparing bread, couscous, cake, loaf, jam, or dough, conserves and mingled with water, ferment in a jar to produce a low-preservation wine.[6,18] In the old ages, the Moroccan nomads have been consumed edible fruits in their travels as a source of energy; which allowed them to feel satiated.[19] This property can be used for weight loss in individuals overweight and obese. Besides, honey collected from the flowers of *Z. lotus* is one of the most expensive in the world for its therapeutic properties against liver diseases, stomach, diabetes, and others. This product is widespread in Morocco, Tunisia, and Yemen and is mainly appreciated for its aphrodisiac properties while the crushed seeds provide a special quality wild oil.[20]

1.4.3 Ecology

Due to the physiological and morphological adaptation mechanisms of *Z. lotus* its intrinsically widely adapted to environmental stresses such as dry and hot climates, which makes it suitable for growth in challenging environments characterized by degraded land and limited water resources.[7,21] This shrub has been used to fight against silting (the improvement of degraded soils), it intervenes in the fixing of mobile substrates by the emission of its roots outside the grounds besides, it constitutes a shelter for the animals (rodents, insects, and reptiles), and allow the installation of a nitrophile flora. The Zizyphus shrub is relatively

resistant to bush fires and generally resumes their vigor 4 months after the passage of fire with only 10% of young sprouts who do not survive.[21]

All these ecological elements militate in favor of the rehabilitation of *Z. lotus* on degraded areas in the arid and semi-arid steppe zone in the context of desertification and decline in agricultural production.

2. General chemical composition of *Zizyphus lotus*

The elemental analyses, as well as the biomass calorific value of *Z. lotus* seeds fraction, are listed in Table 1. The mineral analysis of *Z. lotus* showed that magnesium was the predominance compound in the three parts, namely seeds, pulp, and almond with a value of 153, 397.91, and 1349.06 mg/100 g, respectively (Table 1). Calcium as a blood pressure-lowering agent[22] was found in a significant amount in the seeds (110.58 mg/100 g). Besides, similar amounts for Iron was found in *Z. lotus* fractions, while zinc was absent in the seeds; to quantify in the almond part with a value of 1.38 mg/100 g.[23] The calorific value of the seeds was highlighted (Table 1). Further studies should focus on determining the calorific value of the other parts of *Z. lotus*, in particular, the pulp part.

Table 1: The Proximate analysis, elemental analysis, and energy value of *Zizyphus lotus* (adapted from[20,23]).

Proximate analysis (% dw)	Seeds	Pulp	Almond
Moisture content	6.05		
Ash	1.05	3.20	92.43
Elemental analysis (mg/100g)			
Potassium	92.41		
Calcium	110.58		
Mgnesium	153.92	397.91	1349.06
Sodium	7.30		
Iron	1.21	1.33	1.21
Phosphorus		10.62	24
Natrium		11.45	17.41
Kalium		134.99	97.92
Manganese		2.17	7.84
Zinc	-	0.44	1.38
Calorific value (kJ/ 100 g)	2237.70		

2.1 Vitamins

Table 2 depicts the vitamin composition of several morphological parts of *Z. lotus*. Vitamin C is the major vitamins of *Z. lotus* biomass, ranging from 5.67 mg/100 g in fruits to 19.65 mg/100 g in the pulp. Moreover, vitamin E showed a high content in leaves *Z. lotus* (155.71 mg/100 g), while the seeds are enriched on β-tocopherols.[9] Besides, a small amount of carotenoids were found in seeds and fruit parts (0.634 and 1.47 mg/100 g, respectively). Vitamins B1 and B2 were also present in *Z. lotus* seeds amounting to 0.03 and 0.08 mg/100 g, respectively. Vitamin A was found in *Z. lotus*, varying between 3.8 mg/100 g in the stem to 71.63 mg/100 g in the pulp. Therefore, the significant total amount of tocopherols has only been highlighted in the seeds part (Table 2).[20]

Table 2: Vitamins composition of *Zizyphus lotus* (adapted from[9,20]).

Vitamins	*Z. lotus* (content mg/100 g)					
	Leaves	Seeds	Root	Pulp	Stem	Fruit
Vitamin A	13.52		6.45	71.63	3.8	
Vitamin B2		0.08				
Vitamin C	63.40	31.24-170.84	47.20	190.65	24.65	5.67
Vitamin B1	-	0.03				0.039
Vitamin E	155.71		4.7	11.23	4.5	
carotenoids		0.634				1.47
α-tocopherol						
β-tocopherol		130.47				
γ-tocopherol						
δ-tocopherol		10.60				
Total Tocopherols		141.07				

2.2 Amino acids

Table 3 present the amino acid composition of several morphological parts of *Z. lotus*. Threonine and glutamic were the predominant amino acids in the seeds (26.73 and 17.28 g/100g, respectively). Moreover, an appreciable amount of leucine, arginine, and aspartic acid were observed (Table 3). Besides, the total protein content was determined on seeds and pulp parts, which pulp represents a higher content (19.11%) than in *Z. lotu*s pulp with a value of 1.18% dw.[23] Therefore, the amino acid composition of *Z. lotus* pulp remains to be elucidated.

Table 3: Amino acids composition (g/100g protein) of *Zizyphus lotus* seeds part (adapted from[20]).

Amino acids	Content (g/100 g protein)
Isoleucine	2.85
Leucine	13.11
Lysine	1.55
Glycine	2.67
Phenylalanine	2.65
Threonine	26.73
Valine+methionine	1.80
Tryptophan	1.36
Glutamic acid	17.28
Aspartic acid	7.76
Tyrosine	2.27
Serine+histidine+glutamine	4.57
Alanine	4.56
Arginine	9.47

2.3 Monosaccharides

Mkadmini and co-workers[24] identified six monosaccharides, including arabinose as the main monomeric sugar, followed by rhamnose and glucose. Xylose-sugar was also detected but in smaller amounts accounting for 1.83 % dw.

Table 4: Relative monosaccharides content (%) of *Zizyphus lotus* fruit (adapted from[24]).

Monosaccharides	Content (% dw)
Arabinose	34.00
Rhamnose	23.26
Glucose	19.14
Fructose	12.19
Galactose	9.58
Xylose	1.83

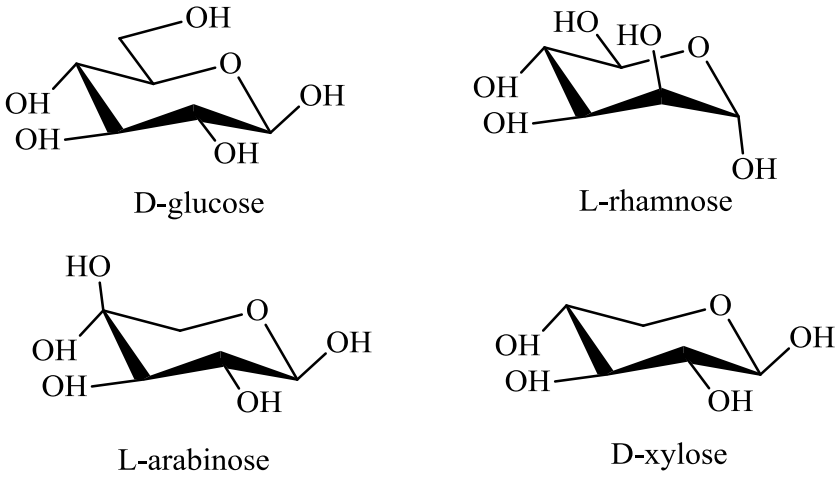

Figure 2: Structures of some monosaccharides identified in *Zizyphus lotus*.

Polysaccharides are constituted by a large number of monosaccharide units, ranging from hundreds to thousands, joined through glycosidic bonds. These macromolecules are structural material and as an energy storage system for plants.[25] Mkadmini et al. (2016)[24] have investigated the extracting polysaccharide optimization from *Z. lotus* fruits by response surface methodology without identifying their main constituent. Under optimal conditions such as extraction time (3h 15min), extraction temperature (91.2 °C), and water/solid ratio (39 mL/g); the experimental extraction yield and uronic acid content are 18.88% and 41.89 mg/mL, respectively.[24]

3. Extractives composition of *Zizyphus lotus*

Extractives are the natural chemical of plants that can be extracted using polar and non-polar solvents.[26] Most of the extractives are secondary metabolites that are preferentially deposited in the cell lumens, albeit they may also be found in cell walls.[27] The overall composition of the extracts varies from plant species to another and certain classes are restricted to a particular taxonomic group (species, genus, family, or closely related group of families).[28]

Plant metabolism can be subdivided into primary metabolisms such as carbohydrates, lipids, and proteins, which encompasses reactions and pathways vital for survival, and secondary metabolism, which is not necessary for survival but is involved in important functions for growth and development, including the interaction of the plant with the environment.[29] In particular, secondary metabolic compounds are shown to be highly valuable products for humans, by commercialized as pharmaceuticals, flavors, fragrances, and pesticides product.[30]

Biosynthetically speaking, plant secondary metabolites (PSMs) can be divided into three major groups: the terpenes, the alkaloids, and the phenylpropanoids and allied phenolic compounds.[31] The PSMs biosynthesis pathways appear in Fig 3. Terpenes are biosynthesized from dimethylallyl pyrophosphate and isopentenyl pyrophosphate. Sterols are also afforded by this pathway. Phenolic compounds or polyphenols are mostly produced through the shikimate and phenylpropanoid pathways. Finally, alkaloids are mainly generated within the pathway of the amino acids.[29,32]

Several studies supported the evolution of secondary metabolism by the recruitment of enzymes and pathways from primary metabolism yielded new compounds that we're able to increase plant adaptation to particular environments and were gradually converted into specialized metabolites.[29,33] For instance, in the case of fatty acids and glucosides, the largest part is better described as primary metabolites, whilst some of them are extremely rare, being referred as secondary metabolites.[33] As indicated in Figure 3, fatty acids are formed in the acetate pathway.

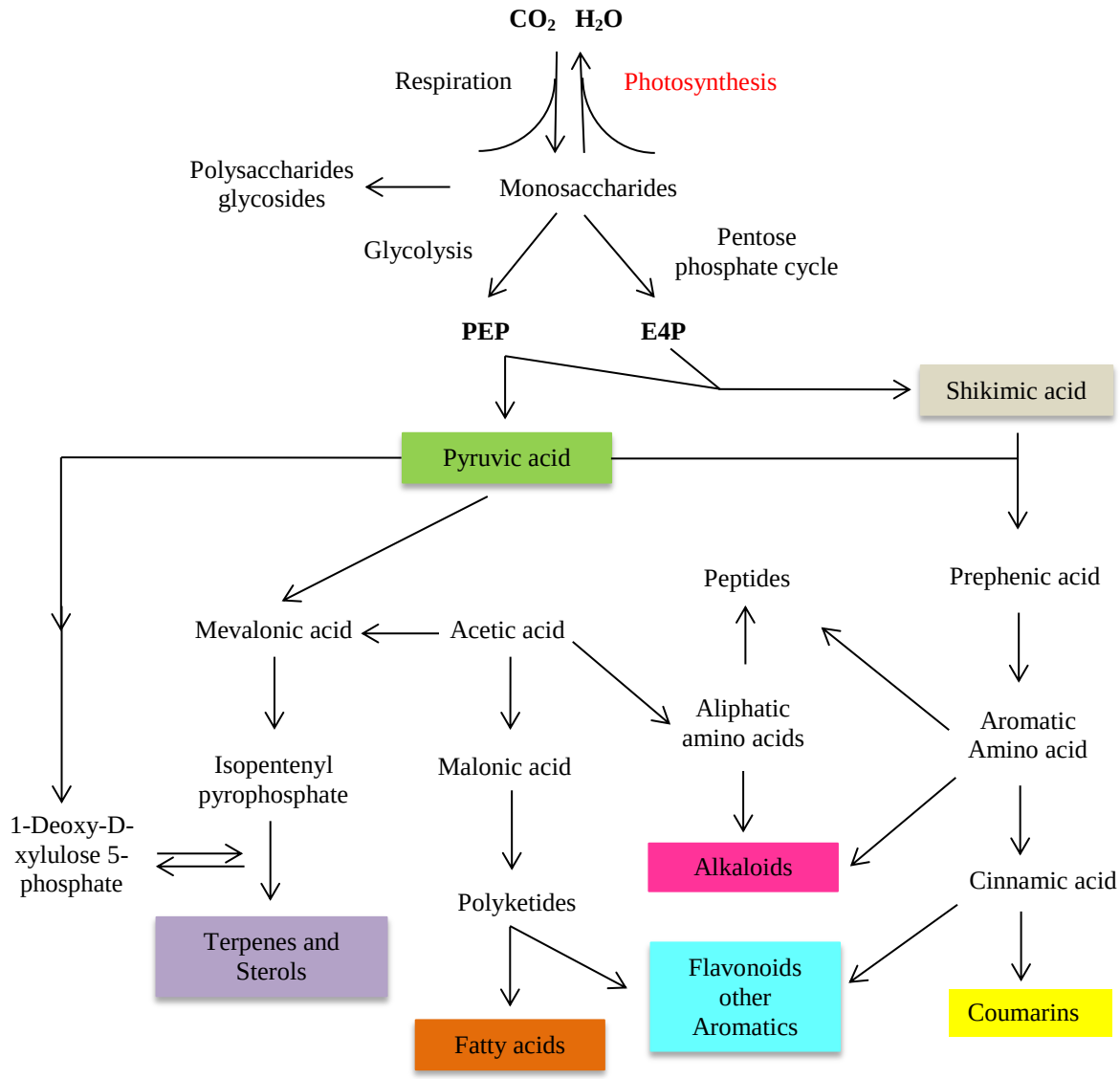

Figure 3: Secondary metabolism pathways for the biosynthesis of terpenes, phenolic compounds and alkaloids. Abbreviations: PEP, phosphoenolpyruvate; E4P, D-erythrose 4-phosphate (adapted from[34]).

Table 5: Extractives yields (% dw) of aerial parts, fruits roots and root barks of *Zizyphus lotus*, by using organic solvents and water (adapted from[35–36]).

Z. lotus	Extractives yields %							
	Hexane	EtOAc	MeOH	H_2O	Butanol	MeOH/ H_2O	$CHCl_3$	Sce
Aerial parts	4.00	4.74	26.30	0.31	-	-	-	[35]
Fruit	-	-	-	8.9-11.9	-	-	-	[37]
Root	-	1.8	-	-	1.1	13.9	-	[38]
Root barks	-	1.29	25.27	-	-	-	0.03	[36]

Abbreviations: EtOAc, Ethyl actate; MeOH, Methanol; H_2O, Water; $CHCl_3$, Chloroform; Sce, Source.

The extractives yields, obtained from *Z. lotus* aerial and root barks extracts, were higher with methanol (26.30 and 25.27% dw, respectively) than with other solvents, such as ethyl

acetate (4.74 and 1.29% dw, respectively).[35,36] The extractives yields of *Z. lotus* roots part were also found to be higher with methanol and water, compared to those with butanol and ethyl acetate (Table 5).[38] Moreover, the fruit aqueous extractive yield showed to be higher than that reported for the aerial parts.[37] The variation in the extractive yields is associated with the type of solvent, the part studied, and the extraction method.

The chemical composition of *Z. lotus*, in terms of lipophilic extractives namely: fatty acids, triacylglycerol, sterols, alkaloid, saponins, and phenolic compounds, will be discussed above in detail.

3.1 Fatty Acids

Plants synthesize a huge variety of fatty acids (FAs) though the acetate pathway, albeit only a few are major and common constituents.[39,40] Fatty acids consist of a long hydrocarbon chain (–CH_2–CH_2–) with a carboxyl group, typically at the terminus of the molecule.[41] The hydrocarbon chain is formed by an even number of carbon atoms, from 4-C to 30-C, although the most common have 16-C or 18-C carbon atoms. Fatty acids can be saturated, unsaturated, monounsaturated or polyunsaturated depending on the number of double bonds. Among the unsaturated fatty acids, the Z-isomers are the most commonly present in plants.[40]

FAs compositions vary widely in the proportion of the different morphological parts of *Z. lotus*, although 18-C unsaturated fatty acids predominate over the saturated ones. Oleic acid, linoleic acid, and linolenic acid are presented in a significant amount, where oleic acid is the most abundant FAs in the *Z. lotus* fruits,[42] seeds,[20] and almond[23] amounting, respectively 88.12%, 61.93%, and 49.88% of the total FAs content. *Z. lotus* seeds oil is rich in FAs, especially oleic acid and linoleic acid, accounting for 56.08% and 18.94% of the total FAs content.[20] Palmitic acid and stearic acid were the main saturated FAs found in *Z. lotus*. Docosenoic and dodecanoic acid were detected only in the fruit part but in very low amount;[42] besides others such as eicosanoic acid docosanoic acid and tetradecanoic acid.[9,20]

Ourzeddine et al. (2017)[43] discovered eleven fatty acid ethyl ester in *Z. lotus* fruit essential oil namely: ethyl decanoate, ethyl undecanoate, ethyl tridecanoate, ethyl pentadecanoate, ethyl (Z)-hexadec-9-enoate, ethyl (E)-hexadec-9-enoate, ethylhexadecanoate, ethyl heptadecanoate, ethyl (Z)-octadec-9-enoate, ethyl (E)-octadec-9-enoate, and ethyl octadecanoate. Besides, methyl hexadecanoate was also detected in the fruit essential oil extract.[43]

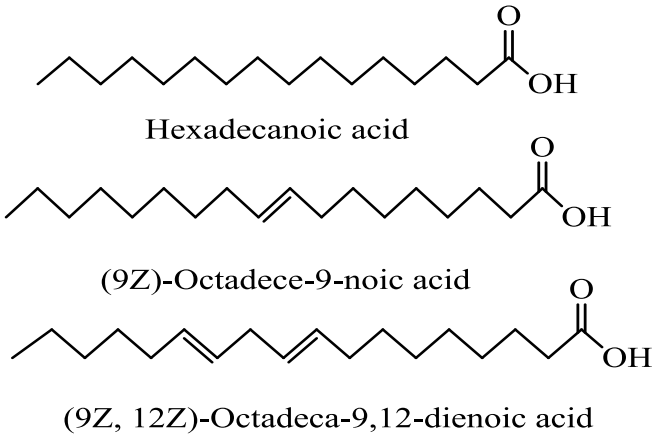

Figure 4: Structure of the most predominance fatty acids in seed oil of *Zizyphus lotus*.

3.2 Pentacyclic triterpene

The mevalonate and non-mevalonate pathway were considered as the universal source of the terpenes (terpenoids), where respectively isopentenyl pyrophosphate (IPP) and 1-Deoxy-D-xylulose 5-phosphate (DXP) were precursors[44] as shown in Figure 3. Terpenes are made up of isoprene molecules, which contain five carbon atoms with double bonds. The simplest terpenes are monoterpenes that contain two isoprene molecules, while the complex contains six molecules which are triterpenes.[45]

Several pentacyclic triterpenes have been identified in the genus Zizyphus.[46,47] Although these compounds have not been explored so far in *Z. lotus* despite their various pharmacological activity such as anti-HIV and antitumor properties.[44] However unique terpene glycosides i.e. oleoside was identified in stem barks and branches of *Z. lotus*.[48]

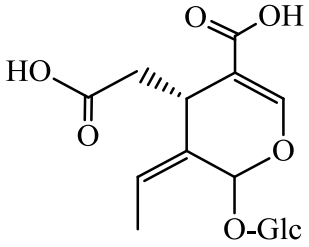

Figure 5: Structures of oleoside identified in *Zizyphus lotus*. Abbreviation: Glc, glucoside.

3.3 Sterols

Sterols are derived from squalene, which is, in turn, derived from hydroxymethylglutaryl CoA (HMG-CoA) via mevalonic acid (MVA). They are considered as triterpenoid, steroidal alcohols characterized by a 3β-hydroxyl group and generally present in fruits, vegetables, vegetable oils, nuts, and grains.[49,50] sterols can be selectively removed from plants by sequential extraction with nonpolar solvents, such as hexane and chloroform.[51]

The photosynthetic tissues of *Z. lotus* species have a remarkable ability to synthesize various sterols. Seven sterols were identified from seeds oil extract of *Z. lotus*, where Δ7-Campesterol, β-sitosterol, and campesterol illustrated in Figure 6, are the most abundant. Δ7-Campesterol was the major accounting of 51.86% of the total sterol identified in seeds oil. Other sterols were also detected in a moderate amount, namely stigmasterol, Δ5- avenasterol, Δ5-24 stigmatadienol, and cholesterol.[20] It is important to indicate that there is no available data on the sterol content in the other parts of *Z. lotus* this issue remains to be determined.

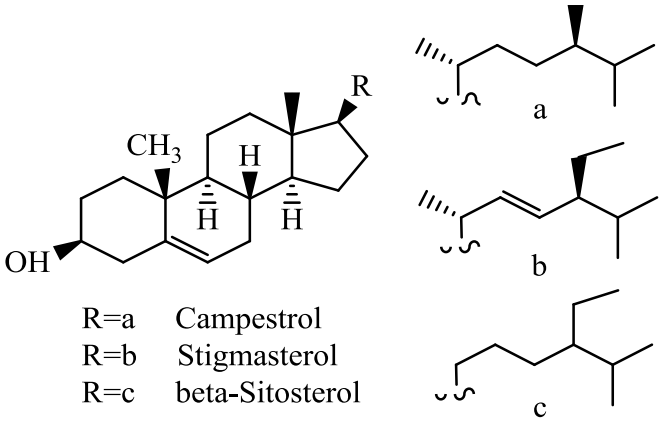

Figure 6: Structures of the most predominance sterols identified in *Zizyphus lotus* seed oil.

3.4 Triacylglycerols

Triacylglycerols (TG) comprise three FAs esterified with a glycerol skeleton, and they are important storage lipids and the main constituents (~99%) of vegetable oils and food lipids.[52]

Eleven TG were identified in *Z. lotus* seed oil. The glycerol-trioleate is regarded as the main TG accounting for 26.48g/100 g, along with glycerol-palmitate-dioleate with 18.78g/ 100g (Fig 7).[20] Other TAGs were also detected such as glycerol–oleate–di-linoleate, glycerol–palmitoleate–dioleate, glycerol–palmitate–oleate linoleate, glycerol–stearate–dioleate, and glycerol–dioleate–linolenate.

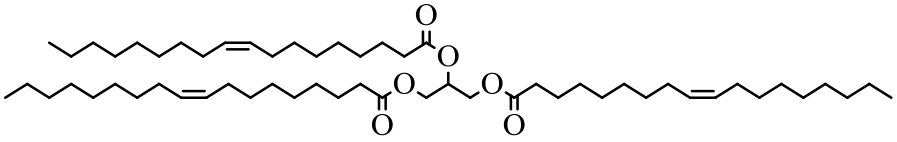

Glycerol-trioleate

Figure 7: Structures of glycerol-trioleate identified in seed volatile oil of *Zizyphus lotus*.

3.5 Cyclopeptide alkaloids

Cyclopeptide Alkaloids are biosynthesized through the Shikimic acid. These plant metabolites are macrocyclic compounds consists of two amino acids and a stryrylamine unit.[53] Six cyclopeptide alkaloids were isolated from *Z. lotus* root bark namely: lotusines, named from A to G.[54–55]

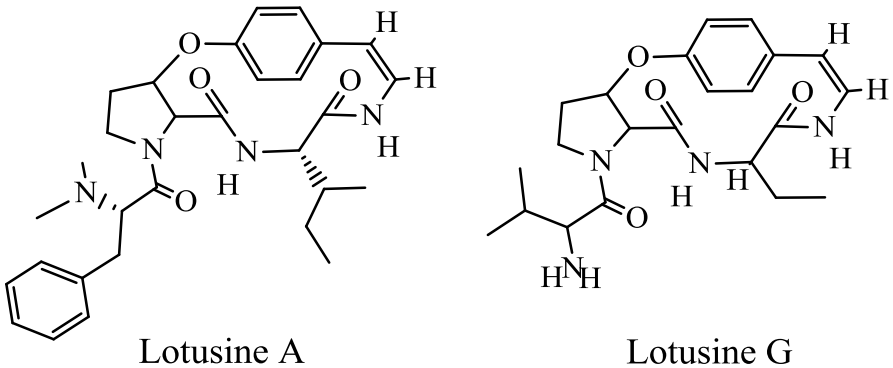

Lotusine A Lotusine G

Figure 8: Structures of lotusine A and G identified in *Zizyphus lotus*.

3.6 Saponins

Saponins consist of an aglycone unit linked to one or more oligosaccharide moieties. The aglycone or sapogenin unit consists of either a sterol or the more common triterpene unit. In both the steroid and triterpenoid saponins, the carbohydrate side-chain is usually attached to the 3 carbon of the sapogenin.[56] Four dammarane-type saponins were isolated from root bark namely: jujuboside C, lotoside I, lotoside II, jujuboside A,[57] along with four dammarane saponins notably jujuboside B, three jujubogenin glycosides and jujubasaponine IV have been also isolated from leaves extract.[58]

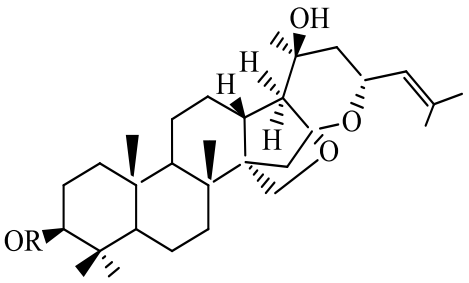

R	
Glu	Jujubogenin glycosides
Tri-Glu	Lotoside I
Hepta-Glu	Jujuboside A

Figure 9: Structures of some saponins isolated from *Zizyphus lotus*. Abbreviation: Glu, Glucose.

3.7 Phenolic compounds

Phenolic compounds (PCs) are a heterogeneous group of secondary metabolites found widely in all plant kingdom which fulfill a very broad range of physiological roles.[59] These secondary metabolites are synthesized through either the shikimate/phenylpropanoid pathway, which directly provides phenylpropanoids, or the "polyketic" acetate/malonate pathway, which can produce simple phenols or both, thus producing monomeric, polymeric phenols and phenolic compounds.[60] PCs are considered to have the most desirable phytochemicals due to their potential to be used as additives in the food industry, cosmetics, medicine, and other fields.

From the chemical point of view, PCs contain benzene rings, with one or more hydroxyl substituents, and range from simple phenolic molecules to highly polymerized compounds.[61] Despite this structural diversity phenolic compounds can be divided into different subgroups, such as:[62]

Class	Structure
Simple phenolics, benzoquinones	C6
Hydroxybenzoic acids	C6–C1
Acethophenones, phenylacetic acids	C6–C2
Hydroxycinnamic acids, phenylpropanoids	C6–C3
Napthoquinones	C6–C4
Xanthones	C6–C1–C6
Stilbenes, anthraquinones	C6–C2–C6
Flavonoids, isoflavonoids	C6–C3–C6
Lignans, neolignans	$(C6–C3)_2$
Biflavonoids	$(C6–C3–C6)_2$
Lignins	$(C6–C3)_n$
Condensed tannins (proanthocyanidins or flavolans)	$(C6–C3–C6)_n$

A summary of the studies of literature regarding the various phenolic compounds such as simple phenols, phenolic acids, and flavonoids identified in different morphological parts of *Z. lotus* shrub is discussed below.

3.7.1 Simple phenols

Pyrogallol with three –OH groups and catechol with two –OH groups (Fig 9) are two hydroxylated phenols identified in *Z. lotus* extract. Pyrogallol was detected in leaves and fruit, accounting, respectively 124.20 and 29.89 mg/kg dw. Although, catechol was found in the fruit part with a low amount (3.31 mg/kg dw).[63]

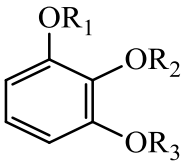

R_1	R_2	R_3	
OH	OH	OH	Pyrogallol
OH	OH	H	Catechol

Figure 9: Structure of pyrogallol and catechol identified in *Zizyphus lotus*.

3.7.2 Phenolic acids

Phenolic acids (PAs) are the most abundant phenolic compounds in our diets, and has been present in plants both as free aglycones and bound in conjugated forms, often with esters, glycosides organic acids, and bound complexes.[62] Phenolic acids have been reported to have powerful antioxidant properties and biological activities including cardioprotective, anti-carcinogenic, antimicrobial, and hepatoprotective properties.[64] Based on the position of the hydroxyl group, PAs can be divided into two subgroups, i.e., the hydroxybenzoic and hydroxycinnamic acids which are derived from the non-phenolic benzoic and cinnamic acids.[62,65]

- **Hydroxybenzoic acids**

Seven PAs have been identified in the leaves and fruits of *Z. lotus*. Gallic acid was the most abundant PAs in leaves and vanillic acid in the fruits fraction, accounting respectively 2715.45 and 254.10 mg/kg dw. Moreover, chlorogenic acid an ester of caffeic acid was found to be concentrated in leaves with the amount of 398 mg/kg dw (Fig 10).

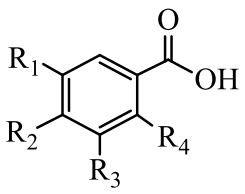

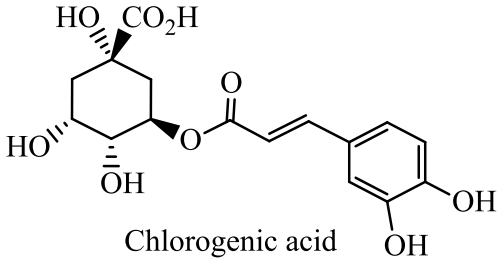

Chlorogenic acid

R_1, R_3=OCH_3, R_2=OH	Syringic acid
R_1, R_2, R_3=OH	Gallic acid
R_1=OCH_3, R_2=OH	Vanilic acid
R_2=OH	*p*-Hydroxybenzoic acid
R_4=OH	Salicylic acid

Figure 10: Structures of phenolic acids identified in *Zizyphus lotus*.

- **Hydroxycinnamic acids**

Hydroxycinnamic acids are aromatic compounds with a three-carbon side chain. Caffeic acid being the most abundant hydroxycinnamic acid found in *Z. lotus* leaf and fruit fractions (247.90 and 56.26 mg/kg dw, respectively) along with its esterified form, i.e. rosmarinic acid.

Other hydroxycinnamic acids were identified with a significant amount as illustrated in figure 11.[63,66]

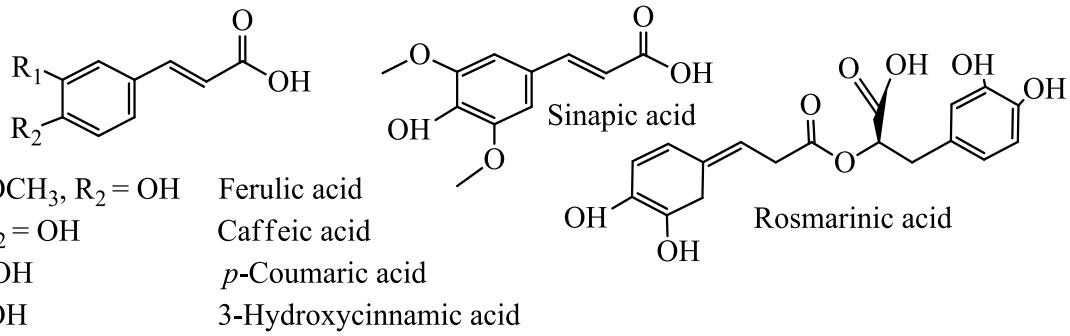

R_1= OCH_3, R_2 = OH	Ferulic acid
R_1, R_2 = OH	Caffeic acid
R_2 = OH	*p*-Coumaric acid
R_1= OH	3-Hydroxycinnamic acid

Figure 11: Structures of hydroxycinnamic acids identified in *Zizyphus lotus*.

- **Stilbenes**

Stilbenes are another class of compounds that are part of nonflavonoid polyphenols with 1,2-diphenylethylene as a basic structure. These compounds can be categorized as monomeric and oligomeric stilbenes.[67] Stilbenes are limited in plants since the stilbene synthase (core enzyme) is not universally expressed.[68] Resveratrol is, so far, the unique monomers stilbene, identified in *Z. lotus* leaves and fruits fraction, amounting respectively 0.88 and 0.43 mg/kg dw (Fig 12). This stilbene capable of preventing several diseases due to its antioxidant and anti-inflammatory properties.[69]

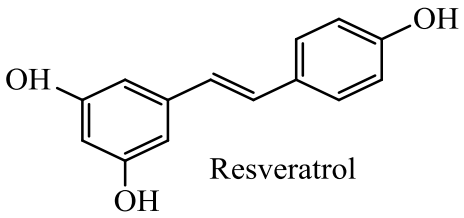

Figure 12: Structures of resveratrol acid identified in *Zizyphus lotus*.

3.7.3 Flavonoids

Flavonoids are the largest and most diverse sub-group of phenolic compounds that are produced as plant secondary metabolites.[70] These compounds are found in various fruits and vegetables, including several medicinal plants, and they are associated with a wide range of biological effects on human health, including antibacterial, anti-inflammatory, anti-allergic, and antithrombotic activities.[68,71] Flavonoids consisting of fifteen carbon atoms divided onto two aromatic rings A and B, joined by a 3-carbon bridge, usually in the form of a heterocyclic ring C (Fig 13). Variations in substitution patterns to ring C result in the major flavonoid classes, i.e., flavonols, flavones, flavanones, flavan-3-ols (or catechins), isoflavones, flavanonols, and anthocyanidins.[62]

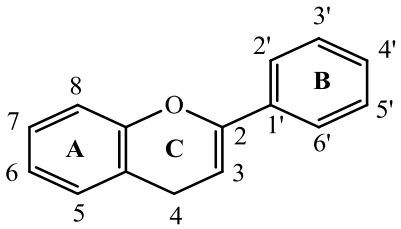

Figure 13: Basic flavonoid structure (2-phenyl-1-benzopyran).

- **Flavanols**

The flavanols are also called the flavan-3-ols due to holding a hydroxyl unit at position 3 of the heterocyclic C-ring.[72] They are the most varied and complex subgroup of flavonoids and exist in states ranging from single molecules to oligomers, polymers, and other derivatives.[73] These compounds are the most abundant subclass of polyphenols found in fruits, berries, and even beverages such as grapes, lychees, strawberries, cacao, black tea, and green tea.[68] Flavanols are responsible for many physiological effects by acting as a free radical scavenger.[69] Catechin and epicatechin represent the two forms of flavanol monomers found in leaves, fruit, and root bark of *Z. lotus* while their polymeric forms are detected in root bark as shown in the table below.

Table 6: Flavanols identified in Z*izyphus lotus* morphological parts (adapted from[63,74]).

Flavanols	*Z. lotus*
(Epi)catechin-(epi)gallocatechin	rb
(+)-Catechin	l, f, rb
Type B (epi)catechin dimer	rb
(-)-Epicatechin	l, f, rb

Abbreviation: rb, root barks; l, leaves; f, fruit.

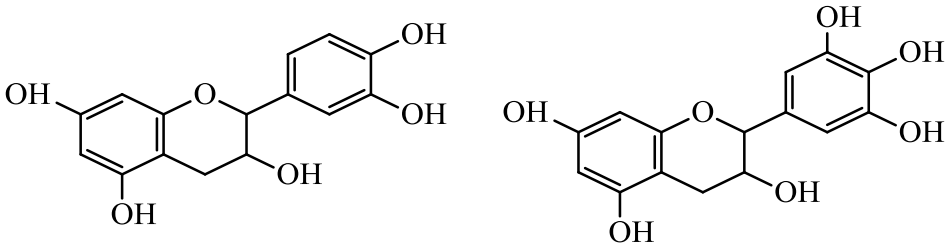

Figure 14: Structure of (epi)-catechin and (epi)-gallocatechin identified in *Zizyphus lotus*.

- **Flavonols**

Flavonols are called 3-hydroxyflavones since they have a hydroxyl group attached to position-3 of the flavones.[68] These hydroxyl groups are present in a glycosylated form in plant species in combination with a sugar moiety (e.g. glucose, rhamnose, or/and rutinoside). Flavonols are extensively distributed in the plant foods mainly in the leaves and in the outer parts of the higher plants.[75] Twelve flavonols were identified as components of *Z. lotus*.

Quercetin, kaempferol, and their several glycosylated derivatives were the most common flavonols found in *Z. lotus* as shown in the table below.

Table 7: Flavonols identified in *Zizyphus lotus* morphological parts (adapted from[63,74,66]).

Flavonols	*Z. lotus*
Quercetin-3-O-(2,6-di-O-rhamnosyl-glucoside)-7-O-rhamnoside	rb
Quercetin-3-O-(2,6-di-O-rhamnosyl-glucoside)	rb, l, f,
Myricetin-3-O-rutinoside	l, rb
Myricetin-3-O-galactoside	l
Quercetin-3-O-(2,6-di-O- rhamnosyl-glucoside)-7-O-glucuronide	rb
Kaempferol-3-O-(2,6-di-O-rhamnosyl-glucoside) isomer 1	rb
Quercetin-3-O-rutinoside	Rb, f, l
Quercetin-O-deoxyhexoside	br, sb
Kaempferol-O-hexoside	rb
Kaempferol-3-O-(2,6-di-O-rhamnosyl-glucoside) isomer 2	rb
Kaempferol-3-O-rutinoside	rb
Kaempferol-3-O-(6-O-rhamnosyl-glucoside)	rb
Quercetin	l, f
Quercetin-3-rhamnoside	l
Kaempferol	l
Quercetin-3-O-galactoside	l

Abbreviations: rb, root barks; l, leaves; f, fruits; br, branches; sbs, stem barks.

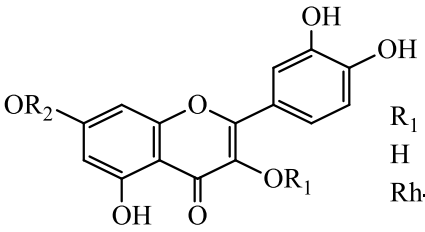

R_1	R_2	
H	H	Quercetin
Rh-Glu	Rh	Quercetin-3-O-(2,6-di-O-rhamnosyl-glucoside)-7-O-rhamnoside
Rh-Glu	H	Quercetin-3-O-(2,6-di-O-rhamnosyl-glucoside)
Rh-Glc	Glu	Quercetin-3-O-(2,6-di-O- rhamnosyl-glucoside)-7-O-glucuronide
Rh-Glu (rhamnosyl(1➔6)-glucoside)	H	Quercetin-3-O-rutinoside
Rh	H	Quercetin-3-rhamnoside
Gla	H	Quercetin-3-galactoside

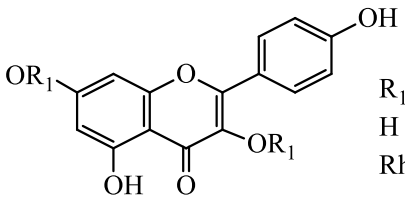

R_1	R_2	
H	H	Kaempferol
Rh-Glu	H	Kaempferol-3-O-(2,6-di-O-rhamnosyl-glucoside)
Rh-Glu (rhamnosyl(1➔6)-glucoside)	H	Kaempferol-3-O-rutinoside

Figure 15: Structures of quercetin, kaempferol, and their derivatives identified in *Zizyphus lotus* L. varieties. Abbreviations: Rh, rhamnoside; Gluc, glucoronide; Glu, Glucoside; Gla, galactoside.

Myricetin derivatives (Table 7, Fig 16) are other flavonols identified as components of *Z. lotus*. Myricetin-3-O-rutinoside was found in leaves and root barks, while myricetin-3-O-galactoside identified in leaves extract.[66]

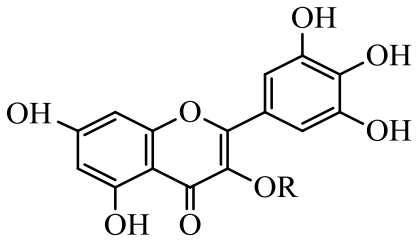

R	
Rh-Glu	Myricetin-3-O-rutinoside
Gla	Myricetin-3-O-galactoside

Figure 16: Structures of myricetin-3-O-rutinoside and myricetin-3-O-galactoside identified in *Zizyphus lotus*. Abbreviations: Rh, rhamnoside; Glu, Glucoside; Gla, galactoside.

- **Flavanones**

Flavanones are characterized by the absence of the double bond between C2 and C3 and have the precursor 2-phenyl-benzopyrone. Flavanones are non-planar flavonoids that are derived chiefly in mono- and di-glucoside forms, but are less frequently present in aglycone form.[68] The main sources of flavanones are citrus fruits and juices and have an important role in generating these fruit taste.[75] Naringenin was found in leaves and fruits, accounting for

105.59 and 5.21 mg/kg dw, respectively. Three glycosidic isomers of eriodictyol such as eriodictyol-O-hexoside, eriodictyol-O-deoxyhexoside, and eriodictyol-O-pentoside were mainly detected as components of stem braks while eriodictyol-O-deoxyhexoside found also in leaves fraction.

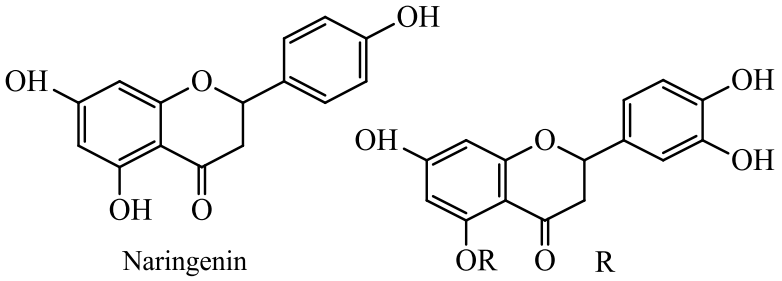

Naringenin

R	
Hx	Eriodictyol-O-hexoside
Dhx	Eriodictyol-O-deoxyhexoside
Pde	Eriodictyol-O-pentoside

Figure 17: Structure of naringenin and eriodictyol derivatives identified in *Zizyphus lotus*. Abbreviations: Hx, hexoside; Dhx, deoxyhexoside; Pde, pentoside.

- **Flavones**

Flavones are structurally very similar to flavonols and differ only in the absence of hydroxylation at the 3-position on the C-ring.[76] They are the single class of flavonoids present in almost all edible cereal species, including maize, wheat, rye, barley, oats, sorghum, and millets.[77] The main flavones in *Z. lotus* are apigenin and luteolin that have distributed with significant concentrations in leaves extract (Fig 18).[66]

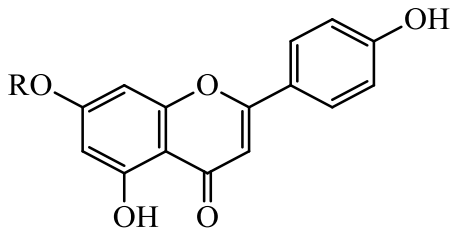

R	
H	Apigenin
Glu	Apigenin-7-O-glucoside

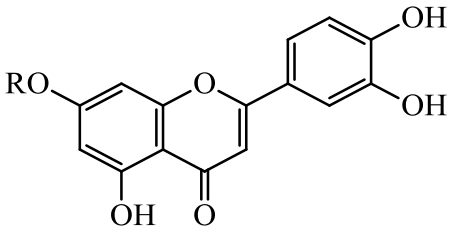

R	
H	Luteolin
Glu	Luteolin-7-O-glucoside

Figure 18: Apigenin, luteolin, and their derivatives identified in *Zizyphus lotus*.

3.7.4 Other flavonoid subclasses

Phloretin 3' 5'-di-c-glucoside and oleuropein derivative are, so far, the unique chalcone and Phenylethanoid acid identified respectively in *Z. lotus* (Table 8, Fig 17). Phloretin 3' 5'-di-c-glucoside was found in *Z. lotus* leaves, while oleuropein and oleuropein-O-hexoside were detected in branches and leaves extracts.

Table 8: Phenylethanoid acid identified in *Zizyphus lotus* morphological parts (adapted from[74])

Phenylethanoid acid	*Z. lotus*
Oleuropein-hexoside	br
Oleuropein-O-hexoside	l
Oleuropein	br, l
Oleuropein isomer1	br
Oleuropein isomer2	br

Abbreviations: l, leaves; br, branches

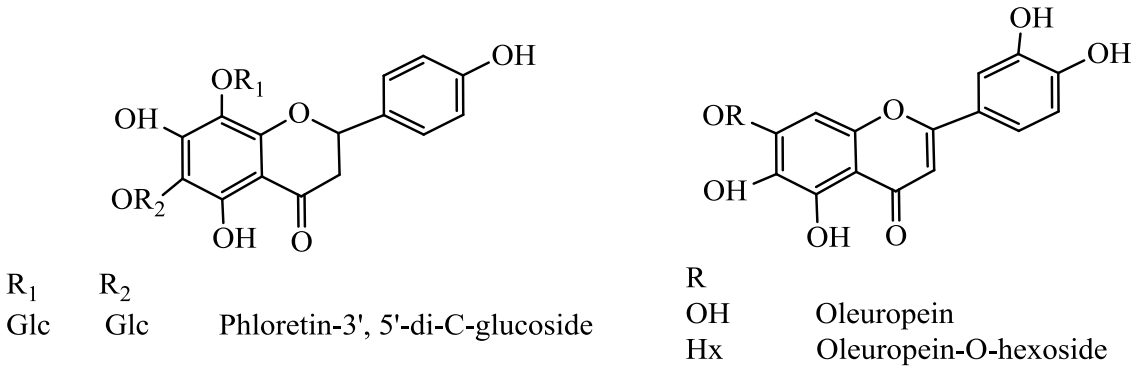

Figure 19: Structure of phloretin 3', 5'-di-C-glucoside, oleuropein derivatives identified in *Zizyphus lotus*. Abbreviations: Glu, glucoside; Hx, hexoside.

3.8 Other compounds identified in *Zizyphus lotus*

Three chlorophyll derived compounds such as 13[1]-oxophorbines, pheophorbide A, and protopheophorbide A were isolated from *Z. lotus*, along with chlorophyllide A, which is the immediate precursor of chlorophyll A.[78] These compounds contain a large heterocyclic aromatic molecule (chlorin), consisting of a core of three pyrrole rings and one reduced pyrrole ring coupled through four methine linkages. Compounds have chlorin ring are usually used as photosensitizers in photochemotherapy due to their photosensitivity.[79]

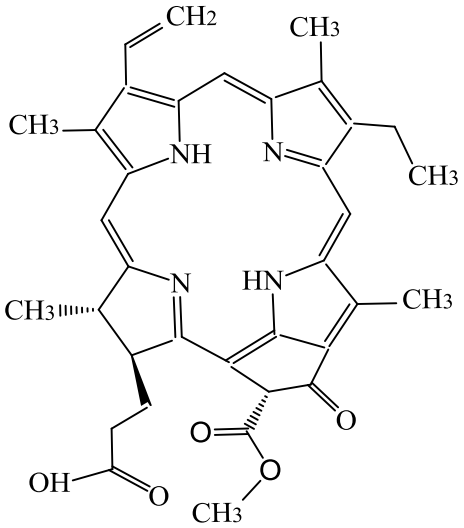

Figure 20: Structure of chlorophyllide A.

4. Extraction and chemical analysis of plants extractives

4.1 Extraction methods

Extraction is the first step in the purification and fractionation of the bioactive constituents from the raw materials.[80] According to the extraction principle several techniques were placed such as solvent extraction, distillation method, pressing, and sublimation. Solvent extraction is the most widely used method that can progress through the penetration of the solvent into the solid matrix followed by the removal of target compounds from the adsorbed sites. The partition coefficient, the particle size of the raw materials, the extraction temperature, and the extraction duration controlled the extraction efficiency.[81]

Various solvent systems are available to extract bioactive compounds from natural products.[82] The selection of the solvent is crucial for solvent extraction that largely depends on the specific nature of the bioactive compound being targeted which is polar or non-polar.[81] The most common solvent extraction methods are those using methanol/water with acid or not to extract phenolic compounds while; dichloromethane was shown as an efficient solvent to extract the lipophilic fraction such as fatty acids, sterol, and triterpenic acids.[83,84]

The methods of extraction must be also considered for their importance in the quality and quantity of biologically active compounds from plant materials. The extraction of plant biomass can be done by various extraction procedures.[85] Conventional extraction methods, such as Soxhlet and maceration extraction are still considered as one of the well-established practice techniques, which gives a better performance, as well as Soxhlet extraction, which is considered as a reference for estimating the action of the newly developed methodology.[86]

4.1.1 Soxhlet

Soxhlet extractor was first proposed by German chemist Franz Ritter Von Soxhlet (1879)[85] to extract the lipid fraction. Thereafter, the Soxhlet extraction remains one of the most relevant techniques in the environmental extraction field and has widely been used for extracting valuable bioactive compounds from various natural sources.[87]

In the conventional Soxhlet system, as shown in Figure 21, plant substance is placed in a porous bag or a thimble. This latter is then placed in the extractor of the Soxhlet apparatus.

The solvent in the distillation flask is heated, and its vapors condensed into the thimble containing the crude simple, and extract it by contact. When the liquid reaches an overflow level, a siphon aspirates the whole contents of the thimble-holder and unloads it back into the distillation flask, carrying the extracted analytes in the bulk liquid. This operation is repeated until the complete extraction is achieved.[88]

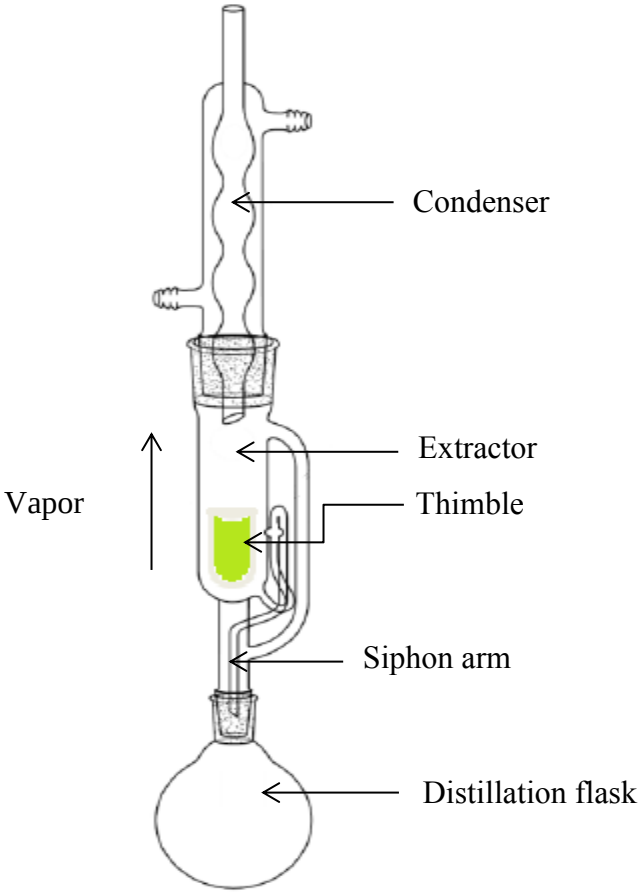

Figure 21: Schematic diagram of Soxhlet extractor.

Soxhlet extraction is a cheap and very simple technique allowed to use a large amount of simple that can be extracted with a much smaller quantity of solvent and even it allows to evaporate and collected the solvent, further improving efficiency.[86] However, the long extraction time in the solvent boiling point makes this technique not suitable for extracting thermolabile compounds such as phenolic compounds.[81]

4.1.2 Maceration

Solid-liquid extraction is another conventional technique aiming at the selective removal of soluble components from a solid matrix in a solvent phase. This technique is prevented to making wine but widely it has been adopted in the extraction of bioactive compounds from the plant.[89]

In this process, the whole or coarsely powdered crude plant is placed in a stoppered container with the solvent and allowed to stand at room temperature for at least 3 days with frequent agitation until the soluble matter has dissolved. The process intended to soften and break the plant's cell wall to release the soluble phytochemicals. The mixture then is strained,

the damp solid material is pressed, and the combined liquids are clarified by filtration or decantation after standing. This method is time-consuming but still the best suited to extract thermolabile drugs such as phenolic compounds.[90]

4.2 Identification and characterization of plants extractives

The extracted obtained from plants are relatively occur as a combination of various types of bioactive compounds or phytochemicals with different polarities.[80] The analysis of the plant extractives can be made at three different levels (i) determination of total extractives, (ii) determination of different component groups, and (iii) analysis of individual components.[91]

Determination of the total extractives could be sufficient for regular process and quality control, while the quantitative determination of the main plant components such as determination of the total phenolic compounds, or anthocyanins, using spectrophotometric analysis (UV-Vis) considered as the first survey of chemical information that is sufficient in some studies.[92] However, UV-Vis analysis gives relative and no-absolute results as a consequence of interference of many compounds that absorbed at the same wavelengths or interact with each other such as protein-phenols interaction which influence the quantitative view of phenolic compounds.[93]

Therefore, for more detailed chemical process studies as well as for research purposes, information on individual compounds is frequently required. The qualitative and quantitative determination of components groups in extracts can be performed by a number of chromatographic techniques such as gas chromatography (GC and GC-MS), also preferred for determination of individual components, high-performance liquid chromatography (HPLC), gel permeation chromatography (GPC), thin-layer chromatography (TLC) and supercritical fluid chromatography (SFC). In addition, qualitative analysis of extracts can also be achieved by nuclear magnetic resonance (NMR) and by Fourier transform infrared spectroscopy (FTIR).[94]

4.2.1 Chromatographic techniques

The applications of chromatography start with the separation of plant pigments into colored bands using noninstrumental techniques, such as column and paper chromatography. Therefore, these techniques are still used; however, to achieve a satisfactory separation with quantitative analysis within a suitable time interval, various chromatography instrumental techniques have been developed: Gas chromatography (GC) and High-Performance Liquid Chromatography (HPLC).[95]

Chromatography is a method of separation in which the components are separated based on their differential interactions with two phases such as a mobile phase (e.g. liquid or inert gas) and a stationary phase (liquid or solid), according to their size, shape, and charge.[96] Regardless of the type of chromatography, samples components are dissolved in the mobile phase, which travels through the stationary phase once has been applied or injected. The components that have the strongest interactions with the stationary phase will be more highly retained by this phase and move through the system more slowly than components that have weaker interactions with the stationary phase and spend more time in the mobile phase.[97,98]

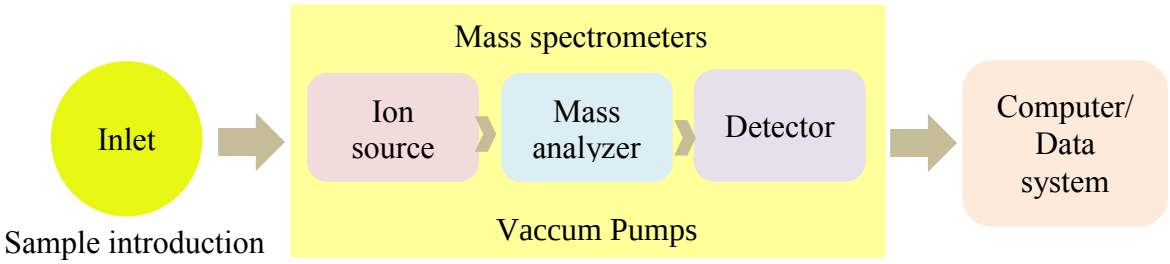

Figure 22: Basic chromatography apparatus coupled to mass spectrometers.

The separated compounds transferred to mass spectrometers apparatus, which was divided into three compartments placed in series allowed successively, after the introduction of the sample, the ionization, and accelerated the eluted compound to gas-phase ionic. This molecular ion undergoes fragmentation by the excess energy transferred during ionization. This process takes place on (i) ion source. Thereafter, the ions sent to the (ii) mass analyzer were separated by their mass-to-charge ratio value and are measured by converting the ions into electrical signals in the (iii) detector (Fig 22).[99]

The sample introduction system is necessary to admit the samples to be studied to the ion source whereas maintaining the high vacuum requirements (~10^{-6} to 10^{-8} mm of mercury) of the technique. Moreover, the computer is required to control the instrument, to manipulate data, and also to compare the fragment ions with different relative abundances to the reference libraries.[100]

5. Phytotherapy

Phytotherapy refers to the use of plant extracts or their natural active ingredients as therapeutic agents for supporting the vital body and preventing or treating health problems.[101] It is one of the oldest forms of treatment that still plays an important role in African countries (e.g. Morocco), especially in rural areas where people have hardly access to allopathic health care.[102] In fact, the World Health Organisation (WHO) reported that 80% of the worldwide population still depends solely on herbal or traditional medicines for their primary health care due to the limited availability or affordability of pharmaceutical medicines.[103]

The plant kingdom includes a high number of species, producing a diversity of bioactive compounds with different chemical scaffolds. However, despite their extensive studies, only 6% of the plants have been studied for their biological activity and about 15% have been investigated phytochemically.[32,104] Although, natural products, and particularly medicinal plants have received considerable attention of pharmaceutical industry as an alternative in the search for new chemical entities (NCEs) among the secondary metabolites.[32] For instance, about a third of the Food and Drug Administration (FDA)-approved drugs over the past 20 years are based on natural products or their derivatives.[105] Moreover, since the 1940s, most molecules involved in cancer treatment have been of natural source, with nearly half being either natural products (NPs) or natural product derivatives (NPD).[104]

Drug discovery from medicinal plants follows a logical pathway; further that process is very complicated, expensive, and time-consuming. It has been estimated to take an average from a few years to as many as 20 years upwards and that only one in 5000 lead compounds will successfully advance through clinical trials and be approved for use.[106,107] For instance

the structure of paclitaxel (Taxol®) extracted from *Taxus brevifolia* illustrated in 1971 and its approved marketing as a cancer chemotherapeutic agent was at the end of 1992 mean after 20 years.[107] On average, new pharmaceuticals require a decade for development and commercialization.

Several scientific papers were reported that different morphological parts of *Z. lotus* exhibited several biological activities such as antimicrobial, antioxidant, antispasmodic, anti-inflammatory, as well as cytotoxic properties on humans T-cell activation, analgesic, immunosuppressive and hypoglycemic properties which emphasize their traditional use.[19,36, 48,63,108,109] This makes *Z. lotus* a richly natural material to isolate NCEs.

6. Biological activity of *Zizyphus lotus* extracts

Therapeutic benefits of *Z. lotus* extracts have been emphasized by several experimental models (cell and animal) through in vivo and in vitro studies.

Aqueous and methanolic extracts of Tunisian *Z. lotus* root barks showed significant anti-inflammatory effects on the carrageenan-induced paw edema.[36] Besides, the flavonoid and saponin fractions from the leaf and root barks for the same species exhibited moderate anti-inflammatory potential on carrageenan-induced paw edema in rats by inhibiting a nitrite (NO) production in lipopolysaccharide (LPS) activated RAW 264.7 macrophages. Moreover, saponins root barks and methanol *Z. lotus* extracts were found to prevent the delayed hypersensitivity-induced by oxazolone.[108] The hydro-alcoholic aerial parts of *Z. lotus* extract from Algeria also could inhibit lipoxygenase.[110] Moreover, aqueous extracts of leaves and branches from Algeria showed an effect on the pro-inflammatory mediators NO in activated RAW 264.7 cells.[48] These data highlight the ability of phenolic compounds to exert anti-inflammatory activity through the inhibition of NO and other markers of inflammation.

Ghalem et al. (2018)[111] found that *Z. lotus* fruit pulp reduced the mRNA expression of Monocyte chemoattractant protein-1 (MCP-1), pro-inflammatory cytokines (IL-6, TNF-α), and increased the level of IL-10, an anti-inflammatory cytokine, in LPS-stimulated RAW 264.7 cells. Moreover, they reported the decrease in NO synthesis and the expression of iNOS in RAW 264.7 cells.[111]

Besides, the aqueous extract of root barks, as well as flavonoid and saponin from the leaf and root barks of Tunisian *Z. lotus*, exhibited an analgesic agent by inhibited the writhing response in mice inducing by acetic acid.[36, 108] *Zizyphus lotus* leaf methanolic extract shows a significant relaxation of spontaneous contractions in Wistar rat and produced a concentration-dependent inhibition compared to those obtained by positive control (atropine and papaverine). The isolated rat duodenum indicate that *Z. lotus* extracts exert anti-spasmodic activities by modulating Ca^{2+} signaling via cholinergic receptors.[112]

Benammar et al. (2014)[113] noted that *Z. lotus* aqueous leaf and root extracts exhibited hypoglycemic activity in streptozotocin-diabetic rats along with an increase in the rate of hemolysis and glutathione reductase, a decrease in catalase and glutathione peroxidase activity and an improvement in the status of antioxidant. According to this study, the current effects can be correlated by the presence of Vitamin A known to improve hyperglycemia and glucose-intolerance, through the regulation of intracellular signaling and glycogen synthesis pathways of muscle and liver.[113,114] Therefore, aqueous leave and fruit extracts showed to have antidiabetic activity by inhibiting the effects of α-amylase, and α-glucosidase which are

compared to the standard drug. These extracts inhibit the tyrosinase effect which reveals the dermatoprotective property of *Z. lotus*.[63] Berrichi et al. (2019)[115] noted that *Z. lotus* fruits play a protective role against insulin resistance, hyperglycemia, dyslipidemia and fatty liver disease observed during obesity but not the severity of high-fat-diet (HFD)-induced obesity in mice.

Several studies highlight the ability of different morphological parts of *Z. lotus* to exert an anti-ulcer activity on the Wistar rat. The aqueous root barks, leaves, and fruits extracts as well as fruits methanol extracts of *Z. lotus* showed a significant reduction in gastric juice secretion, total acidity, and an increase in pH value in pylorus ligated rats. These effects were compared with cimetidine and omeprazole.[19,116]

As shown above, *Z. lotus* is a wealth shrub species in many antioxidant compounds such as phenolic acids, flavonoids, alkaloids, and saponins. These components have been shown to prevent several diseases by reducing reactive oxygen species (ROS).[109]

6.1 Antioxidant activity

Most living beings need oxygen to ensure their existence, while oxygen can produce free radicals, which are also called ROS such as hydrogen peroxide (H_2O_2), superoxide radical anion ($O2^{\bullet-}$), and hydroxyl radical ($OH^{\bullet}$), among others.[117] These ROS are toxic to the integrity of the cell. However, the body has internal defense mechanisms such as antioxidants (tocopherols, ascorbic acid, and glutathione) or enzymes (catalase, peroxidase, and superoxide dismutase) to prevent damage to cell components such as DNA, lipids, and proteins.[118] Therefore, when the concentration of ROS is not controlled by the internal defense, this leads to oxidative stress associated with the pathophysiology of several diseases and health conditions, including inflammation, atherosclerosis, and aging, among others.[119]

To compensate this imbalance between the ROS and their degradation by antioxidant systems, the body use exogenous antioxidants supplied through food, nutritional supplements, or pharmaceuticals. The most important exogenous antioxidants are antioxidant vitamins (A, C, and E), carotenoids, coenzyme-Q, lycopene, and phenolic compounds (phenolic acids, flavonoids, flavonols, anthocyanins, tannins, and lignins).[120]

The antioxidant can be classified as either "primary antioxidants" or "secondary antioxidants" based on their mechanism of action. Primary antioxidants can react directly with free radicals and convert them to more stable, non-radical products although secondary antioxidants inhibit oxidation by different mechanisms such as chelation of transition metals, oxygen scavenging, and quenching of singlet oxygen. Some secondary antioxidants can regenerate primary antioxidants synergistically.[121]

Zizyphus lotus contains a wide range of bioactive substances that all exhibit multiple antioxidant properties, especially phenolic compounds, which have shown to exhibit excellent antioxidant skills.[38,110,122]

Phenolic compounds, as primary antioxidants, act according to two mechanisms: hydrogen-atom transfer (HAT) or single-electron transfer (SET). The HAT mechanism occurs through one or more hydroxyl groups of phenolic compounds, which are effective in breaking antioxidants by donating H-atoms to the free radicals.

$$RO_2^{\bullet} + AOH \rightarrow ROOH + AO^{\bullet} \qquad (1)$$

The phenoxyl radical ($AO^{\bullet}$) formed is relatively unreactive due to resonance delocalization throughout the phenolic ring structure. The SET mechanism occurs in cases where PCs transfers a single electron to aid in the reduction of potential target compounds:

$$RO_2^{\bullet} + AOH \rightarrow RO_2^{-} + [AOH]^{\bullet +} \quad (2)$$

The resultant radical-cationic PCs is then deprotonated by interacting with water:

$$[AOH]^{\bullet +} + H_2O \leftrightarrow AO^{\bullet} + H_3O^{+} \quad (3)$$

$$RO_2\text{-} + H_3O^{+} \leftrightarrow RCOOH + H_2O \quad (4)$$

The HAT and SET chemical processes can occur simultaneously as a sequential proton-loss electron transfer (SPLET), which is also termed as a proton-coupled electron transfer (PCET). The reaction schemes below illustrate a SPLET mechanism:

$$AOH \rightarrow AO^{-} + H^{+} \quad (5)$$

$$AO^{-} + ROO^{\bullet} \rightarrow AO^{\bullet} + ROO^{-} \quad (6)$$

$$ROO^{-} + H^{+} \leftrightarrow ROOH \quad (7)$$

Transition metals such as copper and iron are known to aggravate oxidative stress. These ionic metals can promote the production of hydroxyl radicals by the Fenton reaction:

$$Fe^{2+} (Cu^{+}) + H_2O_2 \rightarrow Fe^{3+} (\text{or } Cu^{2+}) + {}^{\bullet}OH + OH^{-} \quad (8)$$

Phenolic compounds can operate as “secondary” antioxidants in a chelation process by inhibiting oxidation without directly interacting with oxidative species. A high chelation activity is often characteristic of phenolic compounds that have a 5-OH and/or 3-OH moiety with a 4-oxo group in the A/C ring structure.[123]

Several in vitro methods have been utilized to investigate the antioxidant activity of *Z. lotus* extracts, based on the HAT and SET assays, as well as on the ROS scavenging effect.

6.1.1 2,2'-Azino-bis (3-ethylbenzothiazoline-6-sulfonic acid (ABTS) radical scavenging assay

The Trolox equivalent antioxidant capacity (TEAC) assay was developed by Miller et al. (1993)[124] for the measurement of the antioxidant capacity of human plasma-based on the scavenging of the free-radical cation ($ABTS^{\bullet+}$) by antioxidants. This method was modified by Re et al. (1999)[125] for the direct generation of $ABTS^{\bullet+}$ without radical intermediates. The ABTS assay measures the ability of antioxidants to scavenge the stable radical cation $ABTS^{\bullet+}$ produced by the oxidation of 2,2′-azinobis(3-ethylbenzothiazoline-6-sulphonic acid (ABTS). The antioxidants can neutralize the radical cation $ABTS^{\bullet+}$ by both direct reductions via SET assay or by HAT assay, and the balance of these two mechanisms is generally determined by antioxidant structure and pH of the medium.[126]

$$ABTS^{\bullet +} (\text{green at 734 nm}) + AOH \rightarrow ABTS (\text{colorless}) + [AOH]^{\bullet +} \quad (9)\ (\text{SET})$$

$$ABTS^{\bullet +} (\text{green at 734 nm}) + AOH \rightarrow ABTS (H) (\text{colorless}) + AO^{\bullet} \quad (10)\ (\text{HAT})$$

The extent of discoloration of the blue-green color, quantified as a decrease in absorbance at 734 nm, depends on the duration of reaction, the intrinsic antioxidant activity and concentration in the sample.[126]

Boulanouar et al. (2013) investigated the scavenging ABTS activity of the hydro-alcoholic aerial part of *Z. lotus*. The results revealed that the extract exhibited a strong ABTS with a value of 49 µg/mL.[110] Therefore, four aerial part fractions (Hexane, ethyl acetate, methanol, and water) of *Z. lotus* were found to have a strong scavenging ABTS activity with hexane being the most potent fraction compared with positive control.[35] Ghazghazi et al. (2014)[122] assessed the ABTS-scavenging activity of methanol leaf and fruit extracts.[122] They indicated that leaf extract (IC50 =50 µg/mL) has strong antioxidant activity with significant correlations with the total phenolic compounds. Indeed Marmouzi et al. (2019)[63] found that *Z. lotus* aqueous leaves extract exhibited the best scavenging ABTS activity compared with aqueous fruit extract.[63]

6.1.2 2,2-Diphenyl-1-picrylhydrazyl (DPPH) radical scavenging assay

DPPH radical scavenging assay is among the most frequently used methods and offers the first approach for evaluating antioxidant activity. This assay was based on the principle of reduction of DPPH free radical by accepting an electron or a hydrogen atom from the scavenger compound; hence, the color was seen changing from violet to yellow. The absorption intensity was measured at 517 nm, and the discoloration acts as an indicator of the antioxidant efficacy.[127]

The DPPH scavenging assay is based HAT or SET or mixed mechanisms to neutralize DPPH radical according to the following reaction schemes:

$$DPPH^{\bullet} + AOH \rightarrow H{-}DPPH + AO^{\bullet} \quad (HAT) \quad (11)$$

$$DPPH^{\bullet} + AOH \rightarrow DPPH^{-} + AO^{\bullet +} \quad (SET) \quad (12)$$

Even though the DPPH assay is easy to perform and commercial availability compared to other methods. One major limitation of this technic is the overlapped spectra of compounds that absorb in the same wavelength range as DPPH such as anthocyanins (500–550 nm) which may introduce interference with the results and their interpretation.[127,128]

Aqueous, ethyl acetate, hexane, and methanolic aerial part of *Z. lotus* possessed potent antioxidant activity with aqueous extract being the most effective fraction compared with the butylated hydroxytoluene (BHT). Indeed, the *Z. lotus* aqueous extract is very rich in phenolic compounds (340 mg/100g extracts) include 37 mg/100g of flavonoids and 25 mg/100g of flavonols.[35] Other study indicated that the *Z. lotus* hydro-alcoholic aerial part exhibited a strong DPPH and was found to be negatively correlated with the total phenolic compounds and positively with flavanone and dihydroflavonol content.[110] Moreover, hydromethanolic fruit extract exerted a moderate but concentration-dependent DPPH activity compared with quercetin used as a positive control.[19]

Polysaccharide has been identified as compounds of *Z. lotus* and is thought to be involved in its antioxidant activity. Rich-polysaccharide fruit extract of this shrub species exhibited a significant effect on scavenging DPPH, especially at high concentrations. However, the result was lower than that of BHT.[37] Four roots fractions (flavonoids-containing butanol and ethyl

acetate phase, tannins, and phenolic compounds) extract of *Z. lotus* exhibited high antioxidant activity, and some even showed higher potency than the standard synthetic antioxidants. Flavonoids-containing butanol phase and tannins fractions showed a strong DPPH that is similar to the activity of butylated hydroxyanisole (BHA). Therefore, ethyl Flavonoids-containing acetate phase and phenolic compounds fractions showed a good activity compared to ascorbic acid.[38]

Mkadmini et al. (2015)[129] described the DPPH scavenging effect of hydroethanolic fruits extract of *Z. lotus* under optimized condition (concentration of solvent; extraction time, extraction temperature, and the ratio of solvent to solid). The results showed that the DPPH scavenging effect of *Z. lotus* was dependent on the both ratio of solvent to solid and extraction temperature.[129] Therefore, Ghazghazi et al. (2014)[122] referenced that the DPPH scavenging effects of methanol leaf and fruits extract of *Z. lotus* were linearly correlated with the total phenolic and total flavonoid contents. They observed that leaves extract exhibited a strong activity when compared with fruit extract.[122]

Marmouzi et al. (2019)[63] reveal a moderate DPPH scavenging activity, especially attributed to the aqueous leaf extract. Moreover, methanolic stem extract of *Z. lotus* found to have strong antioxidant activity correlated with the presence of high content of phenolic compounds.[130]

6.1.3 Ferric reducing antioxidant power (FRAP) assay

The FRAP assay was developed by Benzie and Strain (1996)[131] to measure the ferric reducing power of human plasma. Pulido et al. (2000)[132] adapted this method to quantify the ferric reducing antioxidant power of plant extracts. In FRAP, the assay is based on the ability to reduce yellow ferric tripyridyltriazine complex Fe^{3+} to blue ferrous complex Fe^{2+} by SET antioxidants in an acidic medium (pH = 3.6) to maintain iron solubility and more importantly drive electron transfer (Equation 13). This assay is determined as an increase of absorbance at 593 nm, and results are expressed as micromolar Fe^{2+} equivalents or relative to an antioxidant standard.[126]

$$Fe^{3+} + AOH \rightarrow Fe^{2+} \text{ (blue at 595 nm)} + [AOH]^{+\bullet} \quad (13)\ (SET)$$

FRAP assay is simple, rapid (generally 4–6min), inexpensive, and can be performed using semiautomatic or automated protocols. This method may predict the free radical scavenging action of phenolic compounds, however, cannot detect the compounds that act by radical quenching (hydrogen transfer), particularly thiols (as glutathione) and proteins. Using this method, Ghalem et al. (2014)[38] indicated that four *Z. lotus* root fractions have significantly reducing antioxidant power FRAP along with a strong positive correlation with the total of phenolic compounds. Moreover, leaf extract showed the highest scavenging assay capacities, compared with fruit extract conducted by Marmouzi et al. (2019).[63] Rich-polysaccharides fruits (pulp and peel) extract of *Z. lotus* revealed ferric reducing capacity but least compared to the positive control BHT.[24] Therefore, the ferric-reducing antioxidant powers of *Z. lotus* pulp extracts, expressed as ascorbic acid equivalents showed that phenolic compounds phase had the highest antioxidant capacity compared with the tannins, flavonoids-containing butanol phase, and the ethyl acetate phase containing flavonoids.[111]

Boulanouar et al. (2013)[110] reported the scavenging effect of hydro-alcoholic aerial parts of *Z. lotus* extracts upon several radical products, such as scavenging lipoxygenase, peroxyl, superoxide anion radicals. The result showed a correlation between inhibiting lipoxygenase and diverse classes of compounds such as hydroxycinnamic acid derivatives, flavonols, and flavones. The inhibition of lipoxygenase substantiates the use of *Z. lotus* not as an antioxidant but as well as an anti-inflammatory agent as shown above. Therefore, the scavenging peroxyl radicals of the same species are positively correlated with phenol, hydroxycinnamic acid derivative contents. Moreover, the capacity for scavenging superoxide anion radicals by *Z. lotus* was strong but significantly less active than the standard ascorbic acid.[110] Adeli et al. (2014)[37] stated the strong hydroxyl radical-scavenging activity of fruit rich-polysaccharide extract of *Z. lotus* compared to ascorbic acid.[37]

The aerial parts of *Z. lotus* extract were found to exhibit a good capacity for chelating metal ions.[110] In the same vein, *Z. lotus* seed oil display ferrous ion chelating abilities compared with that of Trolox as a positive control. This ability may be attributed to the total phenolic compounds and flavonoids.[133] The propriety of *Z. lotus* to chelating metal ions is very important it will reduce the concentration of the catalyzing transition metals in lipid peroxidation. On the other hand, the rich-polysaccharide fruit extract exhibit a moderate anti-lipid peroxidation activity.[24]

Boulanouar et al. (2013)[110] have tested the ability to scavenge the byproduct ions of lipid peroxidation. Thiobarbituric acid reactive substances and liposomes assay were performed. The results indicated that *Z. lotus* extract has no scavenging effect against these product ions.[110]

Benammar et al. (2010)[9] have studied in vitro the sensitivity of aqueous root, leaf, stem, fruit pulp, and seeds extracts of *Z. lotus* to free radical aggression, upon the capacity of red blood cell (RBC) to withstand free radical-induced hemolysis. They report that different extracts of *Z. lotus* exerted the antioxidant activity with fruit pulp being the most potent fraction. The antioxidant power of these extracts might be due to the presence of different vitamins.[9]

Ghalem et al. (2014)[38] assessed the capacity of four root fractions (phenolic compounds, ethyl acetate, butanol flavonoid, and tannins) of *Z. lotus* to minimize the oxidation of β-carotene by hydroperoxides. The β-carotene bleaching method was current out. *Z. lotus* fractions show to neutralized hydroperoxides radical with phenolic compounds being the most powerful fraction when compared with BHA.[38] The total antioxidant capacity assay of *Z. lotus* has also been determined in this study. This assay is based on the reduction of phosphomolybdenum Mo(VI) by *Z. lotus* root and the formation of a green phosphate/Mo(V) complex at acid pH. The phosphomolybdenum method is quantitative since the antioxidant activity is expressed as the number of equivalents of ascorbic acid.[134] *Zizyphus lotus* showed to have significant TAC with tannins roots fraction being the most potent fraction.[38] Although, Ghalem et al. (2018)[111] found that pulp rich-extract had a higher TAC than the tannin extract and flavonoids-containing butanol phase.[111]

6.2 Antimicrobial activity

6.2.1 Antibacterial activity

It has been estimated that microbial species (MS), found in almost every habitat present in nature, comprise about 60% of the Earth's biomass. This, together with their extraordinary genetic, metabolic, and physiological diversity, makes them a major threat to the health and development of populations across the world.[31] Microbial species were first observed in 1683 by the inventor of the microscope, Antoine van Leeuwenhoek, have a size generally between 1 and 10 µm with three typical shapes (Fig 23): spheroidal (cocci), rod (bacillus), or wound in a helix (spirilla), but they all have the same general layout.[135]

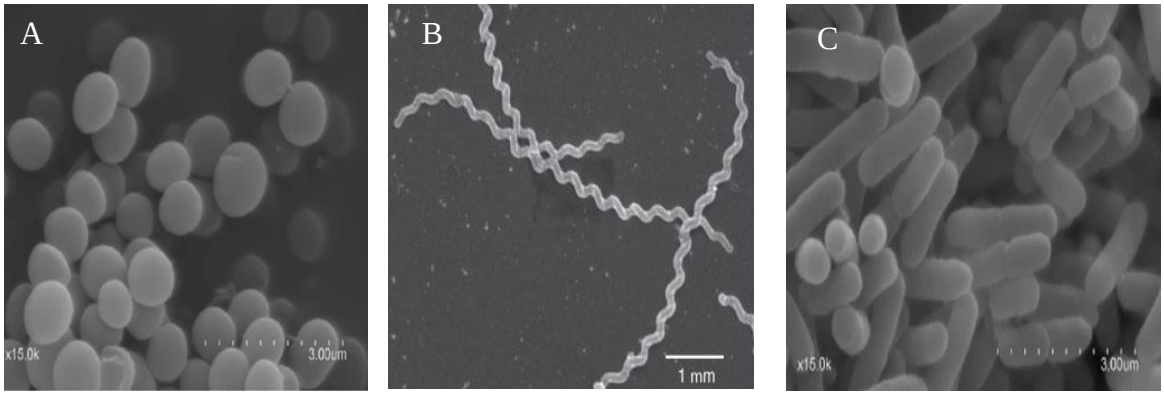

Figure 23: Scanning electron microscopy of morphology of *Escherichia coli* ATCC 25922 (B), *Staphylococcus aureus* ATCC29213 (A), and *Leptospira interrogans* (C) (adapted from [136,137]).

The mainly synthetic and currently available antimicrobials are almost inefficient and most of these agents elicit terrible effects on recipients.[138] Apart from this, there are other concerns like serious irreversible side effects associated with them. Therefore, there is a definite need to develop alternative antimicrobial drugs for the treatment of prevailing infectious diseases.[139] Many initiatives and programs have been set up by many countries/organizations to develop new, effective, and safe antimicrobials.[140] For instance, the 10x'20 initiative proposed in 2010 is aimed at developing 10 new, safe, and effective antibiotics by 2020.[141] Thus, researchers/scientists are now looking at every ecological source including soil, plant, animal, and marine for potentially new and safe antimicrobial agent.[138]

Since the advent of antibiotics in the 1950s, the use of plant derivatives as antimicrobials has been virtually nonexistent.[142] Although, herbal medicines have been used for thousands of years to treat infectious diseases in various parts of the world.[143] For instance several parts of *Z. lotus* have been reported to exhibit promising antimicrobial activity.[19,35,48,66,122,144,145]

Tlili et al. (2019)[66] investigated the antibacterial effect of *Z. lotus* leaf acetonic extract by determining the Minimum Inhibitory Concentration (MIC) and the Minimum Bactericidal Concentration (MBC) values. *Zizyphus lotus* revealed significant MIC (from 250 to 1000 µg/mL) and MBC values (from 500 to 2000 µg/mL) among the six Tunisian spontaneous species studied; it is probably due to their highest amount of phenolic compounds (1087.8 µg/g). Although, *Z. lotus* not active toward Gram-negative bacteria such as *Pseudomonas aeruginosa* (*P. aeruginosa*) and *Escherichia coli* (*E. coli*).[66]

Naili et al. (2010)[144] inspected the antibacterial of leaf methanolic extract of *Z. lotus* from Libya by defining the MIC values and diameter of inhibition zone of five strains namely; *Bacillus subtilis* (*B. subtilis*), *P. aeruginosa*, *E. coli*, *S. aureus*, and *Salmonella typhi*. Among these bacteria, *S. aureus* and *Bacillus subtilis* are more susceptible to the *Z. lotus* methanolic extract with the MIC value of 25 and 12.5 µg/mL, respectively. Moreover, it was shown that methanolic extract was active against negative-bacteria such as *E. coli* and *P. aeruginosa* (1000 µg/mL, MIC value). Nevertheless, the antibacterial effects of the methanolic extract were less active than tetracycline and ceftazidime, except in the case of *Bacillus subtilis* (29 mm diameter of inhibition zone).[144]

Bouaziz et al. (2009)[35] examined the antibacterial activity of wild *Z. lotus* aerial hexane, ethyl acetate, methanol, and water extracts by determining the diameter of the inhibition zone of *S. aureus*, *E. coli*, *Salmonella enterica* (*S. enterica*), *B. subtilis*, and *P. aeruginosa*. The aqueous extract was the only active fraction against *S. enterica* and *E. coli* (10 mm diameter of inhibition zone), along with methanolic extract which prevents the growth of *B. subtilis* with the inhibitory zone of 11 mm diameter.[35]

Ghazghazi et al. (2014)[122] assessed the antibacterial effect of *Z. lotus* leaf and fruit methanolic extracts against seven strains namely; *Listeria monocytogenes*, *Bacillus cereus* (*B. cereus*), *Salmonella typhimurium* (*S. typhimurium*), *Aeromonas hydrophila*, *E. coli*, *P. aeruginosa*, and *S. aureus*. The maximum inhibition zone diameters, MIC values for tested bacteria were evaluated. All the studied strains are sensitive to the leaf and fruit extracts. Moreover, methanolic leaf extract was a more active fraction, especially against *E. coli* and *P. aeruginosa*. Though, the inhibitory action of *Z. lotus* was weaker compared to Gentamicin.[122]

Rsaissi et al. (2013)[145] studied the antibacterial effect of fruit ether, dichloromethane, and methanolic derived from *Z. lotus*. All extracts showed antibacterial activity against different studied strains species with etheric and methanolic were the most active fractions by inducing significant growth inhibition on *Bacillus subtilis*, *B. cereus*, *S. aureus*, *Klebsiella pneumoniae*, *S. typhimurium*, *E. coli*, *Enterococcus faecalis*, and *P. aeruginosa*. Although, the inhibitory actions of *Z. lotus* were less potent compared to Amoxicillin.[145]

Helicobacter pylori (*H. pylori*) know to play a role in different digestive diseases including, chronic gastritis, peptic ulcer, and gastric cancer. Bakhtaoui et al. (2014)[19] investigated the anti-*H. pylori* activity of *Z. lotus* fruit methanolic extract. This latter showed to inhibit the growth of the three *H. pylori* clinical strains among which two were resistant to metronidazole and clarythromycine.[19]

The aqueous and hydroethanolic extracts of the different parts of *Z. lotus* were assessed by Rached et al. (2019)[48] for their antibacterial action against Gram-positive and Gram-negative multi-resistant bacterial strains. Meticillin-Sensitive *Staphylococcus aureus* (MSSA) was highly susceptible to the decoction and hydroethanolic extracts of the branches (MIC = 0.3125 mg/mL), while methicillin-resistant *Staphylococcus aureus* (MRSA) showed higher sensitivity to the leaves infusion (MIC = 0.625 mg/mL). The hydroethanolic of branches, the leaf of infusion, and the barks of decoctions showed significant action on *P. aeruginosa*, which was the most sensitive Gram-negative bacteria. Ait Abderrahim et al. (2019)[130] reported an antibacterial activity of a methanolic stem extract obtained from *Z. lotus* against *S. aureus* (MIC = 7 mg/mL), *E. coli* (MIC = 6 mg/mL), and *P. aeruginosa* (MIC = 6 mg/mL).[130]

6.2.2 Antifungal and anticandidal activities

Antifungal and anticandidal activities have also been investigated with different extractives of *Z. lotus*. Rsaissi et al. (2013)[145] assessed the antifungal effect of *Z. lotus* fruits under etheric, methanolic, and dichloromethane solvents against the growth of four fungi, namely *Fusarium culmorum* (*F. culmorum*), *Aspegillus ochraceus*, *Penicillium italicum* (*P. italicum*), and *Rhizomucor sp*. Methanolic fraction, containing the highest total phenolic content, is evidenced to be the most active in preventing the growth of those fungi. Therefore, the etheric extract was active in preventing the growth of *F. culmorum*, *P. italicum*, and *Rhizopus sp*, while dichlormethanolic extract was active against these species but with less degree. However, these extracts were less potent than difenocazole, except methanolic extract showed a strong antifungal effect against *F. culmorum*.[145]

Ghazghazi et al. (2014)[122] investigated the antifungal effect of *Z. lotus* methanolic extract by the maximum inhibition zone diameters, MIC and MBC values. Leaf was the most active fraction in preventing the tested fungi (*Aspergillus flavus* and *Aspergillus niger*), with MIC values of 3.1 mg/mL and MBC values of 6.2 mg/mL. Moreover, the strains tested were sensitive to the *Z. lotus* methanolic extract were in the range of 15–17mm diameter, and even more active compared to amphotericin. Therefore, it was shown that methanol fruits extract exhibited significant activity against *Aspergillus niger* (6.2 mg/mL of MICs and minimum bactericidal concentrations MBCs).[122]

Bouaziz et al. (2009)[35] studied also the antimicrobial activity of wild *Z. lotus* aerial hexane, ethyl acetate, methanol, and water extracts by determining the maximum inhibition zone diameters. The tested extracts were not active toward *candida albicans* and *aspergillus niger* except methanol extract with an inhibitory zone of 11 mm diameter. Although, Ait Abderrahim et al. (2019)[130] confirmed that *Z. lotus* methanolic stem extract does not effect on *candida albicans* species.

6.3 Anticancer activity

The development of cancer consists of the transformation of a normal cell into a malignant cell. Carcinogenesis is the process whereby cancer starts, which occurs in several stages and reflects the different genetic alterations suffered by the cell.[146] This process can be compared to Darwinian evolution, in which each genetic modification would confer an advantage on the mutated protein, thus causing the transformation of a healthy cell into a cancer cell. In reality, this mechanism is very complex, which gives each cancer its own particularities. Hanahan and Weinberg (2011)[147] suggest as shown in Figure 24 that cancer is a manifestation of ten physiological alterations that together characterize cancer cells. These include the ability of cancer cells to induce angiogenesis, sustaining proliferative signaling, evading growth suppressors and immune destruction, enabling replicative immortality, activating invasion and metastasis, resisting cell death, deregulating cellular energetics, tumor-promoting inflammation, genome instability, and mutation.[147]

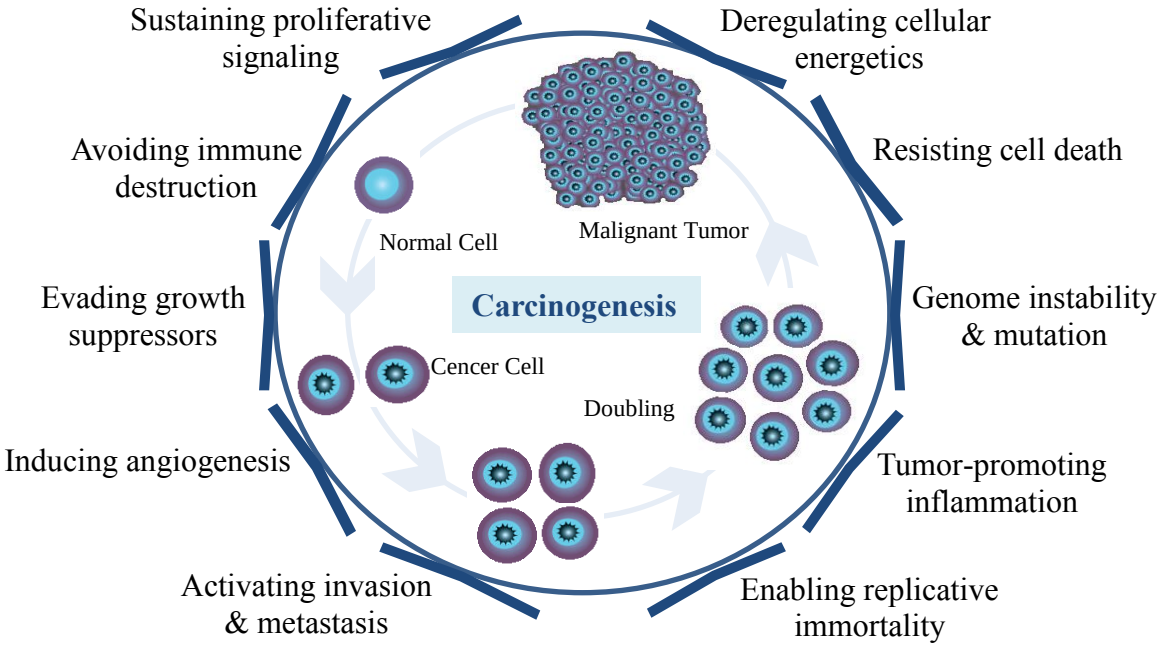

Figure 24: Summary diagram of the various events leading to the transformation of a healthy cell into a cancer cell.

- **Resisting cell death**

Apoptosis is a cellular suicide program that organisms have evolved to eliminate unnecessary or unhealthy cells from the body in the course of development or following cellular stress. Apoptosis can be initiated by intra- and extracellular mechanisms. This leads to the activation of proteases (caspase-2,-8,-9, or -10), inducing proteolysis and disassembly of the cell.[148] The apoptotic trigger' is controlled by the balance of pro- and anti-apoptotic effectors. Inhibitors of apoptosis are members of the Bcl-2 family, pro-apoptotic signaling proteins are, for example, Bak and Bax, which are released from mitochondrial membranes, and cytochrome C, which activates intracellular caspases.[149]

When there is too much DNA damage the TP53 protein activates apoptosis. Many cancers evade cellular apoptosis by inactivation of the function of this protein. Other tumor cells can increase the expression of anti-apoptotic regulators (e.g. Bcl-2), can downregulate pro-apoptotic factors (Bax, PUMA), or can increase survival signals (e.g. insulin-like growth factors).[148]

- **Avoiding immune destruction**

To survive, tumor cells acquire the capability of avoiding immune surveillance by targeting the regulatory T cell function or their secretions, modifying the production of immune-suppressive mediators, tolerance, and immune deviation as well as expressing the immune antigens (e.g. PDL1, MAC387, DAP12, and CD15) which facilitate their escape from the local anti-tumor immune response.[150,151] Studies reveal that the development of cancer-specific "Immune resistance" can be orchestrated either by cooperation with tumor microenvironment or by successive rounds of genetic/epigenetic changes.[150]

- **Inducing angiogenesis**

The blood vessels supply the cells with their needs such as oxygen and nutrients as well as to evacuating their metabolic waste products and CO_2. To survive, a cell must be located no more than 100 µm from a blood vessel.[152] Cancer can grow to roughly 10^6 cells without its own blood supply. For further growth, the tumor builds a new blood vessel (angiogenesis) growth from preexisting vasculature by altering the transcription of genes leading to a suddenly increased expression of an angiogenesis activating factors such as VEGF (Vascular Endothelial Growth Factor) or a decrease in the synthesis of negative regulators of angiogenesis such as thrombospondin-1 protein.[153]

- **Activating invasion and metastasis**

Metastasis describes the ability of cancer cells to penetrate into lymphatic and blood vessels, circulate through these systems and invade normal tissues elsewhere in the body. Approximately 90% of all cancer patients die from metastases.[154] The process is composed of several sequential events that must be completed for the tumor cell to successfully metastasize, the so-called metastatic cascade.[155,156] The metastatic cascade can be broadly separated into three main processes: (i) invasion consists of the loss of cell-cell adhesion capacities such as integrins or E-cadherins following the secretion of substances to degrade the basement membrane and extracellular matrix and also the expression/ suppression of proteins involved in the control of motility and migration. (ii) Intravasation represents the initialization of angiogenesis which without it the tumor would fail to develop. The blood vessel within the tumor's vicinity can then provide a route for the detached cells to enter the circulatory system and metastasize to distant sites.[153] (iii) Extravasation consists of a proliferation of new tumor cell after the cell arrived and develops adhesion to the endothelial cells to form stronger bonds.[155]

- **Genome instability and mutation**

Genomic instability is a characteristic of most cancer cells. It is an increased tendency of genome alteration during cell division. Cancer frequently results from damage in DNA (Deoxyribonucleic acid) which results, in a progressive accumulation of mutations that are even more aggressive when they alter the DNA repair machinery.[157]

- **Tumor-promoting inflammation**

Inflammation is a complex biological response to cellular damage caused either by sterile injury (cell death) or infection, in which the immune system attempts to eliminate or neutralize injurious stimuli and initiates healing and regenerative processes[151] Chronic inflammation can lead to the promotion of tumor cell growth and angiogenesis. During the inflammatory process, immune cells release cytokines such as growth factors, agents that allow cell migration, or even mutagenic ROS and reactive nitrogen species (RNS).[158]

- **Enabling replicative immortality**

Normal cells are only able to pass through a limited number of cycles of cell division. After repetitive cell cycles, either senescence is induced, or cells undergo apoptosis. Very few

cancer cell populations attain immortality with an unlimited number of cell cycles. A crucial factor for achieving immortality seems to be the expression of the enzyme telomerase.[159]

Telomeres are the ends of chromosomes and consist of arrays of shorter DNA sequences (TTAGGG). As DNA polymerases are unable to replicate the very ends of a double-standed DNA molecule, a reverse transcriptase (telomerase)- if expressed- adds repetitive TTAGGG sequences to the ends of the chromosomes.[160] Most normal human loss of TTAGGG repeats from the chromosomal ends (telomeres) with each cell cycle limiting the number of further possible cell divisions. The progressive loss of telomeres is thought to be a mechanism of human aging. Cancer cells that express telomerase can attain cellular immortality.[161]

- **Sustaining proliferative signaling**

In the same vein as before, there are anti-proliferation signals secreted by the surrounding cells to keep it in a quiescent state. Tumor cells show deregulated signaling cascades that enable them to be more or less independent of proliferation signals, which results in unlimited growth. To achieve this independence, tumor cells produce (i) their growth factors (autocrine stimulation), (ii) by inducing cells of the tumor stroma to produce growth factors (iii), or by becoming hyper-responsive to normal levels' growth factors.[162] Some cancer types, somatic mutations lead to the continuous activation of intracellular signaling pathways downstream from the activation of cell membrane receptors (e.g.B-Raf/MAP-kinase pathway, PI3-kinase).[159]

- **Evading growth supressors**

In normal cells, potent pathways negatively regulate cell proliferation, and some of these depend on intact tumor suppressor genes (e.g. Rb, Tp53), which are often inactivated in cancer cells. This genes products are central control nodes of two complementary regulatory cellular circuits that control whether cells go into proliferation or into senescence or apoptosis.[162,159] Rb transduces mainly growth-inhibitory signals that originate largely outside of the cell. TP53 receives input from stress and abnormality sensors within the cell.[147] If there is excessive genomic damage or disturbed metabolism, TP53 can arrest further cell cycle progression until things have normalized or it can trigger apoptosis.

Cancer cells also need to evade "contact inhibition" some known effectors of normal contact are proteins such as the Merlin protein (product of the NF2 gene), which acts on the cell surface adhesion molecules (e.g. E-cadherin), and the LKB1 protein, which may be deregulated or deficient in cancer cells.[163]

- **Deregulating cellular energetics**

Cancer cells have an increased need for energy compared to healthy cells due to their higher activity. They exhibit fundamentally altered cellular energetics, such as increased aerobic glycolysis which may contribute to tumorigenesis and malignancy.[164,165] Tumor cells increase glucose uptake and metabolism by overexpressing glucose transporters (GLUTs) and glycolysis enzyme. Besides, part of the glucose is diverted to be used for the synthesis of other biomolecules such as nucleotides and amino acids.[166]

The causes of cancer are a complex issue, but the risk factors are well-known such as exposing human cells to undesirable chemicals, drugs, foods, and agents including ultraviolet

light and radiation as well as the lack of physical activity, and environmental pollutants. It is estimated that tobacco and obesity or poor diet caused 22% and 10% of cancer deaths, respectively whereas, the remaining 5-10% are due to inherited cancer genetics.[146]

Various therapeutic approaches such as surgery, immunotherapy, chemotherapy drugs, and/or radiation are used to treat all types of cancers.[167] Plant secondary metabolism has garnered increasing attention in cancer chemotherapy due to are (i) more biologically friendly; (ii) reduced toxicity to normal cells; (iii) desired range of efficacy and (iiii) ability to influence simultaneously multiple signaling pathways.[29]

Different parts of *Z. lotus* such as branches, leaves, root barks, and stem barks were tested for their cytotoxic effects against human tumor cells lines (HeLa: Cervical carcinoma, HepG2: hepatocellular carcinoma, MCF-7: breast carcinoma, NCI-H460: non-small lung cancer) and non-tumor porcine liver cells PLP2. Decoction and infusion preparations of leaves fraction exerted the most potent cytotoxic activity, specifically against HepG2 (GI50 values of 18.6 and 41.7 µg/mL, respectively), while decoctions of the leaves revealed the strongest activity on HeLa and NCI-H460 cell lines with GI50 values of 44 and 66 µg/mL, respectively. Therefore, the root barks of both preparations showed modest cytotoxicity against HepG2 (GI50 from 48.3 to 59.8 µg/mL), MCF-7 (GI50 from 74 to 111 µg/mL), and HeLa (GI50 from 69 to 99 µg/mL) carcinoma. Branches and stem barks showed no-cytotoxicity effect against cell line tested. On the other hand, the majority of the tested sample presented effects on the PLP2 cells.[48]

Other studies reported the cytotoxic effect of decoctions extractive of different morphological parts of *Z. lotus* from Algeria (pulp, seeds, leaves, and stems). The result showed that *Z. lotus* exhibited an inhibitory effect against T-cell blastogenesis by the incorporation of 3H–thymidine.[9] Methanolic and ethyl acetate extracts of *Z. lotus* fruit part from Morocco modulate cell signaling and exert immunosuppressive effects in human Jurkat T-cells.[168]

Three isolated compounds (13^1–oxophorbines, pheophorbide A, and protopheophorbide A) from the leaf part were tested against breast cancer cell lines such as MDA-MB-231 and MCF-7. Protopheophorbide A exhibited the highest antiproliferative effect against MDA-MB-231 cells (IC50 = 6.5 µM) by targeting the kinase domain of multiple c-Met crystal structures. Moreover, this compound exhibited anti-migratory properties through impacting the expression levels of adherent proteins (such as: E-cadherin, vimentin, β-catenin, among others) and displayed as a photosensitizer, inducing ROS accumulation, generating oxidative stress and triggering both extrinsic and intrinsic apoptosis in MDA-MB-231 cells.[78]

Hence T-cell is considered a key player in many autoimmune diseases. The aqueous extracts of five parts of *Z. lotus* (root, stem, leaves, fruit pulp, and seeds) were screened for human T-cell proliferation. The results showed that all extracts exhibit the highest inhibitory effect in T-cell proliferation and IL-2 mRNA expression with seed being the powerful immunosuppressant extract with a percentage of inhibition of 86%. Moreover, n-3 fatty acids were postulated responsible for the immunosuppressive activity.[17]

Souleymane et al. (2013)[168] were demonstrated that *Z. lotus* fruits phenolic-rich extract modulate human cell signaling mechanisms and apply immunosuppressive effects by regulate thapsigargin (TG, an inhibitor of Ca^{2+}–ATPase)-mediated calcium signaling at endoplasmic reticulum level, modulate plasma membrane and, thus, block the entry of ions, decrease

ERK1 and ERK2 activation, diminish cell proliferation and IL-2 expression by arresting S cell cycle and increase intracellular acidification in a dose-dependent manner.[168]

7. References

(1) Maraghni, M.; Gorai, M.; Neffati, M. South African J. Bot. **2010**, 76 (3), 453–459.
(2) Mishra, T.; Paice, A. G.; Bhatia, A. In Nuts and Seeds in Health and Disease Prevention; Elsevier Inc., **2011**; pp 733–739.
(3) Mirghani Ismail Hussein, A. A. E. Unconventional Oils eeds and Oil Sources; **2017**; pp 243–249.
(4) Sheng, J. P.; Shen, L. In Woodhead Publishing Limited; China, **2011**; pp 299–326.
(5) Dorie, M. Rev. Hist. Pharm. (Paris). **1967**, 55 (195), 573–584.
(6) Chevalier, A. Rev. Int. Bot. appliquée d'agriculture Trop. Les **1947**, 470–483.
(7) Boussaid, M.; Taïbi, K.; Abderrahim, L. A.; Ennajah, A. Arid L. Res. Manag. **2018**, 0 (0), 1–14.
(8) Nabli, M. B. N.-A. and M. A. Int. Jujube Symp. **2009**, 46 (840), 337–342.
(9) Benammar, C.; Hichami, A.; Yessoufou, A.; Simonin, A. M.; Belarbi, M.; Allali, H.; Khan, N. A. BMC Complement. Altern. Med. **2010**, 10 (54), 1–9.
(10) Saissi, R. N.; Ouhache, B. M.; Encharki, B. B. Rev. marocaine Prot. des plantes **2012**, 3, 13–27.
(11) BRAHLP, D. L. R. R. and A. E. L. B. Weed Technol. **1995**, 9 (2), 326–330.
(12) DOUIRA, J. B. et A. Acta Bot. Malacit. **2002**, 27, 131–145.
(13) Hachi, M.; Hachi, T.; Belahbib, N.; Dahmani, J.; Zidane, L. Int. J. Innov. Appl. Stud. **2015**, 11 (3), 754–770.
(14) Fatiha, E.A, Lahcen, Z. In Journal of Applied Biosciences; **2015**; pp 8493–8502.
(15) Guy, M. In Revue d'Histoire de la Pharmacie; **1998**; pp 465–466.
(16) Boukef, M. K.. In Agence de Coopération Culturelle et Technique; **1986**; p 350.
(17) Simonin, A.; Benammar, C.; Hichami, A.; Bendahmane-Salmi, M.; Allali, H.; Khan, N. Fundam. Clin. Pharmacol. **2011**, 25, 47.
(18) Regehr, D. L.; El Brahli, A. Weed Technol. **1995**, 9 (02), 326–330.
(19) Bakhtaoui, F. Z.; Lakmichi, H.; Megraud, F.; Chait, A.; Gadhi, C. E. A. J. Appl. Pharm. Sci. **2014**, 4 (10), 81–87.
(20) Chouaibi, M.; Mahfoudhi, N.; Rezig, L.; Donsì, F.; Ferrari, G.; Hamdi, S. J. Sci. Food Agric. **2012**, 92 (6), 1171–1177.
(21) Moussa, A.; Khaloufi, B. J. Appl. Environ. Biol. Sci **2017**, 7 (11), 1–8.
(22) Pressure, B.; Osborne, C. G.; Mctyre, R. B.; Ph, D.; Dudek, J.; Roche, K. E.; Scheuplein, R.; Ph, D.; Silverstein, B.; Weinberg, M. S.; Nutr. Rev. **1996**, 54 (12), 365–381.
(23) Abdeddaim, M.; Lombarkia, O.; Bacha, A.; Fahloul, D.; Abdeddaim, D.; Farhat, R.; Saadoudi, M.; Noui, Y.; Lekbir, Ann. Food Sci. Techgnology **2014**, 15 (1), 75–81.
(24) Mkadmini Hammi, K.; Hammami, M.; Rihouey, C.; Le Cerf, D.; Ksouri, R.; Majdoub, H. Food Chem. **2016**, 212, 476–484.
(25) M.Partain, E. Appl. Polym. Sci. 21st Century **2000**, 303–323.
(26) Rohloff, J. Molecules. **2015**, 20 (2), 3431–3462.
(27) Hillis, W. E. Higuchi, T., Ed.; Academic Press; **1985**; pp 209–228.
(28) Balandrin, M. F.; Klocke, J. A.; Wurtele, E. S.; Bollinger, W. H. Natural Plant Chemicals: Sources of Industrial and Medicinal Materials. In Science; **1985**; pp 1154–1160.
(29) Seca, A. M. L.; Pinto, D. C. G. A. Int. J. Mol. Sci. **2018**, 19 (263), 1–22.
(30) Hussain, M. S.; Fareed, S.; Ansari, S.; Rahman, M. A.; Ahmad, I. Z.; Saeed, M. C J. Pharm. Bioallied Sci. **2012**, 4 (1), 10–20.

(31) Radulovi, N. S.; Blagojevi, P. D.; Stojanovi, Z. Z.; Stojanovi, N. M. Curr. Med. Chem. **2012**, 20, 932–952.
(32) Atanasov, A. G.; Waltenberger, B.; Linder, T.; Wawrosch, C.; Uhrin, P.; Temml, V.; Schwaiger, S.; Heiss, E. H.; Rollinger, J. M.; Schus-, D.; Biotechnol. Adv. **2015**, 33 (8), 1582–1614.
(33) Pott, D. M.; Osorio, S.; Vallarino, J. G. Frontiers in Plant Science. 31, **2019**.
(34) Isah, T.; Umar, S.; Mujib, A.; Sharma, M. P.; Rajasekharan, P. E.; Zafar, N.; Frukh, A. Plant Cell. Tissue Organ Cult. **2018**, 132 (2), 239–265.
(35) Bouaziz, M.; Dhouib, A.; Loukil, S. African J. Biotechnol. **2009**, 8 (24), 7017–7027.
(36) Borgi, W.; Ghedira, K.; Chouchane, N. Fitoterapia **2007**, 78 (1), 16–19.
(37) Adeli, M.; Samavati, V. Int. J. Biol. Macromol. **2014**, 72 (March 2014), 580–587.
(38) Ghalem, M.; Merghache, S.; Belarbi, M. Pharmacogn. J. **2014**, 6 (4), 32–42.
(39) Li, N.; Xu, C.; Li-Beisson, Y.; Philippar, K. Trends Plant Sci. **2016**, 21 (2), 145–158.
(40) Dewick, P. M. A Biosynthetic Approach. 2nd Ed.; **2002**; Vol. 45.
(41) Bajpai, P. In Recycling and Deinking of Recovered Paper; **2014**; pp 121–137.
(42) Ghazghazi, H.; Aouadhi, C.; Riahi, L.; Maaroufi, A.; Hasnaoui, B. Nat. Prod. Res. **2014**, 28 (14), 1106–1110.
(43) Widad, O.; Hamza, F.; Youcef, M.; Jean-claude, C.; Pierre, C.; Fadila, B.; Samir, B.; Université, B.; El, A. Int. J. Pharmacogn. Phytochem. Res. **2017**, 9 (2), 228–232.
(44) Kumar, D.; Dubey, K. K. Elsevier B.V., **2019**.
(45) Sandjo, L. P.; Kuete, V. Elsevier Inc., 2013.
(46) Guo, S.; Duan, J. A.; Tang, Y. P.; Yang, N. Y.; Qian, D. W.; Su, S. L.; Shang, E. X. J. Agric. Food Chem. **2010**, 58 (10), 6285–6289.
(47) Masullo, M.; Montoro, P.; Autore, G.; Marzocco, S.; Pizza, C.; Piacente, S. Food Res. Int. **2015**, 77 (2), 109–117.
(48) Rached, W.; Barros, L.; Ziani, B. E. C.; Bennaceur, M.; Calhelha, R. C.; Heleno, S. A.; Alves, M. J.; Marouf, A.; Ferreira, I. C. F. R. Food Funct. **2019**, 10 (9), 5898–5909..
(49) M.Srivastava, L. Plant Growth and Development Hormones and Environment; **2002**; pp 205–215.
(50) Hu, F. B. International Encyclopedia of Public Health; **2018**; pp 181–190.
(51) Horwath, W. In Soil Microbiology, Ecology and Biochemistry; Elsevier Inc., **2015**; pp 339–382.
(52) Wool, R. P. **2005**; pp 202–255.
(53) El-Seedi, H. R.; Zahra, M. H.; Goransson, U.; Verpoorte, R. Phytochem. Rev. **2007**, 6 (1), 143–165.
(54) Ghedira, K.; Chemli, R.; Richard, B.; Nwllard, J.; Men-olivier, L. L. E. **1993**, 32 (6), 1591–1594.
(55) Le Crouéour, G.; Thépenier, P.; Richard, B.; Petermann, C.; Ghédira, K.; Zèches-Hanrot, M. Fitoterapia **2002**, 73 (1), 63–68.
(56) Savage, G. P. Encycl. Food Sci. Nutr. **2003**, 5095–5098.
(57) Maciuk, A.; Lavaud, C.; Thépenier, P.; Jacquier, M. J.; Ghédira, K.; Zèches-Hanrot, M. J. Nat. Prod. **2004**, 67 (10), 1639–1643.
(58) Renault, J.; Ghedira, K.; Thepenier, P.; Lavaud, C.; Zeches-hanrot, M.; Men-olivier, L. L. E. Phytochemistry **1997**, 44 (7), 1321–1327.
(59) Rocher, F.; Dédaldéchamp, F.; Saeedi, S.; Fleurat-Lessard, P.; Chollet, J. F.; Roblin, G. Plant Physiol. Biochem. **2014**, 84, 240–250.
(60) Lin, D.; , Mengshi Xiao, Jingjing Zhao, Zhuohao Li, B. X. 2; Xindan Li , Maozhu Kong, Liangyu Li, Q. Z.; Liu, Y.; Chen, H.; Qin, W.; Chen, H. W. and S. Molecules **2016**, 21 (10), 2–19.
(61) Ho, C.-T. In American Chemical Society; **1992**; pp 2–7.

(62) Nagendran Balasundram, Kalyana Sundram, S. S. Food Chem. **2006**, 99, 191–203.
(63) Marmouzi, I.; Kharbach, M.; El, M.; Bouyahya, A.; Cherrah, Y.; Bouklouze, A.; Vander, Y.; El, M.; Faouzi, A. Ind. Crop. Prod. **2019**, 132, 134–139.
(64) Kaushik, P.; Andújar, I.; Vilanova, S.; Plazas, M.; Gramazio, P.; Herraiz, F. J.; Brar, N. S.; Prohens, J. Molecules **2015**, 20 (10), 18464–18481.
(65) Heleno, S. A.; Martins, A.; Queiroz, M. J. R. P.; Ferreira, I. C. F. R. Food Chem. **2015**, 173, 501–513.
(66) Tlili, H.; Marino, A.; Ginestra, G.; Cacciola, F.; Mondello, L.; Miceli, N.; Taviano, M. F.; Najjaa, H.; Nostro, A. Nat. Prod. Res. **2019**, 1–7.
(67) Shen, T.; Wang, X. N.; Lou, H. X. Nat. Prod. Rep. **2009**, 26 (7), 916–935.
(68) Shin, S. A.; Moon, S. Y.; Kim, W. Y.; Paek, S. M.; Park, H. H.; Lee, C. S. International Journal of Molecular Sciences; 2018; Vol. 19, pp 1–33.
(69) Srivastava, A.; Srivastava, P.; Pandey, A.; Khanna, V. K.; Pant, A. B. Phytomedicine; Elsevier Inc., **2019**.
(70) Ravishankar, D.; Rajora, A. K.; Greco, F.; Osborn, H. M. I. Int. J. Biochem. Cell Biol. **2013**, 45 (12), 2821–2831.
(71) Maru, G. B.; Kumar, G.; Ghantasala, S.; Tajpara, P. Elsevier Inc., 2013; Vol. 2.
(72) Sies, H.; Hollman, P. C. H.; Grune, T.; Stahl, W.; Biesalski, H. K.; Williamson, G. Adv. Nutr. **2012**, 3 (2), 217–221.
(73) Mena, P.; Domínguez-Perles, R.; Gironés-Vilaplana, A.; Baenas, N.; García-Viguera, C.; Villaño, D. IUBMB Life **2014**, 66 (11), 745–758.
(74) Wahiba Racheda, Lillian Barrosa, Borhane E.C. Ziania, Malika Bennaceur, Ricardo C. Calhelha, Sandrina A. Helenoa, Maria José Alvesa, Abderrazak Marouff, I. C. F. R. F. Food Funct. **2019**, 1–34.
(75) Manach, C.; Scalbert, A.; Morand, C.; Rémésy, C.; Jiménez, L. Am. J. Clin. Nutr. **2004**, 79 (5), 727–747.
(76) Jaganath, I. B.; Crozier, A. Woodhead Publishing Limited, **2008**.
(77) Duodu, K. G.; Awika, J. M. AACCI, 2019.
(78) Souid, S.; Elsayed, H. E.; Ebrahim, H. Y.; Mohyeldin, M. M.; Siddique, A. B.; Karoui, H.; El Sayed, K. A.; Essafi-Benkhadir, K. Mol. Carcinog. **2018**, 57 (11), 1507–1524.
(79) Juzeniene, A. Photodiagnosis Photodyn. Ther. **2009**, 6 (2), 94–96.
(80) S. Sasidharan, Y. Chen, D. Saravanan2, K.M. Sundram, L. Y. L. Afr J Tradit Complement Altern Med **2011**, 8 (1), 1–10.
(81) Zhang, Q. W.; Lin, L. G.; Ye, W. C. Chinese Med. (United Kingdom) **2018**, 13 (1), 1–26.
(82) Hemantaranjan, D. A. Advances in Plant Physiology (Vol.16); **2015**.
(83) Vilela, C.; Santos, S. A. O.; Coelho, D.; Silva, A. M. S.; Freire, C. S. R.; Neto, C. P.; Silvestre, A. J. D. Ind. Crops Prod. **2014**, 52, 373–379.
(84) Touati, R.; Santos, S. A. O.; Rocha, S. M.; Belhamel, K.; Silvestre, A. J. D. Ind. Crops Prod. **2015**, 76, 936–945.
(85) Azmir, J.; Zaidul, I. S. M.; Rahman, M. M.; Sharif, K. M.; Mohamed, A.; Sahena, F.; Jahurul, M. H. A.; Ghafoor, K.; Norulaini, N. A. N.; Omar, A. K. M. J. Food Eng. **2013**, 117 (4), 426–436.
(86) Norulfairuz, D.; Zaidel, A.; Muhamad, I. I.; Shafinas, N.; Daud, M.; Azyati, N.; Muttalib, A.; Khairuddin, N.; Lazim, N. A. Elsevier Ltd, **2019.**
(87) Azmir, J.; Zaidul, I. S. M.; Rahman, M. M.; Sharif, K. M.; Mohamed, A.; Sahena, F.; Jahurul, M. H. A.; Ghafoor, K.; Norulaini, N. A. N.; Omar, A. K. M. J. Food Eng. **2013**, 117 (4), 426–436.
(88) Ayuso, M. D. L. de C. E. G. Encyclopedia of Separation Science; **2000**; pp 2701–2709.
(89) Nn, A. Med. Aromat. Plants **2015**, 4 (3), 3–8.

(90) Pandey, A.; Tripathi, S.; Pandey, C. A. J. Pharmacogn. Phytochem. **2014**, 2 (5), 115–119.
(91) Vek, V.; Oven, P.; Poljanšek, I. Drv. Ind. **2016**, 67 (1), 85–96.
(92) Vek, V.; Oven, P.; Poljanšek, I. Drv. Ind. **2013**, 64 (1), 25–32.
(93) S eczyk, L.; Swieca, M.; Kapusta, I.; Gawlik-Dziki, U. Molecules **2019**, 24 (3), 308.
(94) Amit Koparde, A., Chandrashekar Doijad, R., & Shripal Magdum, C. Pharmacognosy - Medicinal Plants; **2019**; pp 1–19.
(95) Hage, D. S. In Principles and Applications of Clinical Mass Spectrometry; **2018**; pp 1–32.
(96) Lobo Roriz, C.; Barros, L.; Carvalho, A. M.; Santos-Buelga, C.; Ferreira, I. C. F. R. **2008**.
(97) Meyer, V. R. Elsevier Inc., **2013**.
(98) Coskun, O. North. Clin. Istanbul **2016**, 3 (2), 156–160.
(99) Menet, M. C. Rev. Francoph. des Lab. **2011**, 2011 (437), 41–53.
(100) Mandal, S. C.; Mandal, V.; Das, A. K. Essentials of Botanical Extraction; **2015**; pp 187–201.
(101) Ghosh, D. In Nutraceuticals; Elsevier Inc., **2016**; pp 925–931.
(102) World Health Organization. In Strategy, WHO Traditional Medicine 2002-2005; **2002**.
(103) Nyeko, R.; Tumwesigye, N. M.; Halage, A. A. BMC Pregnancy Childbirth **2016**, 16 (296), 1–12.
(104) Ferreira, M. P.; Palmer, J.; McKenna, E. B.; Gendron, F. Elsevier Inc., **2015**.
(105) Thomford, N. E.; Senthebane, D. A.; Rowe, A.; Munro, D.; Seele, P.; Maroyi, A.; Dzobo, K. Int. J. Mol. Sci. **2018**, 19 (6).
(106) Balunas, M. J.; Kinghorn, A. D. life Sci. **2005**, 78, 431–441.
(107) Mcchesney, J. D.; Venkataraman, S. K.; Henri, J. T. Phytochemistry **2007**, 68 (2007), 2015–2022.
(108) Borgi, W.; Recio, M. C.; Ríos, J. L.; Chouchane, N. South African J. Bot. **2008**, 74 (2), 320–324.
(109) Forni, C.; Facchiano, F.; Bartoli, M.; Pieretti, S.; Facchiano, A.; D'Arcangelo, D.; Norelli, S.; Valle, G.; Nisini, R.; Beninati, S. Biomed Res. Int. **2019**, 1–16.
(110) Boulanouar, B.; Abdelaziz, G.; Aazza, S.; Gago, C.; Miguel, M. G. Ind. Crops Prod. **2013**, 46, 85–96.
(111) Ghalem, M.; Murtaza, B.; Belarbi, M.; Akhtar Khan, N.; Hichami, A. J. Food Biochem. **2018**, 42 (6), 1–15.
(112) Borgi, W.; Chouchane, N. J. Ethnopharmacol. **2009**, 126 (3), 571–573.
(113) Benammar, C.; Baghdad, C. J. Nutr. Food Sci. **2014**, s8, 8–13.
(114) Jeyakumar, S. M.; Sheril, A.; Vajreswari, A. Preventive Nutrition and Food Science. **2017**, pp 172–183.
(115) Berrichi, M.; Benammar, C.; Murtaza, B.; Hichami, A.; Belarbi, M.; Khan, N. A. Arch. Physiol. Biochem. **2019**, 1–8.
(116) Wahida, B.; Abderrahman, B.; Nabil, C. J. Ethnopharmacol. **2007**, 112 (2), 228–231.
(117) Phaniendra, A.; Jestadi, D. B.; Periyasamy, L. Indian J. Clin. Biochem. **2015**, 30 (1), 11–26.
(118) Gagné, F. Oxidative Stress. Biochem. Ecotoxicol. Princ. Methods **2014**, 103–115.
(119) Shahidi, F.; Zhong, Y. J. Funct. Foods **2015**, 18, 757–781.
(120) Akar, Z.; Küçük, M.; Doğan, H. J. Enzyme Inhib. Med. Chem. **2017**, 32 (1), 640–647.
(121) Jacobsen, C.; Lyngby, K. Oxidative Rancidity; Elsevier, 2018.
(122) Ghazghazi, H.; Aouadhi, C.; Riahi, L.; Maaroufi, A.; Hasnaoui, B. Nat. Prod. Res. **2014**, 28 (14), 1106–1110.
(123) Amarowicz, R.; Pegg, R. B. 1st ed.; Elsevier Inc., **2019**; Vol. 90.

(124) Miller, N. J.; Rice-Evans, C.; Davies, M. J.; Gopinathan, V.; Milner, A. Clin. Sci. **1993**, 84 (4), 407–412.
(125) Roberta Re, Nicoletta Pellegrini, Anna Proteggente, Ananth Pannala, Min Yang, and C. R.-E. Free Radic. Biol. Med. **1999**, 26, 1231–1237.
(126) Cerretani, L.; Bendini, A. Elsevier Inc., **2010**.
(127) Kedare, S. B.; Singh, R. P. J. Food Sci. Technol. **2011**, 48 (4), 412–422.
(128) Chavan, D. U. D. 2018, pp 133–135.
(129) Hammi, K. M.; Jdey, A.; Abdelly, C.; Majdoub, H.; Ksouri, R. Food Chem. **2015**, 184, 80–89.
(130) Ait Abderrahim, L.; Taïbi, K.; Ait Abderrahim, C. Iran. J. Sci. Technol. Trans. A Sci. **2019**, 43 (2), 409–414.
(131) Benzie, I. F. F.; Strain, J. J. Anal. Biochem. **1996**, 239 (1), 70–76.
(132) Pulido, R.; Bravo, L.; Saura-calixto, F. J. Agric. Food Chem **2000**, 48 (8), 3396–3402.
(133) Chouaibi, M.; Rezig, L.; Mahfoudhi, N.; Arafa, S.; Donsì, F.; Ferrari, G.; Hamdi, S. J. Food Biochem. **2013**, 37 (5), 554–563.
(134) Kumar, S.; Sandhir, R.; Ojha, S. BMC Res. Notes **2014**, 7 (1), 1–9.
(135) Gest, H.; Leeuwenhoek, A. V. A. N.; Of, F.; Royal, T. H. E. Notes Rec. R. Soc. **2004**, 58 (2), 187–201.
(136) Hu, F.; Wu, Q.; Song, S.; She, R.; Zhao, Y.; Yang, Y.; Zhang, M.; Du, F. BMC Microbiol. **2016**, 16 (287), 1–10.
(137) Ristow, P.; Bourhy, P.; Kerneis, S.; Schmitt, C.; Prevost, M.; Lilenbaum, W.; Picardeau, M. Microbiology **2008**, 154, 1309–1317.
(138) Anyanwu, M. U.; Okoye, R. C. J Intercult Ethnopharmacol **2017**, 6 (2), 240–259.
(139) Nasir, B.; Fatima, H.; Ahmad, M. Austin J. Microbiol. **2015**, 1 (1), 1002.
(140) Roca, I.; Akova, M.; Baquero, F.; Carlet, J.; Cavaleri, M.; Coenen, S.; Cohen, J.; Findlay, D.; Gyssens, I.; Heure, O. E. New Microbes New Infect. **2015**, 6, 22–29.
(141) America, I. D. S. of. Clin Infect Dis **2010**, 50, 1081–1083.
(142) Cowan, M. M. Clin. Microbiol. Rev. **1999**, 12 (4), 564–582.
(143) Joshi, R. K. Am. J. Clin. Microbiol. Antimicrob. **2018**, 1 (1), 1–5.
(144) Naili, M. B.; Alghazeer, R. O.; Saleh, N. A.; Al-Najjar, A. Y. Arab. J. Chem. **2010**, 3 (2), 79–84.
(145) Rsaissi, N.; Kamili, E. L.; Bencharki, B.; Hillali, L.; Bouhache, M. Int. J. Sci. Eng. Res. **2013**, 4 (9), 1521–1528.
(146) Cole, L., Kramer, P. R. In biochemistry and basic medecine; **2016**; pp 197–200.
(147) Hanahan, D.; Weinberg, R. A. Cell **2011**, 144, 646–674.
(148) Fernald, K.; Kurokawa, M. Trends Cell Biol. **2013**, 23 (12), 620–633.
(149) Safa, A. R. Crit Rev Oncog. **2016**, 21, 203–219. h
(150) Parcesepe, P.; Giordano, G.; Laudanna, C.; Febbraro, A.; Pancione, M. Gastroenterol. Res. Pract. **2016**, 2016, 1–8.
(151) Vinay, D. S.; Ryan, E. P.; Pawelec, G.; Talib, W. H.; Stagg, J.; Elkord, E.; Lichtor, T.; Decker, W. K.; Whelan, R. L.; Kumara, H. M. C. S.; Semin. Cancer Biol. **2015**, 35, S185–S198.
(152) Dewhirst, M. W.; Secomb, T. W. T Nat. Rev. Cancer **2017**, 17 (12), 738–750.
(153) Zuazo-Gaztelu, I.; Casanovas, O. Unraveling the Role of Angiogenesis in Cancer Ecosystems. Front. Oncol. **2018**, 8, 1–13.
(154) Thomas N. Seyfried, and L. C. H. Crit Rev Oncog **2013**, 18, 43–73.
(155) Tracey A. Martin, Lin Ye, Andrew J. Sanders, Jane Lane, and W. G. J. In Metastatic Cancer Clinical Biological Perspectives; **2013**; pp 135–168.
(156) Wittekind, C.; Neid, M. Oncology **2005**, 69, 14–16.
(157) Yixin Yao, W. D. J Carcinog Mutagen **2014**, 5, 1–3.

(158) Shalapour, S.; Karin, M.; Shalapour, S.; Karin, M. J. Clin. Invest. **2015**, 125 (9), 3347–3355.
(159) Aboumarzouk, O. M. Blandy's Urology; **2019**.
(160) Childs, B. G.; Baker, D. J.; Kirkland, J. L.; Campisi, J.; Deursen, J. M. Van. EMBO Rep. **2014**, 15, 1139–1153.
(161) Yaswen, P.; MacKenzie, K. L.; Keith, W. N.; Hentosh, P.; Rodier, F.; Zhu, J.; Firestone, G. L.; Matheu, A.; Carnero, A.; Bilsland, A. Semin. Cancer Biol. **2015**, 1–25.
(162) Taylor, P.; Stadler, P. F. RNA Biol. **2012**, 9 (6), 703–719.
(163) Scoles, D. R. Biochim. Biophys. Acta - Rev. Cancer **2008**, 1785, 32–54.
(164) Dang, C. V. Genes Dev. **2012**, 26 (9), 877–890.
(165) Zhang, C.; Moore, L. M.; Li, X.; Yung, W. K. A.; Zhang, W. Neuro. Oncol. **2013**, 15 (9), 1114–1126.
(166) Nowak, N.; Kulma, A.; Gutowicz, J. Open Life Sci. **2018**, 13 (1), 569–581.
(167) Subramaniam, S.; Selvaduray, K. R.; Radhakrishnan, A. K. Biomolecules **2019**, 9, 2–15.
(168) Abdoul-Azize, S.; Bendahmane, M.; Hichami, A.; Dramane, G.; Simonin, A. M.; Benammar, C.; Sadou, H.; Akpona, S.; El Boustani, E. S.; Khan, N. A. Int. Immunopharmacol. **2013**, 15 (2), 364–371.

Chapter III

Chemical characterization of *Zizyphus lotus* lipophilic fraction

Abstract

Zizyphus lotus is a perennial shrub whose individual morphological parts (root barks, leaves, pulp, and seeds) from Morocco were studied for the first time by gas chromatography-mass spectrometry in terms of lipophilic profile. Fatty acids and triterpenic acids are the main chemical families of all *Z. lotus* extracts, representing 4.1–88.1% and 3.6–92.6% of the total amount of lipophilic components, respectively. Betulinic acid was the most abundant triterpenic acids (119–9838 mg/kg dw), while linoleic (50-737 mg/kg dw), linolenic (9–2431 mg/kg dw), oleic (59–6255 mg/kg dw), and hexadecanoic acids (152-877 mg/kg dw) are the main fatty acids. Sterols were also detected as *Z. lotus* components with β-sitosterol (68–208 mg/kg dw) as the major compound. Fatty acid methyl and ethyl ester and long-chain aliphatic aldehydes were mainly present in the pulp (5–228 and 80 mg/kg dw, respectively) while tocopherols are identified in leaves extract (128 mg/kg dw). Monoglycerides and long-chain aliphatic alcohols were detected at a moderate amount, along with aromatic compounds that were detected at low abundances.

1. Introduction

Zizyphus a plant genus belong to the angiosperm Rhamnaceae family, order Rhamnales, includes about 135–170 species worldwide,[1] of which *Zizyphus jujuba* Mill. and *Ziziphus mauritiana* Lam. are the most important in terms of distribution and economic significance.[2] Recently, other Zizyphus species have been attracted much attention as a natural biomass resource. Among them, *Z. lotus*, is indigenous to Morocco and known as "Sedra" has a wide ecological and geographical distribution in arid and semi-arid in plateau regions and along the sandy riverbeds in the Saharan region.[3] Although in Europe, has restricted to some semiarid areas in the southeast of Spain and the island of Sicily.[4] This wild shrub is mainly appreciated for its brown delicious and nutritive small fruits which have been contributed to the spread of this species, however; their vegetative parts have been associated with a wide range of health benefits, including the treatment of variety of diseases and disorders such as liver complaints, urinary troubles, diabetes, skin infections, insomnia, inflammation and peptic ulcers, and among others.[5]

Several biologically active compounds have been identified in *Z. lotus*. Seven cyclopeptide alkaloids termed lotusines[6–8] were isolated from root barks, and four dammarane saponins from leaves and root barks.[9,10] Moreover, there is a significant amount of work focused on *Z. lotus* fatty acids composition.[4,12–14] However, less attention dedicated to triacylglycerol and sterols beyond their identification in the seeds oil.[12,15,16] Besides, various triterpenic acids have been identified in genus Zizyphus[17,18] although these compounds have not been explored so far in this shrub species despite their valuable properties such as anti-tumor and anti-angiogenic activities.[19–21] Aside from that, anti-inflammatory, analgesic,[22] anti-diabetic,[23] anti-ulcerogenic,[24,25] anti-spasmodic,[26,27] and anti-oxidant proprieties of *Z. lotus* rich-extract were studied[4,23,24] with the lack of a comprehensive composition of the main compounds in charge of these activities. In this context, a detailed study of the composition of *Z. lotus* fraction is, therefore, an important step.

Z. lotus is one of Morocco's forgotten fruits, although used since ancient times to prepare bread, wine, and reserves.[3] The comprehensive study of the profile of the chemical

characterization of this shrub species can be functional to increase its economic value, health potential, and consequently to host its production. Therefore, considering our interest in the exploitation of of bioactive compounds from natural biomass, and the lack of detailed information on the extractives composition of *Z. lotus*, it is given here a detailed chemical characterization of the lipophilic fractions of different parts of *Z. lotus* namely: root barks, leaves, seeds, and pulp by gas chromatography-mass spectrometry (GC-MS) analysis.

2. Materials and methods

2.1 Chemicals

Nonadecan-1-ol (99% purity), hexadecanoic acid (99% purity), β-stigmasterol (93% purity), vanillin (99%), anhydrous pyridine (99.8% purity), dichloromethane (99% purity), bis(trimethylsilyl)trifluoroacetamide, trimethylchlorosilane (≥99% purity), and tetracosane (99% purity) were obtained from Sigma Chemicals Co. (Madrid, Spain). Ursolic acid (98% purity) was purchased from Aktin Chemicals (Chengdu, China).

2.2 Samples

Wild *Z. lotus* was collected from the regions of Beni Mellal, Morocco (32°20'21.998" N; 6°21'38.999" W) between September and October of 2016. The shrub was separated manually into four different morphological parts namely; root barks, leaves, pulp, seeds; each fraction was shade-dried (15 days) and milled into to granulometry lower than 2 mm prior to extraction.

2.3 Extraction

Adequate mass (15 g of dry weight) of either of the following parts of *Z. lotus*, i.e, root barks, leaves, pulp, and seed were Soxhlet extracted with dichloromethane (1:25 w/v) for 8h, in order to obtain the lipophilic extractives. The solvent was evaporated until dryness under vacuum on rotavapor. The extracts were weighed and the results were expressed in percent of dry biomass material (% w/w).

2.4 Derivatization

Before GC–MS analysis, approximately 20 mg of each dried dichloromethane extract were dissolved in 250 µL of pyridine containing 1 mg of the internal standard tetracosane (0.3–1mg). The compounds with carboxylic and hydroxyl groups were converted into their volatile trimethylsilyl (TMS) derivative, adding 250 µL of N, O-bis (trimethylsilyl)trifluoroacetamide, 50 µL trimethylchlorosilane and 250 µL of pyridine. The mixture was heated at 70 °C for 30 min. The TMS derivatives were analyzed by GC–MS.

2.5 GC–MS analysis

Shimadzu GC–MS-QP2010 Ultra was used to analyze the derivatized extracts. A DB-1 J&W capillary column (30 m × 0.32 mm i.d., 0.25 µm film thickness) was used for separation and helium was the carrier gas at a flow rate of 35 cm s^{-1}. The chromatographic conditions were as follows: initial temperature, 80 °C for 5 min; first temperature gradient, 4 °C min^{-1} up to 260 °C; second temperature gradient, 2 °C min^{-1} up to 285 °C for 8 min; injector temperature, 250 °C; transfer-line temperature, 290 °C; split ratio, 1:50.

Lipophilic compounds were identified by comparing their mass spectra with commercial GC-MS spectral libraries (Wiley 275 and U.S. National Institute of Science and Technology (NIST14)), their retention time obtained at the same conditions[28–30] and comparing their MS fragmentation profiles with literature data (as mentioned in the results and discussion).

2.6 GC-MS quantification

The main identified lipophilic extractives families were quantified by peaks area and by a pure reference mixture, namely hexadecanoic acid, nonadecan-1-ol, vanillin, β-stigmasterol, and ursolic acid relative to tetracosane (the internal standard). The respective response factors were calculated as the average of six GC−MS runs. The results were expressed in milligrams per kilogram of dry weight of shrub biomass.

3. Results and discussion

3.1 Dichloromethane extractive yield

Dichloromethane (DCM) extracts from the different morphological parts of *Z. lotus* give rise to a very distinct amount of extractives, with seeds showing the highest yield (9.4%) followed by leaves (4.1%), root barks (2%), and then pulp with the amount of 1.7 % of dry weight (Table 1). The value found for pulp fraction was already reported[31] while, DCM extraction yields from leaves, seeds, and root barks were described here for the first time.

Table 1: Dichloromethane extraction yields (%, w/w) for different morphological part of *Zizyphus lotus*.

Morphological part of *Z. lotus* L.		Extraction yield (%, w/w)
Fruit	Pulp	1.7
	Seeds	9.4
Leaves		4.1
Root barks		2.0

Results represent the mean estimated from three extracts.

3.2 GC/MS analysis of *Zizyphus lotus* lipophilic extractives

The chemical composition of lipophilic extractives of four morphological parts of *Z. lotus* e.g; root barks, leaves, pulp, and seeds obtained by Soxhlet with DCM were detailed characterized by chromatography coupled with a mass detector (GC–MS) analysis. GC-MS is a very useful analysis technique in the identification of lipophilic metabolites. This technique is only intended for the analysis of volatile compounds or that can become volatile by derivatization, allowing their separation, identification and quantification. Trimethylsilylated derivatives are advantageous in a GC–MS analysis as silylation increases the volatility of the compounds and, consequently, improve the chromatographic separation. The components identified and their corresponding quantification is displayed below. As an example, the GC–MS chromatogram of the derivatized lipophilic extract of pulp is presented in Figure 1.

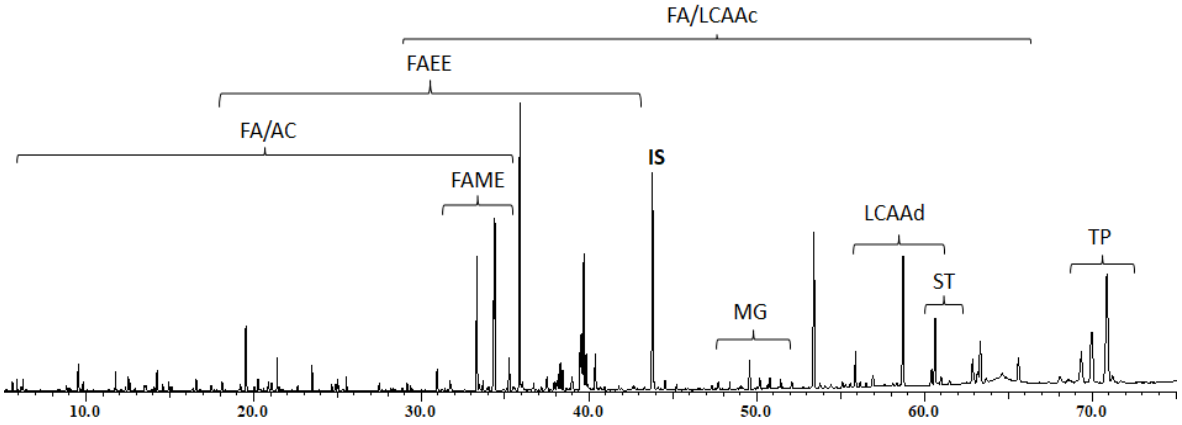

Figure 1: GC−MS chromatogram of the TMS-derivatized dichloromethane extract from *Z. lotus* pulp. Abbreviations: AC, aromatic compounds; IS, internal standard (tetracosane); FA, fatty acids; FAEE, fatty acid ethyl ester; FAME, fatty acid methyl esters; LCAAc, long-chain aliphatic alcohols; LCAAd, long chain aliphatic aldehydes; MG, monoglycerides; PT, triterpenes; ST, sterols.

The compounds corresponding to each chromatographic peak are identified using mass spectra.[32–34] The fragmentation pattern is typical for each family of compounds, which allows unambiguous identification of the class of compounds in question. The relative abundance and the mass/charge ratio (m/z) values of the peaks present in the mass spectrum are an excellent tool for determining the structure of the metabolites detected in the chromatogram.

The following are some of the characteristic fragments displayed in the mass spectra obtained by electronic ionization, for each of the families of compounds identified in the chromatograms of the DCM extracts of *Z. lotus*.

3.2.1 Fatty acids

3.2.1.1 Saturated fatty acids

Sixty-five fatty acids were detected in the *Z. lotus* dichloromethanolic extracts, where 24 were saturated, 13 were unsaturated, 6 were diacids, 10 were hydroxyfatty acids, 2 fatty acid methyl esters, and 10 were fatty acid methyl esters. These compounds were identified based on the EI-MS data of the corresponding TMS esters.

Trimethylsilylated derivatives of fatty acids (fatty acids-TMS) are easily identifiable by GC-MS. Their mass spectra show a typical fragmentation pattern that is characterized by the presence of peaks at m/z 117, 129, 132, and 145. The formation of the corresponding fragments is exemplified in Schemes 1, 2, 3, and 4.[35] The product ions at m/z 145 and 129 resulted from 1,3-hydrogen transfer (at m/z 145), followed by loss of methane (at m/z 129). The other two product ions at m/z 132 and 117 resulted from McLafferty rearrangement (at m/z 132) and successive loss of a methyl radical (at m/z 117).[36]

Scheme 1:

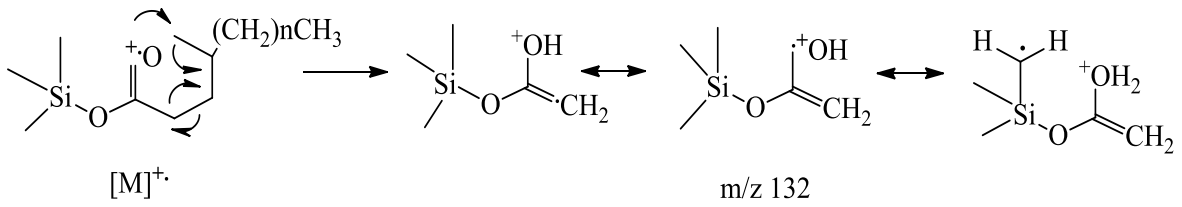

Scheme 2:

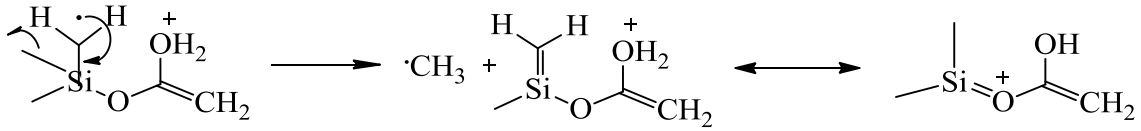

Scheme 3:

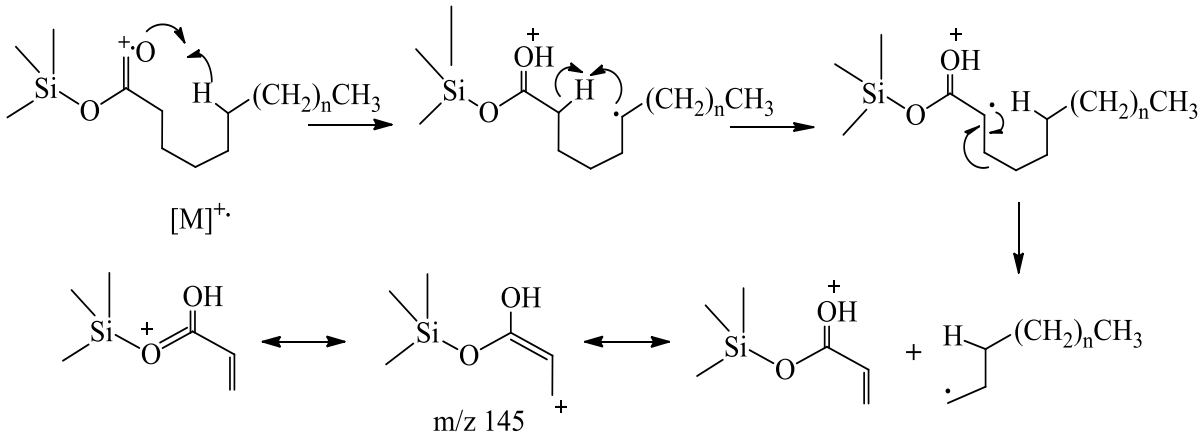

Scheme 4:

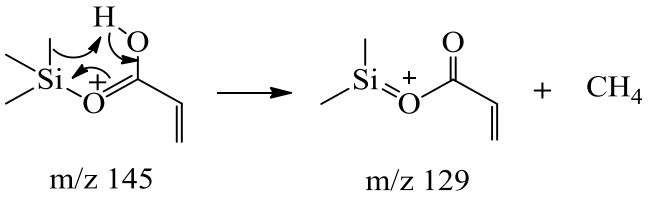

The resulting fragments of the derivatizing group, peaks at m/z 73 $[(CH_3)_3Si]^+$, 75, $[(CH_3)_2SiOH]^+$ and the one corresponding to the ion $[M–90]^+$ (Fig 2) are also common in the mass spectra of fatty acids-TMS. The $[M–15]^+$ fragment corresponds to the loss of a methyl radical from the TMS group (Scheme 5) and is often the most abundant ion in the fatty acid mass spectra.[37] This is an asset in identifying the molecular weight of the fatty acid in question.[35] Another characteristic feature of this family is that the peak corresponding to the molecular ion ($M^{+\bullet}$) has a relatively low or nonexistent abundance.[35]

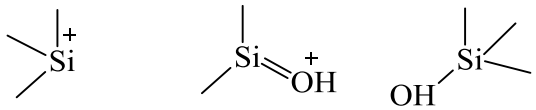

m/z 73 m/z 75 90

Figure 2: Characteristic fragments of the derivatizing group, in saturated fatty acids-TMS.

Scheme 5:

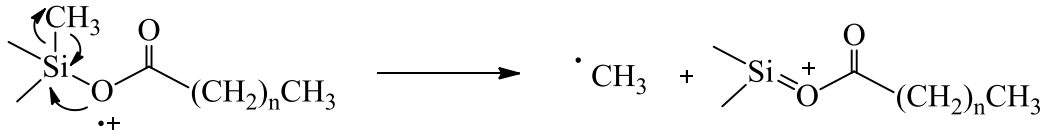

$[M]^{\bullet+}$ $[M\text{-}15]^{+}$

3.2.1.2 Unsaturated fatty acid

The mass spectrum of an unsaturated fatty acid-TMS shows the same peaks as that of saturated fatty acids i.e. m/z 73, 75, 117, 129, 132, and 145, and the corresponding to the fragment ion $[M–90\ ]^+$ and $[M–15]^+$. The big difference in the mass spectra of the unsaturated, in comparison with the saturated ones, is the relative abundance of the peak corresponding to the fragment $[M–15]^+$. As the degree of unsaturation increases, this peak decreases in intensity. However, there is little information regarding the determination of the position of unsaturation, and it is not known which of the peaks in the spectrum indicates the exact location of the double bonds.[35] The determination of the position and geometry of the double bonds is only possible by comparison with the compound mass spectra standard and spectra of the library of the device used.

3.2.1.3 Diacids

In the same way, as the other acids discussed above, the TMS-diacids spectra show the peaks at m/z 73, 75, 117, 129, 132, and 145 and the peaks corresponding to the fragments $[M\text{-}90]^+$ and $[M–15]^+$. The fragments corresponding to m/z 73 and 75 are characterized by very high abundances, and in some cases, one of them corresponds to the base peak. Besides, the peak corresponding to the ion $[M–15]^+$ shows reduced relative abundance.[38]

The characteristic fragments of TMS derivatives of diacids include ions at m/z 147 (Fig 3) with very high relative intensity, and the peak corresponding to the fragment ion $[M–15–44]^+$, with moderate intensity. The ion at m/z 147 results from the transposition of the TMS group, with the further decomposition of the molecule, while the fragment ion $[M–15–44]^+$ corresponds to the loss of methyl radical ($^{\bullet}CH_3$) from the molecular ion (mentioned above) followed by decarboxylation.[38]

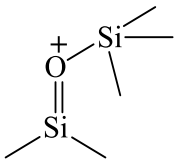

m/z 147

Figure 3: Characteristic fragment of TMS-acids.

3.2.1.4 Hydroxyfatty acids

The mass spectra of the TMS derivatives of all hydroxyfatty acids contain mass peaks characteristic of aliphatic TMS esters (m/z 117, 129, and the intense peak at $[M–15]^+$). The α, β, and γ-hydroxyfatty acids showed a base peak at $[M–117]^+$ indicate the α, β, and γ-cleavage, which confirms the presence of the hydroxy group in the α, β, and γ-position of the fatty acid (Fig 4).[28] Therefore, the mass spectra of ω-hydroxyfatty acids TMS derivatives showed prominent mass peaks at m/z 204 and 217, resulting from rearrangements of trimethylsilyl groups in long-chain compounds.[28]

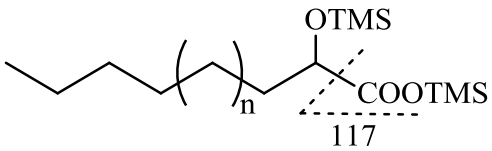

Figure 4: Characteristic fragments of hydroxyfatty acids

3.2.1.5 Fatty acid methyl and ethyl esters

The mass spectra of the methyl ester fatty acids TMS derivatives characteristic by the presence of a peak corresponding to the molecular ion and the loss of a product ion at m/z 74 by a McLafferty rearrangement of the methyl ester (Fig 5).[39,40]

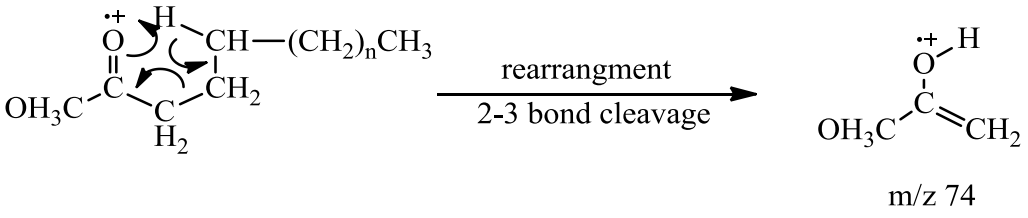

m/z 74

Figure 5: McLafferty rearrangement

Other product ions were also observed at m/z 87, 143, and $[M–43]^+$ in the mass spectra characteristic of aliphatic chain breakdown of methyl ester fatty acid (Scheme 6).[40,41]

Scheme 6:

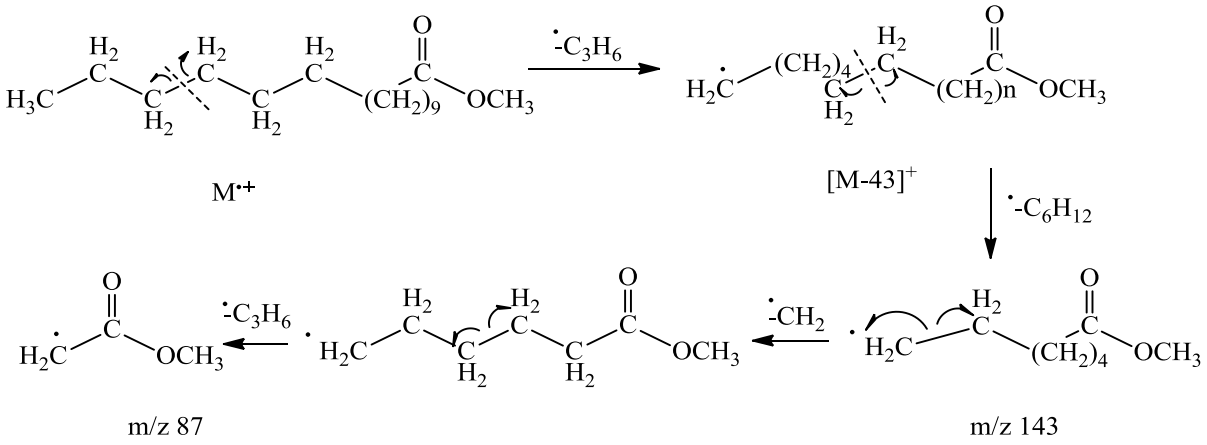

The mass spectra of the TMS derivatives of fatty acid ethyl esters also contain mass peaks characteristic of the molecular ion and the presence of a product ion at m/z 88 (McLafferty rearrangement) as a base peak and fragments resulting from the aliphatic chain breakdown as shown in methyl ester.[40]

3.2.2 Long chain aliphatic

Eleven long-chain aliphatic alcohols (LCAAc) and 2 long-chain aliphatic aldehydes (LCAAd) were identified in DCM extracts of *Z. lotus*. The access of these families has been done by comparing the Electron Ionization Mass Spectrometry (EI–MS) data and elution order of their corresponding TMS derivatives with literature data.[42–44]

3.2.2.1 Long chain aliphatic alcohol

The TMS derivatives of alcohols are a class of compounds in which the mass spectrum is observed only at peaks m/z 73 and 75 with reduced abundance. The molecular ion of TMS ether derivatives are also observed but with very low abundance or sometimes absent. The base peak was observed at fragment ion $[M–15]^+$, due to the loss of a methyl radical from the TMS group.[36] The base peak is very important for determining the molecular weight of the long chain aliphatic alcohol TMS derivative. Ions at m/z 89 and 103 $[TMSOCH_2]^+$ are also usually present in the mass spectra of TMS derivatives of fatty alcohols that help to distinguish them from the TMS derivatives of fatty acids.[36] The former was afforded by C1–C2 bond cleavage (at m/z 103) (Scheme 7), while the latter resulted from the bond cleavage between C1 and oxygen, and transition of a methyl radical from the TMS group to the oxygen (at m/z 89).[36] The characteristic product ion at m/z 117 is also observed as earlier explained.

TMS derivatives of alcohol's linear primers are characterized by the presence of the ion at m/z 103 (Scheme 6), with reduced abundance. In the case of a secondary alcohol, the characteristic ion appears at m/z 117 (Scheme 8).

Scheme 7:

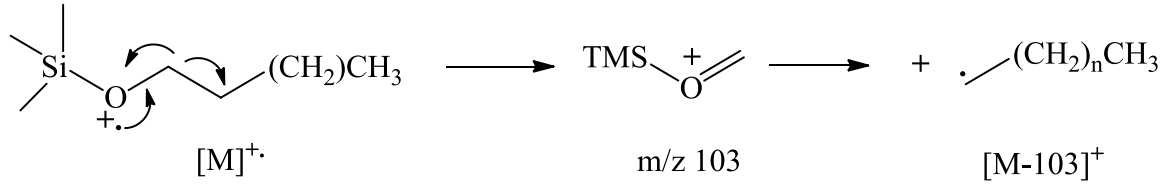

Scheme 8:

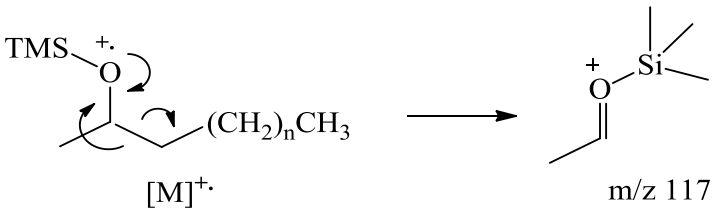

The mass spectrum of unsaturated alcohols-TMS differs from the previous ones only in the relative abundance of the peaks. The typical fragments are the same as in the saturated correspondent, however, the most abundant ion is the peak at m/z 75, instead of ion $[M–15]^+$. The molecular ion is generally detectable in relative abundance from low to reasonable.

3.2.2.2 Long chain aliphatic aldehydes

The EI mass spectrum of TMS-aldehyde displayed an ion $[M–18]^+$, which was yielded by the loss of water molecule. The molecular ion of TMS ether derivatives is generally absent in the mass spectrum of LCAAd. Additionally, the successive loss of methylene (CH_2) group from the molecule ion which gives rise to product ion at m/z 96 and 82 was also observed.[44,40]

3.2.3 Aromatic compound

Thirteen aromatic compounds were identified in the *Z. lotus* dichloromethane extracts. This family was detected as components of *Z. lotus* by comparing their mass spectra with commercial GC–MS spectral libraries and literature data.[28,29,45,46]

The benzene ring of aromatic compounds is a stable structure and for this reason, it does not normally undergo much fragmentation. However, derivatization by silylation gives rise to characteristic fragmentation patterns. In most cases, the peaks corresponding to the molecule ion and the fragment ion $[M–15]^+$ are the most abundant.[37] Two characteristic ions were registered $[M–59]^+$ and $[M–89]^+$. The fragment ion $[M–15]^+$ undergoes rearrangement and decarboxylation, giving rise to the fragment $[M–59]^+$, according to the mechanism illustrated in Scheme 9. The fragment $[M–89]^+$ is characterized by an abundance relatively higher, which may be related to the stability of the cation formed (total conjugation of unsaturated bonds). The mechanism that exemplifies the formation of this cation is shown in Scheme 10.[37]

Derivatives of cinnamic acid–TMS with a methoxy substituent on the aromatic ring are characterized by the presence of the peak corresponding to the fragment ion $[M–30]^+$ (loss of an additional methyl group). Fragmentation involves the loss of a formaldehyde molecule and represents the cleavage of the methoxy substituent on the ring, giving rise to the cation $[M–30]^+$ (Scheme 11).[37]

Scheme 9:

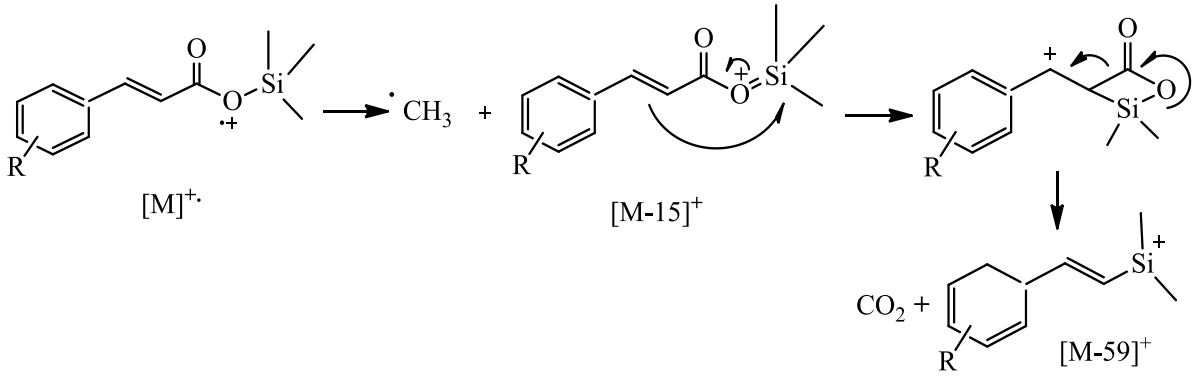

Scheme 10:

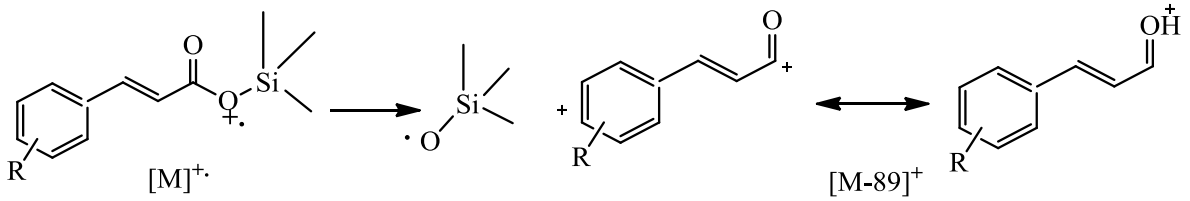

Scheme 11:

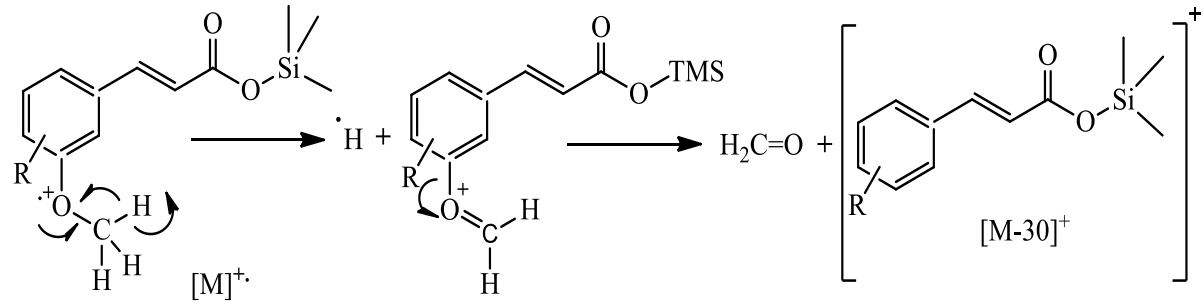

3.2.4 Monoglycerides

Six monoglycerides were identified in dichloromethane extracts of *Z. lotus* by comparing their EI-MS data and the elution order with literature data[47] and by comparing the EI-MS data of the corresponding TMS derivatives with the equipment mass spectral library.

The EI mass spectrum of monoglyceride TMS ether is characteristic by the presence of a base peak, arising from the loss of trimethylsilyloxymethyl radical (–103 Da) formed by the heterolytic cleavage between C1 and C2 of the glycerol moiety (Fig 6).[48] The loss of methylene group $[M–15]^+$ from the molecule ion was observed with a low abundance along with the ion at m/z 73, corresponding to trimethylsilyl radical. Moreover, ions containing one or both of the silicon atoms dominate the spectrum, e.g. m/z 103, 129, 147, and 218, and depending on the molecular weight and degree of unsaturation of the fatty acid chain that at m/z 129 or 218 can be the most abundant. Additionally, the ion at m/z 218 was more prominent in the EI mass spectrum of the 2-monoglyceride derivatives than in those of 1-monoglycerides. The intensity of the acyl ion (palmitoyl, linoleyl, linolenoyl, oleoyl, and stearoyl) is less than in those of the parent monoglycerides.[49]

Therefore, the glycerol part is susceptible to the loss of water molecule or a hydroxy-methylene group to produce peaks of m/z 116 or m/z 103, respectively. These losses take place either from the parent ion or after the loss of the hydrocarbon fragment from the parent ion. Other product ions were also observed at m/z 147 and 205 which are associated with the silylated glycerol backbone.[49]

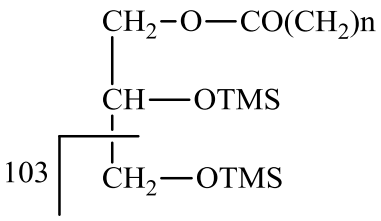

Figure 6: Characteristic fragments of monoglyceride TMS ether derivatives.

3.2.5 Tocopherols

Two tocopherols isomers were identified in the *Z. lotus* dichloromethane extracts based on the EI-MS data of the corresponding TMS esters. The EI fragmentation of tocopherol TMS ether yielded the molecular ion as a base peak. A product ion arose from the loss of the side aliphatic chain and part of the epoxide ($[M–265]^+$) was also observed as an intense peak. Besides, a low relative abundance peak was detected due to the loss of side aliphatic chain ($[M–225]^+$) (Fig 7).[50]

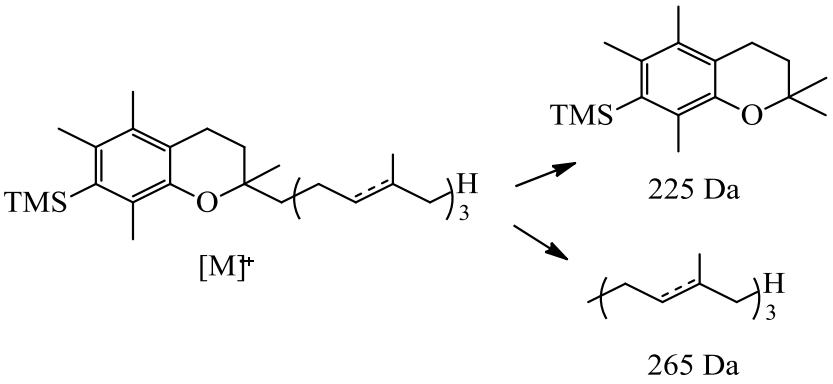

Figure 7: Characteristic fragments of tocopherol TMS ether derivatives.

3.2.6 Sterols

The identification of three sterols in *Z. lotus* dichloromethane extracts was approached by comparing the EI-MS data, elution order, and retention time of the corresponding TMS ethers with the literature data. The mass spectra of TMS-sterol derivatives are characterized by the presence of a large number of peaks with moderate to high relative abundances. Not all fragments found in these spectra are essential for the identification of sterols. The spectra of TMS-sterols are characterized by the presence of a very abundant peak at m/z 257 corresponds to the fragment $[M–CL–TMSOH]^+$ which results from a double fragmentation (Fig 8). The loss of the complete side chain (CL) occurs, with a break in the C-17/C-20 carbons, accompanied by the transfer of two protons (17α-H and 14α-H) and migration of the methyl group from C-18 to C-17. In position C-3 there is a loss of derivatizing group in the form of TMS–OH.[51,52]

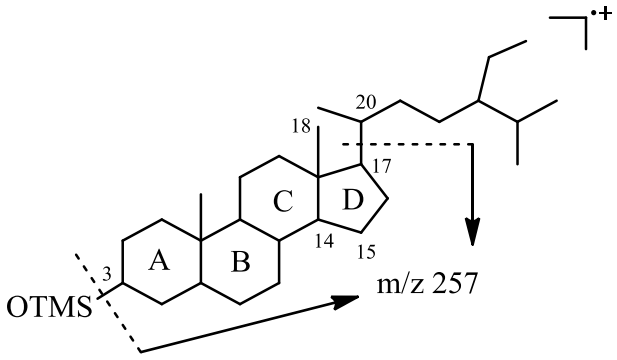

Figure 8: Characteristic fragments site to give rise to the ion with m/z 257.

A consequent fragmentation gives rise to the ion $[M–CL–42–TMSOH]^+$ that corresponds to the peak at m/z 215 (Fig 9). The loss of fragment 42 corresponds to the loss of C_3H_6 in D-ring.[51]

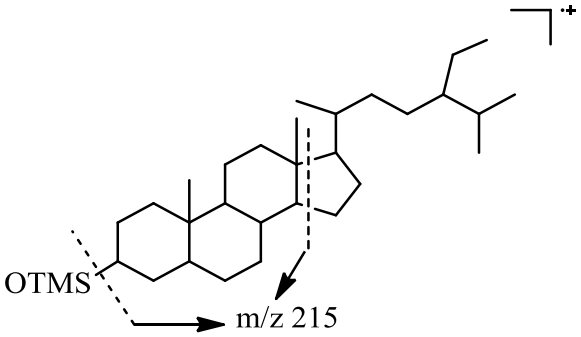

Figure 9: characteristic fragments site to give rise to the ion with m/z 215.

The peaks described at m/z 257 and 215 refer to saturated sterols. In the case of sterols with unsaturation in the ABC ring system (the site of unsaturation is indifferent), the same fragmentation processes occur, obtaining the fragments with m/z 255 and 213. The product ion at m/z 213 was formed by the loss of the side chain and the D-ring (C15-C17), followed by the loss of the trimethylsilanol (–90 Da). The peak at m/z 255 is due to the loss of the side chain, followed by the loss of trimethylsilanol.[36] The $[M–CL–42–TMSOH]^+$ is preponderant to identify the number of unsaturation's in rings A, B, and C.[32,51] On the other hand, this fragment allows determining the mass of the side chain of the sterols. The difference in mass between the molecular ion and the fragment $[M–CL–42–TMSOH]^+$ (note that 42+90 must be added) corresponds to the mass of the side chain.[32]

Other moderate abundances peaks were noticed at m/z 73, 75, $[M–15]^+$, $[M–89–H]^+$, $[M–89–H–CH_3]^+$, 129, and $[M–129]^+$, which provide the structural information. The pair of product ions observed by m/z 129 and $[M–129]^+$ derived, respectively from the C1-C10 and C3-C4 bonds cleavages, being characteristic of the EI fragmentation of TMS derivatives (Fig 10).[32,36]

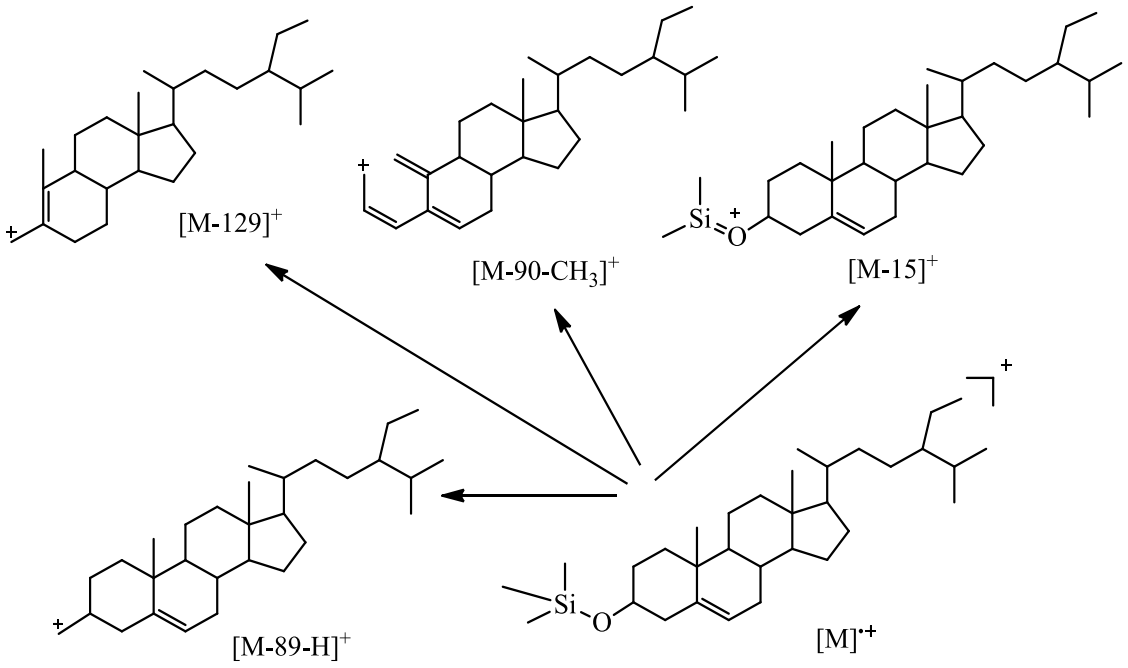

Figure 10: Ion fragmentation sites of $[M\text{-}15]^+$, $[M\text{-}89\text{-}H]^+$, $[M\text{-}90\text{-}CH_3]^+$, and $[M\text{-}129]^+$.

3.2.7 Pentacyclic triterpenes

Four triterpenic acids were identified in *Z. lotus* dichloromethane extracts by systematic interpretation of their mass spectra and also by their elution order.[30,42,53,54]

Oleanolic (oleA) and ursolic acids (ursA) are structurally isomeric pentacyclic triterpene acids that can be well distinguished by order of elution during gas chromatography (ursA is retained longer than oleA) and by intensities of the fragment ion signals in their mass spectra, where the retro-Diels-Alder (rDA) reaction was primarily observed.[42] The most important signals are found at m/z 600 $[M]^{+\bullet}$, 585 $[M–CH3]^+$, 510 $[M–TMSOH]^+$, 495 $[M–TMSOH–CH_3]^+$, 482 $[M–TMSOOCH]^+$, 393 $[M–TMSOH–TMSOOC]^+$, and 392 $[M–TMSOH–TMSOOCH]^+$ (Fig 11). The presence of a double bond C12=C13 originates a rDA reaction, resulting in the formation of two fragments containing rings A, B, and part of C, on one side, and the rings D, E, and part of C on the other.[30] The generated fragments results in the characteristic signals at m/z 320, 279, 203, and 133 shown in Figure 11. At this point, the mass spectrum for oleA becomes different from that of ursA. Observable differences are the intensities of the fragment ion signals at m/z 133 and 320, where both of them are more intense for ursA than for oleA.[42,53]

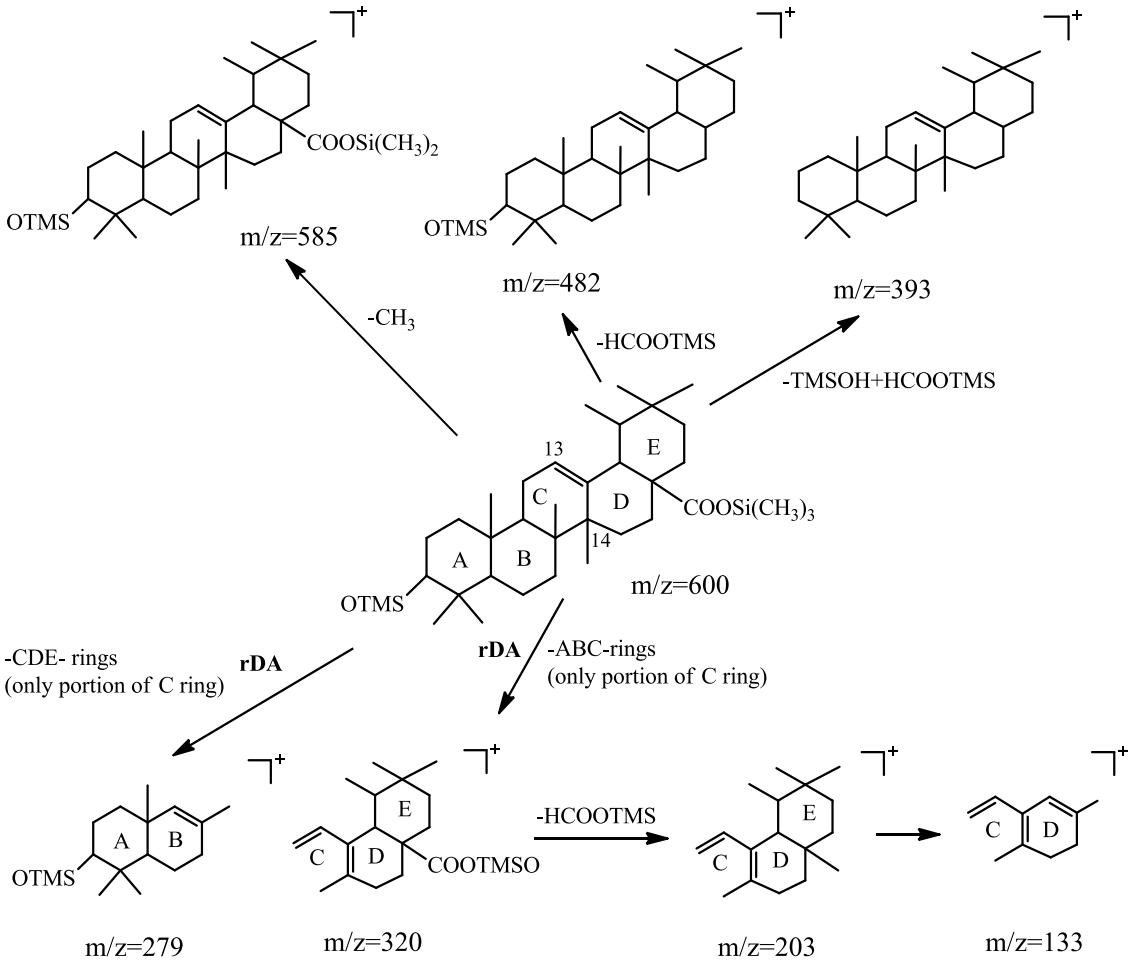

Figure 11: Characteristic fragmentation of oleanolic and ursolic acids TMS ether derivatives.

Otherwise, the EI mass spectrum of the lupeol TMS ether displayed the molecular ion at m/z 498 and the base peak at m/z 189 which contained the D and E rings, after C12-C13 and C8-C14 bonds cleavages (Fig 12). The loss of the propenyl moiety from molecular ion yielded a product ion at m/z 456. Two product ions were formed due to the cleavage of C9-C11 and C8-C14 bonds, namely at m/z 279, containing the A and B rings, and at m/z 218, presenting the D and E rings. An intense peak was noted at m/z 161, whose product ion was due to the loss of CH_2 from the ion at m/z 175. Cleavages of the C18-C19 and C21-C22 bonds in the ion at m/z 203 gave origin to the product ion at m/z 135.[36]

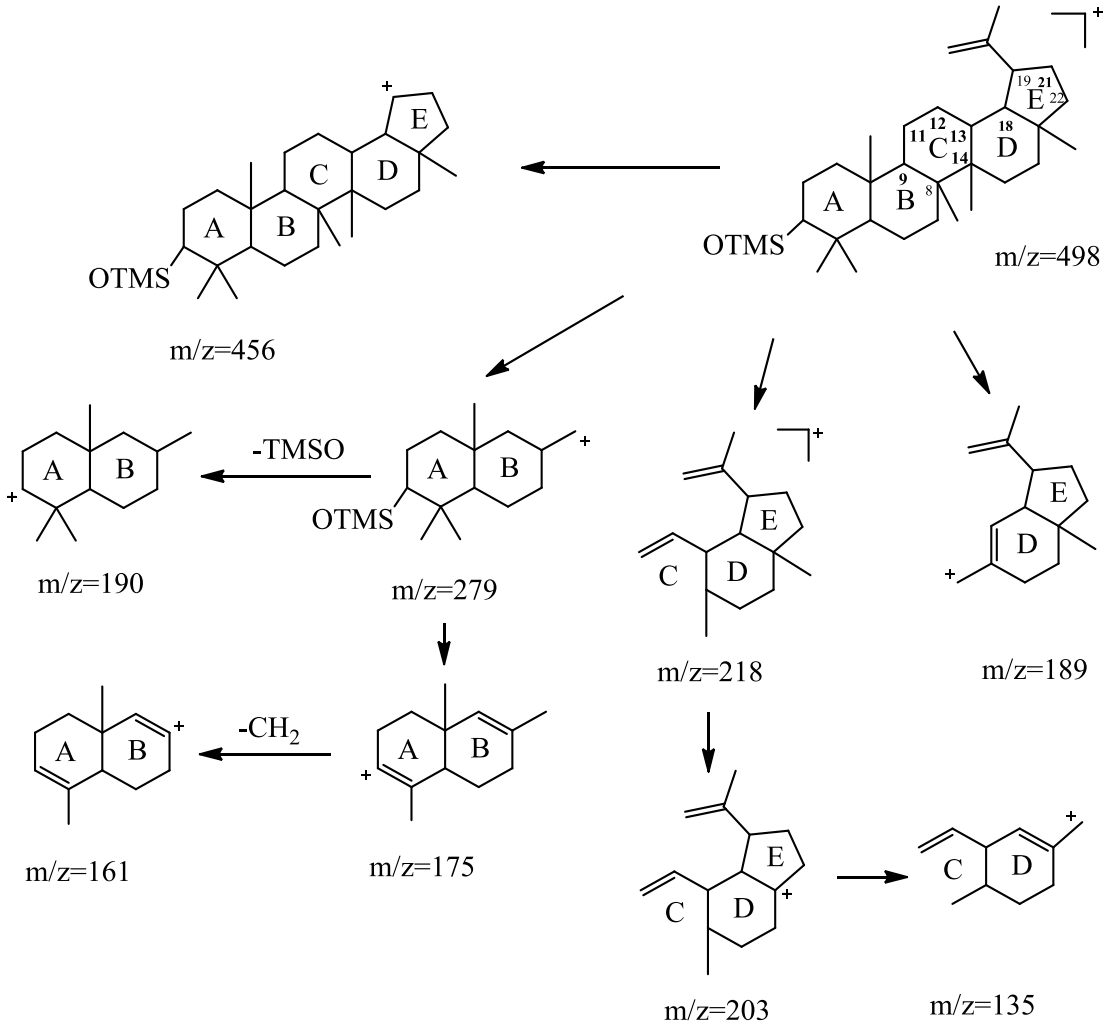

Figure 12: Characteristic fragments of lupeol TMS ether derivatives.

The chemical structure of betA is very similar to that of lupeol except for the presence of an additional carboxylic group in the ring of the lupane-type triterpenes structure (Fig 13). Thus, the mass spectra were very similar to those of oleA and ursA with base peaks of the lupeol structure at m/z 189. In this case, the spectrum of betA shows the molecular ion at m/z 600 and the fragment ions at m/z 585 and 557, corresponding to the respective loss of methyl and the isopropyl units, respectively. Other characteristic fragments of the TMS derivative of this compound are found at m/z 279, 292, and 320 as explained in the Figure 13. Besides, the loss of the TMSOH and TMSOOCH groups resulted in m/z 510 and 483, respectively.[42,53,54]

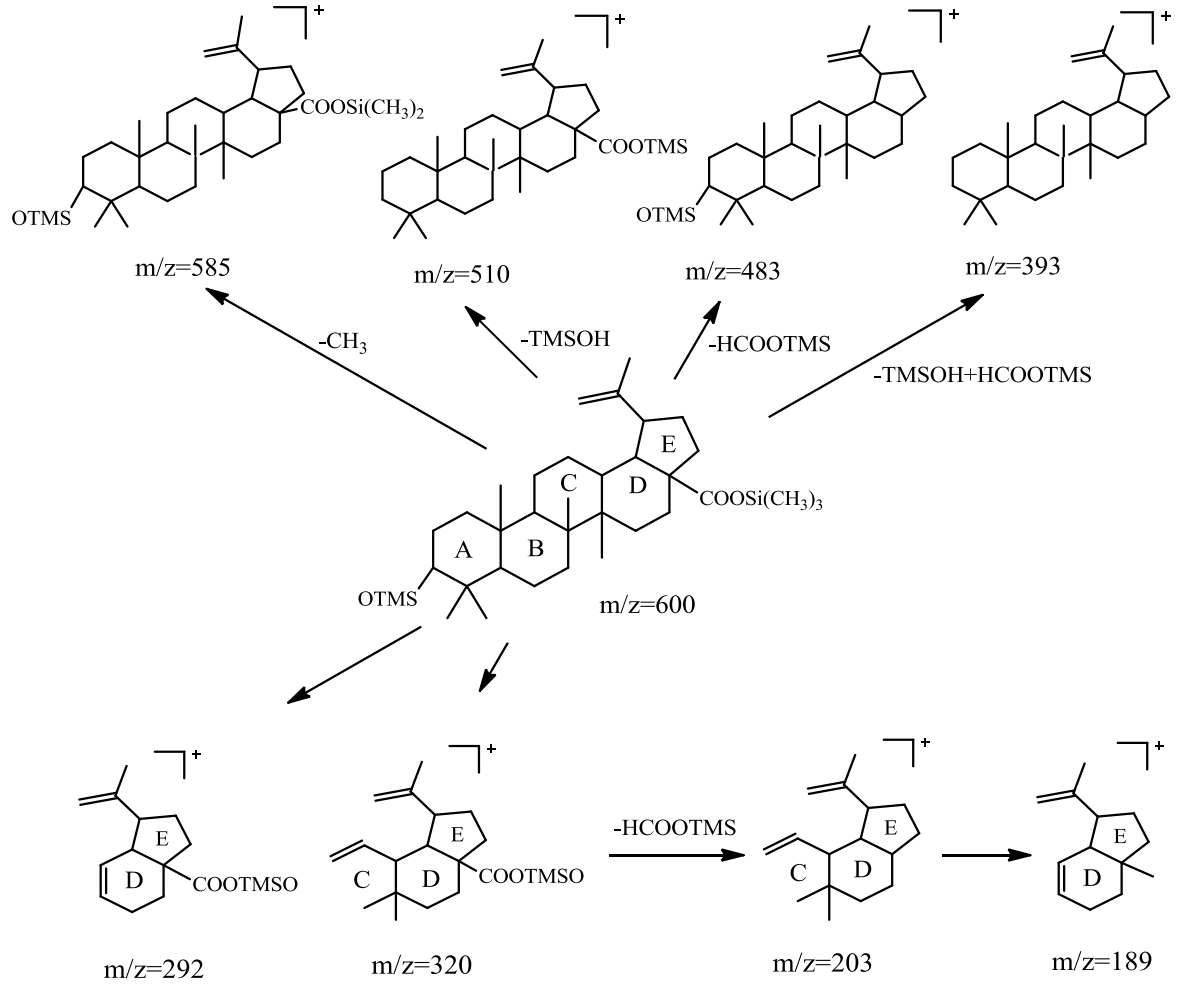

Figure 13: Characteristic fragmentation of betulinic acid TMS ether derivatives.

3.2.8 Other compounds

Besides the beyond families, other compounds were identified in *Z. lotus* dichloromethane extracts, especially in the leaf extract. The identification of phytol, squalene, inositol, erythrono-1,4-lactone, 2-furoic acid, loliolide, solerol, butane-2,3-diol, 1,2,3-butanetriol, tetracosyl acetate, nonacosan-10-one, and neophytadiene was performed by comparing the EI mass spectroscopic data with the literature.[36,55–60]

The EI mass spectrum of the phytol TMS derivative ($[M]^{+\bullet}$ at m/z 296) depicts the dominated peak at m/z 143 which most likely involves an allyl-cleavage. The peak at m/z 123, involving further fragmentation into the $[C_9H_{15}]^+$ fragment ion, consisting of carbons C–1 to C–7 of phytol and a low abundant ion at m/z 353 ($[M–15]^+$) at the higher mass characteristic of the loss of a methylene group of TMS.[55,36]

The EI mass spectrum of squalene TMS derivative ($[M]^{+\bullet}$ at m/z 410) revealed the base peak at m/z 69, due to the cleavage of the C4–C5 bond. A product ion at m/z 137 resulted from the C8–C9 bond cleavage.[36]

The EI mass spectrum of the inositol TMS derivative ($[M]^{+\bullet}$ at m/z 612) depicts the base peak at m/z 73 due to the formation of the $[(CH_3)_3Si]^+$ ion. The peak at m/z 75, regarding the

$[(CH_3)_2SiOH]^+$ ion, also exhibited high relative abundance. The product ion at m/z 305 also revealed high relative abundance, resulting from cleavages on the C1–C2 and C4–C5 bonds.[61]

The EI mass spectrum of the 2-furoic acid TMS derivative ($[M]^{+\bullet}$ at m/z 169) displayed a peak at m/z 73 (TMS) as a base peak, 95 (OTMS) with a high intensity along with $[M–15]^+$.[57]

The EI mass spectrum of the neophytadiene TMS derivatives ($[M]^{+\bullet}$ at m/z 278) demonstrated the major product ions at m/z 57($[C_4H_9]^+$), 66, 82, 95 ($[C_7H_{11}]^+$), and 123 ($[C_9H_{15}]^+$) correspond to the break-down of the aliphatic chain.[58]

3.3 Quantification analysis of the identified compounds in *Z. lotus* dichloromethane extracts

The GC–MS analysis revealed a remarkable diversity prevailing in the *Z. lotus* extracts, with fatty acid and triterpenes being the predominant families of all Z. *lotus* extracts, followed by sterols, and long-chain aliphatic alcohols. Apart from the aforementioned families, fatty acid esters, monoglycerides, aromatic compounds, and other minor components were also identified in the four morphological parts of *Zizyphus lotus*.

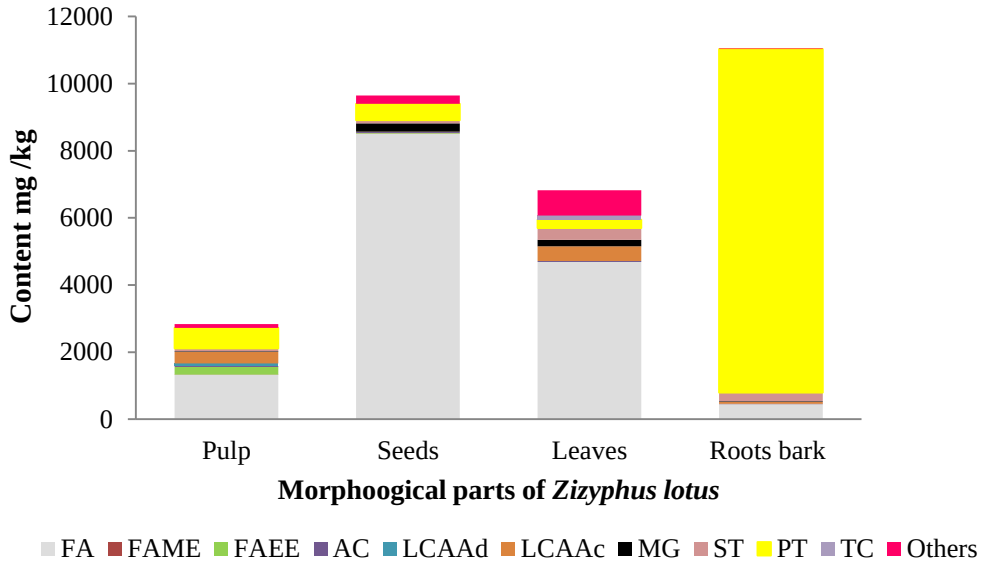

Figure 14: Major families of lipophilic compounds identified in dichloromethane extracts of *Zizyphus lotus.* Abbreviations: AC, aromatic compounds; FA, fatty acids; FAEE, fatty acid ethyl esters; FAME, fatty acid methyl esters; LCAAc, long chain aliphatic alcohols; LCAAd, long chain aliphatic aldehydes; MG, monoglycerides; PT, pentacyclic triterpenes; ST, sterols; TC, tocopherols.

3.3.1 Fatty acids

Twenty four saturated fatty acids, 13 unsaturated fatty acids, among others, belong to the diacids and hydroxyfatty acids were identified and quantified in the four morphological parts of *Z. lotus* (Table 2). Fatty acids represented the major family of lipophilic components of all *Z. lotus* fractions, except for the root barks. To the best of our knowledge, this family is described for the first time in root barks, while the presence of some identified saturated and unsaturated fatty acids has already been reported in leaves, seeds, and pulp extracts.[4,12,13]

Table 2: Semi-quantitative analysis (mg/kg of dry weight) of dichloromethane fatty acids extracts from four morphological parts of *Zizyphus lotus*.*

RT (min)	Fatty acids	Pulp	Leaves	Root barks	Seeds
	Saturated fatty acids	**812**	**1470**	**278**	**1274**
6.12	Propanoic acid	n.d.	n.d.	1	n.d.
6.22	Hexanoic acid	6	5	7	11
12.88	Octanoic acid	4	3	2	4
16.28	Nonanoic acid	3	1	3	n.d.
19.50	Decanoic acid	67	5	1	5
22.58	Undecanoic acid	9	n.d.	n.d.	n.d.
25.49	Dodecanoic acid	17	4	2	2
28.25	Tridecanoic acid	4	n.d.	n.d.	n.d.
30.89	Tetradecanoic acid	28	52	n.d.	10
33.40	Pentadecanoic acid	9	5	2	4
35.82	Hexadecanoic acid	366	877	152	594
38.10	Heptadecanoic acid	22	8	7	7
40.32	Octadecanoic acid	42	276	49	570
42.43	Nonadecanoic acid	2	n.d.	1	n.d.
44.48	Eicosanoic acid	16	40	7	48
46.48	Heneicosanoic acid	5	3	3	n.d.
48.34	Docosanoic acid	10	25	13	19
50.16	Tricosanoic acid	n.d.	n.d.	9	n.d.
52.04	Tetracosanoic acid	10	26	14	n.d.
54.02	Pentacosanoic acid	3	9	5	n.d.
56.10	Hexacosanoic acid	10	52	n.d.	n.d.
58.30	Heptacosanoic acid	11	n.d.	n.d.	n.d.
60.56	Octacosanoic acid	114	79	n.d.	n.d.
65.51	Triacontanoic acid	54	tr	n.d.	n.d.
	Unsaturated fatty acids	**421**	**3175**	**159**	**7222**
30.19	Tetradec-9-enoic acid isomer	2	n.d.	n.d.	n.d.
35.05	Hexadecenoic acid isomer	4	4	2	10
35.19	(9*Z*)-Hexadec-9-enoic acid	40	23	2	11
35.44	(9*E*)-Hexadec-9-enoic acid	7	n.d.	2	n.d.
37.44	Heptadec-10-enoic acid isomer	24	n.d.	n.d.	7
37.52	(9*Z*)-Heptadec-9-enoic acid	n.d.	n.d.	1	n.d.
37.60	(9*E*)-Heptadec-9-enoic acid	n.d.	n.d.	1	n.d.
39.42	(9*Z*,12*Z*)-Octadeca-9,12-dienoic acid	60	544	50	737
39.50	(9*Z*,12*Z*,15*Z*)-Octadeca-9,12,15trienoic acid	45	2431	9	n.d.
39.62	(9*Z*)-Octadec-9-enoic acid	179	120	59	6255

39.78	(9*E*)-Octadec-9-enoic acid	50	54	18	135
41.72	Nonadecenoic acid isomer	7	n.d.	n.d.	n.d.
43.83	Eicos-11-enoic acid	2	0.2	14	66
	Diacids	**22**	**28**	**9**	**5**
8.03	Ethanedioic acid	1	n.d.	n.d.	n.d
14.62	Butanedioic acid	7	1	n.d.	n.d.
21.01	Hexanedioic acid	2	n.d.	n.d.	n.d.
21.13	2-Hydroxybutanedioic acid	n.d.	8	3	n.d.
29.45	Nonadioic acid	4	19	6	5
45.19	Hexadecanedioic acid	7	n.d.	n.d.	n.d.
	Hydroxyfatty acids	**67**	**19**	**9**	**n.d.**
6.12	2-Hydroxypropanoic acid	7	2	tr	n.d.
6.46	2-hydroxyethanoic acid	6	2	n.d.	n.d.
8.79	3-Hydroxypropanoic acid	12	7	n.d.	n.d.
12.12	4-Hydroxybutanoic acid	tr	1	n.d.	n.d.
12.30	3-Hydroxypentanoic acid	4	n.d.	n.d.	n.d.
12.49	2-Hydroxyhexanoic acid isomer a	14	n.d.	n.d.	n.d.
12.58	2-Hydroxyhexanoic acid isomer b	9	n.d.	n.d.	n.d.
14.03	3-Hydroxyhexanoic acid	6	n.d.	n.d.	n.d.
55.04	22-Hydroxydocosanoic acid	5	7	9	n.d.
55.24	2-Hydroxytetracosanoic acid	5	n.d.	n.d.	n.d.
	Fatty acid methyl esters	**5**	**n.d.**	**1**	**15**
32.53	Methyl hexadecanoate	5	n.d.	n.d.	n.d.
36.67	Methyl (9*Z*)-octadec-9-enoate	n.d.	n.d.	1	15
	Fatty acid ethyl esters	**228**	**n.d.**	**n.d.**	**16**
17.08	Ethyl decanoate	1	n.d.	n.d.	n.d.
29.11	Ethyl tetradecanoate	11	n.d.	n.d.	n.d.
31.74	Ethyl pentadecanoate	4	n.d.	n.d.	n.d.
33.62	Ethyl hexadec-9-enoate isomer a	12	n.d.	n.d.	n.d.
33.86	Ethyl hexadec-9-enoate isomer b	3	n.d.	n.d.	n.d.
34.26	Ethyl hexadecanoate	104	n.d.	n.d.	5
38.24	Ethyl (9*Z*)-octadec-9-enoate	33	n.d.	n.d.	11
38.39	Ethyl (9*E*)-octadec-9-enoate	25	n.d.	n.d.	n.d.
38.95	Ethyl octadecanoate	29	n.d.	n.d.	n.d.
43.27	Ethyl eicosanoate	6	n.d.	n.d.	n.d.
	Total	**1322**	**4692**	**455**	**8501**

*Results represent the average of the concordant values obtained for the six aliquots of each sample. Abbreviations: n.d, not detected; tr, traces.

Different assortment of saturated fatty acids (SFA) was identified in this shrub species with hexadecanoic acid as the most abundant SFA in all *Z. lotus* extracts, ranging from 152 mg/kg dw in root barks to 877 mg/kg dw in the leaves. However, an equivalent quantitative distribution of octadecanoic acid in pulp and root barks was measured, with a maximum amount in the seeds fraction (570 mg/kg dw). Other SFA ranging from propanoic (n-$C_{3:0}$) to triacontanoic (n-$C_{30:0}$) acids, were also detected but in low amounts in the studied extracts. Moreover, tetradecanoic, octadecanoic, eicosanoic, docasanoic, and tetracosanoic acid were identified here for the first time as *Z. lotus* constituents.[4,12]

The unsaturated fatty acids (UFA) represented about 31.8-84.9% of the total identified fatty acids of *Z. lotus* with (9Z)-octadec-9-enoic acid (oleic acid), being the most abundant UFA in all *Z. lotus* extracts (59–6255 mg/kg dw in root barks and seeds, respectively), except in the leaves. The abundance of UFA observed in the leaves, is mainly due to the presence of octadeca-9,12,15-trienoic (linolenic acid; ω-3) (**3**) and octadeca-9,12-dienoic acids (linoleic acid; ω-6), accounting together 2975 mg/kg, and corresponding 93.7% of the total UFA detected in the leaves extract.

Omega-3 and ω-6 polyunsaturated fatty acids (PUFAs) are known to be essential fatty acids for humans that must be derived from the diet. Both types offer health benefits.[62,63] However, the importance of a balanced intake of ω-6 and ω-3 PUFAs is necessary to prevent and manage many diseases. The ideal ratio (ω-6/ω-3) would be approximately between 1 and 5 which related to a significant decreased in inflammatory, cancer, cardiovascular, and autoimmune diseases.[64] The PUFAs ω-6 and ω-3 fatty acids ratio (ω-6/ω-3, correspond to the ratio linoleic/linolenic acids) detected in pulp lipophilic fraction of *Z. lotus* is 1.33. This value should be taken into account in the overall assessment of *Z. lotus* benefits. Moreover, minor amounts of (9E)-otadec-9-enoic acid (18-135 mg/kg), and eicos-11-enoic acid (0.2-66 mg/kg dw) which were also detected for the first time as lipophilic components of *Z. lotus* species.

A wide range of fatty acid esters (FAEE) were identified as components of *Z. lotus* at low abundance, with ethyl hexadecanoate remains the major FAEE, accounting up to 45.6% of the total FAEE content identified in the pulp extract (Table 2). According to the results, the FAEE family was only detected in the pulp part, except ethyl hexadecanoate and ethyl (9*Z*)-octadec-9-enoate were also detected in seeds with respective amounts of 5 and 11 mg/kg dw. Other FAEE from C_{12} (Ethyl decanoate) to C_{22} (Ethyl eicosanoate) were also detected, although in lower amounts (Table 2). Two fatty methyl esters were identified namely methyl (9Z)-octadec-9-enoate in seeds and root barks while, methyl hexadecanoate is present only in the pulp extract. So far, the investigation of these compounds has been quite scarce despite their promising biological activities.[65] However, it should be noted that these components were previously detected in seeds oil of this shrub species, except ethyl eicosanoate and the two methyl ester fatty acids which were reported here for the first time as components of *Z. lotus*.[66]

Finally, six diacids were detected among the minor components, with nonadioic acid (**6**), being the most abundant diacids in all *Z. lotus* lipophilic extracts, except for the pulp extract. Besides, ten hydroxyfatty acids were mainly found concentrated in the pulp fraction as shown in Table 2, with a value of 67 mg/kg dw.

3.3.2 Pentacyclic triterpenes

Triterpenes are another abundant family that characterizes the lipophilic profile of *Z. lotus* species, accounting from 3.6% to 92.6% of the total lipophilic components detected (Table 3). Indeed lupeol, oleanolic, betulinic, and ursolic acids are common triterpenoids in genus Zizyphus species[67,68] however, as far as our literature survey could ascertain a detailed identification and quantification of these compounds in *Z. lotus*, as described here, has not been reported so far.

Table 3: Semi-quantitative analysis (mg/kg of dry weight) of dichloromethane pentacyclic triterpenes extracts from four morphological parts of *Zizyphus lotus*.*

RT (min)	Pentacyclic triterpenes	Pulp	Leaves	Root barks	Seeds
63.86	Lupeol	n.d.	78	105	n.d.
69.21	Oleanolic acid	103	51	287	164
69.82	Betulinic acid	160	119	9838	238
70.72	Ursolic acid	345	n.d.	n.d.	81
	Total	**608**	**248**	**10230**	**483**

*Results represent the average of the concordant values obtained for the six aliquots of each sample. Abbreviations: n.d, not detected; tr, traces.

According to the results, root barks extract shows a composition quite similar to that described for leaves but with a much higher abundance of triterpenic compounds, which account for around 10230 mg/kg dw, mainly due to betulinic acid which individually accounts for 9838 mg/kg dw (Table 3). The presence of betA in root barks with such amount, besides its outstanding pharmacological activities,[69] will enhance the value of this shrub species as an edible plant through its exploitation as the biomass of betA extraction.

A noteworthy aspect of this shrub presented in the attendance of ursA exclusively in fruit part with an amount of 81 mg/kg dw in the seeds and 345 mg/kg dw in the pulp fraction, and the absence of lupeol, which in turn exists only in the leaves and root barks lipophilic extracts of *Z. lotus* (78-105 mg/kg dw, respectively). OleA is another triterpenic acid detected as a component of *Z. lotus*, accounting from 51 mg/kg dw in the leaves to 287 mg/kg dw in the root barks.

3.3.3 Sterols

GC-MS analysis also allowed the identification of three sterols concentrated in the root barks and leaves with the amounts of 257 and 355 mg/kg dw, respectively (Table 4).

Table 4: Semi-quantitative analysis (mg/kg of dry weight) of dichloromethane sterols extracts from four morphological parts of *Zizyphus lotus*.*

RT (min)	Sterols	Pulp	Leaves	Root barks	Seeds
60.70	Campesterol	n.d.	28	4	n.d.
61.41	Stigmasterol	13	119	126	n.d.
62.79	*β*-sitosterol	68	208	127	96
	Total	**81**	**355**	**257**	**96**

*Results represent the average of the concordant values obtained for the six aliquots of each sample. Abbreviations: n.d, not detected.

β-Sitosterol is the main sterols present in all morphological parts of *Z. lotus*, ranging from 68 mg/kg dw in the leaves to 208 mg/kg dwin the seeds extract. Stigmasterol is present in all morphological parts, except in the seeds, while campesterol is only detected in the root bark and leaves with a low amount (4 and 28 mg/kg dw, respectively). The sterols components were identified based on their very characteristic fragmentation patterns.[70] As far as we know, this is the first study, reporting the sterols as constituents of *Z. lotus*. Therefore, the three sterols have previously been reported in the *Z. lotus* seed oil.[12] The presence of these sterols as lipophilic phytochemicals in the *Z. lotus* with their various beneficial health effects[71] will increase the value of this shrub as an edible plant.

3.3.4 Long chain aliphatic alcohols and aldehydes

Long chain aliphatic alcohols, were reported here for the first time as a component of lipophilic fractions of *Z. lotus* species, corresponding from traces to 11.9% of the total amount of detected compounds (Table 5).

Table 5: Semi-quantitative analysis (mg/kg of dry weight) of dichloromethane long chain aliphatic alcohols extracts from four morphological parts of *Zizyphus lotus*.*

RT (min)	Long chain aliphatic alcohols	Pulp	Leaves	Root barks	Seeds
28.89	Tetradecan-1-ol	n.d.	n.d.	2	n.d.
33.96	Hexadecan-1-ol	4	4	9	2
37.87	9*Z*-Octadec-9-en-1-ol	9	11	14	n.d.
38.60	Octadecan-1-ol	4	2	6	n.d.
46.83	Docosan-1-ol	3	n.d.	3	n.d.
50.51	Tetracosan-1-ol	n.d.	5	3	n.d.
54.36	Hexacosan-1-ol	7	118	3	n.d.
56.46	Heptacosan-1-ol	8	23	n.d.	n.d.
58.65	Octacosan-1-ol	207	230	11	n.d.
60.91	Nonacosan-1-ol	19	13	n.d.	n.d.
63.24	Triacontan-1-ol	79	31	n.d.	n.d.
	Total	**340**	**438**	**51**	**2**

*Results represent the average of the concordant values obtained for the six aliquots of each sample. Abbreviations: n.d, not detected.

This family is concentrated in the pulp (340 mg/kg dw) and leaves extracts (438 mg/kg dw), with octacosan-1-ol remains the predominant LCAAc (11–230 mg/kg dw), presents in all *Z. lotus* samples, except in the seeds. Other LCAAc from C_{14} (Tetradecan-1-ol) to C_{60} (Triacontan-1-ol) were detected in root barks, leaves, and pulp extracts of *Z. lotus*, except in the seeds, which characterized by the only presence of hexadecan-1-ol (2 mg/kg dw).

Two long chain aliphatic aldehydes were detected for the first time and only as a component of pulp extract, with octasosanal being the most abundant LCAAd accounting for 65% of the total LCAAd content.

Table 6: Semi-quantitative analysis (mg/kg of dry weight) of dichloromethane long chain aliphatic aldehydes extracts from four morphological parts of *Zizyphus lotus*.*

RT (min)	Long chain aliphatic aldehydes	Pulp	Leaves	Root barks	Seeds
55.82	Octacosanal	52	n.d.	n.d.	n.d.
60.35	Triacontanal	27	n.d.	n.d.	n.d.
	Total	**80**	**n.d.**	**n.d.**	**n.d.**

*Results represent the average of the concordant values obtained for the six aliquots of each sample. Abbreviations: n.d, not detected.

3.3.5 Monoglycerides

Particular attention should be paid to the values acquired by several monoglycerides detected in all morphological parts of *Z. lotus* (Table 7).

Table 7: Semi-quantitative analysis (mg/kg of dry weight) of dichloromethane monoglycerides extracts from four morphological parts of *Zizyphus lotus*.*

RT (min)	Monoglycerides	Pulp	Leaves	Root barks	Seeds
47.05	2-Palmitoylglycerol	n.d.	5	n.d.	3
47.67	1-Palmitoylglycerol	13	47	12	44
50.61	1-Linoleylglycerol	n.d.	30	3	35
50.72	1-Linolenoylglycerol	n.d.	84	n.d.	n.d.
50.73	1-Oleoylglycerol	14	n.d.	4	155
51.28	1-Stearoylglycerol	n.d.	24	4	17
	Total	**27**	**189**	**24**	**255**

*Results represent the average of the concordant values obtained for the six aliquots of each sample. Abbreviations: n.d, not detected.

This family was concentrated in the leaves and seeds (189 and 255 mg/kg dw, respectively) due to the presence of 1-linolenoylglycerol in leaves and 1-oleoylglycerol in the seeds extract, representing 44.4% and 60.7% of the total monoglycerides content, respectively. To our knowledge, the six monoglycerides were described here for the first time as components of *Z. lotus*.

3.3.6 Aromatic and other compounds

Apart from the major families reported above, aromatic compounds are represented by thirteen compounds distributed unequally in the four morphological parts of *Z. lotus* in quite

low amounts, ranging from 11 mg/kg dw in the root barks to 31 mg/kg dw in the seeds extract (Table 8). Benzoic acid (**18**) is the major aromatic compound detected in the pulp, while vanillin (**19**) was mainly concentrated in the seeds extract.

Table 8: Semi-quantitative analysis (mg/kg of dry weight) of dichloromethane aromatic compounds extracts from four morphological parts of *Zizyphus lotus*.*

RT (min)	Aromatic compounds	Pulp	Leaves	Root barks	Seeds
11.71	Benzoic acid	23	5	n.d.	2
21.00	Vanillin	n.d.	n.d.	3	20
21.02	2-hydroxybenzoic acid	n.d.	4	n.d.	n.d.
24.65	4-hydroxybenzoic acid	n.d.	3	n.d.	n.d.
24.99	Vanillyl alcohol	n.d.	n.d.	1	5
25.93	Syringaldehyde	n.d.	n.d.	1	n.d.
27.00	Homovanillyl alcohol	n.d.	n.d.	2	n.d.
28.39	Vanillic acid	4	n.d.	2	4
28.96	Hydroxytyrosol	n.d.	n.d.	2	n.d.
30.42	Protocatechuic acid	n.d.	n.d.	0.3	n.d.
31.86	Syringic acid	n.d.	n.d.	1	n.d.
32.88	*p*-Coumaric acid	2	5	n.d.	n.d.
36.54	*E*-Ferulic acid	n.d.	7	n.d.	n.d.
	Total	**29**	**24**	**11**	**31**

*Results represent the average of the concordant values obtained for the six aliquots of each sample. Abbreviations: n.d, not detected.

From eight isomers of vitamin E, only α-tocopherol and *γ*-tocopherol were detected as a component of the lipophilic leaves extract with a total amount of 128 mg/kg dw (Table 9). The acquaintance about the content of α-tocopherols in the four morphological parts of *Z. lotus* was already reported.[4] Therefore, and to the best of our knowledge, *γ*-tocopherols were described here for the first time in leaves, pulp, and root barks although, this isomer had previously been reported in the seeds oil of this shrub species.[12]

The detection of considerable amounts of tocopherols in leaves, namely, the α-tocopherol that is the most biologically active form of vitamin E can constitute an important income to leaves residues. α-Tocopherols is essential for normal growth and development of the human body, and its deficiency often leads to clinical abnormalities. α-, δ-, and γ-Tocopherols are used as additives in various food products, such as fats and oils, and α-tocopherol, in particular, is used in pharmaceuticals and in cosmetics formulations.[72]

Table 9: Semi-quantitative analysis (mg/kg of dry weight) of dichloromethane tocopherols extracts from four morphological parts of *Zizyphus lotus*.*

RT (min)	Tocopherols	Pulp	Leaves	Root barks	Seeds
55.21	γ-Tocopherol	n.d.	54	n.d.	n.d.
58.19	α-Tocopherol	n.d.	74	n.d.	n.d.
	Total	**n.d.**	**128**	**n.d.**	**n.d.**

*Results represent the average of the concordant values obtained for the six aliquots of each sample. Abbreviations: n.d, not detected; tr, traces.

Three isomers of neophytadiene have been identified, besides phytol, tetracosyl acetate, inositol, and squalene which also found in a significant amount in the seeds extract. Other minor components were also identified as components of *Z. lotus*. 2-furoic acid was found as the only furan in pulp a long with solerol, and cyclohexane carboxylic acid, while loliolide terpenoid flavor, detected in leaves dichloromethane extract of *Z. lotus* with 2-piperidinecarboxylic acid. Two isomer of butane-2,3-diol were identified in the four morphological parts of *Z. lotus*. Thus, two isomers of 1,2,3-butanetriol and erythrono-1,4-lactone were identified in pulp and leaves along with 1,2,3-butanetriol a and 1,2,3-butanetriol (E) in the seeds extract (Table 10).

Table 10: Semi-quantitative analysis (mg/kg of dry weight) of dichloromethane extracts from four morphological parts of *Zizyphus lotus*.*

RT (min)	Other compounds	Pulp	Leaves	Root barks	Seeds
5.58	Butane-2,3-diol isomer a	3	2	3	8
5.87	Butane-2,3-diol isomer b	5	5	6	8
7.72	2-Furoic acid	0.3	n.d.	n.d.	n.d.
8.96	Cyclohexane carboxylic acid	2	n.d.	n.d.	n.d.
9.14	2-Piperidinecarboxylic acid	n.d.	1	n.d.	n.d.
13.45	Solerol	6	n.d.	n.d.	n.d.
14.21	Glycerol	41	251	9	148
14.91	1,2,3-butanetriol isomer a	13	7	n.d.	2
15.08	1,2,3-butanetriol isomer b	6	5	n.d.	n.d.
16.52	Erythrono-1,4-lactone (*E*)-isomer a	10	18	n.d.	2
18.06	Erythrono-1,4- lactone, (*Z*)-isomer b	9	5	n.d.	n.d.
28.26	Loliolide	n.d.	39	n.d.	n.d.
30.76	Neophytadiene isomer a	tr	141	n.d.	n.d.
31.29	Neophytadiene isomer b	n.d.	29	n.d.	n.d.
31.75	Neophytadiene isomer c	n.d.	49	n.d.	n.d.
36.94	Inositol isomer	n.d.	13	n.d.	n.d.
39.04	Phytol	n.d.	117	n.d.	n.d.
51.53	Squalene	n.d.	39	n.d.	79

55.33	Tetracosyl acetate	n.d.	26	n.d.	n.d.
56.86	Nonacosan-10-one	24	n.d.	n.d.	n.d.
	Total	**118**	**747**	**17**	**249**

*Results represent the average of the concordant values obtained for the six aliquots of each sample. Abbreviations: n.d, not detected; tr, traces.

4. Conclusions

This chapter reflects one of the first detailed studies of the lipophilic composition of seeds, pulp, leaves, and root barks of *Z. lotus* from the region of Beni Mellal, Morocco. One hundred twenty-three compounds were identified in the dichloromethane extracts of *Z. lotus*, by GC-MS analysis. Lipophilic extracts from seeds, pulp, leaves, and root barks differ significantly in the content of the major identified families. Pentacyclic triterpenes were the main lipophilic compounds of wild *Z. lotus* root barks, accounting for 10230 mg/kg dw. BetA was the most abundant triterpenic acid in *Z. lotus* lipophilic root barks, accounting for 9838 mg/kg dw. Regarding, fatty acids were the main lipophilic components of seeds and leaves, accounting for 877 mg/kg dw in leaves. Hexadecanoic acid was the main saturated fatty acids (594 mg/kg dw), followed by octadecanoic acid (570 mg/kg dw), particularly concentrated in the seeds. The seeds lipophilic fraction is composed also of unsaturated fatty acids, especially oleic acid (6255 mg/kg dw), while in leaves linolenic acid is the most abundant (2431 mg/kg dw) unsaturated fatty acid. Considerable amounts of sterols compounds are also present in *Z. lotus* fractions (81–355 mg/kg dw), particularly in leaves. Low contents of other families of lipophilic compounds were also noted in the morphological parts of *Z. lotus*, namely long-chain aliphatic alcohols (2–438 mg/kg dw), long-chain aliphatic aldehydes (80 mg/kg dw in pulp), monoglycerides (24–255 mg/kg dw), and aromatic compounds (11–31 mg/kg dw). The presence of high amounts of pentacyclic triterpenes, in particularly betA in root barks fraction, can open new perspectives for the valorization of this fraction as health-promoting natural biomass.

5. References

(1) Maraghni, M.; Gorai, M.; Neffati, M. South African J. Bot. **2010**, 76 (3), 453–459.
(2) Sheng, J. P.; Shen, L. Woodhead Publishing Limited, **2011**; pp 299–326.
(3) Brahlp, D. L. R. R. and A. E. L. B. Weed Technol. **1995**, 9 (2), 326–330.
(4) Benammar, C.; Hichami, A.; Yessoufou, A.; Simonin, A. M.; Belarbi, M.; Allali, H.; Khan, N. A. BMC Complement. Altern. Med. **2010**, 10 (54), 1–9.
(5) Abdoul-Azize, S.; Bendahmane, M.; Hichami, A.; Dramane, G.; Simonin, A. M.; Benammar, C.; Sadou, H.; Akpona, S.; El Boustani, E. S.; Khan, N. A. Int. Immunopharmacol. **2013**, 15 (2), 364–371.
(6) Ghedira, K.; Chemli, R.; Richard, B.; Nwllard, J.; Men-olivier, L. L. E. **1993**, 32 (6), 1591–1594.
(7) Ghedira, K.; Chemli, R.; Caron, C.; Nuzilard, J. M.; Zeches, M.; Le Men-Olivier, L. Phytochemistry **1995**, 38 (3), 767–772.
(8) Le Crouéour, G.; Thépenier, P.; Richard, B.; Petermann, C.; Ghédira, K.; Zèches-Hanrot, M. Fitoterapia **2002**, 73 (1), 63–68.
(9) Renault, J.; Ghedira, K.; Thepenier, P.; Lavaud, C.; Zeches-hanrot, M.; Men-olivier, L. L. E. Phytochemistry **1997**, 44 (7), 1321–1327.
(10) Maciuk, A.; Lavaud, C.; Thépenier, P.; Jacquier, M. J.; Ghédira, K.; Zèches-Hanrot, M. J. Nat. Prod. **2004**, 67 (10), 1639–1643.

(11) Maciuk, A.; Ghedira, K.; Thepenier, P.; Lavaud, C.; Zeches-Hanrot, M. Pharmazie **2003**, 58 (2), 158–159.
(12) Chouaibi, M.; Mahfoudhi, N.; Rezig, L.; Donsì, F.; Ferrari, G.; Hamdi, S. J. Sci. Food Agric. **2012**, 92 (6), 1171–1177.
(13) Ghazghazi, H.; Aouadhi, C.; Riahi, L.; Maaroufi, A.; Hasnaoui, B. Nat. Prod. Res. **2014**, 28 (14), 1106–1110.
(14) Abdeddaim, M.; Lombarkia, O.; Bacha, A.; Fahloul, D.; Abdeddaim, D.; Farhat, R.; Saadoudi, M.; Noui, Y.; Lekbir, A. Ann. Food Sci. Techgnology **2014**, 15 (1), 75–81.
(15) Elaloui, M.; Laamouri, A.; Albouchi, A.; Cerny, M.; Mathieu, C.; Vilarem, G.; Hasnaoui, B. Emirates J. Food Agric. **2014**, 26 (7), 602–608.
(16) El Aloui, M.; Mguis, K.; Laamouri, A.; Albouchi, A.; Cerny, M.; Mathieu, C.; Vilarem, G.; Hasnaoui, B. Karst. Acta Bot. Gall. **2012**, 159 (1), 25–31.
(17) Guo, S.; Duan, J. A.; Tang, Y. P.; Yang, N. Y.; Qian, D. W.; Su, S. L.; Shang, E. X. J. Agric. Food Chem. **2010**, 58 (10), 6285–6289.
(18) Masullo, M.; Montoro, P.; Autore, G.; Marzocco, S.; Pizza, C.; Piacente, S. Food Res. Int. **2015**, 77 (2), 109–117.
(19) Li, J.; Guo, W. J.; Yang, Q. Y. World J. Gastroenterol. **2002**, 8 (3), 493–495.
(20) Sogno, I.; Vannini, N.; Lorusso, G.; Cammarota, R.; Noonan, D. M.; Generoso, L.; Sporn, M. B.; Albini, A. In: Senn, H.J., Kapp, U., Otto, F. (Eds.), 5th International Cancer Prevention Conference. St Gallen, Switzerland; **2009**; pp 209–212.
(21) Tolstikova, T. G.; Sorokina, I. V.; Tolstikov, G. A.; Tolstikov, A. G.; Flekhter, O. B. Russ. J. Bioorganic Chem. **2006**, 32 (1), 37–49.
(22) Borgi, W.; Ghedira, K.; Chouchane, N. Fitoterapia **2007**, 78 (1), 16–19.
(23) Benammar, C.; Baghdad, C. J. Nutr. Food Sci. **2014**, s8, 8–13.
(24) Bakhtaoui, F. Z.; Lakmichi, H.; Megraud, F.; Chait, A.; Gadhi, C. E. A. J. Appl. Pharm. Sci. **2014**, 4 (10), 81–87.
(25) Wahida, B.; Abderrahman, B.; Nabil, C. J. Ethnopharmacol. **2007**, 112 (2), 228–231.
(26) Borgi, W.; Recio, M. C.; Ríos, J. L.; Chouchane, N. South African J. Bot. **2008**, 74 (2), 320–324.
(27) Borgi, W.; Chouchane, N. J. Ethnopharmacol. **2009**, 126 (3), 571–573.
(28) Freire, C. S. R.; Silvestre, A. J. D.; Neto, C. P. Holzforschung **2002**, 56 (2), 143–149.
(29) Villaverde, J. J.; Domingues, R. M. A.; Freire, C. S. R.; Silvestre, A. J. D.; Neto, C. P.; Ligero, P.; Vega, A. J. Agric. Food Chem. **2009**, 57 (9), 3626–3631.
(30) Domingues, R. M. A.; Sousa, G. D. A.; Silva, C. M.; Freire, C. S. R.; Silvestre, A. J. D.; Neto, C. P. Ind. Crops Prod. **2011**, 33 (1), 158–164.
(31) Rsaissi, N.; Kamili, E. L.; Bencharki, B.; Hillali, L.; Bouhache, M. Int. J. Sci. Eng. Res. **2013**, 4 (9), 1521–1528.
(32) Sparkman, O. D.; Penton, Z.; Kitson, F. G. Gas Chromatography and Mass Spectrometry: A Practical Guide. **2011**.
(33) Kraj, D. A.; Desiderio, D. M.; Nibbering, N. M. Mass Spectrometry Instrumentation, Interpretation, and Applications; **2009**.
(34) Zhang, A.; Sun, H.; Wang, P.; Han, Y.; Wang, X. Analyst **2012**, 137, 293–300.
(35) Murphy, R. C. Handbook of Lipid Research: Mass Spectrometry of Lipids; **1993**; Vol. 7.
(36) Ramos, P. A. B. Chemical Characterization and Evaluation of Biological Activity of Cynara Cardunculus Extractable Compounds; **2015**.
(37) Robbins, R. J. Agric. Food Chem **2003**, 51, 2866–2887.
(38) Petersson, G. Org. Mass Spectrom. **1972**, 6 (5), 565–576.
(39) GoŁeębiowski, M.; Cerkowniak, M.; Dawgul, M.; Kamysz, W.; Boguś, M. I.; Stepnowski, P. Parasitology **2013**, 140 (8), 972–985.

(40) Prugel, B.; Lognay, G. Phytochem. Anal. **1996**, 7 (1), 29–36.
(41) Maulidiyah; Nurdin, M.; Fatma, F.; Natsir, M.; Wibowo, D. Anal. Chem. Res. **2017**, 12, 1–9.
(42) Ramos, P. A. B.; Guerra, A. R.; Guerreiro, O.; Freire, C. S. R.; Silva, A. M. S.; Duarte, M. F.; Silvestre, A. J. D. J. Agric. Food Chem. **2013**, 61 (35), 8420–8429.
(43) Silvério, F. O.; Barbosa, L. C. A.; Silvestre, A. J. D.; Piló-Veloso, D.; Gomide, J. L. J. Wood Sci. **2007**, 53 (6), 533–540.
(44) Coelho, D.; Marques, G.; Gutiérrez, A.; Silvestre, A. J. D.; del Río, J. C. Ind. Crops Prod. **2007**, 26 (2), 229–236.
(45) Saitta, M.; Salvo, F.; Bella, G. Di; Dugo, G.; Torre, G. L. La. Food Chem. **2009**, 112 (3), 525–532.
(46) Canini, A.; Alesiani, D.; Arcangelo, G. D.; Tagliatesta, P. J. Food Compos. Anal. **2007**, 20, 584–590.
(47) Zhao, X.; Shen, J.; Chang, K. J.; Kim, S. H. J. Agric. Food Chem. **2013**.
(48) Karaś, M. A.; Russa, R. Lipids **2014**, 49 (4), 369–383.
(49) Myher, J. J.; Marai, L.; Kuksis, A. J. Lipid Res. **1974**, 15 (6), 586–592.
(50) Melchert, H. U.; Pabel, E. J. Chromatogr. A **2000**, 896 (1–2), 209–215.
(51) Chuanphongpanich, S.; Nipon, T. J. Sci **2006**, 33 (1), 109–116.
(52) Elliott, W. H. Lipids **1980**, 15 (9), 764–769.
(53) Caligiani, A.; Malavasi, G.; Palla, G.; Marseglia, A.; Tognolini, M.; Bruni, R. Food Chem. **2013**, 136 (2), 735–741.
(54) Horváth, K.; Molnár-Perl, I. Chromatographia **1998**, 48 (1–2), 120–126.
(55) Schröder, M.; Lehnert, K.; Hammann, S.; Vetter, W. Eur. J. Lipid Sci. Technol. **2014**, 116 (10), 1372–1380.
(56) Petersson, G.; Samuelson, O.; Anjou, K.; von Sydow, E.; Eriksson, G.; Blinc, R.; Paušak, S.; Ehrenberg, L.; Dumanović, J. Acta Chemica Scandinavica. **1967**, pp 1251–1256.
(57) Klinke, H. B.; Ahring, B. K.; Schmidt, A. S.; Thomsen, A. B. Bioresour. Technol. **2002**, 82 (1), 15–26.
(58) Profile, C. J. Brazilian Chem. Soc. **2016**, 27 (10), 1872–1880.
(59) Brown, G. K.; Cromby, C. H.; Manning , N. J.; Pollitt, R. J. J. Inher. Metab. Dis. **1987**, 10, 367–375.
(60) Baas, M.; Cox, H. C.; Leeuw, D.; Schenck, P. A. Tetrahedron Lett. **1984**, 25 (48), 5577–5580.
(61) Oh, T. J.; Hyun, S. H.; Lee, S. G.; Chun, Y. J.; Sung, G. H.; Choi, H. K. PLoS One **2014**, 9 (3), 1–13.
(62) Jordan, R. G. J. Midwifery Women's Heal. **2010**, 55 (6), 520–528.
(63) Isca, V. M. S.; Seca, A. M. L.; Pinto, D. C. G. A.; Silva, H.; Silva, A. M. S. Food Chem. **2014**, 165, 330–336.
(64) Simopoulos, A. P. Biomed Pharmacother **2002**, 56 (8), 365–379.
(65) Pinto, M. E. A.; Araújo, S. G.; Morais, M. I.; Sá, N. P.; Lima, C. M.; Rosa, C. A.; Siqueira, E. P.; Johann, S.; Lima, L. A. R. S. An. Acad. Bras. Cienc. **2017**, 89 (3), 1671–1681.
(66) Widad, O.; Hamza, F.; Youcef, M.; Jean-claude, C.; Pierre, C.; Fadila, B.; Samir, B.; Université, B.; El, A. Int. J. Pharmacogn. Phytochem. Res. **2017**, 9 (2), 228–232.
(67) Yang, B.; Yang, H.; Chen, F.; Hua, Y.; Jiang, Y. Analyst **2013**, 138, 6881–6888.
(68) Hossain, M. J.; Sikder, M. A. A.; Kaisar, M. A.; Haque, M. R.; Chowdhury, A. A.; Rashid, M. A. Bol. Latinoam. y del Caribe Plantas Med. y Aromat. **2015**, 14 (3), 179–189.
(69) Mbaveng, A. T.; Hamm, R.; Kuete, V. Toxicological Survey of African Medicinal

Plants; Elsevier Inc., **2014**; pp 557–576.
(70) Pizzoferrato, L.; Nicoli, S.; Lintas, C. Chromatographia **1993**, 35 (5–6), 269–274.
(71) Vanmierlo, T.; Husche, C.; Schött, H. F.; Pettersson, H.; Lütjohann, D. Biochimie **2013**, 95 (3), 464–472.
(72) Oliveira, L.; Freire, C. S. R.; Silvestre, A. J. D.; Cordeiro, N. J. Agric. Food Chem. **2008**, 56 (20), 9520–9524.

Chapter IV

Chemical characterization of *Zizyphus lotus* phenolic-rich fraction

Abstract

The phenolic composition of *Z. lotus* from the region of Beni Mellal, Morocco was determined by analyzing the methanol/water/acetic acid (49.5:49.5:1) extracts of the different morphological parts of the plant, through high temperature-ultra high-pressure liquid chromatography-tandem mass spectrometry. Seventy-eight phenolic compounds were identified and classified as 2 phenolic acid, 2 flavanones, 16 flavan-3-ols, 23 flavones, 34 flavonols, and one dihydrochalcone. Phenolic compounds were essentially retained in the root barks, accounting for 7692 mg/kg dw. Both leaves and pulp parts showed the highest flavonols content (2129 mg/kg and 5055 mg/kg dw, respectively), and seeds demonstrated the major flavone concentration (360 mg/kg dw). Leaves and root barks also evidenced considerably high phenolic acid contents, while flavan-3-ols were the main phenolic compounds found in root barks (7579 mg/kg dw). The quercetin 3-O-rhamnosyl(6-O-hexoside) and (epi)catechin isomers represented the main flavonoids of wild *Z. lotus*, while quinic acid isomer was the only phenolic acid identified in leaves and root barks.

1. Introduction

Zizyphus lotus (L.) Desf. (Rhamnaceae) is a shrub found in Northern African i.e Morocco, and invasive the southern European countries with particular relevance in Spain, Sicily, Greece, and Cyprus.[1] This shrub species produce edible brown-colored fruits, appreciated for both unprocessed consumptions and for preparing bread, wine, and conserves.[2] In the old ages, the Moroccan nomads have been consumed edible fruits in their travels as a source of energy; which allowed them to feel satiated.[3] Furthermore, several parts of *Z. lotus* have been used in traditional and ancestral medicine for the treatment of several pathologies including liver complaints, obesity, urinary troubles, diabetes, skin infections, fever, diarrhea, insomnia, inflammation, and peptic ulcers.[4] Many of these potential health benefits may have attributed to phenolic compounds, especially flavonoids.

Phenolic compounds are one of the biggest groups of secondary metabolites that are on the upswing in the field of science although they are not nutrients; their dietary intake has several health-promoting effects.[5] Most researchers have made efforts to illustrate the effectiveness of different morphological parts of *Z. lotus* as antioxidant agents[3,6,7] and with the attempt to characterize the antioxidant compounds like alkaloids[8–10] and saponins[11,12] but relatively little information are available regarding the phenolic profile of *Z. lotus*. Recently some research entities start to investigate the composition of phenolic compounds in this shrub species.[13–15] Nevertheless, there is still missing systematic detailed chemical characterization of the phenolic compounds, regarding all morphological parts of *Z. lotus*.

The beneficial effects of *Z. lotus* phenolic compounds on health might be generated by their antioxidant and radical scavenging properties. Borgi et al. (2008),[16] shows that flavonoid fraction of root bark was responsible for a significant and dose-dependent anti-inflammatory in carrageenan-induced paw edema in rats and being considered *Z. lotus* as a potential source of analgesic drugs.[17] Another study demonstrated that rich-phenolic compounds pulp fruit extract of *Z. lotus* modulate the cell signaling and exerts immunosuppressive effects in human T-cells.[4] Additionally, the etheric and methanolic rich-phenolic extract of *Z. lotus* fruits presented the most bactericidal effects to induce growth inhibition.[18]

Z. lotus as potential low-cost material with all these health potential, unfortunately, has received less major emphasis. In this scenario, the detailed study of its phenolic chemical composition remains requested. This investigation of such traditional shrub is a relevant topic, as these analyses reveal the possible functional properties that can add value to the plant and encourage the exploitation of this natural source in the food, pharmaceutical, and cosmetics industries. The presence of nutrients and bioactive compounds in different parts of *Z. lotus*, like vitamins, dietary fiber, minerals, essential oils, sterols, triacylglycerol, and tannins makes this thorny shrub an interesting material to study.[12]

Basing on these data the aim of the present chapter was a comprehensive characterization and quantification of phenolic compounds of four morphological parts e.g. root barks, leaves, pulp, and seeds through high temperature-ultra high-performance liquid chromatography (HT-UHPLC) with UV detection coupled with tandem mass spectrometry analysis (MS^n). Quantitative analysis of total phenolics compounds in extracts was also determined with the Folin-Ciocalteu method along with the total anthocyanins.

2. Materials and methods

2.1 Chemicals

Dichloromethane (99% purity), apigenin (≥95.0% purity), naringenin (98% purity) were obtained from Aldrich Chemical Co. (Madrid, Spain). Gallic acid (>97.5% purity), phloretin (≥99% purity), and quercetin (>98% purity) were supplied by Sigma Chemical Co. (Madrid, Spain). HPLC-grade methanol, water and acetonitrile, were supplied from Fisher Scientific Chemicals (Loures, Portugal). Glacial acetic acid (≥99.7% purity) was purchased from Panreac (Castellar del Vallès, Spain) Methanol (>99.8% purity), catechin (>96% purity), and Formic acid (≥98% purity) were purchased from Fluka Chemie (Madrid, Spain). Sodium carbonate (≥99.9% purity) and hydrochloric acid (HCl) used for anthocyanin determination were obtained from Pronalab (Lisbon, Portugal). Folin-Ciocalteu's phenol reagent was supplied by Sigma Chemical Co (Madrid, Spain). Ascorbic acid (>99.5% purity), were purchased from Fluka Chemie (Madrid, Spain). Solvents were further filtered using a Solvent Filtration Apparatus 58061 from Supelco (Bellefonte, PA, USA).

2.2 Samples preparation

Z. lotus was collected between September and October of 2016 from a different region of Beni Mellal, Morocco. The seeds were separated manually from the pulp, bark from roots then air-dried with the leaves at room temperature until constant weight. The four morphological parts of *Z. lotus* were grounded to granulometry lower than 2 mm prior for extraction.

2.3 Extraction

Samples were first submitted to Soxhlet extraction with dichloromethane for 8 h to remove the lipophilic components. Subsequently, the solid residues (2 g) from the dichloromethane extraction were used to extract phenolic compounds by suspended in methanol/water/acetic acid (49.5:49.5:1) mixture.

Acetic acid has been used to protect the anthocyanins if they exist in *Z. lotus* samples. After 24 h of constant stirring at room temperature, the suspension was then filtered then the methanol and acetic acid were removed by low-pressure evaporation and water by freeze-drying. The dried extracts were weighted, and the extraction yield was determined as the percentage of dry biomass material (w/w, %). The extracts were kept at room temperature protected from light until analysis. Two extracts were prepared for each morphological part of *Z. lotus*.

2.4 Total phenolic content

The total phenolic content (TPC) of the extracts was quantified using the Folin-Ciocalteu assay following the methods reported by Dewanto et al. (2002).[19] The dried extracts were firstly dissolved in methanol/water (1:1), to obtain stock solutions with concentrations ranging from 0.5 to 2 mg/mL. Briefly, aliquots of 0.125 mL of each extract solution were mixed with 0.625 mL of Folin Ciocalteu's reagent, previously diluted with water (1:5, v/v). The absorbance was then measured against a blank at 760 nm, using a UV/Vis V-530 spectrophotometer (Jasco, Tokyo, Japan) after 6 min of adding 1.25 mL of 7% sodium carbonate aqueous solution and 1 mL of water. The TPC was expressed as milligrams of gallic acid equivalent per g of dry weight material (mg GAE/kg dw). The analyses were carried out in triplicate for each extract and the average value from the two extracts was calculated for each morphological part.

2.5 Total Anthocyanins

The total anthocyanin content was estimated using the pH-differential method, as described by Lee et al. (2005).[20] The dried extracts were first dissolved in an adequate solvent to obtain stock solutions at a concentration of 50 mg/mL, then combined in a ration of 1:10 or 1:5 (v:v) with potassium chloride pH 1.0 (0.025 M), and with sodium acetate pH 4.5 (0.4 M) buffers in separate vessels. The absorbance was measured at 510 and 700 nm. Wells containing buffer without the sample solution was used as the blanks. The results were expressed as milligrams of cyanidin-3-glucoside equivalents (cyn-3-glcEq)/g extract. The absorbance (A) was calculated according to the following formula:

$$A = (A_{510\ nm} - A_{700\ nm})_{pH\ 1.0} - (A_{510\ nm} - A_{700\ nm})_{pH\ 4.5}$$

2.6 HT-UHPLC-UV analysis

The analysis was performed using Hewlett–Packard (HP) 1050 liquid chromatograph system equipped with an Accela 600 LC pump, an Accela autosampler (set at 16 ºC) and an Accela 80 Hz photo DAD. The compounds were separated according to the gradient elution program which applied at a flow rate of 0.6 ml min^{-1} by Hypersil Gold RP C18 column (100 mm × 2.1 mm; 1.9 µm particle size) supplied by Thermo Fisher Scientific (San Jose, CA, USA), maintained at 45 ºC. The injection volume in the HPLC system was 15 µL prepared by dissolving, the extracts of *Z. lotus* in HPLC grade methanol/water mixture (1:1) at 10 mg/mL, and then filtered through a 0.2 µ.m PTFE syringe filter. The mobile phase has consisted of water: acetonitrile (99:1, v/v) (A) and acetonitrile (B), both with 0.1% of formic acid. The following linear gradient was applied: 0–1.50 min: 99% B; 1.50–6 min: 99–91% B; 6–11 min:, 91–88% B; 11–12 min:, 88–87% B; 12–23 min:, 87–69% B; 23–24 min: 69–65% B;

24–29 min: 65–46% B, finally 100% A from 29 to 31 min. Before the next run, the percentage of A decreased from 100% to 1% for 4 min and they were maintained at 1% A for 8 min. The chromatograms were recorded at 280, 320, and 340 nm and UV/Vis spectra recorded from 210 to 600 nm.

2.7 HT-UHPLC–MS^n analysis

The HT-UHPLC–MS^n analysis was performed following previously optimized conditions by Santos et al (2013).[21] The HPLC system was coupled to a LCQ Fleet ion trap mass spectrometer (ThermoFinnigan, San Jose, CA, USA), equipped with electro-spray ionization (ESI) source. The ESI-MS was operated under the negative ionization mode with a spray voltage of 5 kV and capillary temperature of 320 ºC. The flow rates of nitrogen sheath and auxiliary gas were 40 and 5 (arbitrary units), respectively. The capillary and tube lens voltages were set at −44 V and −125 V, respectively.

CID-MS^n experiments were performed on mass-selected precursor ions in the range of m/z 100–2000. The isolation width of precursor ions was 1.0 mass unit. The scan time was equal to 100 ms and the collision energy was 15 and 45 (arbitrary units), using helium as collision gas. Data acquisition was carried out by using Xcalibur® data system (ThermoFinnigan, San Jose, CA, USA).

2.8 Quantification of phenolic compounds by HT-UHPLC-UV

Calibration curves were obtained by UHPLC injection of gallic acid, catechin, quercetin, apigenin, isorhamnetin, luteolin, naringenin, and phloretin solutions in methanol/water (1:1), with six different concentrations each ranging from 0.088 to 60.2µg/mL. The quantification of individual compounds was done by using the linear equation (Table 1) obtained with the aglycone standard since no pure reference compounds were available. Therefore, the acylated flavonoids were quantified as equivalents of the most similar compound, taking into account their molecule weight. The concentrations were calculated based on triplicate for each extract and the mean value calculated for each morphological part.

Table 1: standard data used for the HT-UHPLC-UV quantification of phenolic compounds of methanol/water/acetic acid extracts from *Zizyphus lotus*.

Standard	λ(nm)[a]	Concentration range (µg/ml)	Linear equation[b]	r^2	LOD[c] (µg/mL)	LOQ[d] (µg/mL)
Gallic acid	280	0.104-41.6	y=475396x-8708.1	0.999	1.53	4.63
Catechin	280	0.102-60.2	y=119442x-9251.6	0.997	4.83	14.64
Quercetin	370	0.098-9.8	y=110572x+21824	0.998	9.11	27.60
Apigenin	340	1.115-11.5	y=82591x-234101	0.996	1.07	3.25
Isorhamnetin	317	0.088-52.8	y=242887x-331459	0.995	4.84	14.66
Luteolin	340	0.14-14	y=362178x-130178	0.917	6.73	20.40
Naringenin	280	0.108-21.6	y=414598x+254398	0.998	1.42	4.30
Phloretin	280	0.1-20	y=322385x+117003	0.994	2.22	6.73

[a] Detection wavelength; [b] y = peak area, x = concentration in µg/mL; [c] LOD, limit of detection; [d] LOQ, limit of quantification.

3. Results and Discussion

3.1 Extraction yield, total phenolic and anthocyanin content

The hydromethanolic extraction yields of the different morphological parts of *Z. lotus* e.i seeds, pulp, leaves, and root barks, as well as the corresponding total phenolic compounds content (TPCs) and total anthocyanin content (TAC), are shown in Table 2.

The pulp fraction shows a considerably higher extraction yield (70.9%) followed by leaves and root barks extract; therefore, seeds fraction sowed the lowest extraction yield with a value of 5.9%. These values displayed higher extraction yields than those reported for methanol extract of leaves (15.3%). However, the extraction yield of root barks was in the same range as what previously described (25.3%) for methanol extracts of *Z. lotus* root barks.[22,23]

Table 2: Extraction yield, total phenolic content and total anthocyanin content of methanol/water/acetic acid (49.5:49.5:1) extracts from *Zizyphus lotus*.

Z. lotus	**Extraction yields (% w/w)**	**Total phenolic content**		**Total anthocyanin content**	
		mg GAE/g extract	mg GAE/kg dw	cyn-3-glcEq mg/g extract	cyn-3-glcEq mg/kg dw
Pulp	70.9 ± 0.6	51 ± 2.4	39503 ± 1531.4	2.6 ± 0.5	2038 ± 389.5
Seeds	5.9 ± 0.2	64.4 ± 1.6	4156 ± 205.8	0.7 ± 0.03	46 ± 1.3
Leaves	38.9 ± 1.5	192.6 ± 4.9	80813 ± 1857	2.9 ± 0.4	1202.3 ± 203.5
Root barks	27.6 ± 1.4	83.1 ± 5.6	25710 ± 531.4	9.1 ± 0.8	2826.5 ± 187

Results correspond to the average ± standard deviation estimated from three aliquots of three extracts.

The TPCs varied from 4156 mg/kg dw (64.4 mg/g extract) in seeds to 80813 mg/kg dw (192.6 mg/g extract) in leaves (Table 2). When compared to literature data, TPCs of both parts of leaves and pulp were higher than those previously reported for leaves and pulp *Z. lotus* methanolic extract.[18,24] Moreover, TPCs of hydro-alcoholic aerial parts (leaves and fruits) extract of *Z. lotus* reported by Boulanouar et al. (2013)[25] were much lower relative to those noticed in the current wok. Besides, TPCs of fruit extract (pulp and seeds) were much higher compared with the alcoholic fruits *Z. lotus* extract.[7,24] Additionally, TPCs of root barks were similar relatively to those recorded for an acetone-water extract of *Z. lotus*.[26] These variations in *Z. lotus* biomolecules content might be due to the different factors explained in Chapter II.

In the determination of the total anthocyanin content (Table 2), the highest levels of these compounds were found in the root barks phenolic-rich extract (2826.5 mg/kg dw, 9.1 mg/g extract). The same total anthocyanin content was found for pulp and leaves extracts. Nevertheless, seeds phenolic-rich extract presented lower content of these secondary metabolites (46 mg/kg dw, 0.7 mg/g extract) compared to the four morphological parts of *Z. lotus*. To the best of our knowledge, this is the first study concerning the total anthocyanin content of wild *Z. lotus* species.

3.2 HT-UHPLC-UV-MS^n analysis of *Zizyphus lotus* extracts

A deep screening of phenolic compounds of four morphological parts of *Z. lotus* (seeds, pulp, leaves, and root barks) was carried out. The seeds extracts were considered as a typical

chromatograms model as shown in Figure 1. The compounds were carefully identified by analyzing various information, such as the retention time (t_R), UV absorption, the $[M-H]^-$ ion, and the MS^n fragmentation pattern in the negative ion mode (Table 2) besides, by comparing these data with standard aglycone and scientific literature as discussed below. Whereas, the formation of formic acid adduct $[M+HCOOH]^-$ in seeds and root barks has been observed, which is normal since this phenomen on is often observed during flavonoid analysis in ESI (-ve mode).[27]

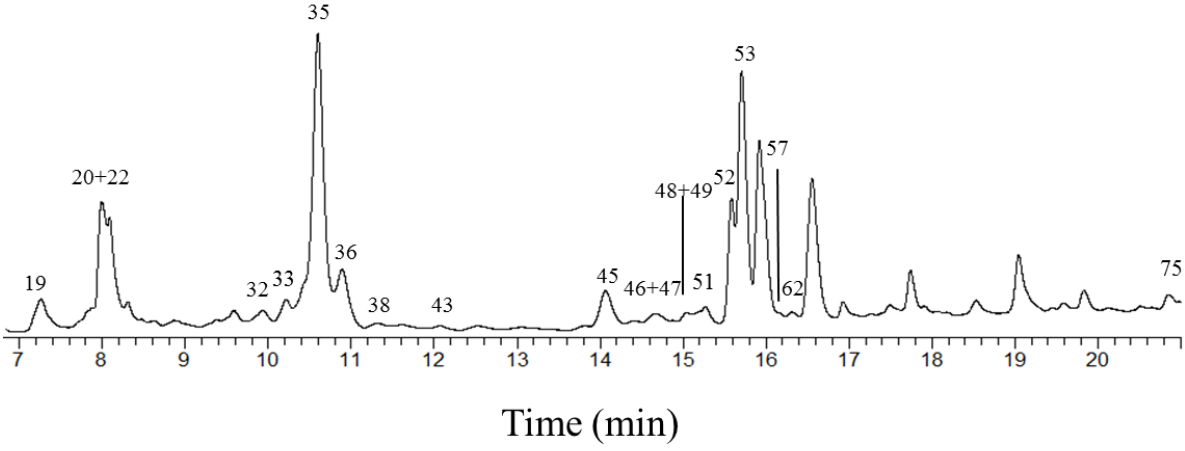

Figure 1: HT-UHPLC-UV chromatograms of methanol/water/acetic acid (49.5:49.5:1) extracts of seeds part of *Zizyphus lotus*.

Eighty-seven phenolic compounds were identified in methanol/water/acetic acid extracts of Z. *lotus*. These compounds are reported here for the first time as *Z. lotus* component, except for phloretin-3',5'-di-C-glucoside, (epi)catechin, (epi)catechin-(epi)gallocatechin, type B procyanidin dimer, myricetin-3-O-rhamnosylhexoside, quercetin-3-O-[(2,6-di-O-rhamnosyl-hexoside)]-7-O-rhamnoside, quercetin-3-O-(2,6-di-O-rhamnosylhexoside), kaempferol-3-O-(6-O-hexosyl-rhamnosyl), and kaempferol-3-O-rutinoside were previously described in leaf *Z. lotus* extract.[14]

3.2.1 Phenolic acid

Two phenolic acid isomers were reported in the methanol/water/acetic acid leaf extract of *Z. lotus*. Their identification relies on the UV spectra, the revealing of molecule ion $[M-H]^-$ and respective MS^n fragmentations (Table 3).

Table 3: HT-UHPLC-UV-MS^n data of quinic acid identified in methanol/water/acetic acid extracts of *Zizyphus lotus*.

Peak	R_t (min)	λ_{max} (nm)	$[M-H]^-$ (m/z)	HT-UHPLC–MS^n product m/z (% base peak)$^{(I)}$	Compound
1	0.50	245, 265	191	MS^2: 127(100), 85(95), 173(55), 155 (30), 171(30), 93(25), 59(25), 137(20), 111(15).	Quinic acid
2	0.71	234, 268	191	MS^2: 127(100), 173(49), 171(30), 111(15).	Quinic acid

[(I)]m/z in bold was subjected to MS^n analysis.

The negative ESI of quinic acid **1** and **2** gave rise to the same molecule ion at m/z 191 $[M–H]^-$. The MS^2 [191] spectrum showed ions at m/z 111 $[M–H–2H_2O–CO_2]^-$, 173 $[M–H–H_2O–H]^-$, 171 $[M–H–H_2O–H_2–H]^-$, and 137 $[M–H–3H_2O]^-$ correspond a dehydrated form of the deprotonated molecular ion.[28,29] The obtained MS data also showed fragment ions at m/z 85 ($[M–H–C_4H_5O_2]^-$) and 93 ($[M–H–C_6H_5O]^-$), along with base peak fragment ion at m/z 127 ($[M–H–CO_2–H_2–H]^-$) which is characteristic of quinic acid (Table 3).[28–30]

3.2.2 Flavonoids

The structure analysis of flavonoids negative ion CID spectra is often considered to be more difficult to interpret. However, it's more sensitive in flavonoid analysis and the fragmentation behavior is different, giving additional and complementary information.[31] Cleavage of the C-ring by an rDA mechanism leads to $^{i,j}A$ and $^{i,j}B$ ions, providing information on the number and type of substituents in the A^- and B–rings.[31,32] The main product ions of which observed in this study are shown in Figure 2, using the nomenclature adapted from that proposed by Ma et al. (1997).[33]

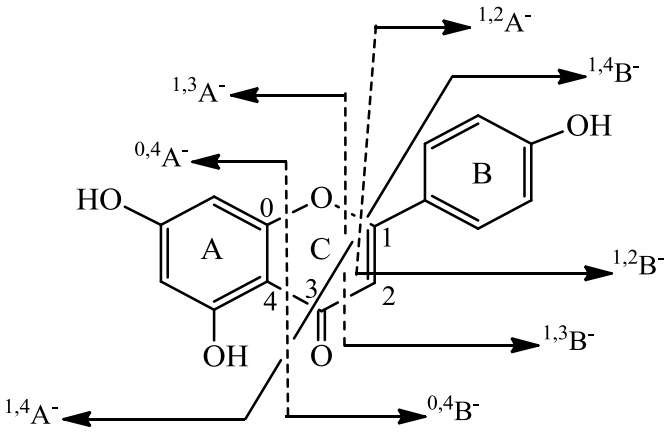

Figure 2: Fragmentation nomenclature for molecule ion of flavonoids (adapted from[32,33]). The superscripts on the left of the A or B ring indicate the broken C-ring bonds.

Flavonoids were the main phenolic compounds found in *Z. lotus* grouped into sixteen flavan-3-ol, forty flavonols, two flavanones, and twelve flavones, based on the UV spectra and MS^n fragmentation as depicted bellow.

3.2.2.1 Flavan-3-ols

Sixteen flavan-3-ols were identified as *Z. lotus* components and were mainly concentrated in leaf and root barks fractions. Their identification relies on the characteristic UV spectra,[34] the neutral loss of catechin (289 Da) and gallocatechin (305 Da) fragment, and the respective MS^n fragmentation (Table 4).

Table 4: HT-UHPLC-UV-MS^n data of flavan-3-ols identified in methanol/water/acetic acid extracts of Z*izyphus lotus*.

Peak	R_t (min)	UVλ_{max} (nm)	$[M–H]^-$ (m/z)	HT-UHPLC–MS^n product m/z (% base peak)[(I)]	Compound

3	0.93	234, 272	609	MS^2: 441(100), 423(80), 452(35), 591(35), 562(35), 473(20), 541(20), **305**(15); MS^3: 261(100).	(epi)gallocatechin dimer
4	1.28	231, 272	609	MS^2: 441(100), 423(75), **305**(15), 483(15); MS^3: 179(100).	(epi)gallocatechin dimer
5	1.41	235, 272	609	MS^2: 441(100), 423(45), 465(15), **305**(15), 591(15), 219(10), 483(10); MS^3: 219(100).	(epi)gallocatechin dimer
6	1.59	235, 270	305	MS^2: 221(100), 219(55), 179(70), 261(55), 175(35), 165(30), 125(25), 287(20), 137(20), 147(15).	(epi)gallocatechin
7	2.06	235, 270	305	MS^2: 219(100), 179(95), 221(90), 261(35), 165(35), 125(30), 137(25), 164(20), 167(10), 287(10).	(epi)gallocatechin
8	4.00	235, 274	593	MS^2: **423**(100), 441(75), 467(50), 575(45), 305(20), 425(20).	(epi)catechin-(epi)gallocatechin
9	4.71	235, 272	305	MS^2: 179(100), 221(100), 219(70), 175(65), 261(45), 287(20), 247(20), 209(20), 203(20), 125(20), 137(20).	(epi)gallocatechin
10	4.90	237, 277	593	MS^2: **423**(100), 441(80), 467(45), 575(45), 305(40), 425(20); MS^3: 282(100).	(epi)catechin-(epi)gallocatechin
11	5.81	237, 276	577	MS^2: 425(100), 407(55), 441(25), 559(20), 451(20), 289; MS^3: 407(100)	Procyanidin (B-type) dimer isomers
12	6.01	237, 278	497*	MS^2: **451**(100), 487, 289; MS^3: 289(100).	(epi)catechin-O-hexoside
13	6.32	238, 278	577	MS^2: **425**(100), 407(35), 441(25), 451(20), 509(20), 559(15), 289; MS^3: 407(100).	Procyanidin (B-type) dimer isomers
14	6.50	238, 278	335*	MS^2: **289**(100); MS^3: 245(100), 205(35), 203(20), 179(15), 271.	(epi)catechin
15	6.73	238, 278	335*	MS^2: 289(100), 245(100), 205(35), 203(20), 179(15), 271.	(epi)catechin
17	6.89	237; 275	335*	MS^2: 289(100), 245(100), 205(25), 203(20), 175(20), 161(15), 271	(epi)catechin
21	7.58	234, 268	471	MS^2: 427(100), 425(95), 403(48), 387(25), 319(15), 289(10).	(epi)gallocatechin methyl gallate
77	19.25	234, 274	951*	MS^2: **905**(100), 789; MS^3: **451**(100), 679(60); MS^4:	(epi)catechin-O-(rutinosyl-

		433(100)	rhamnoside)-O-hexoside

(1)m/z in bold was subjected to MS^n analysis,*: Formic acid adduct (FA).

Compounds **3**, **4**, and **5** exhibited molecule ion at m/z 609 $[M–H]^-$ and were assigned to (epi)gallocatechin dimer (Table 4) which is known as components of Z*izyphus spina-christi* leaves.[35] The MS^2 [609] data produce ions at m/z 441 $[M–H–168]^-$, 423 $[M–H–186]^-$, and 452 $[M–H–157]^-$. The neutral losses indicate the presence of a galloyl moiety. Additional fragment ions were observed at m/z 473 $[M–H–136]^-$ owing to the rDA reaction and loss of the A-ring, m/z 591 $[M–H–18]^-$ due to the loss of water molecule, and m/z 483 $[M–H–126]^-$ resulted from the heterocyclic ring fission (HRF). The presence of a fragment ion at m/z 305, with its main MS^3 fragmentation, pointed out that the top and base units are (epi)gallocatechin.[36,37]

Compounds **6**, **7**, and **9** displayed molecule ion at m/z 305 $[M–H]^-$ ((epi)gallocatechin) generated the MS^2 [305] fragmentation at m/z 261 $[M–H–44]^-$, 221 $[M–H–84]^-$, 219 $[M–H–86]^-$, 179 $[M–H–126]^-$, 167 $[M–H–138]^-$, 165 $[M–H–140]^-$, and 287 $[M–H–18]^-$ in keeping with the loss of one CO_2, $C_4H_4O_2$, $C_4H_6O_2$, $C_6H_6O_3$, $C_7H_6O_3$, $C_7H_8O_3$, and H_2O, respectively. The neutral loss of $C_4H_4O_2$, and $C_4H_6O_2$ was due to the cleavage of the A ring of flavan-3-ol (Table 4). The loss of $C_6H_6O_3$ was due to HRF. The loss of $C_7H_6O_3$ and $C_7H_8O_3$ were through rDA fission.[36,38] The ion at m/z 125 characteristics of (epi)gallocatechin,[39] although the ion at m/z 203, resulting from the cleavage of the A-ring of flavan-3-ol.[40]

Compounds **8** and **10** present a molecule ion at m/z 593 $[M–H]^-$ and were identified as (epi)catechin-(epi)gallocatechin, which has already been appeared as a component of *Z. lotus* leaves.[14] The fragment ion at m/z 423 $[M–H–152–18]^-$, corresponding to the loss of galloyl moiety and a water molecule, m/z 467 $[M–H–126]^-$ resulted from HRF, and the fragment ion at m/z 575n$[M–H–18]^-$ correspond to the loss of water molecule. The precursor ion gave fragment ions at m/z 425 $[M–H–168]^-$ and 441 $[M–H–152]^-$, after the loss of gallic acid and m/z 305 $[M–H–288]^-$ which indicate the presence of (epi)catechin unit.[37]

Compounds **11** and **13** displayed molecule ion at m/z 577 $[M–H]^-$ and were assigned as procyanidin (B-type) dimer, known components of *Z. lotus* leaves.[14] The rDA fragmentation of the dimer produced the fragment $[M−H−152]^-$ at m/z 425 (Table 4). Moreover, the ion at m/z 407 $[M−H−152−18]^-$ resulted from water elimination of m/z 425, most likely from the 3–OH.[40] Interflavanic bond cleavage corresponding to (epi)catechin occurred as well, producing ion at 289.[41]

Compound **12** with molecule ion at m/z 497 $[M+HCOOH]^-$ (formic acid (FA) adduct ion of m/z 451 $[M–H]^-$) was assigned as (epi)catechin-O-hexoside, relies on the UV spectra and MS^n fragmentation (Table 4). The MS^3 [451] data generated ion at m/z 289, corresponding to the deprotonated ion of (epi)catechin and displaying typical loss of hexosyl unit (–162 Da) (Table 4).[42,43]

The identification of compounds **14**, **15**, and **17** was confirmed as (epi)catechin by the UV spectra and MS^n fragmentations of the pure standard. These isomers were already found in *Z. lotus* leaf and fruit extracts.[14,15] The MS^2 spectra of the ion at m/z 335 $[M+HCOOH]^-$ (FA adduct) produced ion at m/z 289, corresponding to the deprotonated ion of (epi)catechin

(Table 4). The MS data showed a major product ion at m/z 245 $[M–H–44]^-$, indicating the decarboxylation of (epi)catechin, along with minor fragments at m/z 203 ($C_4H_6O_2$) and 205 ($C_4H_4O_2$) resulted from the cleavage of A-ring of flavan-3-ols and suggesting (epi)catechin as aglycone (Table 4).[40] Other fragment ions at m/z 161 $[M–H–126–2H]^-$ and 271 were observed and corresponded to the loss of a phloroglucinol molecule (A–ring) and a water molecule, respectively, while the product ion at m/z 179 indicates the HRF.[40]

Compound **21** exhibited a molecular ion at m/z 471 $[M–H]^-$ and was assigned as methyl-epigallocatechin-3-O-gallate (Table 4). The MS^n fragmentation, yielding fragment ion at m/z 319 $[M–H–152]^-$, results from the loss of a galloyl molecule and 289 $[M–H–152–30]^-$, due to the loss of methyl and galloyl group from the C–3 position of (epi)gallocatechin.[38,40,44] The ion at m/z 427 $[M–H–44]^-$, indicate the loss of CO_2 although, ions at m/z 403 $[M–H–68]^-$ and 387 $[M–H–84]^-$, resulting from cleavage of the A^- ring (Table 4).[44]

Compound **77** displayed a molecule ion at m/z 951 $[M+HCOOH]^-$ and corresponding to FA adduct of fragment ion at m/z 905 (Table 4). The MS data present fragment ion at m/z 451 $[M–H–454]^-$, after the loss of triglycosylated unities, consistent with rutinosyl (–308 Da) and hexosyl (–162 Da) moieties. Moreover, the MS^3 [451] fragmentation displayed base peak ion at m/z 433, indicates the loss of water molecule probably from the 3–OH position of the flavonoid.[45,46] Therefore, the fragment 451 Da correspond to the molecule ion of compound **12**, suggesting this compound being (epi)catechin-O-rutinosylrhamnoside-O-hexoside.

3.2.2.2 Flavanones

Two naringenin isomers derivatives (**16** and **18**) were identified in *Z. lotus* leaf extract, based on the UV spectra, the detection of $[M–H]^-$ and respective MS^n fragmentations (Table 5).

Table 5: HT-UHPLC-UV-MS^n data of flavanones identified in the methanol/water/acetic acid extracts of *Zizyphus lotus*.

Peak	R_t (min)	λ_{max} (nm)	$[M–H]^-$ (m/z)	HT-UHPLC–MS^n product m/z (% base peak)[(I)]	Compound
16	6.87	235, 282	595	MS^2: **385**(100), 475(85), 355(65), 313(25), 415(25), 457(25), 577(25); MS^3: 313(100)	Naringenin-6,8-di-C-hexoside isomers
18	6.94	235, 282	595	MS^2: **385**(100); 355(70), 475(50), 457(25), 415(20), 505(15), 577(10); MS^3: 313(100).	Naringenin-6,8-di-C-hexoside isomers

[(I)]m/z in bold was subjected to MS^n analysis.

Compounds **16** and **18** demonstrate the MS^2 [385] and MS^3 [385→313] mass spectra and the fragment ions originated by the fragmentation of naringenin-6,8-di-C-hexoside under the negative ESI. The product ions at m/z 577 $[M–H–18]^-$, 505 $[M–H–90]^-$, 475 $[M–H–120]^-$, 415$[M–H–180]^-$, 385$[272+113]^-$, and 355$[272+83]^-$ are typical of trihydroxyflavanone-di-C-hexoside.[47] Therefore, the loss of 272 Da corresponds to the molecular weight of naringenin. Moreover, a weak fragment ion was observed at m/z 457 [M–H–138], indicating the loss of the B ring (Table 5).

3.2.2.3 Flavonols

Thirty-four mono, di, tri, tetra, and penta-glycosides flavonols were detected in methanol/water/acetic acid extracts of *Z. lotus* and were concentrated mainly in the leaves. The tentative characterization of these compounds was based on the appearance of UV spectra, aglycone fragment ions at m/z 300/301, 285/284, 316/317, or 300/315, and to their main MS^3 and/or MS^4 product ions corresponds, respectively, to the deprotonated aglycones ions of quercetin, kaempferol, myricetin, or isorhamnetin.[32] This group of compounds is characterized by the presence of UV spectra typical of flavonols glycoconjugates (341–359 nm) and acylated flavonols glycoconjugates derivatives (311–330 nm) by adding cinnamoyl radical.[48,49]

Compounds **23** was considered as myricetin-3-O-rhamnosyl-hexoside, based on the UV spectra as well as on the detection of molecule ion at m/z 625 $[M–H]^-$ and the respective MS^n fragmentation under negative mode ESI (Table 6).

Table 6: HT-UHPLC-UV-MS^n data of flavonols identified in the methanol/water/acetic acid extracts of *Zizyphus lotus*.

Peak	R_t (min)	λ_{max} (nm)	$[M–H]^-$ (m/z)	HT-UHPLC–MS^n product m/z (% base peak)[(I)]	Compound
23	7.99	235, 254, 350, 358	625	MS^2: 316(100), **317**(70), 271(20), 463(20), 607(15), 287(15); MS^3: 179(100), 192(20), 255(20).	Myricetin-3-O-rhamnosyl-hexoside

[(I)]m/z in bold was subjected to MS^n analysis.

The MS^2 [317] data, releasing a base peak fragment ion at m/z 316/317 $[M–H–308]^-$ and a weak fragment ion at m/z 463 $[M–H–162]^-$ indicated the loss of a rutinosyl unit (–308 Da) and the further loss of hexosyl moiety (–162 Da), respectively (Table 6).[36] Thus, this compound was tentatively identified as flavonoid-O-rhamnosyl-hexoside.[50] The main fragment at m/z 607 $[M–H–18]^-$ is probably due to the cleavage of the hydroxyl group (–OH) at position C-3 of the flavonoid.[45,46] Moreover, the MS data exposed fragmentations pattern characteristic of flavonols at m/z 255 ($[aglycone−CO_2−H_2O]^-$), 179 ($[^{1,2}A]^-$), and 192 ($[aglycone−ring\ B−H_2O]^-$.[32] Although, the observation of a base peak at m/z 317, along with the fragment ions in MS^4 [353] spectrum at m/z 287 ($[M−H−CO−2H]^-$) and 271 $[M−H−CO−H_2O]^-$, confirmed myricetin as aglycone.[32,51]

Twenty four quercetin derivatives were characterized in methanol/water/acetic extracts of *Z. lotus* were grouped into quercetin glycoconjugates (**24**–**31**, **34**, **44**, and **50**) and *p*-coumaroyl quercetin glycoconjugates derivatives (**55**, **56**, **59**, **61**, **63**, **67, 69**, **72**, **78**, **79**–**80**, **84**, and **85**). Their identification relies on the UV spectra, the detection of $[M−H]^-$ and respective MS^n fragmentations (Table 7).

Table 7: HT-UHPLC-UV-MS^n data of flavonols identified in methanol/water/acetic acid extracts of *Zizyphus lotus*.

Peak	R_t (min)	λ_{max} (nm)	$[M–H]^-$ (m/z)	HT-UHPLC–MS^n product m/z (% base peak) [(I)]	Compound
24	8.29	233, 253, 245, 359	755	MS^2: **300**(100), 301(35), 271(35), 609(35), 489(20), 343(20), 325(20), 591(15); MS^3: 255(100), 271(55).	Quercetin-3-O-(2,6-di-O-rhamnosyl-hexoside)
25	8.41	233, 253, 345, 359	755	MS^2: **300**(100), 271(35), 301(30), 591(30), 609(15), 373(15), 343(15); MS^3: **271**(100), 255(55), 272(10); MS^4: 243(100), 253(20), 215(15), 271(100).	Quercetin-3-O-(2,6-di-O-rhamnosyl-hexoside)
26	8.51	233, 254, 345, 359	755	MS^2: **300**(100), 271(35), 301(35), 591(35), 609(15), 573(15), 343(15); MS^3: 271(100), 179(100), 257(55), 229(40), 255(35), 274(20), 151(15), 239(15).	Quercetin-3-O-(2,6-di-O-rhamnosyl-hexoside)
27	8.77	233, 253, 265, 346	901	MS^2: **755**(100); MS^3: 489(100); 465(40), 301(35), 327(25).	Quercetin-3-O-[di-rhamnosyl(2-O-hexoside)]-7-O-rhamnoside
28	9.06	233, 254, 345, 359	609	MS^2: **301**(100), 300(85), 271(20), 343(15), 255(10); MS^3: 151(100), 179(95), 192(15), 273(15), 229(10), 257(10).	Quercetin 3-O-rhamnosyl(6-O hexoside)
29	9.21	233, 253, 265, 346	609	MS^2: **301**(100), 300(85), 271(30), 255(15), 591(15), 343(10); MS^3: 179(100).	Quercetin-3-O-rhamnosyl(6-O hexoside)
30	9.42	233, 250, 345, 359	609	MS^2: **301**(100), 300(55), 271(15), 255(15), 343(10); MS^3: 179(100), 151(75), 273(30), 257(20), 211(20).	Quercetin-3-O-rhamnosyl(6-O hexoside)
31	9.70	232, 255, 264, 349	463	MS^2: **301**(100), 352(20), 395(15), 379(10), 300(10); MS^3: 151(100), 179(100), 257(80), 273(55), 211(50), 107(45), 239(30), 256(25), 229(20).	Quercetin-7-O-hexoside
34	10.03	232, 252, 265, 346	755	MS^2: **609**(100); MS^3: 301(100), 373(50), 300(45), 343(40), 315(39), 179(35).	Quercetin-3-O-[rhamnosyl(6-O-hexoside)]-7-O-rhamnoside
44	13.99	233,	901	MS^2: 781(100), **755**(70); MS^3:	Quercetin-3-O-[(di-O-

		267, 315, 346		301(100), 446(80), 487(65), 226(55); MS^4: 151(100).	rhamnosylhexoside)]-7-O-rhamnoside
50	15.22	233, 256, 267, 346	901	MS^2: **755**(100), 781(25); MS^3: **300**(100), 591(45), 489(40), 283(30), 409(25), 343(20), 285(15), 609(15), 271(15), 301(10); MS^4: 243(100).	Quercetin-3-O-(2, 6-di-O-rhamnosyl-hexoside)-7-O-rhamnoside
55	16.08	233, 255, 267, 330	931	MS^2: 755(100), **769**(65); MS^3: 271(100), 315(75), 300(35).	Isorhamnetin-3-O-[(*p*-coumaroyl-rhamnosyl hexoside)]-7-O-hexoside
56	16.20	233, 255, 267, 315	901	MS^2: **755**(100); 781(60), 300(15), 737(10), 343(10); MS^3: 591(100), 271(80); 300(75), 353(50), 346(35), 343(35).	Quercetin-3-O-[(2,6-O-*p*-coumaroyl-rhamnosyl-hexoside]-7-O-rhamnoside
59	17.06	257, 266, 315	755	MS^2: **609**(100), 301(25); MS^3: **301**(100), 300(25), 255(10), 213(10); MS^4: 273(100), 191(60).	Quercetin-3-O-[(*p*-coumaroyl-hexoside)]-7-O-rhamnoside
61	17.36	233, 250, 268, 313	1047	MS^2: **901**(100); MS^3: **755**(100), 781(10); MS^4: 300(100), 737(80), 427(75), 273(70), 237(45), 255(35), 301(30), 547(30).	Quercetin-3-O-[(*p*-coumaroyl-rhamnosyl hexoside)]-7-di-O-rhamnoside
63	17.57	229, 257, 266, 313	1047	MS^2: **755**(100); MS^3: **609**(100), 300(40), 712(30), 591(20), 299(20), 301(15), 343(10); MS^4: **301**(100), 300(85), 343(55), 271(50), 259(30), 327(10); MS^5: 179(100), 151(65), 233(25), 255(15), 173(15).	Quercetin-3-O-[(2,6-O-*p*-coumaroyl-rhamnosyl-hexoside)]-7-di-O-rhamnoside
67	18.09	233, 257, 266, 313	901	MS^2: **755**(100); MS^3: **300**(100), 591(60), 271(55), 609(25), 489(25), 343(25), 301(20), 573(15), 325(15); MS^4: 271(100), 255(85).	Quercetin-3-O-[(2,6-O-*p*-coumaroyl-rhamnosyl-hexoside)]-7-O-rhamnoside
69	18.18	232, 257, 267, 313	901	MS^2: **755**(100); MS^3: **300**(100), 591(40), 609(25), 271(25), 343(15), 489(15), 255(15), 409(10); MS^4: 271(100), 255(100), 272(20).	Quercetin-3-O-[(2,6-O-*p*-coumaroyl-rhamnosyl-hexoside]-7-O-rhamnoside
72	18.84	233, 251, 267, 311	1047	MS^2: **755**(100); MS^3: **609**(100), 325(10); MS^4: 300(100), 337(75), 301(60).	Quercetin-3-O-[(*p*-coumaroyl-rhamnosyl hexoside)]-7-di-O-rhamnoside
78	19.40	231, 256,	901	MS^2: **755**(100); MS^3: **300**(100), 489(35), 591(35),	Quercetin-3-O-[(2,6-O-*p*-coumaroyl-

		267, 311		301(25), 343(20), 609(20), 271(20), 409(15), 737(15); MS^4: 271(100), 255(20), 272(10).	rhamnosyl-hexoside)]-7-O-rhamnoside
79	19.52	230, 267, 289, 311	901	MS^2: **755**(100), 300; MS^3: 300(100), 343(40), 489(35), 301(30), 355(25), 271(20), 255(15), 609.	Quercetin-3-O-[(2,6-O-*p*-coumaroyl-rhamnosyl-hexoside)]-7-O-rhamnoside
80	19.61	229, 267, 289, 311	755	MS^2: **609**(100), 301(25), 635(15), 300(10); MS^3: 271(100).	Quercetin-3-O-[(*p*-coumaroyl-hexoside)]-7-O-rhamnoside
84	20.92	230, 269, 290, 314	1047	MS^2: **901**(100), 927(15), 755(10); MS^3: **755**(100), 781(10); MS^4: 300(100), 737(80), 427(75), 273(70), 237(45), 255(35), 301(30), 547(30).	Quercetin-3-O-[*p*-coumaroyl-rhamnosyl hexoside)]-7-di-O-rhamnoside
85	21.65	230, 259, 268, 314	1047	MS^2: **901**(100), 927(10), 755(10), 781(10); MS^3: **755**(100), 781(35); MS^4: 300(100), 327(45), 409(40), 591(40), 271(35), 297(35), 343(25), 529(25), 301(15), 517(15).	Quercetin-3-O-[(2,6-O-*p*-coumaroyl-rhamnosyl-hexoside)]-7-di-O-rhamnoside

(1)m/z in bold was subjected to MS^n analysis.

Compound **31** should correspond to quercetin derivatives bearing hexosyl moiety. The observation of MS^2 [463] fragment resulting from the alternative loss of O-hexosyl unit (–162 Da), to yield the aglycone fragment at m/z 301. Moreover, weak fragment ions at m/z 379 and 352, resulting from the loss of flavonoid A ring $[M-H-84]^-$ and B ring $[M-H-110-H]^-$, respectively.[52] Set product ions were observed at m/z 256/257 ($[aglycone-CO_2]^-$), 151 ($^{1,2}A^-$−CO), 273 ($[aglycone-CO]^-$), 211 ($[aglycone-CO_2-CO-H_2O]^-$), 107 ($^{1,2}A^-$−CO−$CO_2$), 239 ($[aglycone-CO_2-H_2O]^-$), and 229 ($[aglycone-CO_2-CO]^-$) (Table 7). These neutral losses, suggesting that aglycone belongs to flavonols.[32] While, the MS^2 spectra showed a weak fragment ion at m/z 395 (<30%), indicated β-hydroxylation on ring A (C_3O_2, 68 Da) which would not be expected in the case of flavonols. However, the MS^3 [463→301] spectrum gave rise to rDA fragment ion at m/z 179 ($^{1,2}A^-$) and 301/300 in MS^2 which characteristic of quercetin in negative ESI fragmentations.[32] A compound with a similar pseudo-molecule ion was reported in *Zizyphus jujube* fruit as quercetin-3-O-galactoside.[53] Although, in our case, an intense fragment ion of aglycone ion (m/z 285 Da) accompanied by a weak radical aglycone ion (m/z 284 Da) confirmed the glycosylation site at the 7-O position.[54] Therefore, this compound was tentatively assigned as quercetin-7-O-hexoside.

Compounds **28**, **29**, and **30** were assigned as quercetin derivatives, through the UV spectra and the MS^n fragmentation which characteristic of flavonol-3-O-(6-O-rhamnosylhexoside), according to Federico Ferreres et al. (2008).[56] The MS-ESI data of these compounds gave origin to the fragment ion at m/z 301/300 [Ag–H/2H], resulting from the alternative loss of

308 Da (146+162 Da) residues which might suggest that glycan was located in the same position of the aglycone (Table 7). In our case, no fragment ion resulting from the rupture of the interglycosidic linkage of sugar moiety was noticed. Instead, it was observed the loss of 266 Da fragment (120+146 Da) from the ion at m/z 343, which indicates a rhamnosylation at position 6 of the hexose (Table 7).[49] Compound **29** showed minor product ion at m/z 591 [M–H–18]$^-$, probably due to the cleavage of the hydroxyl group (–OH) from the 3–OH position of the flavonoid.[45,46] Although, ions at m/z 179 ($^{1,2}A^-$), 151, 229, 273, 257, 211, and 192 ([M−H−ring B])$^-$ were observed in the MS^3 [609→301] spectrum and suggesting quercetin as aglycone.[32] All in all, the compounds were tentatively assigned as quercetin-3-O-rhamnosyl(6-O-hexoside).

Compounds **24**, **25**, **26**, **34**, **59**, and **80** were identified as quercetin derivatives, based on their UV spectra and the production of an MS^2 [755] product ion at m/z 300/301 ([quercetin–2H/H]$^-$) by the loss of rutinosyl residue (308 Da) (Table 7). In the MS spectra, fragments at m/z 609 [M–H–146]$^-$ ([quercetin-3-O-rhamnosyl(6-O-hexoside)]), 591 [M–H–146–18]$^-$, and 573 [M–H–146–36]$^-$ (**26**) were observed and suggested the presence of a 2-O-linked rhamnosyl moiety (146 Da).[57,54] The neutral loss of 36 Da ($2H_2O$) may indicate the successive loss of water molecules. Although the fragments at m/z 489 (**24**) and 343 (**24-26**) from further loss of respective 266 Da (120+146 Da) and 412 Da (120+146+146 Da) from the molecule ion indicated an intern rupture of the hexose linked to a rhamnosyl moiety at its 6-position, by positions 0,2 (fragment of 120 Da) (Table 7), since the linkage 1→6 is very stable.[56,57] Other fragments were observed at m/z 325 [M–H–284]$^-$ (**24**), 373 [M–H–236]$^-$ (**25** and **34**), and 315 [M–H–294]$^-$ (**34**), corresponding to the radical anion species of quercetin instead of kaempferol since the MS^3 [300] data showed ions at m/z 179, 255, 257, and 229 correspond to the main fragmentation of quercetin in negative mode ESI (as explained above) (Table 7).[32] Otherwise, the fragments 325, 373, and 315 designated the successive loss of sugar moiety. According to this data, compound **24-26** were tentatively identified as quercetin-3-O-(2,6-di-O-rhamnosylhexoside), which were previously reported in *Z. lotus* leaves.[14]

In the MS^2 [755] fragmentation of compounds, **34**, **59**, and **80** a base peak ion at m/z 609 [quercetin-3-O-rhamnosyl(6-O-hexoside)] was produced by the cleavage of rhamnosyl unit (146 Da) from the hydroxyl in position C-7 as being much more favored in ESI-MS than from position C-3.[58,59] Moreover, in the MS^3 fragmentation, the observation loss of 308/309 fragments (at m/z 301/300) suggested the loss of rutinosyl moiety linked at 3–OH position, although the main fragment at m/z 179 could be interpreted as corresponding to the partial fragmentation of the quercetin (Table 7).[32]

Compound **34** showed UV spectra similar to those of **24-26** with less MS^n data, display the neutral loss of 266 Da fragment, corresponding to the ion at m/z 343, which as referred above, indicates rhamnosylation at position 6 (Table 7).[49] Besides, compound **80** showed a weak fragment ion at m/z 635 (<30%) corresponding to the neutral loss of a fragment of 120 Da, indicated the breakdown of 0,2 hexosyl moiety (162 Da).[58,60] The later elution, as well as the higher retention time (t_R: 17.06–19.61 min) of compounds **59**/**80**, allowed their identification as acylated forms of compounds **24-26** and **34** (Table 7).[61] Their UV spectra were characterized by a distinct (315–311 nm) hypsochromic shift in Band I, indicating that they might be acylated with hydroxycinnamic acid that was interpreted as a *p*-coumaric moiety.[61,62]

Thus, the retention time of compound **80** is too much higher than those of earlier described compounds, indicating that it may contain more than one acyl group. This hypothesis isn't confirmed due to the leak of MS-ESI fragmentation and literature data so that compound could be only speculated to be as an isomer of compound **59**.[57] Therefore, these compounds could be labeled as quercetin-3-O-[rhamnosyl(6-O-hexoside)]-7-O-rhamnoside (**34**), and quercetin-3-O-(*p*-coumaroylhexoside)-7-O-rhamnoside (**59** and **80**).

As in the case described above, the MS analysis of compounds **27**, **44**, **50**, **56**, **67**, **69**, **78**, and **79** ($[M–H]^-$, m/z 901 Da) displayed ion produced after the loss of rhamnosyl residue (146 Da) from 7-OH position ($–MS^2$ $[(M−H)→755(M−H−146)]^-$) (Table 7). Accordingly, the tri-saccharide losses ([Ag−2H], m/z 300 Da) were easily detected in the MS^3 spectrum.[58] In the MS^3 [300] product ion, the observation of ions at m/z 151, 243, 271, and 255, suggesting quercetin as aglycone.[32] The MS^2 [901] spectrum of compounds **44**, **50**, and **56** exhibited additional fragment ion at m/z 781, pointed to the partial fragmentation of the hexosyl residue (–120 Da), and the observation of ions at m/z 737 (**56**) and 591 (**50**, **56**, **67**, **69**, and **78**) from the loss of 164 Da that suggested the presence of a 2-O-linked rhamnosyl moiety. Other product ions were observed in the MS^3 [755] spectrum at m/z 343 and 489, corresponding, respectively, to the loss of 412 Da (146+146+120 Da) and 266 Da (120+146 Da).[49] This would indicate O-glycosylation at position 6 of the O-attached sugar.[57] Compound with the same molecule ion was detected in *Z. lotus* and *Zizyphus spina-christi* leaves by Elsadig Karar et al. (2016)[35] and Rached et al. (2019),[14] respectively and suggested to correspond to the quercetin-3-O-(2,6-di-O-rhamnosylhexoside)-7-O-rhamnoside, so that those identities were also tentatively assumed in the case of compound **50**.

Compounds **56**, **67**, **69**, **78**, and **79** shared the same basic skeleton as **27**, **44**, and **50**, with a fragmentation pattern indicated O-substituted quercetin. However, their UV spectra pointed to the acylated flavonoid derivatives with hydroxycinnamic acid.[61,62] The MS^3 [755] spectrum exhibited a fragment at m/z 609 (**56**, **67**, **69**, **78**, and **79**) together with product ions at m/z 346 (146+263 Da), 353 (146+256 Da), 325 (146+284 Da), 355 (146+254 Da), 327 (146+282 Da) (**27**), and 487 (–263 Da) correspond to the successive loss of rhamnosyl or *p*-coumaric acid moieties, along with the radical anion species of quercetin.[32] Further ions were observed at m/z 409 (146+162+38 Da) (**50**, **69**, and **78**), 573 (162+18+2H Da) (**67**), 465 (–290 Da) (**27**), and 446 (146+162 Da) (**44**) indicated breakdown with partial loss of sugar residue. Therefore, these compounds could be assigned as quercetin-3-O-[di-rhamnosyl(2-O-hexoside)]-7-O-rhamnoside (**27)**, quercetin-3-O-[(di-O-rhamnosylhexoside)]-7-O-rhamnoside (**44**), quercetin-3-O-[(2,6-di-O-rhamnosylhexoside)]-7-O-rhamnoside (**50**), and quercetin-3-O-[(2,6-O-*p*-coumaroyl-rhamnosyl-hexoside)]-7-O-rhamnoside (**56**, **67**, **69**, **78**, and **79**).

The fragmentation pattern of compounds **61**, **63**, **72**, **84**, and **85** ($[M–H]^-$, m/z 1047 Da) indicated the presence of four sugar-moiety conjugated with by five or four O-sugar linkages. These compounds produced two fragment ions at m/z 901 and 755 which are the molecule ion of compounds discussed above and indicating the loss of di-rhamnoside residues from position 7. The MS^4 [755→300] (neutral loss of triglyosides (–454 Da) moieties) were reminiscent to that of quercetin 3-O-(di-O-rhamnosyl-hexoside). In the case of compounds **63** and **72**, an ion at m/z 609 was appeared, resulting from the simultaneous loss of the rhamnose at position 3. Their MS^4 fragmentation showed ion at m/z 301 corresponds to the loss of

rutinosyl moiety (O-rhamnosylhexoside). The assignment of substitution position of the sugar moiety was based on the observation of fragment ions at m/z 343 and 591 characteristics of an interglycosidic linkage in compounds **63** and **85**.[56,57] These data suggested that these compounds were derivatives of compounds **56**, **67**, **69**, **78**, and **79** with an additional of O-rhamnoside (–146 Da) substituent at position 7, which is preferential.[58,59] A compound with the same molecular ion and fragmentation characteristics was identified in *Zizyphus spina-christi* leaf by Elsadig Karar et al. (2016)[35] as quercetin 3-O-(2,6-di-O-rhamnosyl-glucoside)-7-di-O-rhamnoside. However, the low value of UV spectra for Band I (315 nm) and the high retention time indicate that these compounds were acylated with *p*-coumaric acid.[61,62] The observation of MS^2 fragment ions at m/z 737 (**61** and **84**), 712 (**63**), and 781/927 (**61**, **84**, and **85**) were characteristic loss of 18, 43, and 120 Da, respectively indicate the loss of hydroxyl group from the 3-OH position, CO_2 group, and the cross-ring cleavage of hexose moiety. Thus, these compounds could be identified as quercetin-3-O-[(2,6-O-*p*-coumaroyl-rhamnosyl-hexoside)]-7-di-O-rhamnoside (**63** and **85**), and quercetin-3-O-[(*p*-coumaroyl-rhamnosyl-hexoside)]-7-di-O-rhamnoside (**61**, **72**, and **84**).

Compounds **55** showed a molecule ion at m/z 931 $[M–H]^–$, MS^2 fragment ions at m/z 755 $[M–H–162–14]^–$ and 769 $[M–H–162]^–$ from the putative loss of methyl and hexosyl moieties. The MS^3 fragmentation showed neutral loss of triglyosides (–454 Da) moieties to yield the aglycone fragment at m/z 315. The fragment ion at m/z 300, arising from the loss of methyl radical from molecular ion ($[M–H]^–$, m/z 315, Isorhamnetin),[55] while m/z 271, corresponding to the characteristic ion of quercetin in negative ESI fragmentation.[32] Therefore, and according to MS-ESI information and to the UV spectra, this compound suggested to be isorhamnetin-3-O-[(*p*-coumaroyl-rhamnosyl-hexoside)]-7-O-hexoside.

Nine kaempferol derivatives were identified in methanol/water/acetic acid extracts of *Z. lotus*. The deprotonated molecule ion of these compounds ($[M–H]^–$, m/z 885, 739, and 593) were already identified in the work of Del Rio et al. (2004)[48] and Ikeda, M et al. (2016)[63] as unknown kaempferol-*p*-coumaroyl-sugar and kaempferol-sugar conjugates, respectively.

Table 8: HT-UHPLC-UV-MS^n data of flavonols identified in the methanol/water/acetic acid extracts of *Zizyphus lotus*.

Peak	R_t (min)	λ_{max} (nm)	$[M–H]^–$ (m/z)	HT-UHPLC–MS^n product m/z (% base peak)[(I)]	Compound
37	10.37	228, 265, 345	593	MS^2: **285**(100), 284(95), 255(25), 327(15); MS^3: 257(100), 229(65), 267(55), 241(50), 256(40), 179(40), 163(35), 151(15), 169(10).	Kaempferol-3-O-[6-O-rhamnosylhexoside]
40	11.77	232, 265, 344	593	MS^2: **285**(100); MS^3: 257(100), 267(50), 229(45), 241(35), 213(25), 197(25), 163(15), 151(10), 173(10).	Kaempferol-3-O-rutinoside
41	11.85	232, 266, 344	593	MS^2: **285**(100), 257(15).	Kaempferol-3-O-rutinoside

70	18.52	232, 264, 311	593	MS^2: **285**(100), 447(30), 257(10); MS^3: 151(100), 214(85), 215(75).	Kaempferol-3-O-[hexosyl(2-O-*p*-coumaroyl)]
71	18.70	233, 267, 314	739	MS^2: 593(100), **285**(60), 255(25), 575(25); MS^3: 163(100), 257(80), 227(50), 199(45), 151(30), 285(25).	Kaempferol-3-O-[hexosyl(2-O-*p*-coumaroylrhamnoside)]
73	18.99	231, 267, 314	885	MS^2: **739**(100); MS^3: 284(100), 575(100), 285(95), 255(45), 393(30), 593(20), 327(20), 473(15), 257(15), 339(15).	Kaempferol-3-O-[2,6-O-*p*-coumaroylrhamnosyl-hexoside]-7-O-rhamnoside
74	19.07	231, 267, 314	885	MS^2: **739**(100); MS^3: 575(100), 284(50), **285**(40), 327(15), 593(15), 393(15), 255(15); MS^4: 151(100), 257(95), 213(85), 241(60), 267(55), 285(45), 169(40).	Kaempferol-3-O-[2,6-O-*p*-coumaroylrhamnosyl-hexoside]-7-O-rhamnoside
81	19.85	229, 267, 311	739	MS^2: **285**(100), 593(85); MS^3: 257(100), 241(15).	Kaempferol-3-O-[hexosyl(2-O-*p*-coumaroylrhamnoside)]
83	20.26	233, 266, 311	885	MS^2: **739**(100), 575(15), 721(10); MS^3: 284(100), 327(25), 457(25), 256(25), 473(20), **285**(20), 338(15); MS^4: 151(100), 163(90), 226(85), 267(85), 212(55).	Kaempferol-3-O-[2,6-O-*p*-coumaroyl-rhamnosyl-hexoside]-7-O-rhamnoside

[(1)] m/z in bold was subjected to MS^n analysis.

The EI-MS data (Table 8) of the chromatographic peak **37**, **40**, **41**, and **70** showed a molecular ion at m/z 593 $[M–H]^-$ followed by product ion at m/z 285 [aglycone–H], due to the loss of rutinosyl moiety (–308 Da). Further ions were observed at m/z 257 ([aglycone–$CO]^-$), 229 ([aglycone–2$CO]^-$), 267 ([aglycone–$H_2O]^-$), 241 ([aglycone–$CO_2]^-$), 213/214/215 ([aglycone–CO_2–$CO]^-$), 151 ([aglycone–($^{1,2}A^-$)–$CO]^-$), and 163 ($[^{1,2}A^-$]), resulting from kaempferol fragmentation; the last product ion was formed through the rDA fragmentation pathway.[32] Compound **37** characterized by additional loss of a 266 Da fragment (120+146 Da) correspond to the fragment ion at m/z 327. This neutral loss indicates a rhamnosylation at position 6 of a hexose.[57] A compound with the same molecule ion was detected in *Z. lotus* leaves by Rached et al. (2019),[14] and suggested to correspond to the kaempferol-3-O-[6-O-rhamnosylhexoside] and kaempferol-3-O-rutinoside, so that those identities were also assumed in the case of compounds **37** and **40**/**41**, respectively.[14] Therefore, compound **70** showed additional fragment ion at m/z 447 $[M–H–146]^-$ corresponds to cleavage of a *p*-coumaric acid rather than rhamnosyl moiety. This hypothesis is reinforced by the UV spectra (311 nm, characteristic of *p*-coumaric acid) and the higher retention time (t_R: 18.52).[48,61] Therefore, and according to MS data, these compounds could be assigned to kaempferol-3-O-[6-O-rhamnosylhexoside] (**37**), kaempferol-3-O-rutinoside (**40** and **41**), and kaempferol-3-O-[hexosyl(2-O-*p*-coumaroyl)] (**70**).

Compounds **71** and **81** can be kaempferol-3-O-[hexosyl(2-O-*p*-coumaroylrhamnoside)], according to the UV spectra, molecular ion at m/z 739 $[M–H]^-$, and its MS^2 fragmentation suggested the presence of triglyosides units (454 Da) linked at 3-OH positions (Table 8).[48,49] Similar compound was identified in *Zizyphus spina-christi* leaf and assigned to kaempferol 3-O-(2,6-di-O-rhamnosyl-glucoside).[35] According to the UV spectrum, these compounds were monoacylated with hydroxycinnamic acid[61] and could be considered as derivatives of compound **70** (kaempferol-3-O-[hexosyl-*p*-coumaroyl], $[M–H]^-$, m/z 593 Da) by addition of a rhamnosyl moiety.[57] The MS^2 [739] fragmentation of these isomers showed ions at m/z 575 $[M–H–146–18]^-$ (**71**) and 593 $[M–H–146]^-$ (**81**), arising from the successive loss of rhamnosyl or coumaric acid moieties. Moreover, the m/z 285 [aglycone–H] formed after the loss of pair of hexosyl and rhamnoside moieties was considered as kaempferol flavonoid, which confirmed by the presence of set product ions in MS^3 [285→739] spectrum at m/z 163 ($[^{1,2}A^-]$), 227 ($[aglycone–CH_2O–CO]^-$), 199 ($[aglycone–C_2H_2O–CO_2]^-$), 151 ($[aglycone–(^{1,2}A^-)–CO]^-$), 257 ($[aglycone–CO]^-$), and 241($[aglycone–CO_2]^-$).[32]

Compounds **73**, **74**, and **83** exhibited a molecular ion higher by 146 Da than that of **71**/**81** ($[M–H]^-$, m/z 739) (Table 8). Their MS^n fragmentation showed losses of 146 Da (MS^2 [885], m/z 575 and 721 (**83**)) and 292 Da (MS^3 [739]→ m/z 575 (**73/74**)) with the corresponding ion indicated the interglycosidic linkage 1→2.[57] Additionally, product ion was detected at m/z 327 (266+146 Da) with additional losses of 266 Da and 146 Da fragments at m/z 473 (**73** and **83**) and 593 (**73/74**), respectively. Moreover, The MS^n data exposed ions at m/z 255, 257, 151, 213, 243 ($[aglycone–C_2H_2O]^-$), and 241($[aglycone–CO_2]^-$) characteristic of flavonols as well as the typical product ion of kaempferol at m/z 163 ($[^{1,2}A^-]$).[32] Therefore, the loss of fragment ion corresponds to the aglycone being also detected in a weak peak at m/z 457 (**83**) (Table 8). These compounds having UV spectra of acylated flavonoid with *p*-coumaric acid (the band I: 311–314 nm) and mass spectra corresponds to kaempferol-sugar derivatives. Thus, these compounds could be assigned as kaempferol-3-O-[2,6-O-*p*-coumaroylrhamnosyl-hexoside]-7-O-rhamnoside.

3.2.2.4 Flavones

Three luteolin derivatives (**42**, **58**, and **82**), seven apigenin glycoconjugates (**19**, **20**, **22**, **33**, **35**, **36**, and **38**), and twelve acylated apigenin glycoconjugates (**43**, **45-49**, **51- 53**, **57**, **62**, and **75**) were identified in the methanol/water/acetic acid extracts of *Z. lotus*, based on their UV spectra and the MS^n fragmentations data (Tables 9 and 10).

3.2.2.4.1 Flavones glycosides

Ten flavones derivatives were identified for the first time as a component of *Z. lotus* and were mainly concentrated in the leaves and seeds. The identification of these compounds was attained based on MS^n fragmentation and on the characteristic UV spectra (Table 9).

Table 9: HT-UHPLC-UV-MS^n data of flavone identified in methanol/water/acetic acid extracts of *Zizyphus lotus*.

Peak	R_t (min)	λ_{max} (nm)	$[M–H]^-$ (m/z)	HT-UHPLC–MS^n product m/z (% base peak) [I]	Compound
19	7.38	232, 274, 326	593	MS^2: **473**(100), 353(73), 547(50), 413(38), 383(35), 379(28), 545(28); MS^3: 353(100), 383(25).	Apigenin 6,8-di-C-glucoside
20	7.57	231, 271, 326	593	MS^2: **473**(100), 353(75), 503(38), 383(30), 297(10), 575(10); MS^3: 353(100), 383(25), 297(10).	Apigenin 6,8-di-C-glucoside
22	7.68	232, 271, 330	593	MS^2: **473**(100), 353(60), 383(45), 503(28), 575(10); MS^3: 353(100), 383(15).	Apigenin 6,8-di-C-glucoside
32	9.77	232, 268, 334	653*	MS^2: **607**(100); MS^3: 445(100), 487(80), 427(55), 335(15), 325.	7-O methyl apigenin-2″-O-glycosyl-6-C-glucoside
33	9.93	237, 270, 335	607	MS^2: **427**(100), 307(15), 445(15), 487(15); MS^3: **307**(100), 292(20); MS^4: 292(100).	7-O methyl apigenin-2″-O-glycosyl-6-C-glucoside
35	10.07	237, 270, 334	607	MS^2: **427**(100), 307(15), 445(15), 487(15); MS^3: **307**(100), 292(20); MS^4: 292(100).	7-O methyl apigenin-2″-O-glycosyl-6-C-glucoside
36	10.36	232, 269, 334	607	MS^2: **427**(100), 325(20), 292(20), 283, 307; MS^3: **307**(100), 292(80), 367(60), 283(45), 325(40), 297(25); MS^4: 292(100).	7-O methyl apigenin-2″-O-glycosyl-6-C-glucoside
38	10.61	231, 272, 333	445	MS^2: **297**(100), 325(75), 282(43), 231(30), 216(25), 323(23), 355(20), 295(19), 261(15), 377(10), 269(10); MS^3: 269(100), 267(40), 241(40), 197(40), 295(20), 149(15).	7-O-methyl apigenin-6-C-glucoside
42	12.02	229, 265, 341	447	MS^2: **285**(100), 284(85), 255(65), 379(65), 311(15), 327(15); MS^3: 199(100), 257(95).	Luteolin-7-O-hexoside
58	16.58	230, 267, 316	885	MS^2: **739**(100), 593(15), 445(10); MS^3: 243(100), 257(65), 285(25).	Luteolin-3-O-[hexosyl(*p*-coumaroylrhamnoside)]-7-O-rhamnoside

82	20.17	230, 266, 311	885	MS^2: **739**(100), 721(10), 575(10); MS^3: 575(100), **285**(85), 284(35), 255(25), 393(20), 339(15), 429(10), 593(10); MS^4: 241(100).	Luteolin-O-[(hexosyl(6-O-*p*-coumaroylrhamnoside)] -O-rhamnoside

(I)m/z in bold was subjected to MS^n analysis, *: Formic acid adduct (FA).

The negative ESI of compound **42** gave origin to the molecule ion at m/z 447 $[M–H]^-$. The MS^2 fragmentation showed base peak fragment ion at m/z 284/285 $[Ag–H/2H]^-$ indicated the flavonoid-O-hexosyl moiety (Table 9). In the same, a product ion at m/z 311 $[M–H–135–H]^-$ was detected in MS data and was attributed to $^{1,3}A^-$ cleavage, indicating the presence of one hydroxyl group on ring A[46] although, 327 $[M–H–120]^-$ formed after the cross-ring cleavage of hexoses moiety.[60] Besides, the MS data showed characteristic product ions of flavonoids aglycone at m/z 257 ($[aglycone–CO]^-$) and 199 ($[aglycone–C_2H_2O–CO_2]^-$).[32] A compound with similar pseudomolecule ion and characteristics fragment was already reported in *Zizyphus spina-christi* leaves by Elsadig et al. (2016)[35] and has been assigned as kaempferol-3-O-glucoside. Indeed, a high peak at m/z 255 ($[aglycone–2H–CO]^-$) was observed in the MS^2 fragmentation and consisting of the reported data for flavonols.[59] However, the same fragment has also been observed for several flavonoids.[64] A loss of 68 Da (C_3O_2), at m/z 379 (>60%) has also been observed and has been suggested to be indicative of flavones.[32] Therefore and according to the intensity of ion at m/z 199 (base peak), UV spectra, and on what discussed above this compound could be assigned as luteolin-7-O-hexoside.[32]

As detailed reported above, compounds **58** and **82** have a UV spectra characteristic of acylated flavonoids derivatives. Their MS-ESI analysis gave a molecule ion at m/z 739 $[M–H–146]^-$, resulting from the simultaneous loss of the rhamnose unit at position 7, undergoes MS fragmentations similar to those of compounds **73**, **74**, and **83**. The fragment ion at m/z 285 was formed by the loss of triglyoside moieties and pointed to luteolin as aglycone. This fact was confirmed by the relative intensities of the observed ion signals at m/z 241, 243, and 257 in the $MS^{3,4}$ spectra.[32] On the other hand, compound **58** is characterized by the presence of additional ion at m/z 445 $[M–H–146–146–2H]^-$ in the MS^2 spectrum that corresponds to the loss of rhamnose and coumaric acid. Consequently, these data indicated that the current compounds corresponding to luteolin-O-[hexosyl(*p*-coumaroylrhamnoside)]-7-O-rhamnoside (**58**) and luteolin-O-[hexosyl(6-O-*p*-coumaroylrhamnoside)]-7-O-rhamnoside (**82**).

Compounds **19**, **20**, and **22** produced the same molecule ion at m/z 593 $[M–H]^-$, and they shared the same major ions in MS^2 spectra. The fragment ions at m/z 353 $[M–H–(Ag+83)]^-$, 383 $[M–H–(Ag+113)]^-$, 473 $[M–H–120]^-$, 503 $[M–H–90]^-$, and 575 $[M–H–18]^-$ are typical of di-*C*-glycosylflavone, suggesting apigenin as an aglycone (MW 270).[65,66] The fragment ion at m/z 575 may be due to sugar structures linked directly to the aglycone, while m/z 297 (**20**) corresponds to the aglycone with two CH_3 groups derived from the C-bonded sugar still attached.[67] The three compounds were producing in the MS^3 [473] spectra, the same fragment ions at m/z 353 and 383 due to the further neutral loss of 120 and 90 Da from the other sugar moiety (Table 9). According to MS data and the UV spectra[65,66] these compounds could be assigned as apigenin 6,8-di-C-glucoside isomers.

Compounds **33**, **35**, and **36** were identified based on UV spectra[68] and to the displayed molecule ion at m/z 607 $[M-H]^-$. The MS^2 [607] fragmentation showed ions at m/z 427 $[M-H-180]^-$ and 445 $[M-H-162]^-$ (**33**/**35**); the loss of 180 Da (162+18 Da) resulted in the base peak, which is characteristic of an O-glycosylation on the hydroxyl group on position 2 of the C-glycosylation sugar (Table 9).[55,69,70] The loss of hexosyl moiety and a fraction of C-glycosylation generated fragment ions at m/z 487 $[M-H-120]^-$ (**33**/**35**) and 307 $[M-H-(162-18)-120]^-$, suggesting a 6″-O-hexosyl-C-hexosyl structure.[65] Other fragment ions located at m/z 325 $[M-H-282(Ag+13)]^-$, 283 and 297 (**36**) led to the aglycone (apigenin, 270 DW).[67,71] The neutral loss of 60 Da (CH_3+H_2O+CO) gives ion at m/z 367 (60%) in MS^2 spectrum characteristic fragment of flavones which having a higher or lower degree of methoxylation. Moreover, the MS^4 [307] give a rise to the fragment ion at m/z 292 correspond to the loss of the methyl group (15 Da, CH_3). Compound **32** produce a $[M+HCOO]^-$ at m/z 653 suffered the loss of −46 Da (FA) to produce an ion at m/z 607 which had similar UV spectra, along with pattern fragmentation similar to those of compounds **33**, **35**, and **36** (Table 9). Based on the obtained data, these compounds were concluded to be isomers of 7-O methyl apigenin-2″-O-glycosyl-6-C-glucoside which had already been identified in *Zizyphus jujuba* and *Zizyphus spinosae* seeds.[53,72]

Compound **38** displayed a molecule ion at m/z 445 $[M-H]^-$ which already identified in *Zizyphus jujuba* seeds as swertish ($[M-H]^-$, m/z 607 Da).[53] The MS^2 [445] spectrum showed a base peak fragment ion at m/z 297 $[M-H-148]^-$, indicating the loss of $^{1,4}B^-$ ring by rDA reaction.[32] The m/z 297 corresponds probably to the aglycone with two CH_3 groups.[67] Further fragment ions were observed at m/z 325 $[M-H-120]^-$ and 355 $[M-H-90]^-$ which are typical of C-glycosidic flavonoid. The presence of base peak fragment ion at m/z 269 in MS^3 [445] spectrum with other fragment ions at m/z 267 $[aglycone-H-H_2O]^-$, 241 $[aglycone-CO]^-$, 197 $[aglycone-CO_2-CO]^-$, and 149 ($^{1,4}B^-$+2H) confirmed apigenin as aglycone (Table 9).[73] Taking into account these obtained data this compound was concluded to be 7-O-methyl apigenin-6-C-glucoside (swertish).

3.2.2.4.2 Acylated Flavone

Twelve acylated flavones were detected for the first time as a component of *Z. lotus* and were mainly concentrated in the seeds fraction. The identification of these compounds was achieved based on literature data,[49,65,67] and on the characteristic UV spectra[70,74] The analysis fragmentation pathways of flavone exception of compounds **43**, **46**, **47**, **53**, and **75** showed that they behave similarly with loss of an O-(acyl) group to yield an ion with high relative abundance, which is the pseudo-molecule ion (MW 607) of compounds **33**, **35**, and **36**. Therefore, these compounds could be considered as acylated derivatives of 7-O-methyl-mono-6-C-glycosylapigenin differing only in their putative hydroxycinnamic acid namely: sinapic, ferulic, caffeic, dihydroferulic, hydroxyferulic, methoxymalonic, methylmalonic, methylacetyl, *p*-coumaric, and dihydrophaseolic acid. However, the positions of the acyl group on the glycosidic part of the molecule and that of the acylhexose group on the aglycone could be reported in the literature to be predominantly in position 6 of the hexose probably in position 2 of the terminal hexose and 7 of the aglycone.[57]

Table 10: HT-UHPLC-UV-MS^n data of acylated flavone identified in methanol/water/acetic acid extracts of *Zizyphus lotus*.

Peak	R_t (min)	λ_{max} (nm)	$[M–H]^-$ (m/z)	HT-UHPLC–MS^n product m/z (% base peak)$^{(I)}$	Compound
43	13.51	231, 272, 325	857	MS^2: **783**(100), 663(10); MS^3: **427**(100), 487(60), 292(40), 307(25); MS^4: 307(100) 391(45), 283(20).	7-O-methyl (2″-methylacetyl) apigenin-O-(6‴-hydroxyferuloyl)glucosyl-6-C-glucoside.
45	14.44	231, 272, 330	707	MS^2: **649**(100), 689(40), 427(39), 607(20); MS^3: **427**(100), 589(30), 608(25), 309(20), 292(15), 267(10), 487(10); MS^4: 307(100), 292(40), 325(25), 309(20), 295(19).	7-O-methyl apigenin-2″-O-(6‴-methylmalonyl)glycosyl-6-C-glucoside.
46	14.69	232, 274, 330	385	MS^2: **353**(100), 243(25), 249(19), 317(19), 225(15), 309(10); MS^3: 225(100), 243(85), 309(40), 269(10).	7-O-methoxymalonyl-apigenin isomer
47	14.93	232, 272, 334	385	MS^2: **353**(100), 243(29), 225(25), 309(10); MS^3: 243(100), 309(70), 225(55), 291(40), 335(30), 269(25), 199(15), 226(15).	7-O-methoxymalonyl-apigenin isomer
48	15.13	238, 273, 330	813	MS^2: **607**(100), 427(95), 693(86), 325(40), 307(25), 311(25),798(20), 487(20), 295(20), 281(15), 265(15), 251(10); MS^3: **307**(100), 427(45), 385(35), 355(25), 445(15), 592(10), 311(10), 337(10); MS^4: 292(100).	7-O methyl apigenin-2″-O-(2‴-sinapoyl)glucosyl-8-C-glycoside
49	15.22	236, 273, 317	799	MS^2: **307**(100), 607(82), 413(55), 771(50), 785(45), 381(28); MS^3: 279(100).	7-O methyl apigenin-2″-O-(2‴-hydroxyferuloyl)glucosyl-C-glucoside
51	15.47	233, 273, 330	783	MS^2: **607**(100), 483 (85), 445(80), 427 (35), 325(20); MS^3: 307(100), 487(85), 427(80), 349(70), 325(65), 239(40), 367(35).	7-O methyl apigenin O-(2‴-feruloyl)glucosyl-C-glucoside
52	15.56	232, 273, 334	783	MS^2: 325(100), 251(65), 239(62), 287(60), 307(35).	7-O methyl apigenin O-(feruloyl)glucosyl-C-glucoside
53	15.79	232, 275, 330	979	MS^2: **783**(100); MS^3: **427**(100), 295(60); MS^4: 292.	7-O methyl-(2''-dihydroferuloyl)apigenin O-(feruloyl)glucosyl-C-glucoside

57	16.52	232, 274, 330	873	MS^2: **608**(100), 609(55); 283(55), 428(50), 842(25), 292(20), 589(10); MS^3: 488(100), 322(30).	7-O methyl apigenin-O-(2'''-dihydrophaseoyl)glucosyl-C-glucoside
62	17.37	232, 272, 335	869	MS^2: **607**(100), 427(39), 839(39), 589(20); MS^3:**427**(100), 307(20), 445(15), 487(15), 325(10); MS^4: 307(100), 292(35), 379(15).	7-O methyl apigenin-O-(2'''-dihydrophaseoyl)glucosyl-C-glucoside
75	19.19	233, 276, 317	737	MS^2: **589**(100), 427(75), 307(47), 309(20), 283(20), 445(15), 229(10); MS^3: 433(100), 324(95), 469(85), **427**(60), 293(25), 411(20), 321(20); MS^4: 307(100), 292(40), 311(25), 367(20).	7-O methyl apigenin O-(2'''-*p*-coumaroylrhamnoside)-6-C-hexoside

(1) m/z in bold was subjected to MS^n analysis, *: Formic acid adduct (FA).

Compound **43** displayed a molecule ion at m/z 857 $[M-H]^-$ and displayed a base peak fragment at m/z 783 $[M–H–(56–18)]^-$ accompanied by a minor ion at m/z 663 $[M–H–194]^-$ (10%) in agreement with the loss of an O-(methylacetyl) and O-(hydroxyferuloyl), respectively. The primary residue was concluded to be linked to the phenolic hydroxyl by 1→2 due to the relative intensity of the ions observed at m/z 783.[75] Moreover, the MS^3 [783] spectrum showed product ion at m/z 427, corresponding to the loss of an O-(6‴-hydroxyferuloyl)hexosyl (194+162 Da).[75] The ion at m/z 307 in MS^4 of [857→427] generated by the cleavage of –120 Da and the successive loss of water molecule (36 Da, $2H_2O$) in m/z 391 designate the presence of mono-6-C-glucoside.[70,76] The absence of aglycone ion in MS spectra consistent with an O-,C-diglycoside structure.[66] Further, ions were observed at m/z 283 (Ag+14), 296, and 292 led to the aglycone as methylapigenin[67,71] although, the ion at m/z 292 indicates the loss of methyl group (15 Da, CH_3). This suggested the identification of this compound as 7-O-methyl (2″-methylacetyl)apigenin-O-(6'''-hydroxyferuloyl)glucosyl-6-C-glucoside.

Compound **45** showed a molecule ion at m/z 707 $[M-H]^-$ and exhibited MS^2 fragmentation which was characterized by the loss of –44 Da (CO_2) and –18 Da (H_2O) to yield the base peak at m/z 649 $[M–H–44–14]^-$, this behavior being typical of compounds acylated with a dicarboxylic acid.[57] In the same spectrum fragment ions were observed at m/z 607 $[M–H–100]^-$ (acyl−18) and 427 $[M–H–(100–18)–162]^-$, suggesting an O-(acyl)-glycosylation.[65] The product ion at m/z 427 appears again as a base peak in MS^3 [649] data, corresponding to the loss of 162 and 42 Da residues. The loss of 42 Da would be related to the rest of the acyl decarboxylate, which for this compound would correspond to malonic acid.[57] Moreover, the revealing of fragment ion at m/z 307 (cross ring of hexosyl unit, 120 Da) accompanied to the loss of water molecule at m/z 689 might indicate the 6-C substitution.[70,76] Other fragment ions were observed at m/z 487 and 292, corresponding to the putative loss of hexosyl unit (–162 Da) and methyl group (–15 Da), respectively although, the ion at m/z 589 indicates the loss of methyl, water molecule, and a carboxyl group.[77] The fragment ion observed at m/z 295, 292,

and 267 may characterize the aglycone as methylapigenin. Based on these observations and on the fact that the ion observed at m/z 607, showed a very low relative intensity (20%),[75] this compound was proposed to be 7-O-methyl apigenin-2″-O-(6'''-methylmalonyl)glycosyl-6-C-glucoside.

Compounds **46** and **47** displayed similar molecule ion at m/z 385 $[M–H]^-$. The MS data showed fragment ion at m/z 353 $[M–H–32]^-$, with a very high relative intensity (base peak), indicating the loss of the methoxy group. In the same MS data, fragment ions were observed at m/z 317 and 243 explained by the loss of 68 and 110, respectively from the original compound. These residues are probably due to the cleavage of C_3O_2, and C_3O_2-C_2H_2O which are characteristic losses of flavone fragmentations in the ESI negative ion mode.[32] Other fragment ion was observed at m/z 309, suggesting the loss of fragment 44 Da from the cleavage of CO_2 or malonic acid. However, the MS^3 [353] spectrum gives rise to the loss of 84 Da corresponds to m/z 269 established the presence of the malonyl group. Furthermore, the ions at m/z 225 ($[aglycone–H–CO_2]^-$) (base peak) and 269 with weak abundance confirmed apigenin as aglycone. These results suggested this compound could be 7-O-methoxymalonyl-apigenin.

Compound **48** exhibited a molecule ion at m/z 813 $[M–H]^-$. The MS fragmentation showed ions at m/z 607 $[M–H–206]^-$, 427 $[M–H–(206–18)–162]^-$, 295 $[M–H–206–162–150]^-$, 281 $[M–H–(206–2H)–162–162]^-$, 487 $[M–H–162–162]^-$, and 265 $[M–H–(206–18)–162–162]^-$. These fragment ions were consistent with the loss of an O-(sinapoyl)-di-glucoside with 1→2 interglycosidic linkages.[65] Further loss that characterizes the O-glycosylation on the hydroxyl group in 2″ in the C-glycosylation sugar were also observed in $MS^{2,3}$ at m/z 427 (162+18 Da), 445 (162 Da), and 693 $[M–H–120]^-$.[74] The ion at m/z 311 (Ag+42) is typical of mono C-glycosylflavones and confirmed the substitution in the C-8 position due to the low relative intensity (25%) of the fragment ion at m/z 311.[78] Additional ions were observed at m/z 798 and 592, indicating the successive loss of methyl group (15 Da, CH_3) although, ions at m/z 337 (–270 Da) and 251 ($^{1,3}A^-$) confirmed apigenin as an aglycone.[32] Therefore, this compound could be labeled as 7-O methyl apigenin-2″-O-(2'''-sinapoyl)glucosyl-8-C-glycoside similar to the compound previously reported in *Zizyphus mauritiana* seeds.[79,80]

Compound **49** displayed a molecule ion at m/z 799 $[M–H]^-$. The characteristic fragment ions at m/z 307 $[M–H–(192–18)–162–120]^-$, 607 $[M–H–192]^-$, 413 $[M–H–(192–18)–162–14]^-$, and 381 $[M–H–(192–18)–162–46]^-$ indicate the loss of an O-(acyl)-glucosyl-C-glucoside moiety. The observed loss of 192 Da, indicating loss of dehydrated hydroxyferuloyl acid connected through an interglycosidic 1→2 linkage to the glucoside due to the high relative intensity of the ion at m/z 607.[65] Also the absence of the aglycone ion is consistent with an O-, C-diglycoside structure.[66] The fragment ions at m/z 785 $[M–H–14]^-$, 771 $[M–H–28]^-$, and 279 (–28 Da), representing the loss of methyl group and the putative loss of carboxyl moiety, respectively. Based on the obtained results, this compound was concluded to be 7-O methyl apigenin-O-(2'''-hydroxyferuloyl)glucosyl-C-glucoside.

Compounds **51** and **52** presented a molecule ion at m/z 783 $[M–H]^-$. Compound **51** originates a base peak fragment ion at m/z 607 $[M–H–176]^-$ indicating a loss of an O-acyl moiety. The latter was concluded to be linked through an O-glycosylation, due to the presence

of the fragment ions at m/z 445 $[M–H–176–162]^-$ and 427 $[(176–18)–162]^-$. The observed neutral loss of 176 Da corresponds to a feruloyl group. Another fragment ion was observed at m/z 325 $[M–H–176–162–120]^-$, corresponding to the loss of the O-(feruloyl)-glucosyl-C-glucoside. As well, the MS^3 [607] fragmentation reported an ion at m/z 487, representing the cross-ring of sugar moiety and cleavage of hexosyl unit (120 Da). Based on these results and on the fact that the ion observed at m/z 607, showed a very high relative intensity (base peak),[65] compound **51** was suggested to be 7-O methyl apigenin-O-(2'''-feruloyl)glucosyl-C-glucoside similar to what had already been identified in *Zizyphus jujube* seeds.[53] However, compound **52** could be considered as a derivative of compound **51** and could be assigned as 7-O methyl apigenin-O-(feruloyl)glucosyl-C-glucoside, due to the lack of further ESI-MS fragmentation.

Compound **53** displayed a molecule ion at m/z 979 $[M–H]^-$, suffered a neutral loss of 196 Da (dihydroferulic acid), yielding a fragment ion at m/z 783. The latter ion has already been detected as a pseudo-molecule ion of compound **51/52**. Therefore, similarly to what was exposed above, we could consider it as a derivative of **51**, in which there was the substitution of dihydroferulic acid by 1→2 linkages in the phenolic hydroxyl group.[75] Thus, this compound could be labeled as 7-O methyl-(2''-dihydroferuloyl)apigenin-O-(feruloyl)glucosyl-C-glucoside.

Compound **57** exhibited a molecule ion at m/z 873 $[M–H]^-$, produced MS^2 [873] fragmentation at m/z 608 $[M–H–(264–H)]^-$, 283 $[M–H–(264–2H)–162–162]^-$, 428 $[M–H–(264–18–H)–162]^-$, and 292 $[M–H–(264–18)–162–15]^-$, corresponding to the loss of an O-(acyl)-di-glucosyl moiety. The loss of 264 Da was related to the molecular weight of dihydrohaseic acid (DPA),[49] with interglycosidic 1→2 linkage due to the relative intensity of the fragment ion.[65] The ions at m/z 589 $[M–H–269–15]^-$ and 322 (Ag+17) led to the aglycone. Besides, ions at m/z 842 and 488 would result, respectively, from the loss of (–31 Da) and (–120 Da), characteristics loss of methoxy group, and the partial cleavage of the hexosyl unit. Thus, 7-O methyl apigenin-O-(2'''-dihydrophaseoyl)glucosyl-C-glucoside was attributed to this compound similar to a compound previously reported in *Zizyphus mauritiana* seeds.[79]

Compound **62** displayed molecule ion at m/z 869 $[M–H]^-$, yielding a product ion at m/z 607 $[M–H–262]^-$ and 589 $[M–H–262–18]^-$ by the loss of –262 Da, characteristic of dihydrophaseoyl unit, although fragment ion at m/z 427 $[M–H–(262–18)–162]^-$ is compatible with an O-(acyl)-glucosyl with 1→2 interglycosidic linkage due to the high relative intensity of fragment ion at m/z 607.[65] Further product ion was observed at m/z 839 $[M–H–30]^-$, designates to the loss of methoxy group. Therefore, the absence of the aglycone ion is consistent with an O–,C-diglycoside structure.[66] Therefore, this compound exhibited similar $MS^{3,4}$ product ions to those of compounds **33**/**35** which could be identified as derivatives of spinosin by adding dihydrophaseoyl (262 Da) radical, and isomers of compound **57** so that peak was tentatively assigned as 7-O methyl apigenin-O-(2'''-dihydrophaseoyl)glucosyl-C-glucoside.

Compound **75** exhibited molecule ion at m/z 737 $[M–H]^-$. The MS fragmentation showed ions at m/z 283 $[M–H–146–146–162]^-$ and 229 $[M–H–146–146–162–54]^-$, indicating the loss of tri-saccharide moieties interlinkage with each other. The fragment ion at m/z 283, pointed

to methylated apigenin as aglycone since the MS^3 data exposed a neutral loss of 268 Da at m/z 321. However, the behavior fragmentation patterns of this peak were remarkably similar to the above compounds, which manifested by the loss of an O-(acyl)-glucosyl moiety (m/z 589 $[M–H–(146–2H)]^-$ and 427 $[M–H–(146–18)–146]^-$). Besides, the UV spectra as well as the higher retention times of this compound suggested that they might be acylated by *p*-coumaric acid.[57] Further, fragment ion was observed at m/z 311 (Ag+42) which is typical of mono C-glycosylflavones. This was also confirmed through the neutral loss of a 120 Da at m/z 427. The low intensity of the signal (Ag+42) confirmed the 6-C substitution.[65] Based on the relative intensity of fragment ion at m/z 589 and to what discussed above this compound was concluded to be 7-O methyl apigenin O-(2'''-*p*-coumaroylrhamnoside)-6-C-hexoside.[57]

3.2.3 Dihydrochalcones

Phloretin-3',5'-di-C-glucoside is the unique chalcones identified in methanol/water/acetic acid extracts of *Z. lotus*, according to the MS fragmentations pattern and UV spectra which is in agreement with earlier work.[81]

Table 11: HT-UHPLC-UV-MS^n data of phloretin identified in the methanol/water/acetic acid extracts of *Zizyphus lotus*.

Peak	R_t (min)	λ_{max} (nm)	$[M–H]^-$ (m/z)	HT-UHPLC–MS^n product m/z (% base peak)[(I)]	Compound
39	11.12	239, 284	597	MS^2: **477**(100), 357(20), 387(20), 417(15); MS^3: **357**(100), 387(50), 381(15), 459(15), 315(10); MS^4: 209(100), 163(60), 167(55), 255(25), 251(20), 123(20), 229(15), 137(15).	Phloretin-3',5'-di-C-glucoside

[(I)]m/z in bold was subjected to MS^n analysis.

Compound **39** presents the molecule ion at m/z 597 $[M–H]^-$. The MS^2 [597] data exhibited fragment ion at m/z 477 found after cleavage at ($[M−H]−120]^-$), followed by m/z 357 $[M−H−120−120]^-$, 387 $[M−H−120−90]^-$, and 417 $[M−H−162−18]^-$ were related to the fragmentation of a second glucose unit (Table 11). Moreover, the successive loss of 387 $[aglycone+113]^-$ and 357 $[aglycone+83]^-$ which are typical of di-C-glycosides were observed in MS^3 [597→357] fragmentation.[82,83] Other fragment ions were observed at m/z 381, 315, and 459, corresponding to the 0,3 cross-ring cleavage (90 Da), loss of hexosyl moiety (–162 Da), and loss of water molecule (–18 Da), respectively.[66] Moreover, the aglycone ion was not visible in the MS spectra of this compound whilst, the fragmentation pathways observed in MS^4 [477→357] matched to those of an authentic standard of phloretin, for which the main product ions are observed at m/z 167, 229, and 255/251 assigned to the loss of B ring moiety, carbon dioxide (44 Da, CO_2) and a water molecule (18 Da, H_2O), respectively (Table 11).[84,85] The product ion at m/z 163 originated by the successive loss of CO_2 from 167[85] while, the ion at m/z 209 corresponds to the loss of 148 Da suggested the loss of $^{1,4}B^-$ ring by rDA reaction.[32] Therefore, this compound could be identified as phloretin-3',5'-di-C-glucoside which has been detected in genus *Ziziphus* and *Z. lotus* leaves.[13,86,87]

3.2.4 Unkown Flavonoids

The structure elucidation of compounds **54**, **60**, **64**-**66**, **68**, **76**, and **87** could not be attained only based on the UV spectra and MS^n data (Table 12). Further information is thus needed to elucidate the structure of these compounds.

Table 12: HT-UHPLC-UV-MS^n data of unidentified flavonoids in the methanol/water/acetic acid extracts of *Zizyphus lotus*.

Peak	R_t (min)	λ_{max} (nm)	$[M–H]^-$ (m/z)	HT-UHPLC–MS^n product m/z (% base peak)[(I)]	Compound
54	16.07	234, 276	435*	MS^2: 389(100), **305**(97), 357(70), 371(40), 399(15); MS^3: 175(100), 147(55).	Unknown
60	17.15	232, 275, 317	725*	MS^2: **679**(100); MS^3: 453(100), 452(45), 661(20), 225(25), 226(10).	Acylated flavonoid-sugar conjugates
64	17.60	233, 275, 321	725*	MS^2: **679**(100); MS^3: 453(100), 452(50), 661(20), 225(18).	Aylated flavonoid-sugar conjugates
65	17.74	230, 267, 312	885	MS^2 : **739**(100), 721(35), 619(25); MS^3: 575(100), 285.	Flavonoid-O-[2,6-O-*p*-coumaroylrhamnosyl-hexoside]-O-rhamnoside
66	17.92	230, 266, 316	1031	MS^2: **885**(100), 739(30); MS^3: 739(100).	Flavonoid-O-[*p*-coumaroylrhamnosyl-hexoside]-O-di-rhamnoside
68	18.10	278, 321	725*	MS^2: **679**(100); MS^3:453(100), 452(50), 661(20), 225(20).	Acylated flavonoid-sugar conjugates
76	19.20	233, 267, 315	885	MS^2: **739**(100), 575(10); MS^3: **575**(100), 284(55), 285(35), 593(20), 327(20), 429(15), 255(15), 411(10), 267(10); MS^4: 327(100), 299(30), 285(25), 284(25), 315(25), 357(20).	Flavonoid-O-[2,6-O-*p*-coumaroylrhamnosyl-hexoside]-O-rhamnoside
87	22.89	230, 268, 312	1031	MS^2: **885**(100); MS^3: **739**(100), 575(35); MS^4: 575(100), 284(65).	Flavonoid-O- [*p*-coumaroylrhamnosyl-hexoside]-O-di-rhamnoside

[(I)]m/z in bold was subjected to MS^n analysis, *: Formic acid adduct (FA).

Compound **54** exhibited molecule ion at m/z 435 $[M+HCOOH]^-$ (FA adduct), MS^2 spectrum showed base peak ion at m/z 389 $[M–H–46]^-$, corresponding to the loss of formic acid. The presence of ion at m/z 305, accompanied by the absorption maxima at 276 nm, suggests this compound as (epi)gallocatechin derivatives. Although, the MS^3 [305] fragmentation doesn't give any further information to confirm this hypothesis (Table 12).

Compounds **60**, **64**, and **68** shared the same molecule ion at m/z 725 $[M+HCOOH]^-$ and exhibit the MS^2 product ion, characteristic by the loss of 46 Da to yield a base peak ion at m/z 679. This residue might be related to the formic acid adduct, whose formation has been discussed above. Thus, product ion at m/z 225 results from the loss of 454 Da, characteristics of tri-saccharides, consisting of rutinosyl and rhamnoside residues (Table 12). Therefore, the UV spectra were similar to those of acylated flavonoids. Compound **60** showed a UV spectrum characteristic of *p*-coumaric acid derivatives, with a maximum at λ=317 nm (Table 12) while compounds **64** and **68** were showed a maximum at 321 nm characteristic of caffeic acid derivatives.[62,88] Despite these data, it was not possible to indicate the chemical structure of these isomers but they could be assigned as acylated flavonoid-sugar conjugates.

Compounds **66** and **87** exhibited the molecule ion at m/z 1031 $[M–H]^-$. The MS^2 spectrum showed a base peak fragment ion at m/z 885 (loss of 146 Da), resulted from the loss of a rhamnosyl unit. This ion was already identified as a molecule ion of compounds **73**, **74**, and **83** as kaempferol-3-O-[6-O-hexosyl(2-O-*p*-coumaroylrhamnoside)]-7-O-rhamnoside. The ion at m/z 739, during the MS^3 fragmentation, suffered the loss of 146 Da that may be attributed to the loss of a second rhamnosyl moiety or *p*-coumaric acid. In compound **87**, the ion at m/z 739 exposed two fragment ions at m/z 575 (–146 Da) and 284 (–454 Da). The product ion at m/z 285 corresponds to the aglycone. However, the MS data and UV spectra did not allow identifying the nature of the aglycone. Thus, based on what was discussed above, these compounds could be assigned as flavonoid-O-[*p*-coumaroyl-rhamnosyl-hexoside)]-O-rhamnoside.

Compounds **65** and **76** were monoacylated with *p*-coumaric acid. Both of them shared the same molecule ion ($[M–H]^-$, m/z 885 Da), identical with **73**, **74**, and **83**, which was confirmed with MS and UV spectra. However, the nature of the aglycone moiety could not be established due to the link of further fragmentations. This compound was tentatively assigned as flavonoid O-[2,6-O-*p*-coumaroyl-rhamnosyl-hexoside]-7-O-rhamnoside.

3.3 Quantification analysis of phenolic compounds identified in *Zizyphus lotus* methanol/water/acetic acid extracts

The phenolic composition of seeds, pulp, leaves, and root barks consequential from wild *Z. lotus* was quantified for the first time by HT-UHPLC-UV expressed in mg/kg of dry material are shown in Table 13. Quantification was carried out using calibrations curves of standard representative compounds of each family as summarized in Table 1.

Among the four morphological parts, root barks presenting the higher content of quantified phenolic compounds with 7692 mg/kg of dry material, followed by leaves which account for 5904 mg/kg of dry material, and by pulp (2596 mg/kg dw). The analyzed seeds extract showed lower phenolic content compared to the four *Z. lotus* fractions. The reduced number of studies dealing with the phenolic composition of wild *Z. lotus* with their lack of sufficient qualitative and quantitative information makes it impossible to compare our results. Therefore, the values found were lower than those obtained in the total phenolic contents measured by the Folin Ciocalteu method (Table 2). Nonetheless, it is well-known the non-specificity of this method due to the presence of interfering compounds such as reducing

sugars (i.e. glucose and fructose), ascorbic acid, organic acids, among others, known to react with the Folin-Ciocalteu's reagent, and maybe in those extracts.[89]

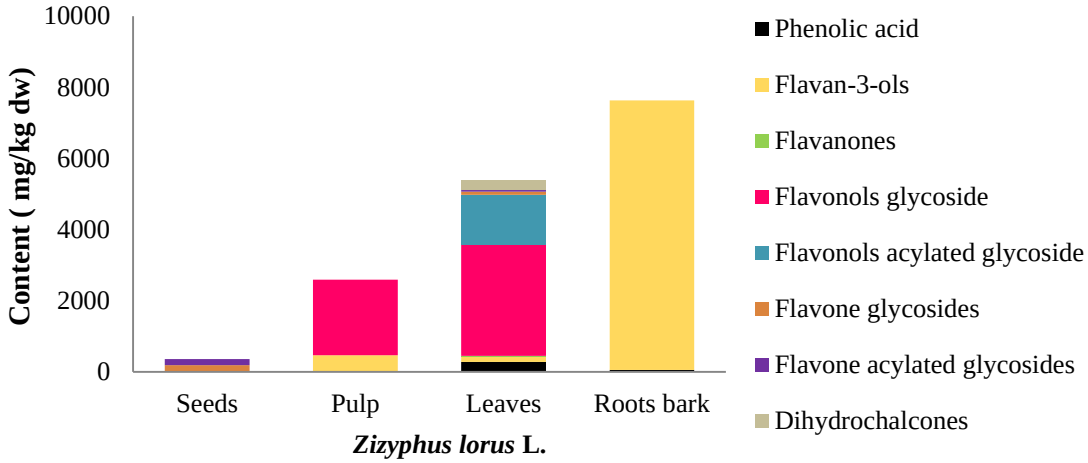

Figure 3: Phenolic composition of *Zizyphus lotus* morphological parts.

According to the HT-UHPLC-UV-MS^n screening, each morphological part of *Z. lotus* has a unique phenolic composition with flavonoids derivatives the most predominant group with a higher variety of compounds. Flavon-3-ols content was very high in root barks, representing the dominant class of compounds in this fraction. Besides, the leaves and pulp extracts of this shrub species differ from root barks by the abundance and diversity in flavonols derivatives. Whilst seeds phenolic-rich extract representing by the predominant flavone group.

3.3.1 Phenolic acid

Quinic acid is a derivative of chlorogenic acid, which is the only phenolic acid found in *Z. lotus* extracts. This compound was detected in root barks and leaves, amounting to 57 and 277 mg/kg of dry material, respectively. This compound could be found in many plant species but to the best of our knowledge it has never been reported in *Z. lotus* extracts.

Table 13: HT-UHPLC-UV quantification of phenolic acid identified in methanol/water/acetic acid extracts of *Zizyphus lotus*.

Compound	**Phenolic acid content (mg/kg dw)**			
	S	P	L	Rb
Total phenolic acid	**n.d.**	**n.d.**	**277**	**57**
Quinic acid	n.d.	n.d.	n.d.	40
Quinic acid	n.d.	n.d.	277	17

Results represent the means estimated from the analysis of three extracts of each fraction of *Z. lotus*. Abbreviation: n.d, not detected; tr, traces; n.q, not quantified; S, Seeds; P, Pulp; L, Leaves; Rb, Root barks.

3.3.2 Flavonoids

From a qualitative point of view, wild *Z. lotus* was found to have a diverse composition (Fig 3). Root barks showed the highest flavonoids concentration (7635 mg/kg dw), mostly due to the contribution of flavan-3-ols (7579 mg/kg dw). Also, leaf extract presents a considerable

flavonoid concentration (5627 mg/kg dw) followed by pulp accounting for 2596 mg/kg of dry weight. Therefore, seeds extract revealed the lowest flavonoid content (360 mg/kg dw).

3.3.2.1 Flavan-3-ols

Flavan-3-ols content was very high in root barks, representing the dominant class of compounds in this part (29–1794 mg/kg dw). The (epi)catechin (**15**) was the major compound of this group representing 1794 mg/kg dw of root barks. The content of this compound was much higher than that previously indicated for leaf aqueous extracts (3 mg/kg dw).[15] In our case this compound doesn't appear in the UHPLC-UV-MS^n spectrum of leaves extract, rejoined the results found in the work of Rached et al. (2019).[14] (epi)Gallocatechin dimer and (epi)gallocatechin isomers were also detected in the leaves and root barks extracts. Besides, two (epi)catechin-sugar conjugated were detected in the root barks with a considerable content (650 and 219 mg/kg dw), namely (epi)catechin-O-hexoside and (epi)catechin-O-(rutinosyl-rhamnoside)-O-hexoside, respectively. (epi)Gallocatechin methyl gallate was only noted in the pulp (467 mg/kg dw) (Table 14). This phenolic subclass was for the first time quantified in *Z. lotus* by UHHPLC-UV-MS^n analysis

Table 14: HT-UHPLC-UV quantification (mg/kg of dry weight) of flavan-3-ols identified in methanol/water/acetic acid extracts of *Zizyphus lotus*.

Compound	**Flavan-3-ols content (mg/kg dw)**			
	S	P	L	Rb
Total flavan-3-ols	**n.d.**	**467**	**157**	**7579**
(epi)gallocatechin dimer	n.d.	n.d.	61	tr
(epi)gallocatechin dimer	n.d.	n.d.	22	58
(epi)gallocatechin dimer	n.d.	n.d.	54	58
(epi)gallocatechin	n.d.	n.d.	tr	n.d.
(epi)gallocatechin	n.d.	n.d.	20	29
(epi)catechin-(epi)gallocatechin	n.d.	n.d.	n.d.	219
(epi)gallocatechin	n.d.	n.d.	tr	667
(epi)catechin-(epi)gallocatechin	n.d.	n.d.	n.d.	659
Procyanidin (B-type) dimer isomers	n.d.	n.d.	n.d.	798
(epi)catechin-O-hexoside	n.d.	n.d.	n.d.	650
Procyanidin (B-type) dimer isomers	n.d.	n.d.	n.d.	969
(epi)catechin	n.d.	n.d.	n.d.	652
(epi)catechin (**15**)	n.d.	n.d.	n.d.	1794
(epi)catechin	n.d.	n.d.	n.d.	806
(epi)gallocatechin methyl gallate	n.d.	467	n.d.	n.d.
(epi)catechin-O-(rutinosyl-rhamnoside)-O-hexoside	n.d.	n.d.	n.d.	219

Results represent the means estimated from the analysis of three extracts of each fraction of *Z. lotus*. Abbreviation: n.d, not detected; tr, traces; n.q, not quantified; S, Seeds; P, Pulp; L, Leaves; Rb, Root barks.

3.3.2.2 Flavonols

Flavonols glycoside were mainly retained in leaves and pulp parts (Table 15), accounting for 3126 and 2129 mg/kg dw, respectively. Quercetin-3-O-rhamnosyl(6-O-hexoside) (**30**) are the main flavonols glycoside identified in *Z. lotus*, contributing to 1757 mg/kg dw and 1069

mg/kg dw in leaves and pulp, respectively and which also represent the dominant compounds in this shrub species. Two other isomers of this compound were detected in *Z. lotus* with **28** were only noted in the leaf part, accounting for 321 mg/kg dw. These compounds were for the first time quantified in *Z. lotus* varieties. Myricetin-3-O-rhamnosyl-hexoside (**23**) was also noted with a moderate amount in pulp and leaf extracts (282 and 153 mg/kg dw, respectively).

Three isomers of quercetin-3-O-(2,6-di-O-rhamnosylhexoside) (**24**, **25**, and **26**) were detected in *Z. lotus* phenolic-rich extract with moderate concentration (Table 15), except for isomer **24** that had only found in leaves fraction, accounting for 283 mg/kg dw. Kaempferol-3-O-rutinoside was determined in leaves and pulp extracts, accounting for 7 and 137 mg/kg dw, respectively. Some other flavonols were also identified in leaves, such as quercetin-7-O-hexoside (**31**), quercetin-3-O-[rhamnosyl(6-O-hexoside)]-7-O-rhamnoside (**34**), kaempferol-3-O-[(6-O-rhamnosyl-hexoside)] (**37**), and quercetin-3-O-[(2,6-di-O-rhamnosyl-hexoside)]-7-O-rhamnoside (**50**).

Twenty acylated flavonols glycosides have been identified for the first time as components of *Z. lotus* which concentrate in the leaves part, accounting for 1403 mg/kg of dry weight. Quercetin-3-O-[(2,6-O-*p*-coumaroylrhamnosyl-hexoside]-7-O-rhamnoside (**67** and **69**) were the most common acylated flavonols glycosides identified in *Z. lotus* leaves extract, representing for 130 and 155 mg/kg dw, respectively, followed by quercetin-3-O-[(*p*-coumaroylrhamnosyl-hexoside)]-7-di-O-rhamnoside (**61**) with 106 mg/kg of dry weight. Three acylated kaempferol glucosides derivatives have been also detected from traces to a moderate amount (Table 15). Isorhamnetin-3-O-[(*p*-coumaroyl-rhamnosyl-hexoside)]-7-O-hexoside was also identified in *Z. lotus* phenolic-rich leaves extract (73 mg/kg dw).

Table 15: HT-UHPLC-UV quantification (mg/kg of dry weight) of flavonols identified in methanol/water/acetic acid extracts of Z*izyphus lotus*.

Compound	**Flavonols content (mg/kg dw)**			
	S	P	L	Rb
Total flavonols	**n.d.**	**2129**	**5055**	**n.d.**
Flavonols glycoside	**n.d.**	**2129**	**3126**	**n.d.**
Myricetin-3-O-rhamnosyl-hexoside (**23**)	n.d.	282	153	n.d.
Quercetin-3-O-(2,6-di-O-rhamnosylhexoside) (**24**)	n.d.	n.d.	283	n.d.
Quercetin-3-O-(2,6-di-O-rhamnosylhexoside) (**25**)	n.d.	470	322	n.d.
Quercetin-3-O-(2,6-di-O-rhamnosylhexoside) (**26**)	n.d.	tr	71	n.d.
Quercetin-3-O-[di-rhamnosyl(2-O-hexoside)]-7-O-rhamnoside	n.d.	n.d.	n.q.	n.d.
Quercetin 3-O-rhamnosyl(6-O-hexoside) (**28**)	n.d.	n.d.	321	n.d.
Quercetin 3-O-rhamnosyl(6-O-hexoside)	n.d.	172	63	n.d.
Quercetin 3-O-rhamnosyl(6-O-hexoside) (**30**)	n.d.	1069	1757	n.d.
Quercetin 7-O-hexoside (**31**)	n.d.	n.d.	tr	n.d.
Quercetin-3-O-[rhamnosyl(6-O-hexoside)]-7-O-rhamnoside (**34**)	n.d.	n.d.	57	n.d.
Kaempferol-3-O-[(6-O-rhamnosylhexoside)] (**37**)	n.d.	n.d.	51	n.d.
Kaempferol-3-O-rutinoside	n.d.	n.d.	7	n.d.
Kaempferol 3-O-rutinoside	n.d.	136	n.d.	n.d.

Quercetin-3-O-[(di-O-rhamnosylhexoside)]-7-O-rhamnoside	n.d.	n.d.	tr.	n.d.
Quercetin-3-O-[(2, 6-di-O-rhamnosyl-hexoside)]-7-O-rhamnoside (**50**)	n.d.	n.d.	41	n.d.
Acylated derivative of flavonols glycoside	**n.d.**	**n.d.**	**1403**	**n.d.**
Isorhamnetin-3-O-[(*p*-coumaroylrhamnosyl-hexoside)]-7-O-hexoside	n.d.	n.d.	73	n.d.
Quercetin-3-O-[(2,6-O-*p*-coumaroylrhamnosyl-hexoside)]-7-O-rhamnoside	n.d.	n.d.	tr	n.d.
Quercetin-3-O-[(*p*-coumaroylhexoside)]-7-O-rhamnoside	n.d.	n.d.	98	n.d.
Quercetin-3-O-[(*p*-coumaroyl-rhamnoside-hexoside)]-7-di-O-rhamnoside (**61**)	n.d.	n.d.	106	n.d.
Quercetin-3-O-[(2,6-O-*p*-coumaroylrhamnosyl-hexoside)]-7-di-O-rhamnoside	n.d.	n.d.	92	n.d.
Quercetin-3-O-[(2,6-O-*p*-coumaroylrhamnosyl-hexoside)]-7-O-rhamnoside (**67**)	n.d.	n.d.	130	n.d.
Quercetin-3-O-[(2,6-O-*p*-coumaroylrhamnosyl-hexoside)]-7-O-rhamnoside (**69**)	n.d.	n.d.	155	n.d.
kaempferol-3-O-[hexosyl(2-O-*p*-coumaroyl)]	n.d.	n.d.	tr	n.d.
Kaempferol-3-O-[(*p*-coumaroylhexoside)]-7-O-rhamnoside	n.d.	n.d.	71	n.d.
Quercetin-3-O-[*p*-coumaroylrhamnosyl-hexoside]-7-di-O-rhamnoside	n.d.	n.d.	74	n.d.
Kaempferol-3-O-[(2,6-O-*p*-coumaroylrhamnosyl-hexoside)]-7-O-rhamnoside	n.d.	n.d.	74	n.d.
Kaempferol-3-O-[(2,6-O-*p*-coumaroylrhamnosyl-hexoside)]-7-O-rhamnoside	n.d.	n.d.	97	n.d.
Quercetin-3-O-[(2,6-O-*p*-coumaroylrhamnosyl-hexoside)]-7-O-rhamnoside	n.d.	n.d.	87	n.d.
Quercetin-3-O-[(2,6-O-*p*-coumaroylrhamnosyl-hexoside)]-7-O-rhamnoside	n.d.	n.d.	tr	n.d.
Quercetin-3-O-[(*p*-coumaroylhexoside)]-7-O-rhamnoside	n.d.	n.d.	68	n.d.
Kaempferol-3-O-[(hexosyl(2-O-*p*-coumaroylrhamnoside)]	n.d.	n.d.	tr	n.d.
Kaempferol-3-O-[2,6-O-*p*-coumaroylrhamnosyl-hexoside]-7-O-rhamnoside	n.d.	n.d.	63	n.d.
Quercetin-3-O-[(*p*-coumaroylrhamnosyl-hexoside)]-7-di-O-rhamnoside	n.d.	n.d.	73	n.d.
Quercetin-3-O-[(2,6-O-*p*-coumaroylrhamnosyl-hexoside)]-7-di-O-rhamnoside	n.d.	n.d.	61	n.d.

(1) Results represent the means estimated from the analysis of three extracts of each fraction of *Z. lotus*. (2) the standard curve of Isorhamnetin was chosen to quantify acylated flavonols, because these compounds were higher at 330 nm compared to 350 nm. Abbreviation: n.d, not detected; tr, traces; n.q, not quantified; ; S, Seeds; P, Pulp; L, Leaves; Rb, Root barks.

3.3.2.3 Flavones

Several derivatives of apigenin and luteolin were detected in the methanol/water/acetic acid extracts of seeds and leaves, respectively. All these flavonoids were identified as glycosides or acylated glycosides containing one or two sugar moieties. Four 7-O methyl apigenin-2″-O-glycosyl-6-C-glucoside isomers (**32**, **33**, **35**, and **36**) were detected in seeds with **35** being the most abundant flavone in *Z. lotus* seeds extract, accounting for 124 mg/kg dw. The 7-O methyl-(2″-dihydroferuloyl)apigenin O-(6‴-feruloyl)glucosyl-C-glucoside (**53**), was also detected in considerable amount (60 mg/kg dw) followed by 7-O methylapigenin-O-(feruloyl)glucosyl-C-glucoside (**52**), accounting for 43 mg/kg of the dry weight. Apigenin glucosides and their acylated derivatives are known to occur in the *Zizyphus* family, but according to our knowledge, this is the first time these flavonoids are detected and quantified in this shrub species. Moreover, leaves fraction exhibited a lower content of total luteolin derivatives ranging from 83 mg/kg dw for luteolin-3-O-glucoside to 20 mg/kg dw for luteolin-O-[hexosyl(6-O-*p*-coumaroylrhamnosyl)]-7-O-rhamnoside (Table 16).

Table 16: HT-UHPLC-UV quantification (mg/kg of dry weight) of flavone identified in methanol/water/acetic acid extracts of *Zizyphus lotus*.

Compound	**Flavones content (mg/kg dw)**			
	S	P	L	Rb
Total flavones	**360**	**n.d.**	**129**	**n.d.**
Flavone glycoside	**186**	**n.d.**	**83**	**n.d.**
Apigenin 6,8-di-C-glucoside	4	n.d.	n.d.	n.d.
Apigenin 6,8-di-C-glucoside	20[(20+22)]	n.d.	n.d.	n.d.
Apigenin 6,8-di-C-glucoside	20[(20+22)]	n.d.	n.d.	n.d.
7-O methyl apigenin-2″-O-glycosyl-6-C-glucoside (**32**)	7	n.d.	n.d.	n.d.
7-O methyl apigenin-2″-O-glycosyl-6-C-glucoside (**33**)	18	n.d.	n.d.	n.d.
7-O methyl apigenin-2″-O-glycosyl-6-C-glucoside (**35**)	124	n.d.	n.d.	n.d.
7-O methyl apigenin-2″-O-glycosyl-6-C-glucoside (**36**)	8	n.d.	n.d.	n.d.
7-O-methyl apigenin-6-C-glucoside	4	n.d.	n.d.	n.d.
Luteolin-3-O-glucoside	n.d.	n.d.	83	n.d.
Acylated derivative of flavone glycoside	**174**	**n.d.**	**46**	**n.d.**
7-O-(2″-methylacetyl) methyl apigenin-O-(6‴-hydroxyferuloyl)glucosyl-6-C-glucoside.	4	n.d.	n.d.	n.d.
7-O-methyl apigenin-2″-O-(6‴-methylmalonyl)glycosyl-6-C-glucoside.	7	n.d.	n.d.	n.d.
7-O-methoxymalonyl-apigenin isomer	9	n.d.	n.d.	n.d.
7-O-methoxymalonyl-apigenin isomer	5	n.d.	n.d.	n.d.
7-O methyl apigenin-2″-O-(2‴-sinapoyl)glucosyl-8-C-glycoside	4	n.d.	n.d.	n.d.
7-O methyl apigenin-2″-O-(2‴-hydroxyferuloyl)glucosyl-C-glucoside	8	n.d.	n.d.	n.d.
7-O methyl apigenin O-(2‴-feruloyl)glucosyl-C-glucoside	9	n.d.	n.d.	n.d.

7-O methyl apigenin O-(feruloyl)glucosyl-C-glucoside (**52**)	43	n.d.	n.d.	n.d.
7-O methyl-(2″-dihydroferuloyl)apigenin O-(6'''-feruloyl)glucosyl-C-glucoside (**53**)	60	n.d.	n.d.	n.d.
7-O methylapigenin-O-(2'''-dihydrophaseoyl)glucosyl-C-glucoside	6	n.d.	n.d.	n.d.
Luteolin-O-[hexosyl(p-coumaryolrhamnoside)]-7-O-rhamnoside	n.d.	n.d.	26	n.d.
7-O methyl apigenin-O-(2'''-dihydrophaseoyl)glucosyl-C-glucoside	7	n.d.	n.d.	n.d.
7-O methyl apigenin O-(2'''-p-coumaroyl)rhamnosyl-6-C-hexoside	12	n.d.	n.d.	n.d.
Luteolin-O-[hexosyl(6-O-p-coumaryol)]rhamnosyl-7-O-rhamnoside	n.d.	n.d.	20	n.d.

(1) Results represent the means estimated from the analysis of three extracts of each fraction of *Z. lotus*. Numbers in parenthesis correspond to compounds whose chromatographic peaks were overlapped. (2)the standard curve of Isorhamnetin was chosen to quantify acylated flavonols, because these compounds were higher at 330 nm compared to 350 nm. (3)In the seeds, the total contents did not include the content of **20**, due to the co-elution with **22**. Abbreviation: n.d, not detected; tr, traces; n.q, not quantified; S, Seeds; P, Pulp; L, Leaves; Rb, Root barks.

3.3.2.4 Flavanones

Flavanones were only detected in leaves extract. Two isomers of naringenin-6,8-di-C-hexoside were quantified with a concentration ranging between traces to 17 mg/kg dw (Table 17). However, to the best of our knowledge, the existence of this isomer in *Z. lotus* has not been reported before.

Table 17: HT-UHPLC-UV quantification (mg/kg of dry weight) of flavanones identified in methanol/water/acetic acid extracts of *Zizyphus lotus*.

Compound	**Flavanones content (mg/kg dw)**			
	S	P	L	Rb
Total flavanones	**n.d.**	**n.d.**	**17**	**n.d.**
Naringenin-6,8-di-C-hexoside	n.d.	n.d.	tr	n.d.
Naringenin-6,8-di-C-hexoside	n.d.	n.d.	17	n.d.

Results represent the means estimated from the analysis of three extracts of each fraction of *Z. lotus*. Abbreviation: n.d, not detected; tr, traces; n.q, not quantified; S, Seeds; P, Pulp; L, Leaves; Rb, Root barks.

3.3.3 Dihydrochalcones

Phloretin-3', 5'-di-C-glucoside was the only dihydrochalcones determined, present only in leaves extract (269 mg/kg dw). A glycosidic form of phloretin was also previously reported as constituent of *Z. lotus* leaves extract with concentration higher than that reported in our study.[14]

Table 18: HT-UHPLC-UV quantification (mg/kg of dry weight) of dihydrochalcones identified in methanol/water/acetic acid extracts of *Zizyphus lotus*.

Compound	dihydrochalcones content (mg/kg dw)			
	S	P	L	Rb
Total dihydrochalcones	**n.d.**	**n.d.**	**269**	**n.d.**
Phloretin-3',5'-di-C-glucoside	n.d.	n.d.	269	n.d.

Results represent the means estimated from the analysis of three extracts of each fraction of *Z. lotus*. Abbreviation: n.d, not detected; tr, traces; n.q, not quantified; ; S, Seeds; P, Pulp; L, Leaves; Rb, Root barks.

4. Conclusions

This study appears as the most complete qualitative and quantitative analysis of the phenolic compound of *Z. lotus* never performed to date. The UHPLC-UV-MS^n was used to separate and quantify 78 phenolic compounds in four morphological parts of wild *Z. lotus* namely: seeds, pulp, leaf, and root barks. To the best of our knowledge, this is the first detailed work describing the phenolic compounds present in methanol/water/acetic acid (49.5:49.5:1) extracts of *Z. lotus*.

Several flavonoids including two naringenin derivatives (**16** and **18**), 2 quinic acid derivatives (**1** and **2**), 16 catechin and gallocatechin derivatives (**3**-**15**, **17**, **21**, and **77**), myricetin derivatives (**23**), 11 quercetin derivatives (**24**-**31**, **34**, **44**, and **50**) 13 acylated quercetin derivatives (**55**, **56**, **59**, **61, 63**, **67**, **69**, **72**, **78**, **79**, **80, 84**, and **85**), 3 kaempferol derivatives (**37**, **40**, and **41**), 6 acylated kaempferol derivatives (**70**, **71**,**73**, **74**, **81**, and **83)**, 8 apigenin derivatives (**19**, **20**, **22**, **32**, **33**, **35**, **36**, and **38**), luteolin derivative (**42**), 12 acylated apigenin derivatives (**43**, **45**-**49**, **51**-**53**, **57**, **58**, **62**, and **75**), and 2 acylated luteolin derivatives (**58** and **82**) were identified in negative mode using full scan mass measurements and MS^n fragmentations. Root barks contained the highest flavan-3-ol abundances (7579 mg/kg dw) while seeds demonstrated the highest flavone (360 mg/kg dw). Flavonols were specially retained in leaf and pulp extracts (2129 and 5055 mg/kg dw, respectively). The obtained results indicated that wild *Z. lotus* could be considered as a rich source of bioactive phenolic compounds that could be exploited as an important supplement in food manufacturing such as functional foods or other herbal preparations.

5. References

(1) Benammar, C.; Hichami, A.; Yessoufou, A.; Simonin, A. M.; Belarbi, M.; Allali, H.; Khan, N. A. BMC Complement. Altern. Med. **2010**, 10 (54), 1–9.
(2) BRAHLP, D. L. R. R. and A. E. L. B. Weed Technol. **1995**, 9 (2), 326–330.
(3) Bakhtaoui, F. Z.; Lakmichi, H.; Megraud, F.; Chait, A.; Gadhi, C. E. A. J. Appl. Pharm. Sci. **2014**, 4 (10), 81–87.
(4) Abdoul-Azize, S.; Bendahmane, M.; Hichami, A.; Dramane, G.; Simonin, A. M.; Benammar, C.; Sadou, H.; Akpona, S.; El Boustani, E. S.; Khan, N. A. Int. Immunopharmacol. **2013**, 15 (2), 364–371.
(5) Gini, T. G.; Jeya Jothi, G. Egypt. J. Basic Appl. Sci. **2018**, 5 (3), 197–203.
(6) Benammar, C.; Baghdad, C. J. Nutr. Food Sci. **2014**, s8, 8–13.
(7) Hammi, K. M.; Jdey, A.; Abdelly, C.; Majdoub, H.; Ksouri, R. Food Chem. **2015**, 184, 80–89.

(8) Ghedira, K.; Chemli, R.; Caron, C.; Nuzilard, J. M.; Zeches, M.; Le Men-Olivier, L. Phytochemistry **1995**, 38 (3), 767–772.
(9) Ghedira, K.; Chemli, R.; Richard, B.; Nwllard, J.; Men-olivier, L. L. E. **1993**, 32 (6), 1591–1594.
(10) Le Crouéour, G.; Thépenier, P.; Richard, B.; Petermann, C.; Ghédira, K.; Zèches-Hanrot, M. Fitoterapia **2002**, 73 (1), 63–68.
(11) Maciuk, A.; Lavaud, C.; Thépenier, P.; Jacquier, M. J.; Ghédira, K.; Zèches-Hanrot, M. FJ. Nat. Prod. **2004**, 67 (10), 1639–1643.
(12) Abdoul-Azize, S. J. Nutr. Metab. **2016**, 1–13.
(13) Maciuk, A.; Ghedira, K.; Thepenier, P.; Lavaud, C.; Zeches-Hanrot, M. Pharmazie **2003**, 58 (2), 158–159.
(14) Rached, W.; Barros, L.; Ziani, B. E. C.; Bennaceur, M.; Calhelha, R. C.; Heleno, S. A.; Alves, M. J.; Marouf, A.; Ferreira, I. C. F. R. Food Funct. **2019**, 10 (9), 5898–5909.
(15) Marmouzi, I.; Kharbach, M.; El, M.; Bouyahya, A.; Cherrah, Y.; Bouklouze, A.; Vander, Y.; El, M.; Faouzi, A. Ind. Crop. Prod. **2019**, 132, 134–139.
(16) Borgi, W.; Recio, M. C.; Ríos, J. L.; Chouchane, N. South African J. Bot. **2008**, 74 (2), 320–324.
(17) Borgi, W.; Ghedira, K.; Chouchane, N. Fitoterapia **2007**, 78 (1), 16–19.
(18) Rsaissi, N.; Kamili, E. L.; Bencharki, B.; Hillali, L.; Bouhache, M. Int. J. Sci. Eng. Res. **2013**, 4 (9), 1521–1528.
(19) Ewanto, V. E. D.; Ianzhong, X. W. U.; Dom, K. A. K. A.; Iu, R. U. I. H. A. I. L. J. Agric. Food Chem. **2002**, 50 (10), 3010–3014.
(20) Lee, J.; Durst, R. W.; Wrolstad, R. E. J. AOAC Int. **2005**, 88 (5), 1269–1278.
(21) Santos, S. A. O.; Vilela, C.; Freire, C. S. R.; Neto, C. P.; Silvestre, A. J. D. J. Chromatogr. B **2013**, 938, 65–74.
(22) Wahida, B.; Abderrahman, B.; Nabil, C. J. Ethnopharmacol. **2007**, 112 (2), 228–231.
(23) Borgi, W.; Chouchane, N. J. Ethnopharmacol. **2009**, 126 (3), 571–573.
(24) Ghazghazi, H.; Aouadhi, C.; Riahi, L.; Maaroufi, A.; Hasnaoui, B. Fatty Acids Nat. Prod. Res. **2014**, 28 (14), 1106–1110.
(25) Boulanouar, B.; Abdelaziz, G.; Aazza, S.; Gago, C.; Miguel, M. G. Ind. Crops Prod. **2013**, 46, 85–96.
(26) Ghalem, M.; Merghache, S.; Belarbi, M. Pharmacogn. J. **2014**, 6 (4), 32–42.
(27) Eva de Rijke, Herman Zappey, Freek Ariese, Cees Gooijer, U. A. T. B. J. Chromatogr. A **2003**, 984, 45–58.
(28) Lay-Keow ng, Pierre Lafonta, and M. V. J. Agric. Food Chem. **2004**, 52, 7251–7257.
(29) Quercus, L.; Santos, S. A. O.; Pinto, P. C. R. O.; Silvestre, A. J. D.; Neto, C. P. C Ind. Crop. Prod. J. **2010**, 31, 521–526.
(30) Li, S.; Lin, Z.; Jiang, H.; Tong, L.; Wang, H.; Chen, S. J. Chromatogr. Sci. **2016**, 54 (7), 1225–1237.
(31) Cuyckens, F.; Claeys, M. J. Mass Spectrom. **2004**, 39 (1), 1–15.
(32) Fabre, N.; Rustan, I.; Hoffmann, E. de; Quetin-Leclercq, J. J. Am. Soc. Mass Spectrom. **2001**, 12 (6), 707–715.
(33) Ma, Y. L.; Li, Q. M.; Van Den Heuvel, H.; Claeys, M. Rapid Commun. Mass Spectrom. **1997**, 11 (12), 1357–1364.
(34) Gori, A.; Ferrini, F.; Marzano, M. C.; Tattini, M.; Centritto, M.; Baratto, M. C.; Pogni, R.; Brunetti, C. Int. J. Mol. Sci. **2016**, 17 (8), 2–13.
(35) Karar, M. G. E.; Quiet, L.; Rezk, A.; Jaiswal, R.; Rehders, M.; Ullrich, M. S.; Brix, K.; Kuhnert, N. Med. Chem. (Los. Angeles). **2016**, 6 (3), 143–156.
(36) Bresciani, L.; Calani, L.; Cossu, M.; Mena, P.; Sayegh, M.; Ray, S.; Del, D. Biochem. Pharmacol. **2015**, 3 (2), 11–19.

(37) Santos, S. A. O.; Vilela, C.; Camacho, J. F.; Cordeiro, N.; Gouveia, M.; Freire, C. S. R.; Silvestre, A. J. D. Food Chem. **2016**, 211, 845–852.
(38) Dou, J.; Lee, V. S. Y.; Tzen, jason T. C.; Lee, M.-R. J. Agric. Food Chem. **2007**, 55, 7462–7468.
(39) Vagiri, M.; Ekholm, A.; Johansson, E.; Rumpunen, K. J. Agric. Food Chem. **2012**, 60, 10501–10510.
(40) Rockenbach, I. I.; Jungfer, E.; Ritter, C.; Santiago-Schübel, B.; Thiele, B.; Fett, R.; Galensa, R. Food Res. Int. **2012**, 48 (2), 848–855.
(41) Figueroa, J. G.; Borrás-linares, I.; Lozano-sánchez, J. Food Res. Int. **2018**, 105 (November 2017), 752–763.
(42) Guimarães, R.; Barros, L.; Maria, A.; João, M.; Queiroz, R. P.; Santos-buelga, C.; Ferreira, I. C. F. R. Food Chem. **2013**, 141, 3721–3730.
(43) Di Lecce, G.; Arranz, S.; Jáuregui, O.; Tresserra-Rimbau, A.; Quifer-Rada, P.; Lamuela-Raventós, R. M. P Food Chem. **2014**, 145, 874–882.
(44) Ikeda, M., Ueda-Wakagi, M., Hayashibara, K., Kitano, R., Kawase, M., Kaihatsu, K., Ashida, H. S molecules **2017**, 22 (2), 1–12.
(45) Falcão, S. I.; Vilas-Boas, M.; Estevinho, L. M.; Barros, C.; Domingues, M. R. M.; Cardoso, S. M. Anal Bioanal Chem **2010**, 396, 887–897.
(46) Ye, M.; Yang, W.-Z.; Liu, K.-D.; Qiao, X.; Li, B.-J.; Cheng, J.; Feng, J.; Guo, D.-A.; Zhao, Y.-Y. C J. Pharm. Anal. **2012**, 2 (1), 35–42.
(47) Federico FN., Daniela G., Patrícia V., Rui G., Rafael P., E. A. C.; Rosa M. Seabra, P. B. A. Food Chem. **2009**, 114 (3), 1019–1027.
(48) Del Rio, D.; Stewart, A. J.; Mullen, W.; Burns, J.; Lean, M. E. J.; Brighenti, F.; Crozier, A. J. Agric. Food Chem. **2004**, 52 (10), 2807–2815.
(49) Ferreres, F.; Magalhães, S. C. Q.; Gil-Izquierdo, A.; Valentão, P.; Cabrita, A. R. J.; Fonseca, A. J. M.; Andrade, P. B. Food Chem. **2017**, 214, 678–685.
(50) Lobo, C.; Barros, L.; Maria, A.; Santos-buelga, C.; Ferreira, I. C. F. R. FRIN **2014**, 62, 684–693.
(51) Santos, S. A. O.; Vilela, C.; Domingues, R. M. A.; Oliveira, C. S. D.; Villaverde, J. J.; Freire, C. S. R.; Neto, C. P.; Silvestre, A. J. D. Ind. Crops Prod. **2017**, 95, 357–364.
(52) Escobar-Avello, D.; Lozano-Castellón, J.; Mardones, C.; Pérez, A. J.; Saéz, V.; Riquelme, S.; Baer, D. von; Vallverdú-Queralt, A. molecules **2019**, 24 (20), 3763.
(53) Choi, S. H.; Ahn, J. B.; Kozukue, N.; Levin, C. E.; Friedman, M. J. Agric. Food Chem. **2011**, 59 (12), 6594–6604.
(54) Francescato, L. N.; Debenedetti, S. L.; Schwanz, T. G.; Bassani, V. L. Talanta **2013**, 105, 192–203.
(55) Ferreres, F.; Pereira, D. M.; Valentão, P.; Andrade, P. B.; Seabra, R. M.; Sottomayor, M. J. Agric. Food Chem. **2008**, 56 (21), 9967–9974.
(56) Ferreres, F.; Pereira, D. M.; Valentão, P.; Andrade, P. B.; Seabra, R. M.; Sottomayor, M. J. Agric. Food Chem **2008**, 56, 9967–9974.
(57) Ferreres, F.; Magalhães, S. C. Q.; Gil-izquierdo, A.; Valentão, P.; Cabrita, A. R. J.; Fonseca, A. J. M.; Andrade, P. B. Food Chem. **2017**, 214, 678–685.
(58) Vallejo, F.; Tomás-Barberán, F. A.; Ferreres, F. J. Chromatogr. Amatography A **2004**, 1054, 181–193.
(59) Zhang, Y.; Xiong, H.; ID, X. X.; Xue, X.; Liu, M.; Xu, S.; Liu, H.; Gao, Y.; Li, X.; Zhang, H. molecules **2018**, 23 (5), 1199.
(60) Davis, B. D.; Brodbelt, J. S. J. Am. Soc. Mass Spectrom. **2004**, 15 (9), 1287–1299.
(61) Falcão, S. I.; Vale, N.; Gomes, P.; Domingues, M. R. M.; Freire, C.; Cardoso, S. M.; Vilas-Boas, M. Phytochem. Anal. **2013**, 24 (4), 309–318.
(62) Victor, H.; Wrolstad, R. E. J. Agric. Food Chem. **1990**, 38, 708–715.

(63) C.M. Bamawa, L.M. Ndjele, F. M. F. J. Nat. Prod. Resour. **2016**, 2 (2), 86–89.
(64) Ibrahim, R. M.; El-halawany, A. M.; Saleh, D. O.; Moataz, E.; El, B.; El-shabrawy, A. E.; El-hawary, S. S. Rev. Bras. Farmacogn. **2015**, 25 (2), 134–141.
(65) Es-Safi, N. E.; Gómez-Cordovés, C. Int. J. Mol. Sci. **2014**, 15 (11), 20668–20685.
(66) Ibrahim, R. M.; El-halawany, A. M.; Saleh, D. O.; Moataz, E.; El, B.; El-shabrawy, A. E. O.; El-hawary, S. S. Rev. Bras. Farmacogn. **2015**, 25 (2), 134–141.
(67) Cao, J.; Yin, C.; Qin, Y.; Cheng, Z.; Chen, D. J. Mass Spectrom. **2014**, 49 (10), 1010–1024.
(68) Gong Cheng, Yanjing Bai, Yuying Zhao, Jing Tao, Yi Liu, Guangzhong Tu, Libin Ma, N. L. and X. X. Spinosa. Tetrahedron **2000**, 56, 8915–8920.
(69) Bao, K.; Ping, L. I.; Ling, Y. I.; Ang, W. W.; Ang, Y. W. Chem. Pharm. Bull. **2009**, 57 (2), 144–148.
(70) Geng, P.; Sun, J.; Zhang, M.; Li, X.; Harnly, J. M.; Chen, P. J Mass Spectrom **2016**, 51 (10), 914–930.
(71) Ye, M.; Yang, W.; Liu, K.; Qiao, X.; Li, B.; Cheng, J.; Feng, J. J. Pharm. Anal. **2012**, 2 (1), 35–42.
(72) Sun, S.; Liu, H.; Xu, S.; Yan, Y.; Xie, P. J. Pharm. Anal. **2014**, 4 (3), 217–222.
(73) Wei WU, Zhiqiang LIU, Fengrui SONG, and S. L. Anal. Sci. **2004**, 20, 1103–1105.
(74) Ferreres, F.; Gil-izquierdo, A.; Vinholes, J.; Grosso, C. Rapid Commun. Mass Spectrom. **2011**, 25, 700–712.
(75) Benayad, Z.; Gómez-cordovés, C.; Es-safi, N. E. J. Food Compos. Anal. **2014**, 35 (1), 21–29.
(76) Hassan, W. H. B.; Abdelaziz, S.; Yousef, H. M. Al. Arab. J. Chem. **2018**, 12 (13), 377–387.
(77) Kachlicki, P.; Piasecka, A.; Stobiecki, M.; Marczak, Ł. Molecules **2016**, 21 (11), 1–21.
(78) Guo, X.; Yue, Y.; Tang, F.; Wang, J.; Yao, X.; Sun, J. Int. J. Mass Spectrom. **2013**, 333, 59–66.
(79) Ang, B. W.; Hu, H. Z.; Ang, D. W.; Ang, C. Y.; Min, X. U.; Hang, Y. Z. Nat. Prod. Bioprospect **2013**, 3, 93–98.
(80) Ferreres, F.; Gomes, D.; Valentão, P.; Gonçalves, R.; Pio, R.; Chagas, E. A.; Seabra, R. M.; Andrade, P. B. Food Chem. **2009**, 114 (3), 1019–1027.
(81) Kokotkiewicz, A.; Luczkiewicz, M.; Sowinski, P.; Glod, D.; Gorynski, K.; Bucinski, A. I Food Chem. **2012**, 133 (4), 1373–1382.
(82) Zangueu, C. B.; Olounlade, A. P.; Ossokomack, M.; Djouatsa, Y. N. N.; Alowanou, G. G.; Azebaze, A. G. B.; Llorent-Martínez, E. J.; de Córdova, M. L. F.; Dongmo, A. B.; Hounzangbe-Adote, M. S. BMC Vet. Res. **2018**, 14 (1), 147.
(83) Roowi, S.; Crozier, A. J. Agric. Food Chem. **2011**, 59 (22), 12217–12225.
(84) Sa´nchez-Rabaneda, F.; Ja´uregui, O.; Lamuela-Ravento´s, R. M.; Viladomat, F.; Bastida, J.; Codina, C. Mass Spectrom. **2004**, 18, 553–563.
(85) Elsadig Karar, M. G.; Kuhnert, N. J. Chem. Biol. Ther. **2016**, 01 (02), 1–23.
(86) Gamaleldin, M.; Karar, E.; Quiet, L.; Rezk, A.; Jaiswal, R.; Rehders, M.; Ullrich, M. S.; Brix, K. Med. Chem. (Los. Angeles). **2016**, 6 (3), 143–156.
(87) Pawlowska, A. M.; Camangi, F.; Bader, A.; Braca, A. Food Chem. **2009**, 112 (4), 858–862.
(88) Ribas-Agustí, A.; Gratacós-Cubarsí, M.; Sárraga, C.; García-Regueiro, J. A.; Castellari, M. Phytochem. Anal. **2011**, 22 (6), 555–563.
(89) Sánchez-Rangel, J. C.; Benavides, J.; Heredia, J. B.; Cisneros-Zevallos, L.; Jacobo-Velázquez, D. A. Anal. Methods **2013**, 5 (21), 5990–5999.

Chapter V

Evaluation of biological activity of
Zizyphus lotus extracts

Abstract

Nowadays, investigations are mostly focused on medicinal plants containing important sources of new chemical substances with potential therapeutic effects. *Z. lotus* shrub species (Rhamnaceae) is known to be used in traditional medicine for the treatment of several diseases and in medicinal applications. The present chapter investigated the antioxidant, antibacterial, and anti-tumor activities of lipophilic and phenolic-rich extracts of *Z. lotus*. The evaluation of the in vitro antioxidant power by colorimetric methods (DPPH, ABTS, and FRAP) showed that the different phenolic rich-extracts of *Z. lotus* have a strong antioxidant activity at low concentrations. Besides, the root barks and leaves phenolic-rich extracts (IC50 = 5.97 µg/mL and 9.68 µg/mL, respectively) exhibited the strongest DPPH scavenging effects and even showed higher potency than the BHT (IC50 = 11.30 µg/mL). A strong correlation was noted between the phenolic content quantified by HPLC in *Z. lotus* extracts and their antioxidant activities. At concentrations ranged between 1024 and 2048 µg/mL, *Z. lotus* extracts were tested against four bacterial species: *E. coli*, MSSA, *S. epidermidis*, and MRSA. Pulp lipophilic and phenolic-rich extracts did not have inhibitory effects against bacterial strains. Seeds extract also did not demonstrate an antibacterial effect on bacterial species but was found to have a considerable antimicrobial effect against *S. epidermidis* together with lipophilic leaves extract (MIC = 1024 µg/mL). Root barks phenolic-rich extract (MIC = 1024 µg/mL) prevented the growth of MRSA. Moreover, the evaluation of the antiproliferative power of *Z. lotus* extracts was studied. Root barks lipophilic extract was the most active extract in inhibiting MDA-MB-231, MCF-7, and HepG2 cellular viability (IC50 = 6.01, 18.78, and 23.27 µg/mL, respectively). BetA was the abundant compound identified in root barks lipophilic extract also prevented MDA-MB-231 cell growth (IC50 = 22.67 µM), within the same period. Moreover, root barks lipophilic extract has been shown to induce cell migration arrest, blocked cell cycle at G2/M, promote cell apoptosis, and downregulating the expression of PI3K/Akt signaling molecules. *Z. lotus* biomass may be considered as a potential lead for the development of an antioxidant, antibacterial, antitumor drug.

1. Introduction

In the last few years, natural compounds, especially those displaying role in the treatment of certain cancer and infectious diseases are of increasing interest to specialists in the field of pharmacology and medicinal chemistry.[1,2] The plant kingdom is one of the low-cost biomass characterized by their availability of compounds in which the number of them has multiple biological activities with minimum side effects.[2] According to the World Health Organization (WHO), a variety of modern drugs have been isolated from different medicinal plants and, around 80% of the world's rural areas of developing countries still depend on traditional medicines for their primary health care needs.[3] *Zizyphus lotus*, a Mediterranean shrub species widely spread in Morocco, is one of the richest sources of materials that possess high biological activities illustrated through traditional medicine and also exploited scientific reports.[4–14]

Several biologically active compounds, including cyclopeptide alkaloids, and dammarane saponins, have been isolated from this shrub species.[15–19] Moreover, some studies so far have investigated the phenolic composition of different morphological parts of *Z. lotus*, and they illustrate their capacity to carry out anti-inflammatory, antibacterial, anti-tumor, and dermatoprotective activities.[20,21] The high antioxidant properties of *Z. lotus* have been also reported and were found to be attributed to the presence of phenolic compounds.[9,12,14] However, the antioxidant effect of methanol/water/acetic acid (49.5:49.5:1) extracts, derived from several morphological parts of wild *Z. lotus* with detailed chemical composition was not been explored so far, particularly in what regards seeds and pulp fractions.

Natural triterpenoids are an abundant lipophilic group in the Zizyphus genus which is found to possesses many promising effects against cancer, immunological disorders, and potential in sustainably enhancing human vitality, and promoting longevity.[22] More importantly, triterpene acid group compounds which have become one of the most prevalent topics recently due to its selective ability between cancer cells and normal cells.[23] Despite the valuable data on the variability among *Z. lotus* species in hydrophilic antioxidant activity, there is still a lack of knowledge on the relation between lipophilic phytochemicals and pharmacological potential. At the current knowledge, only some studies highlighted the fatty acids, triacylglycerol, and sterols composition without any further information about their related biological activities.[14,24–28]

In this context and considering our interest in pursuing plant biological activities, this chapter is centered to investigate in vitro the antioxidant, antitumor, and antibacterial activities of *Z. lotus* lipophilic and phenolic-rich extracts. The current investigation will help to outline the precise pharmacological properties of this shrub species and to determine its value as functional foods and as a source of nutraceutical compounds, such as novel bioactive natural sources.

2. Materials and Methods

2.1 Chemicals

Dichloromethane (≥99% purity), were obtained from Sigma Chemicals Co. (Madrid, Spain). Dimethyl sulfoxide (DMSO) cell culture grade was obtained from PanReac Applichem (Gatersleben, Germany). Acetone (≥99% purity) was supplied by VWR. Mueller Hinton agar or broth was obtained from Liofilchem (Roseto degli Abruzzi, Italy). Brucella Broth was purchased from Fluka Analytical. 1,1-diphenyl-2-picrylhydrazyl (DPPH), 2,2'-azino-bis-3-ethylbenzthiazoline-6-sulphonic acid (ABTS), Ferric reducing antioxidant power (FRAP) and 3,5-di-tert-4-butylhydroxytoluene (BHT) (≥99% purity) were obtained from Sigma Chemicals Co. (Madrid, Spain). Ascorbic acid (≥99.5% purity) was upplied from Fluka Chemie (Madrid, Spain).

2.2 Preparation of *Zizyphus lotus* extracts

Different morphological part of wild *Z. lotus* was collected from the region of Beni Mellal. Before their use pulp and seeds, leaves and root barks were separated manually and each part was shade-dried and milled into granulometry lower than 2 mm prior to extraction. Lipophilic extractives, resulting from *Z. lotus* were prepared and examined by gas chromatography-mass spectrometry (GC-MS), as referred in Chapitre III. Therefore, the

phenolic-rich extract was prepared after the removal of lipophilic components by dichloromethane, and their chemical composition was performed by liquid chromatography-mass spectrometry (UHPLC-UV-MS^n), as previously explained in Chapitre IV.

2.3 Antioxidant activity

The antioxidant activity of *Z. lotus* phenolic rich-extracts was assessed through the DPPH, ABTS free radical scavenging assay, and FRAP assay according to the procedure explained below. Ascorbic acid and BHT were used as reference antioxidants of DPPH assay.

2.3.1 DPPH scavenging effect assay

The free radical scavenging activity of phenolic rich-extract of different morphological parts of *Z. lotus* was estimated according to a procedure described by Santos et al. (2013).[29] The extract concentration ranged between 3 and 100 µg/mL. The absorbance of DPPH free radical was measured at 517 nm using a UV/Vis V-530 spectrophotometer. Ascorbic acid (AA: 1.6-3.8 µg/mL) and 3,5-di-tert-4-butylhydroxytoluene (BHT: 2-20 µg/mL) were used as reference compounds. The capacity to scavenge the DPPH was calculated using the following equation: % scavenging effect = $[(A_{DPPH} - A_S)/ A_{DPPH}] \times 100$, where A_{DPPH} is the control absorbance and A_S is the sample absorbance.

2.3.2 ABTS assay scavenging assay

ABTS scavenging assay was estimated following the method of Roberta et al (1999).[30] The extract concentration ranged between 20 and 100 µg/mL. The absorbance was measured at 734 nm using a UV/Vis V-530 spectrophotometer. The Percent inhibition was calculated using the formula, $ABTS^{\bullet+}$ scavenging effect (%) = ((AB – AA) / AB) × 100; where AB the absorbance of ABTS radical and methanol; AA the absorbance of ABTS radical and sample extract/standard. Trolox was used as a standard substance.

2.3.3 Ferric reducing antioxidant power assay (FRAP)

The ferric reducing antioxidant power assay was performed as previously described by Thaipong et al. (2006).[31] The antioxidant capacity of the samples was measured spectro-photometrically at 593 nm using a UV/Vis V-530 spectrophotometer. An analytical curve with different concentrations of Trolox (linearity: 50–750 µM; R^2 = 0.9997) was plotted to quantify the ferric reducing antioxidant power phenolic rich-extracts. The potential antioxidant activity was expressed as Trolox equivalent antioxidant capacity in µmol Trolox × g^{-1} of the extract.

2.4 Anribacterial activity

The antibacterial activity of *Z. lotus* lipophilic and phenolic-rich extracts was assessed through MIC determination against four bacterial strains namely: *E. coli*, Methicillin-sensitive *Staphylococcus aureus*–MSSA, Methicillin-resistant *Staphylococcus aureus*–MRSA, and *S. epidermis*.

2.4.1 Bacterial strains

Bacterial cultures grown on Mueller-Hinton Agar (MHA) plates incubated overnight at 37 ºC. These bacterial strains were maintained at –80 °C in Brucella Broth with 20% (v/v) glycerol and DMSO (+5%) until use.

2.4.2 MIC determination

Zizyphus lotus lipophilic and phenolic-rich extracts (root barks, leaves, pulp, and seeds) antibacterial activity was determined using Minimal Inhibitory Concentration (MIC), through microbroth dilution method. Extracts were tested against the bacterial strains *E. coli* (ATCC 25922), MSSA and MRSA (ATCC 6538), and *S. epidermis* (clinical isolate), kindly provided by Portuguese Catholic University (Oporto). Briefly, bacterial strains in the exponential growth phase were suspended in Mueller-Hinton Broth (MHB) to obtain a final inoculum concentration of $1x10^5$ CFU/mL, according to Clinical and Laboratory Standards Institute guidelines (CLSI).[32]

In 96-well plates, were performed serial dilutions of lipophilic and phenolic-rich extracts of *Z. lotus* in a range of concentrations of 8 and 2048 µg/mL, using a stock solution of 50 mg/mL in DMSO or Acetone. The following controls were also performed: i) Solvent control: bacterial cultures with 4% (v/v) of DMSO or Acetone; ii) Growth control: pure cultures (only bacterial inoculum); and iii) Sterility control: culture media. Three independent experiments were performed for each extract, each one in triplicate. The MIC values were determined after 24 h of incubation at 37 °C by using the Resazurin assay adapted from Sarker et al. (2007).[33] The MIC value was considered as the minimum concentration of the tested sample at which the blue color of resazurin becomes pink and fluorescent when reduced to resorufin by oxidoreductases within viable cells.

2.5 Anticancer activity

2.5.1 Cell culture

The cell lines were purchased from American Type Cell Culture (ATCC, Manassas, Virginia, USA). Cells were grown in Gibco Dulbecco's Modified Eagle Medium (DMEM) supplemented with 10% (v/v) fetal bovine serum (FBS) and 1% penicillin-streptomycin mixture in a humidified atmosphere with 5% CO_2 (C150, Binder GmbH, Tuttlingen, Germany) under 37 °C. Before confluence, cells were washed with phosphate-buffered saline (PBS), collected the following trypsinization with trypsin (0.5 g/L)/EDTA (0.2 g/L) solution and suspended in fresh growth medium before platting.

2.5.2 Cell viability

The cytotoxicity activity of lipophilic and phenolic-rich extracts of *Z. lotus* against MDA-MB-231 (triple-negative breast cancer), MCF-7 (breast cancer), and HepG2 (liver hepatocellular carcinoma) was tested for 48 h and analyzed for cell proliferation by MTT assay.[34] The stock solution of *Z. lotus* extracts (10 mg/mL), were prepared in DMSO. Cells were seeded in 96-well plates at 2 x 10^5 cells/mL density, and incubated for 24 h at 37 °C afterward; cells were treated with *Z. lotus* extracts (0.1–100 µg/ml) and MDA-MB-231 cell with betA (0.1–150.0 µM). The negative control cells received DMSO (<1% (v/v)) and the blank contains the medium with the cell line. Therefore, cells were incubated for 4 h at 37 °C

with 20 µL, per well, of MTT stock solution (final concentration 0.5 mg/mL) in PBS. Then the medium was discarded, and formazan crystals were solubilized in 100 µL of DMSO/ethanol (1:1) solution. The efficiency of each extract solution was measured at 570 nm using a microplate reader (Thermo Scientific, Waltham, MA, USA). The results were expressed as the percentage of cell viability relative to that of the respective solvent control according to eq.1: % Inhibition = (ODC − ODT)/ ODC × 100%; Where ODC is the optical density of the solution in wells containing cells treated with *Z. lotus* extracts and ODT is the optical density of the solution in wells containing DMSO treated cells (negative control). The IC50 was calculated by plotting the percentage of cell viability in the function of the sample concentration logarithm. Each test sample solution was performed in triplicate independent experiments and then averaged.

2.5.3 Transwell migration assays

For the cell migration analysis, MDA-MB-321 cells (2 x 10^5 cells/mL) were seeded into the upper chamber and 600 µL of medium containing 10% fetal bovine serum was added to the lower chamber. The IC50 value of lipophilic root barks extract (6.01 µg/mL) was added to upper chambers for 48h in a humidified incubator with 5% CO_2 at 37 °C. Then, the migrative cells were fixed with 85% cold ethanol and stained with 0.5% crystal violet, and counted under an inverted microscope. For cell migration assays, the upper chamber was coated with Matrigel. Subsequent operations were similar to cell migration assays. Data are expressed as a migrative rate compared with the DMSO-treated group.

2.5.4 Cell cycle analysis

MDA-MB-231 cells were cultured in six-well plates at a density of 4 x 10^5 cells/mL for 24h at 37 ºC. Then, cells were exposed to the IC50 values of root barks lipophilic extract (6.01 µg/mL). Vehicle solvent control cells received DMSO (0.09% (v/v)). After 48 h-incubation, cells were collected, PBS washed and fixed with 85% cold ethanol. Cell pellets were collected after centrifugation at 300 x g for 5 min at 4°C and resuspended in PBS. Then, cells were incubated with 50 µg/mL RNase and 50 µg/mL propidium iodide staining solution for 20 min at room temperature in dark. Propidium iodide-stained cells were analyzed in the Beckman-Coulter®EPICS-XL (Beckman-Coulter®, Brea, California, USA) flow cytometer equipped with an air-cooled argon-ion laser (15 mW, 488 nm). Results were obtained using the SYSTEM II software (version 3.0 Beckman-Coulter®, Brea, California, USA), in which at least 5000 nuclei per sample were acquired. Analysis of cell cycle distribution was performed by using the Flow Jo software (Tree Star, Ashland, Oregan, USA). Three replicates were performed for each treatment.

2.5.5 Cell-apoptosis analysis

Apoptosis in MDA-MB-231 cells was detected using annexin V-fluorescein isothiocyanate (FITC)/propidium iodide (PI) apoptosis detection kit following the manufacturer's instruction. Briefly, cells were seeded into 6-well culture dishes (4 x 10^5 cells/well) for 48 h before the addition of root barks lipophilic extract (6.01 µg/mL). Following 24h-incubation with the tested extract, the percentage of apoptotic cells was determined by the annexin V-FITC/PI assay. The cells were harvested, washed with cold phosphate-buffered saline and resuspended

in binding buffer. The cells were treated with annexin V-FITC conjugate and incubated for 15 min at room temperature in the dark condition. The cells were then stained with propidium iodide (PI, 5 µg/mL) and analyzed by flow cytometry using a software (version 3.0 Beckman-Coulter®, Brea, California, USA) within 1 h following the staining. In the next step, cells were suspended in a staining buffer. Cell analysis was performed using CytoFlex Flow Cytometer (Beckman-Coulter®, Brea, California, USA). Electronic compensation was used to eliminate bleed-through fluorescence.

2.5.6 Western Blot Analysis

To determine the effect of *Z. lotus* on the signaling pathway involved, some protein MDA-MB-321 cells were evaluated by western blot. Briefly, MDA-MB-231 cells were treated with IC50 of the root barks lipophilic extract (6.01 µg/mL) for 48h; then cells were washed with cold PBS and centrifuged at 492 x g for 3 min, at 4 ºC. This procedure was repeated two more times. Cells were then lysed with RIPA buffer (1% NP-40 in 150 mM NaCl, 50 mM Tris-HCl (pH=8), 2 mM EDTA), containing 1 mM phenylmethylsulfonylfluoride, phosphatase inhibitors (20 mM NaF, 20 mM Na2V3O4), and protease inhibitor cocktail (Roche, Mannheim, Germany), for 10 min, at 4 ºC. Cell lysates were centrifuged at 24104 x g for 10 min, at 4 ºC. Supernatants were collected and total protein concentrations were quantified according to the Lowry method,[35] using BSA as the protein standard. Cell lysates (25-40 µg protein) were electrophoresed on sodium dodecyl sulfate 10% polyacrylamide gel, and then transferred onto poly(vinylidene difluoride) (PVDF) membranes (Amersham Biosciences, Buckinghamshire, UK). PVDF membranes were blocked with 5% (w/v) of non-fat milk at 37°C for 1 h, and incubated overnight at 4 °C with a primary antibody against Akt (1:200), *p*-Akt (1:1000); *p*-PI3K (1:200), and β-actin (1:300). After incubation with the relevant secondary antibodies, their active bands were identified using enhanced chemiluminescence using appropriate horseradish peroxidase-conjugated secondary antibodies, and developed with ECL reagents (Amersham Biosciences, Buckinghamshire, UK), according to manufacturer's instructions. Three independent experiments were performed for each treatment.

2.6 Statistical analysis

Statistical analysis Data are presented as mean±standard deviation. SPSS17.0 software was applied to perform statistical analysis. Pearson correlations (0.01 and 0.05 significance levels) were performed in SPSS, and principal component analysis (PCA) was applied to separate thecultivars according to phenolic composition and antioxidant activity.

3. Results and Discussion

3.1 Antioxidant activities of *Zizyphus lotus* extracts

Phenolic compounds are known to be the main bioactive compounds in plants with antioxidant capacities to scavenge free radicals, participate in the regeneration of other antioxidants, and protect cell constituents against oxidative damage. In this study, we determined the free radical scavenging capacities of *Z. lotus* phenolic-rich extract using DPPH and ABTS assays, and its ferric reducing capacities using the FRAP assay. The corresponding

results are presented in Table 1. The capacity of ascorbic acid and BHT to scavenge DPPH was also assessed for comparative purposes.

Table 1: Antioxidant activities of phenolic-rich extract of different morphological parts of *Zizyphus lotus* by DPPH, ABTS, and FRAP assay.

***Z. lotus* extract**		**Antioxidant Assay**		
		DPPH IC50 (µg/mL)	ABTS IC50 (µg/mL)	FRAP (µM Trolox equiv (TE) /g extract)
Phenolic-rich extracts				
Fruits	Pulp	44.71±1.75	97.20±1.95	86±1.29
	Seeds	75.45±9.04	137.09±1.07	51±1.03
Leaves		9.68±0.9	56.12±0.47	245±6.18
Root barks		5.97±0.57	69.16±0.53	601±4.90
Ascorbic acid		2.44±0.42	-	-
BHT		11.30±2.17	-	-

Data are reported as mean (n=3) ± SD. DPPH (2,2-diphenyl-1-picrylhy- drazyl), ABTS (2,2′-azino-bis(3-ethylbenzothiazoline-6-sulphonic acid)), and FRAP (Ferric reducing/antioxidant power) in µM Trolox equiv (TE) /g extract, Trolox; 6-hydroxy-2,5,7,8-tetramethylchroman-2-carboxylic acid.

DPPH, ABTS, and FRAP assays have been widely used to determine the antioxidant capacities of plant extracts as they require relatively standard equipment and deliver fast and reproducible results. Indeed, an interlaboratory comparison of six methods for measuring antioxidant potential published recently showed that DPPH and ABTS assays are the easiest to implement and yield the most reproducible results.[36] In our study, we have observed that the four morphological parts of methanol/water/acetic acid (49.5:49.5:1) extracts of *Z. lotus* exerted different antioxidant activities behavior. This might be explained by the particular profile of each fraction in phenolic compounds, mainly flavonoids derivatives.

3.1.1 DPPH scavenging effect of *Zizyphus lotus*

In the DPPH assay, the root barks and leaf phenolic-rich extracts of *Z. lotus* exhibited stronger scavenging potential with IC50 values of 5.97 and 9.68 µg/mL, respectively (Table 1). The IC50 value of root barks was higher than the other extracts and also showed good activity compared to the synthetic antioxidant BHT used as a positive control (IC50 = 11.30 µg/mL). Leaves also presented good activity compared to BHT, while both extracts exhibit weak activity against ascorbic acid (IC50 = 2.44 µg/mL). Pulp extract had a moderate scavenging activity, while seeds had lower antioxidant activity and had possessed a higher IC50 value (75.45 µg/mL). *Z. lotus* phenolic-rich extract gives lower DPPH scavenging activity when compared to aerial aqueous and methanolic extracts reported by Bouaziz et al. (2009) (IC50 = 0.69 and 1.1 µg/mL, respectively).[37] Nonetheless, it gave higher DPPH scavenging activity than the aerial hydro-alcoholic extract (IC50 = 42 µg/mL) expect for seeds fraction.[38] Moreover, root barks give higher DPPH scavenging activity when compared with the roots phenolic-rich fraction (IC50 = 816 µg/mL) stated by Ghalem et al. (2014).[39]

3.1.2 ABTS scavenging effect of *Zizyphus lotus*

The ABTS radical scavenging activity results were shown in Table 1. These results were similar to those of the DPPH radical cation radicals scavenging activity. In this assay, leaf extracts had a higher capacity than had the other extracts, followed by root barks with an IC50 value of 69.16 µg/mL. As the results of DPPH scavenging assay pulp and seeds phenolic-rich extracts of *Z. lotus* showed the weakest activity. Leaves extract was similar to that informed for the methanolic leaf extract of *Z. lotus* (IC50 = 50 µg/mL)[25] and to was reported in the hydro-alcoholic aerial part (IC50 = 49 µg/mL) by the work of Boulanouar et al. (2013).[38] While, it gave lower ABTS scavenging activity than hexane extract prepared with aerial part simple (IC50 = 0.25 µg/mL).[37]

3.1.3 FRAP reducing power of *Zizyphus lotus*

The FRAP assessment provides clear information about the electron transfer potency of an antioxidant which is a simple, rapid, and relatively inexpensive assay. According to the results ferric reducing potential was higher in root barks and leaves, followed by pulp and seeds extracts, which was consistent with the $ABTS^{+}$ and DPPH radical scavenging activity. Among the four fractions, root barks and seeds showed the respective highest and lowest FRAP, at the concentrations ranging from 601 and 51 µM (TE)/g extract, respectively. Therefore, leaf extract was found to have a potent FRAP. Marmouzi et al. (2019)[20] were studied the FRAP activity of *Z. lotus* aqueous leaf and fruit extracts. The results have been expressed as ascorbic acid equivalent per gram of extract.[20] They found that *Z. lotus* leaves extract has the highest antioxidant capacities compared to the fruit that is concomitant with our results.

Concerning the total phenolic content determined by HPLC of the different studied *Z. lotus* extracts, the obtained results showed that a high content of phenolic compounds corresponds automatically to high antioxidant activity. Thus the observed antioxidant activity could due, at least partially, to the presence of the flavonoids identified in Chapter IV.

Flavonoids possess many biochemical properties however the best-described property of almost every group of flavonoids is their capacity to act as antioxidants.[40] The scavenging ability of phenolic compounds could be explained by the total content, chemical structure and as well as the position and availability of hydroxyl groups.[41] Root barks phenolic-rich extract is represented by a high concentration of flavan-3-ols (7579 mg/kg dw) that could be explaining its potent scavenging capacity. Catechin derivatives represent the main phenolic compounds of root barks extract (Chapter IV) and are known to have a potent antioxidant activity due to their content in a saturated single bond at 2 and 3 positions.[42] Additionally, it was reported that the adding of galloyl groups to the molecule structure is recognized to enhance the antioxidant activity.[43] Procyanidin structure had a catechol unit on the aromatic B-ring, which stabilizes free radicals and can chelate metals and proteins due to several o-dihydroxy phenolic groups.[43,44] The presence of procyanidin (B-type) dimer with a considerable amount (798–969 mg/kg dw, Chapter IV) could explain the higher antioxidant capacity of root barks phenolic-rich extract.

Flavonols are known for their efficient acts as antioxidants, both as radicals scavengers and as metal chelators.[45] Methanol/water/acetic acid (49.5:49.5:1) leaves extract, constitute by flavonols derivatives, represented by 79.97 % of the total phenolic compounds identified in

leaves. Quercetin derivatives present the predominant flavonols fraction in leaves extracts and have been reported to exhibit good antioxidant activities due to the combination of the catechol moiety with double bonds at C2–C3 and 3–OH in its structure provide an extremely active free-radical scavenger.[40,42] This may increase and explain the observed antioxidant activity. Other possible antioxidants, present in the leaf extract may also have influenced such as myricetin and kaempferol derivatives. Myricetin is known to scavenge different radicals, and it was more effective than α-tocopherol as an antioxidant in liposomes.[46] The significant scavenger activity of pulp phenolic-rich extract might be explained by its peculiar content (2596 mg/kg dw, Chapter IV) along with its profile in phenolic compounds mainly: (epi)gallocatechin methyl gallate and flavonols derivatives. (epi)Gallocatechin methyl gallate has been extensively studied for its potential health- effects related to its antioxidant activity.[49]

The leaves and seeds UHPLC-UV-MS characterization show to have flavonoids glycosides bearing hydroxycinnamic acid. The pharmacological evaluation of several similar flavonoids, especially the one bearing a *p*-coumaric acid revealed that these compounds exhibit various beneficial effects attributed to their antioxidant activity.[47] These facts could explain the potent scavenging activity of leaves phenolic-rich extract. Seeds phenolic-rich extract gave the lowest activity in all the assays, presenting also the lowest phenolic concentrations (360 mg/kg dw, Chapter IV), which might explain the less effect shown by this sample. This could be also explained by the fact that flavone has a lack of a catechol system during the oxidation leads to the formation of unstable radicals.[40] Besides that, the solvents may influence the antioxidant activity of seeds because they may affect the hydrogen-donating ability of antioxidants.[48]

Worth noted that the extracts contain always a mixture of various chemical compounds; it is not possible to relate the antioxidant effect of wild *Z. lotus* to one or a few bioactive compounds. To confirm any relationships among the analyzed variables from the *Z. lotus* samples, principal component analysis (PCA) and Pearson's coefficients were conducted.

3.1.4 Correlations of antioxidant assays and phenolic compounds

3.1.4.1 Pearson's correlation coefficients

Correlations between the antioxidant activities and total phenolic compounds determined by folin (TPC), total anthocyanins content (TAC), phenolic compounds determined by HPLC (PCs), phenolic acids (PA), flavones, flavonoids, flavonols, and flavan-3-ols were performed with factor analysis and Pearson's.

Table 2: Pearson's correlation coefficients (r) for the relationships between antioxidant assays and phenolic contents.

Variables	DPPH	ABTS	FRAP	Fds	Fols	Fone	F3ols	PCs	TPC
ABTS	,999**								
FRAP	-,916	-,904							
Fds	-,913	-,915	,915						
Fols	,040	,009	-,178	,229					
Fone	,838	,856	-,560	-,725	-,307				

F3ols	-,863	-,844	,938	,736	-,489	-,474			
PCs	-,885	-,888	,890	,997**	,290	-,711	,690		
TPC	-,235	-,264	,094	,485	,961*	-,509	-,229	,538	
TAC	-,949	-,953*	,754	,762	-,066	-,920	,761	,725	,182

** Significant correlation with p<0.01; * significant correlation with p<0.05; Abbreviations: PA, phenolic acid; Fds, flavonoids; Fols, flavonols; Fone, flavone; F3ols, flavon-3-ols; Fnone, flavonone; PCs, phenolic compounds-HPLC; DHCs, dihydrochalcones; TPC, total phenolic compounds; TAC, total anthocyanines.

The Pearson correlation test was used to determine the correlation between antioxidant activity (DPPH, ABTS, and FRAP) and the major composition family of phenolic-rich extracts of *Z. lotus* as well as the total amount of phenolic compound and anthocyanins evaluated using the colorimetric method and phenolic compounds determined by HPLC. It is observed that the three antioxidant assays, DPPH, ABTS, and FRAP were strongly correlated with each other, in which the Pearson's correlation coefficient r = 0.999 (p<0.01) were found between ABTS and DPPH assays. Our results are in agreement with previous studies.[50,36] The ABTS assay applies to both hydrophilic and lipophilic antioxidant systems, while DPPH is only applicable to hydrophobic systems due to using a radical dissolved in organic media.[51] The strong correlation between these two parameters in this study indicated that the phenolic compounds that contributed to the free radical scavenging activity were similar compounds with comparable hydrophilicity.[50] FRAP was highly correlated with both DPPH and ABTS with a negative correlation coefficient of r = -0.916 and -0.904 respectively. FRAP tested the reducing capability measured by the ferric ions. The high correlation of FRAP with DPPH and ABTS suggested that the compounds present in the plant extract capable of scavenging DPPH and ABTS free radicals could also reduce ferric ions. The high correlations of FRAP and antioxidant activity assays were previously reported by Pulido et al. (2000)[52] and Vasco et al. (2008).[53]

The HPLC determined phenolic compounds were strongly correlated with the antioxidant measures (DPPH, ABTS, and FRAP) with r=–0,885, –0.888 and 0.890, respectively suggesting that phenolic compounds significantly contributed to the antioxidant activities. Indeed, some authors have found correlations between the phenolic composition and antioxidant activities.[54] Therefore, a weak correlation was found between antioxidant parameters and total phenolic content determined by the Folin-Ciocalteu method (Table 2). These results are likely explained by the reaction of Folin reagents with phenolic compounds and any other reducing substance present in the sample.[89] Besides, flavonols were found to be strongly correlated with TPC (r=0.961, p<0.05) while weak correlated with other parameters, which consistent with the poor correlations of the antioxidant parameters with flavonols and TPC. On the other hand, higher correlations of flavan-3-ols quantified by HPLC, TAC, and antioxidant activities were found, in which the Pearson's correlation coefficient r=0.953 (p<0.05) were found between TAC and ABTS assays. These findings suggest that flavon-3-ols represent a huge part of TAC, and both of them contribute to the antioxidant activities.

The HPLC detected flavonoids were found to be correlated with DPPH, ABTS, and FRAP with -0.913, -0.915, and 0.915, respectively suggested that phenolic compounds were the major contributors to the reducibility of the plant extracts. Whereas, the strong correlation found between flavonoids and PCs with correlation coefficient r=0.997 (p<0.01) indicates that

flavonoids represent a high proportion of the total PCs of the samples. Other compounds such as quinic acids isomers, naringenin-6,8-di-C-hexoside isomers, and phloretin-3',5'-di-C-glucoside, detecting in *Z. lotus* phenolic-rich extract but not analyzed in this study.

3.2 Antibacterial activity

Plant species contain several secondary metabolites such as tannins, terpenoids, alkaloids, and flavonoids that have been found in vitro to have antimicrobial properties for protection against aggressor agents, especially microorganisms.[55] The number of studies dealing with antimicrobial properties of plant secondary metabolites is constantly rising along with the action of their potential mechanisms.

Antibacterial activity of different morphological parts of *Z. lotus* extracts was evaluated through Resazurin assay against Gram-negative and Gram-positive bacterial strains. The results obtained were summarized in Table 3.

Table 3: MIC values of *Z. lotus* extracts against *E.coli*, MSSA, MRSA, and *S. epidermidis*, determined through Resazurin assay.

***Z. lotus* extracts**	**MIC (µg/mL)**			
	E. coli	MSSA	*S. epidermidis*	MRSA
Lipophilic extracts				
Root barks	>2048	2048	2048	>2048
Leaves	1024	2048	1024	>2048
Seeds	>2048	>2048	1024	>2048
Pulp	>2048	>2048	>2048	>2048
Phenolic-rich extracts				
Root barks	2048	2048	>2048	1024
Leaves	2048	2048	>2048	2048
Seeds	>2048	>2048	>2048	>2048
Pulp	>2048	>2048	>2048	>2048

The results showed that lipophilic leaves extract presents the highest activity, among all fractions, with inhibitory effect against strains used, especially for *E. coli* and *S. epidermidis* (MIC = 1024 µg/mL). In contrast, lipophilic pulp fraction did not demonstrate antibacterial activity against any of the bacterial strains in the range of concentrations used. Moreover, the lipophilic extract of leaves and root barks showed a slightly inhibitory effect on MSSA (MIC = 2048 µg/mL), except for pulp fraction. *S. epidermidis* showed susceptibility to *Z. lotus* lipophilic extracts between 1024 and 2048 µg/mL, except for pulp. However, all the tested lipophilic extracts were resistant to MRSA strains (MIC > 2048 µg/mL). It is worthy to note that there is no available data in the literature regarding the anti-bacterial effect of lipophilic wild *Z. lotus* extracts estimated by the microdilution method.

Generally, the antibacterial effectiveness of plants depends on chemical characteristics and their region of origin.[56] Fatty acids particularly, long-chain unsaturated fatty acids (UFA) are known to have antimicrobial activities against Gram-positive bacteria by inhibiting an essential component of bacterial fatty acids synthesis which is enoyl-acyl transporter protein reductase (FabI).[57] Therefore, γ-linolenic acid reported altering the cell membrane properties of *E. coli* directly or by generating the free radical.[58] Linolenic and oleic acids were identified

respectively as the major constituents of UFA in leaves and seeds extracts (2431 and 6255 mg/kg dw, respectively, Chapiter III). These significant amounts could support the antimicrobial effect findings.

According to Lee et al. (2002)[59] the combination of linolenic acid and monoglycerides produces a strongly synergistic effect than the use of linolenic acid alone.[59] The moderate amount of monoglycerides (189 mg/kg dw) with high linolenic acid content in leaves extract may explain its good antibacterial effect. Besides, the leaves lipophilic extract is characterized by the presence of α-tocopherol which would alter the structure of the bacterial lipoprotein membrane, adjust its fluidity, and thus the death of bacteria.[60] Also, it has been shown that phytol and neophytadiene have antimicrobial activity against *S. aureus*.[61] These compounds were identified as a component of leaves lipophilic extract with a significant amount (Chapter III). BetA isolated from the dichloromethane stem bark extract of *Zizyphus joazeiro* was reported to have antimicrobial properties against Gram-positive bacteria.[62] The considerable amount of betA in the root barks could be responsible for the antibacterial activity acquired against MSSA and *S. epidermidis*. Therefore, the moderate amounts of active components identified in the pulp lipophilic fraction may explain its ineffectiveness against bacterial strains in the concentration tested.

The variety of chemical structures of phenolic compounds present in *Z. lotus* phenolic-rich extract makes it a possible effective alternative in the treatment of bacterial infections. Several studies attributed the inhibitory effect of plant extracts against bacterial pathogens to their phenolic composition.[63] In this vein, the strongest activity was recorded by the root barks methanol/water/acetic acid (49.5:49.5:1) extracts registering MIC values in a range of 1024 to 2048 µg/mL. Meanwhile, *S. epidermidis* was not susceptible to the phenolic-rich extracts of wild *Z. lotus* (MIC > 2048 µg/mL), while MRSA showed higher sensitivity to the root barks extract (MIC = 1024 µg/mL). The leaves extract, exert an anti-bacterial effect with similar MIC values of 2048 µg/mL. While, seeds and pulp phenolic-rich extracts did not inhibit bacterial growth, a range of 8–2048 µg/mL.

The antibacterial effect of leaves phenolic-rich extract against *E. coli* was stronger than the methanolic leaves extract (MIC = 12500 µg/mL) shown by Ghazghazi et al. (2014)[25] and even in what found in the work of Wahiba et al. (2019).[21] Nonetheless, the result is comparable (MIC = 1000 µg/mL) with what was informed by Mahboba et al. (2010).[1] The anti-MRSA effect of leaves extract was much weaker compared to the leaves infusion (MIC = 625 µg/mL), and stronger than the antibacterial action of decoction and hydroethanolic *Z. lotus* extracts (MIC = 1250 and 2500 µg/mL, respectively).[21] Besides, the MRSA and MSSA effect of leaves and root barks were stronger than those reported in the work of Wahiba et al. (2019).[21]

The phenolic composition of each shrub parts, characterized in the previous Chapter IV, may be responsible for the antibacterial effect analysis. The mechanism action of phenolic compounds is not fully understood, however, is speculated to involve many sites of action at the cellular level.[64] This ability is related to the molecules' structures; by their hydroxyl (–OH) group and benzene ring. Numerous research results indicate that the hydroxyl group at C-3 in the C ring is required for antibacterial activity which could facilitate the penetration of flavonoids through the cell membrane.[63,65] Among, 11 different flavonoids tested, a positive

correlation was found among the antibacterial activities and with quercetin and kaempferol aglycone.[66] Actually, quercetin derivatives were shown to have significant antibacterial activity against MRSA and *S. epidermidis*, acting by enzyme inhibition of DNA gyrase.[67,68] Besides, kaempferol is known to generate the reactive oxygen species through the interaction of its phenoxyl radical to oxygen that could damage vital molecules inside the cell or alter its redox state, which can lead to cell death.[69] All this is in agreement with the results obtained in the leaf extract were represented by flavonols (e.g. quercetin and kaempferol derivatives) that could explain their potent antibacterial activity. Other compounds such as (epi)-catechin, luteolin, and myricetin derivatives may also contribute to the activity of *Z. lotus* leaves extract.[65,70] Luteolin derivatives were found to be active against *E. coli* and *S. aureus* and its glycoside derivatives were displayed to act as an inhibitor of proteins and peptidoglycan synthesis and by altering the membrane permeability of bacterial strains.[71] Additionally, the current activity may also result from the synergic effect between these compounds.

The results obtained in the phenolic-rich extract of root barks especially against MRSA (MIC = 1024 µg/mL) could be due to the considerably high concentration of flavan-3-ols (7579 mg/kg dw, Chapter IV) that already defined as toxic compounds to microorganisms due to the existence of two hydroxyl groups in its structure. The mechanism of action of this family is attributed to their chelating properties on iron, an important oligo element for heme-utilizing bacteria.[72] Actually, several researchers have discovered that tea catechins can be used against MRSA.[73] It would be worth mentioning that MRSA is one of the clinical infections that are currently difficult to treat. The effect of root barks extract against MRSA probably is part of an antibacterial formulation against this strains bacterium. Therefore, the lower concentration of phenolic compounds in the seeds may explain its ineffectiveness against bacterial strains in the concentration tested.

3.3 Anti-tumor activity

This study was undertaken for the first time to investigate the anti-proliferative effects of wild *Z. lotus* extracts from Morocco on MDA-MB-231, MCF-7, and HepG2 cell lines. Besides, the evaluation of the role of lipophilic root barks extract in the MDA-MB-231 cancer cell line by exploring its effects on cell migration, apoptosis, and the cell cycle as well as the investigation of its effect on the important signaling network, such as the PI3K/Akt signaling pathway.

3.3.1 Toxicity evaluation of *Zizyphus lotus* extracts on MDA-MB-231, MCF-7, and HepG2 cells growth

The antiproliferative effect of different morphological parts of *Z. lotus*, as shown in Table 4, was evaluated against three cell lines namely: MDA-MB-231, MCF-7, and HepG2. Our selection is based on the aggressive form of these cell lines and also on the continued investigation of the antiproliferative potential of triterpenic acid and phenolic compounds as phytotherapeutics agents against triple-negative breast cancer (TNBC) and MCF-7.[74]

Table 4: IC50 values of *Zizyphus lotus* extracts on MDA-MB-231, MCF-7, and HepG2 cell lines using the MTT assay.

***Z. lotus* extracts**	**MDA-MB-231**		**MCF-7** (IC50 µg/mL)	**HepG2** (IC50 µg/mL)
	IC50 µg/mL	IC50 µM		
Lipophilic extracts				
Root barks	6.01± 0.96	-	18.78 ± 0.47	23.27 ± 1.07
Leaves	85.87± 7.09	-	59.27± 2.65	67.34 ± 0.73
Fruits Seeds	>100	-	>100	>100
Pulp	>100	-	>100	>100
Phenolic-rich extracts				
Root barks	>100	-	>100	79.45 ± 2.13
Positive control (BA)	10.80±0.75	22.67±2.22	-	-

In general, *Z. lotus* root barks lipophilic extract showed a significant antiproliferative effect in vitro against the MDA-MB-231 cell line (Table 4). Although, the lipophilic fraction of the leaves had a lower inhibitory activity (IC50 = 85.87 µg/mL) compared to the value of the root barks and that reported for the ethanolic leaves extract of *Z. lotus* (IC50 = 45.5 µg/mL).[75] The root barks lipophilic extract revealed also the strongest activity on MCF-7 and HepG2 cell lines with IC50 values of 18.78 and 23.27 µg/mL, respectively. Besides, the lipophilic preparations of the leaves part also exerted a potent cytotoxic activity, specifically against MCF-7 with an IC50 value of 59.27 µg/mL. Among the phenolic-rich extracts, root bark was the only part tested against HepG2, which has shown to exhibit a moderate cytotoxic activity. The lipophilic extract of seeds and pulp showed an inhibitory activity higher than 100 µg/mL being non-cytotoxic for the cell lines tested.

In qualitative and quantitative terms, leaves lipophilic extract is considered as the richest fraction compared to the root barks, except for triterpenic acids, which represent 10230 mg/kg dw, corresponds to 92.61% of the total triterpenic acids content (Chapiter III). This appreciable amount could be regarded as a suppressor of the tested cell lines. BetA is the main triterpenic acid (96.16% of the total triterpenic acid content) identified in the root barks as discussed previously and known to be a promising compound against different types of cancer by inducing apoptosis in the CD-95 and p53-independent manner.[74,76–78] In addition to its broad specificity for multiple tumor types, betA was reported to be devoid of cytotoxic effects against healthy cells.[78]

The pure betA is used as a positive control for comparing the effect of root barks extract. However, betA showed cytotoxicity towards the MDA-MB-231 cells at a high dose (IC50 = 22.67 µM) which confirmed the hypothesis that the lipophilic root barks cytotoxicity may also have resulted from synergistic or cumulative actions of betA, together with other extract component(s). The dichloromethane bark extract of *Zizyphus mauritiana* has been shown to has a significant antiproliferative activity against the MCF-7 cells by arresting the cell cycle on G2/M. Lupeol and betA were fractionated from this extract and were suggested as being responsible for the cytotoxicity activity of the bark extract.[79] Besides, lupeol was reported to increase at a high-level ERa gene expression in the MDA-MB-231 ERalpha-negative breast cancer cells by stimulation the decoy effect of the RA4 DNA sequence and also found to

inhibit the cell proliferation.[80] Although, oleA is inactive triterpenic acids against the MDA-MB-321 cell line[81] although, it was observed to generate apoptosis of HepG2 cells and also arrest its cell cycle in the G2/M phase through the decreasing of Cyclin Bi/cdc2 activity.[23]

Sterols are another family characterized by their anticancer potential.[82] β-Sitosterol was found to inhibit MDA-MB-231 cell growth by inducing cell cycle arrest at the G2/M phase and as an anti-metastatic agent[83] while, stigmasterol has antiproliferative activity compared to cholesterol and campesterol, which were found to have no cytotoxic effect on MDA-MB-231 cell growth.[84] Taking into account the significant content of sterols in leave and root barks (355 and 257 mg/kg dw, respectively), these compounds could be involved in the results acquired.

HepG2 cells were thus more sensitive to phenolic-rich extract of root barks than other cell lines. Such significant action could be linked to the presence of flavan-3-ols, such as the (epi)catechin-(epi)gallocatechin described as a strong cytotoxic agent through the inhibition of cell proliferation and by inducing apoptosis in different cancer cell lines.[21] Lipophilic extracts of seeds and pulp have no cytotoxic effect (IC50 > 100 µg/mL) on the cell lines tested at the maximum concentration. This fact could be due to the lowest concentration of bioactive compounds present in these parts of this shrub species.

Breast cancer (BC) continues to abruptly disrupt the lives of millions of women. In 2018, an estimated 2.4 million females were newly diagnosed with breast cancer approximately one new case diagnosed every 18 seconds; additionally, 626,679 women with breast cancer died.[85,86] Although, the incidence varies worldwide, with a higher incidence in high-income regions (92 per 100,000 in North America) than in lower-income regions (27 per 100,000 in middle Africa and eastern Asia).[86]

Triple-negative breast cancer (TNBC) is a subtype of BC lacking expression of estrogen and progesterone receptors and human epidermal growth factor receptor 2 (HER2) amplification.[87] Four molecular TNBC subtypes (TNBC type) were identified, based on gene expression and molecular features.[88] The TNBC affects more commonly black women younger than 40 years of age and is associated with the BRCA1 genetic mutation.[89] TNBC constitutes approximately 20%–25% of all BC cases with poor prognosis tending to be the most refractory than other BC subsets, with the absence of FDA–approved targeted therapies.[88,90] Chemotherapy is the main treatment option for patients with TNBC subtype and is based on anthracycline and taxane regimen, either in combination or sequentially.[87,91] However, this type of BC is easy to metastasis in the liver, brain, and lungs and has a higher three-year recurrence rate and five-year mortality rate after treatment.[91] Thus, the development of new effective anti-TNBC drug treatment has become urgent for us. Improved understanding of *Z. lotus* root barks lipophilic extract biochemical mechanisms is crucial to enable their future development as anticancer agonist agents.

3.3.2 Effect of *Zizyphus lotus* root barks lipophilic extract on the MDA-MB-231 cells migration

To explore whether root barks lipophilic extract could affect the mobility of MDA-MB-231 cells, a transwell migration chamber assay was conducted. Treatments with 6.01 µg/mL root barks lipophilic extract inhibited the migration of the MDA-MB-231 colonies, relatively to DMSO control (Fig 2). Additionally, root barks lipophilic extract strongly prevented MDA-

MB-231 cells to migrate regarding control cells. At the current knowledge, this is the first time that inhibitory effects of *Z. lotus* roots bak lipophilic extract, upon TNBC migration, are evidenced.

Cell migration is the key feature of cancer progression, metastasis, and suppression of cell migration may prove essential in the inhibition of metastasis in vivo. This may ensure a comparatively longer survival period of patients.[92] Therefore, the potential of root barks lipophilic extract for inhibition of migration of MDA-MB-231 cancer cells indicates that it may prove to be an efficient fraction in inhibiting the metastasis of cancer and deserves more analysis to understand its proper processing as well as its evaluation in vivo.

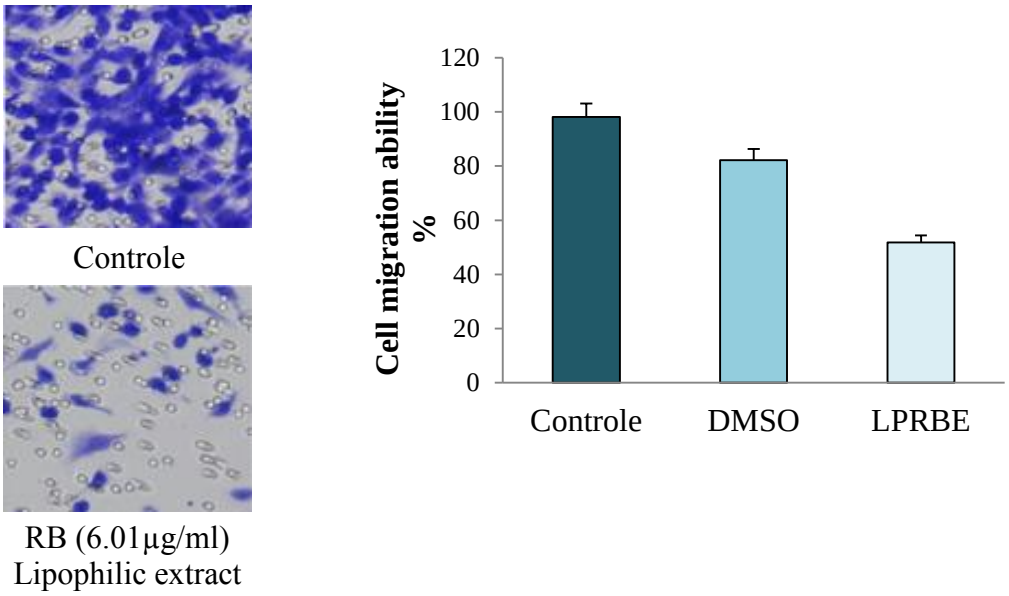

Figure 2: MDA-MB-231cells were seeded in the top chamber of transwell with serum-free medium and treated with vehicle or IC50 value of root barks lipophilic extract. After about 48h, migrated cells were fixed, stained, photographed and quantified. The results shown are representative of three independent experiments. Abbreviation: LPRBE, root barks lipophilic extract.

3.3.3 Effect of *Zizyphus lotus* root barks lipophilic extract treatment on the MDA-MB-231 cell cycle

Several anticancer agents lead to cell cycle arrest and are clinically effective for cancer treatment.[93] In this vein, flow cytometry (FCM) was applied to gain further insights about the suppressive actions of *Z. lotus* root barks lipophilic extract, upon the distribution of the MDA-MB-231 cells through the different cell cycle phases (G0/G1, S, and G2 phases) (Fig 3). The 24h-treatment with 6.01 µg/mL root barks lipophilic extract led to an accumulation of 30.4 % of MDA-MB-231 cells at the G2/M phase, representing a 2.14-fold cell percentage increase, regarding DMSO control cells. A slight decrease in the G0/G1 phases was noted (1.07-fold relative to DMSO control cells, respectively). The data suggest that root barks lipophilic extract treatment of the MDA-MB-231 cell line could lead to the arrest of cells in the G2-phase, eventually restraining the proliferation of cells. Further experiments are needed to

elucidate the mechanism by which *Z. lotus* lipophilic root barks extract causes cell cycle arrest in the MDA-MB-231 cell line.

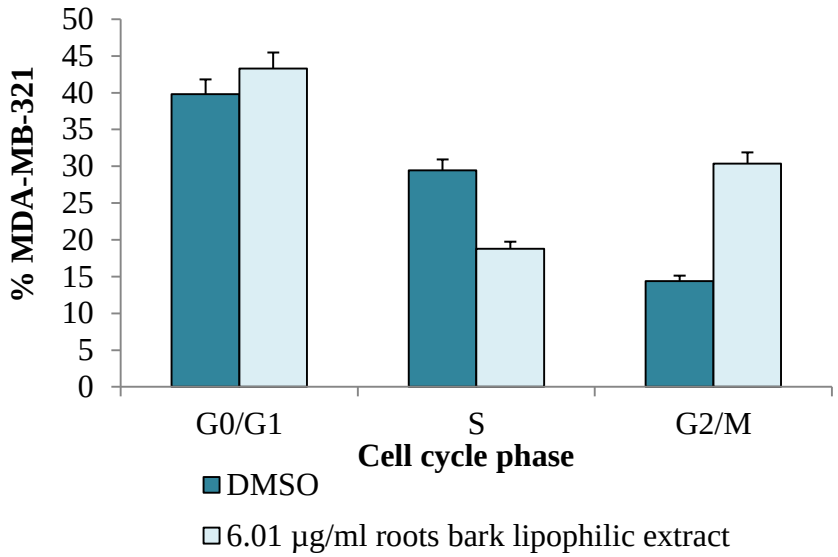

Figure 3: Cell cycle phase distribution of MDA-MB-231 cell was treated for 24h with *Zizyphus lotus* root barkq lipophilic extract. Cell cycle phases distribution by flow cytometry. The results shown are representative of three independent experiments.

3.3.4 Apoptosis-inducing effect of *Zizyphus lotus* root barks lipophilic extract on the MDA-MB-231 cells

Apoptosis is a key feature of cancer cells. Therefore, apoptosis promoting agents in cancer cells are considered as key candidates in anti-cancer treatments.[94] Following the effect upon the MDA-MB-231 cell cycle, more insights were sought to know whether the root barks lipophilic extract, at the respective IC50 value, could also induce the apoptosis of MDA-MB-231 cell colonies. After 48 h-incubation, root barks lipophilic extract increased the apoptotic cells of 68.8 % of MDA-MB-231 cells, representing a 5.9-fold cell percentage increase, regarding the control cells. This result suggesting that the anti-proliferative effect of root barks lipophilic extract might be due to apoptosis induction.

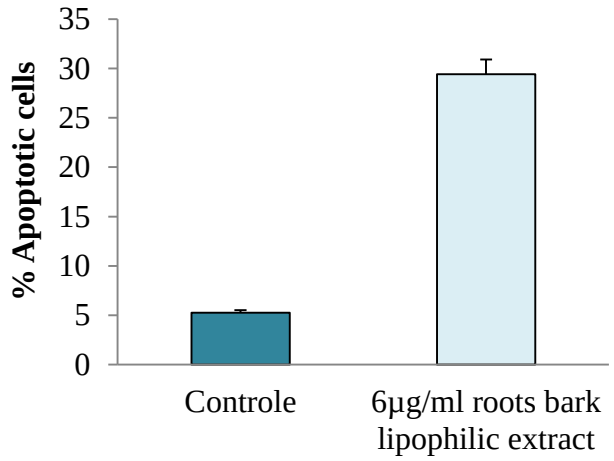

Figure 4: Effect on induction of apoptosis induced by *Zizyphus lotus* root barks lipophilic extract on MDA-MB-231 cell. Apoptosis was evaluated through nuclear condensation assay at 48h of incubation. The results shown are representative of three independent experiments.

3.3.5 Effect of *Zizyphus lotus* root barks lipophilic extract on the p-Ser473-Akt, p-PI3K, and Akt protein expression in MDA-MB-231 cells

Given the significant role of the PI3K/Akt pathway in cancer cells, in the current part, Akt and active *p*-Ser-473-Akt and *p*-PI3K protein expressions, in MDA-MB-231 cells, were thus evaluated after 48 h-incubation with *Z. lotus* root barks lipophilic extract. Notably, treatments with root barks lipophilic extract greatly decreased active p-Ser473-Akt and *p*-PI3K protein expression in MDA-MB-231 cells, relative to the control group (Fig 5). Furthermore, both protein expressions also increased in MDA-MB-231 cells after root barks lipophilic extract treatment, compared to DMSO control cells. Nevertheless, total Akt protein expression in treated MDA-MB-231 cells remained constant compared with the controls (Fig 5). In this way, these data suggest that root barks lipophilic extract inhibited the growth of TNBC by down-regulating the PI3K/Akt signal pathway. Nevertheless, since decreased *p*-Ser473-Akt protein levels, caused by lipophilic root barks extract, were not influenced by variations in Akt protein expression, further investigation is essential to reveal the modulating effect of root barks lipophilic extract on proteins downstream of the PI3K/AKT/mTOR pathway.

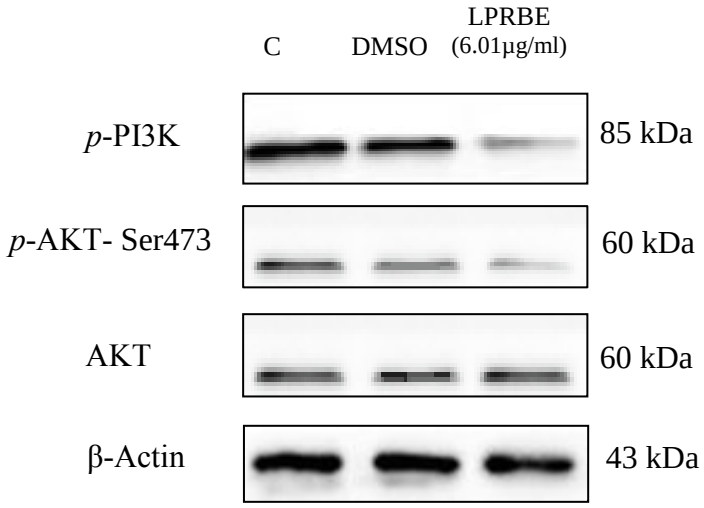

Figure 5: Western blot analysis of total Akt, phospho-Ser-473-Akt, phosphor- PI3K, and β-actin protein expressions in MDA-MB-231 cells after 48 h-treatment with 6. 01 µg/mL of *Z. lotus* root barks lipophilic extract. The blots shown are representative of three independent experiments. Abbreviation: C, Controle; LPRBE, root barks lipophilic extract.

4. Conclusions

The study contributes to enrich the literature data on the pharmacological proprieties of four morphological parts of wild *Z. lotus*. Lipophilic and phenolic-rich extracts of this shrub species were investigated for their antioxidant, anti-tumor, and antibacterial activities.

The antioxidant properties differed significantly among the four parts selected shrub extracts (root barks, leaves, pulp, and seeds). Among these fractions, phenolic-rich extracts of leaves and root barks showed very strong scavenging and ferric reducing activities. The study has also demonstrated a moderate antioxidant activity of pulp and seeds extracts of *Z. lotus*. A significant correlation between antioxidant properties and total phenolic content determined by UHPLC-UV-MS^n was found, indicating that phenolic compounds are the major contributor to the antioxidant properties of these plant extracts. This investigation further supports the view that some plants are promising sources of natural antioxidants.

The results suggested also that *Z. lotus* lipophilic extracts of leaves and seeds may have the potential for the development of anti-*S. epidermidis* and leaves of anti-*E. coli* therapeutics. Moreover, it was also evidenced that root barks could probably be part of an antibacterial formulation against MRSA. The results also reflected that bacterial strains were more resistant towards the pulp lipophilic and phenolic-rich extracts, compared to other fractions, probably due to their low concentration of antibacterial bioactive compounds. The antibacterial activities of pure phenolic compounds from this shrub species have not been investigated yet and therefore might represent an interesting research topic.

About anti-tumor activity, the present study indicated that *Z. lotus* was highly effective against MDA-MB-231, MCF-7, and HepG2 cell lines. *Z. lotus* root barks lipophilic extract and pure betA, representative of the main identified extract compound, inhibited strongly the growth of MDA-MB-231 cells (IC50 = 6.01 µg/mL and 22.67 µM, respectively) for 48h. Additionally, root barks lipophilic extract arrest the MDA-MB-231 cell migration, inducing

apoptosis, and caused G2 cell cycle arrest. The treatment of MDA-MB-231 cells with root barks lipophilic extract affected the PI3K/Akt pathway. A deeper analysis would be necessary to know the components of root barks lipophilic extract implicated in the inhibitory action upon TNBC MDA-MB-231 cellular viability.

Taken all together, the present findings provide a scientific basis to promote the value-adding of wild *Z. lotus* as a safe source of promising antioxidant, antibacterial, and anti-tumor agents.

5. References

(1) Naili, M. B.; Alghazeer, R. O.; Saleh, N. A.; Al-Najjar, A. Y. Arab. J. Chem. **2010**, 3 (2), 79–84.
(2) Aye, M. M.; Aung, H. T.; Sein, M. M.; Armijos, C. Molecules **2019**, 24 (2), 293. https://doi.org/10.3390/molecules24020293.
(3) Tlili, H.; Hanen, N.; Arfa, A. Ben; Neffati, M.; Boubakri, A.; Buonocore, D.; Dossena, M.; Verri, M.; Doria, E. PLoS One **2019**, 14 (9), 1–18.
(4) Abdoul-Azize, S.; Bendahmane, M.; Hichami, A.; Dramane, G.; Simonin, A. M.; Benammar, C.; Sadou, H.; Akpona, S.; El Boustani, E. S.; Khan, N. A. Int. Immunopharmacol. **2013**, 15 (2), 364–371.
(5) Li, J.; Guo, W. J.; Yang, Q. Y. World J. Gastroenterol. **2002**, 8 (3), 493–495.
(6) Sogno, I.; Vannini, N.; Lorusso, G.; Cammarota, R.; Noonan, D. M.; Generoso, L.; Sporn, M. B.; Albini, A. In: Senn, H.J., Kapp, U., Otto, F. (Eds.), 5th International Cancer Prevention Conference. St Gallen, Switzerland; 2009; pp 209–212. h
(7) Tolstikova, T. G.; Sorokina, I. V.; Tolstikov, G. A.; Tolstikov, A. G.; Flekhter, O. B. Russ. J. Bioorganic Chem. **2006**, 32 (1), 37–49.
(8) Borgi, W.; Ghedira, K.; Chouchane, N. Fitoterapia **2007**, 78 (1), 16–19.
(9) Benammar, C.; Baghdad, C. J. Nutr. Food Sci. **2014**, s8, 8–13.
(10) Borgi, W.; Recio, M. C.; Ríos, J. L.; Chouchane, N. South African J. Bot. **2008**, 74 (2), 320–324.
(11) Borgi, W.; Chouchane, N. J. Ethnopharmacol. **2009**, 126 (3), 571–573.
(12) Bakhtaoui, F. Z.; Lakmichi, H.; Megraud, F.; Chait, A.; Gadhi, C. E. A. J. Appl. Pharm. Sci. **2014**, 4 (10), 81–87.
(13) Wahida, B.; Abderrahman, B.; Nabil, C. J. Ethnopharmacol. **2007**, 112 (2), 228–231.
(14) Benammar, C.; Hichami, A.; Yessoufou, A.; Simonin, A. M.; Belarbi, M.; Allali, H.; Khan, N. A. BMC Complement. Altern. Med. **2010**, 10 (54), 1–9.
(15) Ghedira, K.; Chemli, R.; Richard, B.; Nwllard, J.; Men-olivier, L. L. E. **1993**, 32 (6), 1591–1594.
(16) Ghedira, K.; Chemli, R.; Caron, C.; Nuzilard, J. M.; Zeches, M.; Le Men-Olivier, L. Phytochemistry **1995**, 38 (3), 767–772.
(17) Le Crouéour, G.; Thépenier, P.; Richard, B.; Petermann, C.; Ghédira, K.; Zèches-Hanrot, M. Fitoterapia **2002**, 73 (1), 63–68.
(18) Renault, J.; Ghedira, K.; Thepenier, P.; Lavaud, C.; Zeches-hanrot, M.; Men-olivier, L. L. E. Phytochemistry **1997**, 44 (7), 1321–1327.
(19) Maciuk, A.; Lavaud, C.; Thépenier, P.; Jacquier, M. J.; Ghédira, K.; Zèches-Hanrot, M. J. Nat. Prod. **2004**, 67 (10), 1639–1643.
(20) Marmouzi, I.; Kharbach, M.; El, M.; Bouyahya, A.; Cherrah, Y.; Bouklouze, A.; Vander, Y.; El, M.; Faouzi, A. Ind. Crop. Prod. **2019**, 132, 134–139. (21) Rached, W.; Barros, L.; Ziani, B. E. C.; Bennaceur, M.; Calhelha, R. C.; Heleno, S. A.; Alves, M. J.; Marouf, A.; Ferreira, I. C. F. R. Food Funct. **2019**, 10 (9), 5898–5909.

(22) Hsu, C. L.; Yen, G. C. Elsevier Inc., **2014**; Vol. 36.
(23) Zhang, W.; Men, X.; Lei, P. J. Cancer Res. Ther. **2014**, 10 (5), 14.
(24) Chouaibi, M.; Mahfoudhi, N.; Rezig, L.; Donsì, F.; Ferrari, G.; Hamdi, S. J. Sci. Food Agric. **2012**, 92 (6), 1171–1177.
(25) Ghazghazi, H.; Aouadhi, C.; Riahi, L.; Maaroufi, A.; Hasnaoui, B. Nat. Prod. Res. **2014**, 28 (14), 1106–1110.
(26) Abdeddaim, M.; Lombarkia, O.; Bacha, A.; Fahloul, D.; Abdeddaim, D.; Farhat, R.; Saadoudi, M.; Noui, Y.; Lekbir, A. Ann. Food Sci. Techgnology **2014**, 15 (1), 75–81.
(27) Elaloui, M.; Laamouri, A.; Albouchi, A.; Cerny, M.; Mathieu, C.; Vilarem, G.; Hasnaoui, B. Emirates J. Food Agric. **2014**, 26 (7), 602–608.
(28) El Aloui, M.; Mguis, K.; Laamouri, A.; Albouchi, A.; Cerny, M.; Mathieu, C.; Vilarem, G.; Hasnaoui, B. Acta Bot. Gall. **2012**, 159 (1), 25–31.
(29) Santos, S. A. O.; Vilela, C.; Freire, C. S. R.; Neto, C. P.; Silvestre, A. J. D. J. Chromatogr. B **2013**, 938, 65–74.
(30) Roberta, Re.; Nicoletta, P.; Anna, P.; Ananth, P.; Min, Yang, C. R.-E. Free Radic. Biol. Med. **1999**, 26, 1231–1237.
(31) Thaipong, K.; Boonprakob, U.; Crosby, K.; Cisneros-zevallos, L.; Hawkins, D. J. food Compos. Anal. **2006**, 19, 669–675.
(32) Clinical and Laboratory Standards Institute. M07: Methods for Dilution Antimicrobial Susceptibility Tests for Bacteria That Grow Aerobically, 11th Edition; **2018**.
(33) Sarker, S. D.; Nahar, L.; Kumarasamy, Y. METHODs **2007**, 42, 321–324.
(34) Mosmann, T. J. Immunol. Methods **1983**, 65, 55–63.
(35) Lowry, O. H.; Rosebrough, N. J.; Farr, A. L.; Randall, R. J. J. Biol. Chem **1951**, 193 (1), 265–275.
(36) Stéphanie, D.; Xavier, V.; Philippe, C.; Marion, Woillez.; Jean-michel merillon. J. Agric. Food Chem **2009**, 57, 1768–1774.
(37) Bouaziz, M.; Dhouib, A.; Loukil, S. African J. Biotechnol. **2009**, 8 (24), 7017–7027.
(38) Boulanouar, B.; Abdelaziz, G.; Aazza, S.; Gago, C.; Miguel, M. G. Ind. Crops Prod. **2013**, 46, 85–96.
(39) Ghalem, M.; Merghache, S.; Belarbi, M. Pharmacogn. J. **2014**, 6 (4), 32–42.
(40) Kumar, S.; Pandey, A. K. Sci. World J. **2013**, 1–16..
(41) Dueñas, M.; Mingo-Chornet, H.; Pérez-Alonso, J. J.; Paola-Naranjo, R. Di; González-Paramás, A. M.; Santos-Buelga, C. Eur Food Res Technol **2008**, 227, 1069–1076.
(42) Zielinski, A. A. F.; Haminiuk, C. W. I.; Alberti, A.; Nogueira, A.; Demiate, I. M.; Granato, D. Food Res. Int. **2014**, 60, 246–254.
(43) Prothmann, J.; Sun, M.; Spégel, P.; Sandahl, M.; Turner, C.; Scheuba, J.; Wronski, V. K.; Rollinger, J. M.; Grienke, U.; Santos-Buelga, C. J. Agric. Food Chem. **2017**, 53 (6), 1713.
(44) Rice-Evans, C. A.; Miller, N. J.; Paganga, G. Free Radic. Biol. Med. **1996**, 20 (7), 933–956.
(45) Hopia, A.; Heinonen, M. J. Am. Oil Chem. Soc. **1999**, 76 (1), 139–144.
(46) Barzegar, A. Mol. Biol. Res. Commun. **2016**, 5 (2), 87–95.
(47) Li, X.; Tian, Y.; Wang, T.; Lin, Q.; Feng, X.; Jiang, Q.; Liu, Y.; Chen, D. Molecules **2017**, 22 (7).
(48) Kozłowska, M.; Gruczyńska, E.; Ścibisz, I.; Rudzińska, M. Food Chem. **2016**, 213, 450–456.
(49) Brito, S. M. O.; Coutinho, H. D. M.; Talvani, A.; Coronel, C.; Barbosa, A. G. R.; Vega, C.; Figueredo, F. G.; Tintino, S. R.; Lima, L. F.; Boligon, A. A. Food Chem. **2015**, 186, 185–191.
(50) Floegel, A.; Kim, D. O.; Chung, S. J.; Koo, S. I.; Chun, O. K. J. Food Compos. Anal.

2011, 24 (7), 1043–1048.
(51) Kim, D. O.; Lee, K. W.; Lee, H. J.; Lee, C. Y. J. Agric. Food Chem. **2002**, 50 (13), 3713–3717.
(52) Pulido, R.; Bravo, L.; Saura-calixto, F. J. Agric. Food Chem **2000**, 48 (8), 3396–3402.
(53) Vasco, C.; Ruales, J.; Kamal-eldin, A. Food Chem. **2008**, 111 (4), 816–823.
(54) Kowalczyk, D.; Micha, Ś.; Cichocka, J.; Gawlik-dziki, U. J. Inst. Brew. Distill. **2013**, No. April, 103–110.
(55) Cowan, M. M. Plant Products as Antimicrobial Agents. Clin. Microbiol. Rev. **1999**, 12 (4), 564–582.
(56) Al-mariri, A.; Safi, M.; Allium, L.; Houtt, M. Iran J Med Sci **2014**, 39 (1), 36–43.
(57) Ji, C.; Yoo, J.; Lee, T.; Cho, H.; Kim, Y.; Kim, W. FEBS Lett. **2005**, 579, 5157–5162.
(58) Grecka, P.; Giamarellon, H. J. Antimicrob. Chemother. **1995**, 36, 327–334.
(59) Ji-Young Lee, Yong-Suk Kim, and D.-H. S. J. Agric. Food Chem. **2002**, 50, 2193–2199.
(60) Jacqueline, Q.; Andrade, C.; Morais-braga, M. F. B.; Guedes, G. M. M.; Tintino, S. R.; Freitas, M. A.; Menezes, I. R. A.; Coutinho, H. D. M. Biomed. Pharmacother. **2014**, 68 (8), 1065–1069.
(61) Inoue, Y.; Hada, T.; Shiraishi, A.; Hirose, K.; Hamashima, H.; Kobayashi, S. Biphasic Antimicrob. Agents Chemother. **2005**, 49 (5), 1770–1774.
(62) Boual, Z.; Kemassi, A.; Chouana, T.; Michaud, P.; Didi, M.; El, O.; Material, A. P. **2015**, 9 (12), 1194–1197.
(63) Ouerghemmi, I.; Rebey, I. B.; Rahali, F. Z.; Bourgou, S.; Pistelli, L.; Ksouri, R.; Marzouk, B.; Tounsi, M. S. J. Food Drug Anal. **2016**, No. June, 1–10.
(64) Bouarab-chibane, L.; Forquet, V.; Lantéri, P.; Clément, Y. Front. Microbioloy **2019**, 10 (829).
(65) Rasheda, K.; Ciric, A.; Glamoclija, J.; Sokovi, M. Ind. Crops Prod. **2014**, 59, 210–215.
(66) Qin, F.; Yao, L.; Lu, C.; Li, C.; Zhou, Y.; Su, C.; Chen, B.; Shen, Y. Food Chem. Toxicol. **2019**, 129, 354–364.
(67) Farhadi, F.; Khameneh, B.; Iranshahi, M.; Iranshahy, M. Phyther. Res. **2019**, 33 (1), 13–40.
(68) Borrás-Linares, I.; Fernández-Arroyo, S.; Arráez-Roman, D.; Palmeros-Suárez, P. A.; Del Val-Díaz, R.; Andrade-Gonzáles, I.; Fernández-Gutiérrez, A.; Gómez-Leyva, J. F.; Segura-Carretero, A. Ind. Crops Prod. **2015**, 69, 385?394-394.
(69) Del Valle, P.; García-Armesto, M. R.; de Arriaga, D.; González-Donquiles, C.; Rodríquez-Fernández, P.; Rúa, J. Food Control **2016**, 61, 213–220.
(70) Juneja, V. K.; Dwivedi, H. P.; Sofos, J. N. Microbial Control and Food Preservation Theory and Practice; **2018**.
(71) Righi, N.; Boumerfeg, S.; Fernandes, P. A. R.; Deghima, A.; Baali, F.; Coelho, E.; Cardoso, S. M.; Coimbra, M. A.; Baghiani, A. TFood Res. Int. **2020**.
(72) Monagas, M.; Urpi-sarda, M.; Fernando, S. food **2010**, 1 (3), 233–253.
(73) Yamada, H.; Ohashi, K.; Atsumi, T.; Okabe, H.; Shimizu, T.; Nishio, S.; Li, X. D.; Kosuge, K.; Watanabe, H.; Hara, Y. J. Hosp. Infect. **2003**, 53 (3), 229–231.
(74) Guerra, A.; Soares, B.; Guerreiro, O.; Ramos, P.; Oliveira, H.; Silvestre, A.; Freire, C.; Duarte, M. F. Planta Med. **2014**, 80 (16), SL41.
(75) Soumaya Souid, Heba E. Elsayed, Hassan Y. Ebrahim, Mohamed M. Mohyeldin, Abu Bakar Siddique, Habib Karouia, Khalid A. El Sayed, and K. E.-B. Mol. Carcinog. **2018**, 57 (11), 1507–1524.
(76) Sousa, J. L. C.; Freire, C. S. R.; Silvestre, A. J. D.; Silva, A. M. S. Molecules. **2019**, 24 (2), 1–35.
(77) Weber, D.; Zhang, M.; Zhuang, P.; Zhang, Y.; Wheat, J.; Currie, G.; Al-eisawi, Z.

SAGE Open Med. **2014**, 3–12.
(78) Santos, R. C.; Salvador, J. A. R.; Cortés, R.; Pachón, G.; Marín, S.; Cascante, M. Biochimie. **2011**, 93 (6), 1065–1075.
(79) Richard Simo Tagne , Bruno Phelix Telefo, Emmanuel Talla , Jean Noel Nyemb, Sylvain Nguedia Njina , Mudassir Asrar, F. M.; Kamdje, A. H. N.; Paul Fewou Moundipa , Ahsana Dar Farooq, M. I. C. Asian Pacific J. Trop. Dis. **2015**, 5 (4), 307–312.
(80) Lambertini, E.; Lampronti, I.; Penolazzi, L.; Tareq, M.; Khan, H.; Ather, A.; Giorgi, G.; Gambari, R.; Piva, R. Oncol. Res. **2017**, 14, 69–79.
(81) Oprean, C.; Zambori, C.; Borcan, F.; Soica, C.; Zupko, I.; Minorics, R.; Bojin, F.; Ambrus, R.; Muntean, D.; Danciu, C. Pharm. Biol. **2016**, 54 (11), 2714–2722. https://doi.org/10.1080/13880209.2016.1180538.
(82) Jiang, L.; Zhao, X.; Xu, J.; Li, C.; Yu, Y.; Wang, W.; Zhu, L. J. Oncol. **2019**, 1–11.
(83) Barber, M. D.; Fearon, K. C. H.; Tisdale, M. J.; Mcmillan, D. C.; Ross, A.; Ross, J. A. Nutr. Cancer. **2009**, 40 (2), 157–164.
(84) Awad, A. B.; Fink, C. S. J. Nutr. **2000**, 130 (9), 2127–2130.
(85) Zaheer, S.; Shah, N.; Maqbool, S. A.; Soomro, N. M. BMC Public Health. **2019**, 19 (1), 1–9.
(86) Phaniendra, A.; Jestadi, D. B.; Periyasamy, L. Indian J. Clin. Biochem. **2015**, 30 (1), 11–26.
(87) Borri, F.; Granaglia, A. Cancer Biol. **2020**.
(88) Zadeh, A.; Alsabi, Q.; Ramirez-vick, J. E.; Nosoudi, N. Expert Syst. Appl. **2020**, 113253.
(89) Castrellon, A. B. Hematol. Oncol. Stem Cell Ther. **2017**, 4–7.
(90) Lehmann, B. D.; Jovanovi, B.; Chen, X.; Estrada, M. V; Johnson, N.; Shyr, Y.; Moses, H. L.; Sanders, M. E.; Pietenpol, J. A. PLoS One **2016**, 1–22.
(91) Chang-qing, Y.; Jie, L.; Shi-qi, Z.; Kun, Z.; Zi-qian, G.; Ran, X. Prog. Biophys. Mol. Biol. **2019**.
(92) Al-Mahmood, S.; Sapiezynski, J.; Garbuzenko, O. B.; Minko, T. Transl. Res. **2018**, 8 (5), 1483–1507.
(93) Zhang, Q.; Bao, J.; Yang, J. Arch. Med. Sci. **2019**, 15 (4), 1001–1009.
(94) Ediriweera, M. K.; Moon, J. Y.; Nguyen, Y. T.-K.; Cho, S. K. Molecules **2020**, 25 (14), 3164.

Part C

Synthesis and characterization of new alizarin derivatives

Chapter VI

Rubia tinctorum: Synthesis, characterization and computational studies of new alizarin derivatives

Abstract

Rubia tinctorum L. (Rubiaceae) is a perennial herbaceous climbing plant known to have several anthraquinones, mainly in the roots which are used as natural food colorants and as natural hair dyes. Alizarin (1,2-dihydroxyanthraquinone) is the main anthraquinone found in this plant species. It is used not only as a dye but as well for the synthesis of various active derivatives which have shown several chemical and pharmaceutical properties. The present work aims to extract and purify alizarin from *R. tinctorum*, and its scaffold was used as a platform to synthesis a new series of functional compounds. The syntheses of new alizarin derivatives, differing in the position of substitution on the pyridine ring, are described. The structures of these compounds were determined by ^{1}H and ^{13}C NMR, and IR spectroscopy. A detailed DFT study based on B3LYP/6-311G+ (d, p) of geometrical structures and electronic properties of alizarin drivatives was performed. The study was extended to the HOMO-LUMO analysis to calculate the energy gap (Δ), Ionization potential (I), Electron Affinity (A), Global Hardness (η), Chemical Potential (μ), and Global Electrophilicity (ω). All isomers can be considered as promising ligands for use as catalysis, material, or/and as a pharmaceutical agent.

1. Introduction

The overall aim of this chapter was to use the scarfford of alizarin to synthesis new active derivatives. The objectives to achieve this aim were to undertake a study on *Rubia tinctorum*, which could help to successfully isolate the 1,2-dihydroxyanthraquinone (alizarin) molecule from its dried roots.

1.1 Generality about *Rubia tinctorum*

1.1.1 Origin and Botany

Rubiaceae is a family of flowering plants, variously called the coffee family, madder family, or bedstraw family. Its name takes from the madder genus Rubia, which derives from the Latin word ruber, meaning "red". Rubia, as a name for madder was coined by the naturalist philosopher Pliny.[1] It comprises about 70 species distributed in Europe, Africa, and Asia, with two species in Morocco, namely *Rubia tinctorum* and *Rubia peregrine*.[2,3] Common madder *Rubia tinctorum* (*Tinctorum* is derived from the Latin word for dyeing) is one of the most important species belonging to this family,[4] which was cultivated as a source of dyestuff since ancient time in central Asia and Egypt, where it was grown as early as 1500bc. Cloth dyed with madder root pigment was found in the tomb of the Pharaoh Tutankhamun, in the ruins of Pompeii, and ancient Corinth. In the Middle Ages, Charlemagne encouraged madder cultivation.[4] Therefore, the Romans used in medicine as in diuretics, and they called it Rubia passiva.[5]

The botanical description of Rubia *tinctorum* (Linn.) is as follows:

Kingdom	Plantae-Plants
Subkingdom	Tracheophytes-vascular plants
Division	Spermaphytes-seed plants, roots and vessels
Superdivision	Angiosperms
Class	Dicotyledoneae
Subclass	Sympetalae
Order	Rubiales
Family	Rubiaceae
Genus	Rubia
Species	*Rubia tinctorum*

1.1.2 Morphological characterization

Rubia tinctorum is a perennial climbing plant that reproduces fresh aerial parts every year employing its rhizomes. This plant may also be reproduced by seeds, which are produced by the bisexual flowers usually in cymose inflorescences. Stems are lying or climbing up to 1.5 m, long and fitted on the corners with hooked spines.[5] The leaves are fairly large, lanceolate, annual, thin, and deciduous, with thin edges and a network of secondary veins very prominent below (Fig 1, pic A). Apparently whorled, with small prickles at the edges and on the main rib which allow the plant to support itself by leaning on the other plants.[5,6] The flower-shoots spring from the joints in pairs, the loose spikes of yellow, starry flowers blooming only in the second or third year, in June-July. Each flower includes a 4–5 lobed calyx, generally a 4–5 lobed corolla, 4 or 5 stamens and two carpels (Fig 2, pic B).[7] The fruit is a fleshy berry the size of a pea, black at maturity (Fig 1, pic E). The roots part are covered with a black-ish rind, beneath which the color is reddish, and the pith is pale yellow (Fig 1, pic D_1-D_2). These underground parts are wealthy in anthraquinones.[4,5,7]

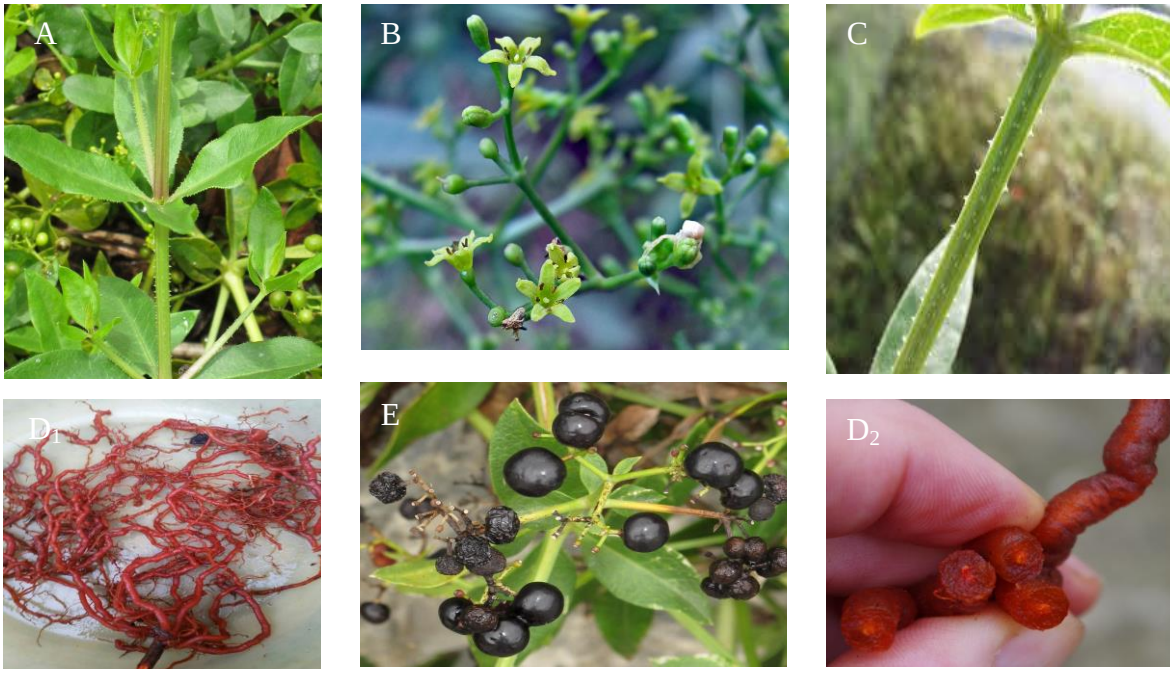

Figure 1: different morphological part of *Rubia tinctorum*.

1.1.3 Geographical distribution

Rubia tinctorum is native in Southern and Southeast Europe, in the Mediterranean area including Morocco, in Asia Minor, and in the Caucasus, which produces a red dye from its roots.[4,8] Nowadays the plant also grows in China and Japan, up to the Malaysian Archipelago, in the Western part of North America, in Mexico and South America. In earlier days madder was cultivated in Central and Western Europe. Nowadays most of the plant is found in the wild, except in the Netherlands where cultivated in the province of Groningen for its roots.[8] *Rubia tinctorum* is a plant that grows on very rich moist and deep soils, but its root is only extractable when the soil also has the characteristic of being very light. It is also growing on limestone soils, hedges, bushes, and roadsides.[9]

1.1.4 Traditional use of *Rubia tinctorum*

R. tinctorum roots are known as a traditional herbal medicine used for the treatment of kidney and bladder stones mainly, those consisting of calcium oxalate and calcium phosphate in the urinary tract.[10] The plant has been used as a laxative mixture and as a mild sedative. Madder root has reportedly also been used medicinally for menstrual and urinary disorders.[11] The Greek physicians have been used this plant as a diuretic and for treatment of jaundice, sciatica, and paralysis. In Europe, the plant was used for the treatment of rheumatic disorders. In the traditional medical texts of Iran, Makhzan-ol-advieh and Tohfat-ol-momenin, the plant was recommended for the treatment of inflammatory disorders.[12] People from many parts of Serbia and other Balkan countries used this plant for the treatment of bladder infections.[13] In the Middle Atlas, the infusion of madder flowers is used as an aphrodisiac. In some cases the madder mixed with Maghreb curry, olive oil, and barley flour to make bread that has fortifying and aphrodisiac properties.[14]

1.2 Chemical composition of *Rubia tinctorum*

The aboveground and underground parts of *R. tinctorum* are rich in anthracene quinone derivatives, mainly anthraquinones.[5] Benzoquinones and naphthoquinones are also part of this group. Anthraquinones are found in a wide range of species, especially in the families Rubiaceae, Polygonaceae, and Rhamnaceae, and they constitute the largest group of natural pigments, with approximately 700 compounds described. About 200 of these compounds were isolated from plants, while the rest were isolated from lichens and fungi. About 90% of these compounds are derived from 9,10-anthracenedione with several hydroxy and other functional groups.[15,16] Glycosylated anthraquinones are also present in the plant, for instance in rhizomes to favor their accumulation and storage in the plant but they are converted into aglycone anthraquinones by β-glucosidases or oxidative processes.[16]

1.2.1 Generality on anthraquinones

Anthraquinones are a group of secondary metabolites structurally constructed from an anthracene ring with carbonyl groups at positions 9 and 10 and their glycosides.[17] Anthrones and their tautomeric form; anthranol, are reduced forms of anthracene derivatives.[5,18]

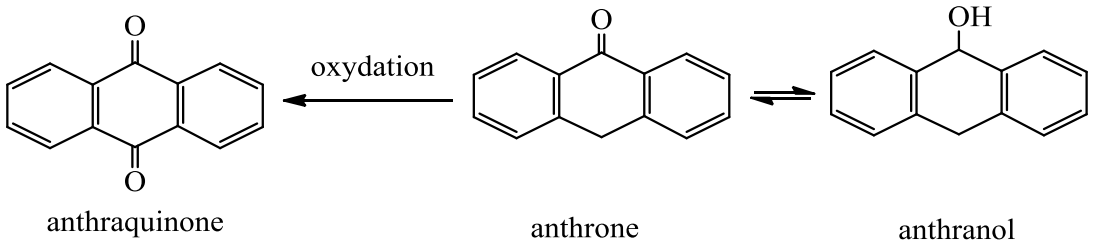

Figure 2: Interconversion of the anthrone with its tautomeric forms.

In most anthraquinones, hydroxyl groups are normally found at positions C-1 and C-8. Only C-3 and C-6 carbon may also be substituted: methyl, hydroxymethyl, or carboxyl group at C-3, and phenolic or methyl group at C-6. Anthrones and anthraquinone are found in plants mainly as O-glycosides or rarely C-glycosides at the C-8 or C-6 hydroxyl groups or as C-glycosides at the C-10 position.[18]

1.2.2 Biosynthesis

Plants and their derived cell and tissue cultures in the family Rubiaceae accumulate several anthraquinones. Despite the numerous medicinal qualities of anthraquinone, very few of its biosynthetic pathways have been elucidated so far including polyketide or shikimate pathway.[19,15] The polyketide pathway (1), which provides polyketide anthraquinones with two rings hydroxylated by cyclization of the intermediate chain of octa-β-ketoacyl-CoA, produced by the addition of an acetyl-CoA to three malonyl-CoA units (Schemes 1). These types of AQs often exhibit a characteristic substitution pattern, i.e. they are substituted in both ring A and C of AQ structure. Anthraquinones (tricyclic aromatic ketones) such as emodin (Schemes 3) and chrysophanol are typical candidates for biosynthesis via the polyketide pathway. Enzymes responsible for polyketide biosynthesis have been well documented in bacteria but detected only rarely in higher plants.

Schemes 1:

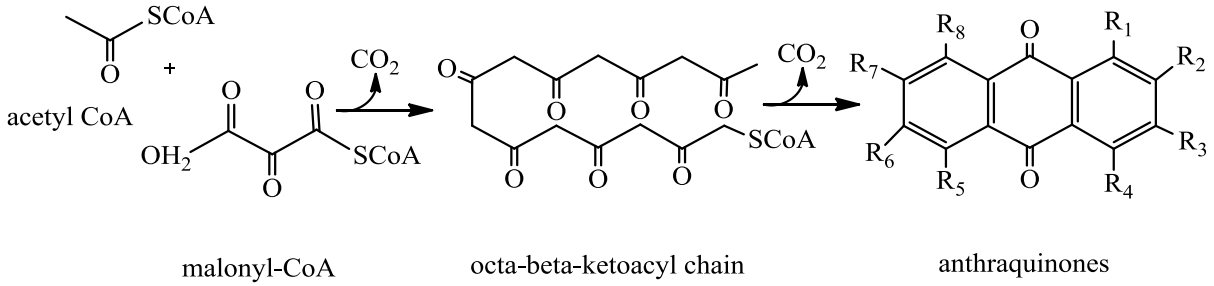

The shikimate or chorismate/o-succinylbenzoic acid pathway (2), which occurs by the addition of succinoyl benzoic acid, formed from shikimic acid and α-ketoglutaric acid to mevalonic acid. This pathway is used to produce anthraquinones with only one hydroxylated ring, such as 1,2-dihydroxylated anthraquinones (Schemes 2). Alizarin (1,2-dihydroxy-9,10-anthraquinone) an example of anthraquinone produced by the shikimate pathway (Schemes 3). The enzymes necessary for the formation of polyketides are the so-called polyketide synthases.

Schemes 2:

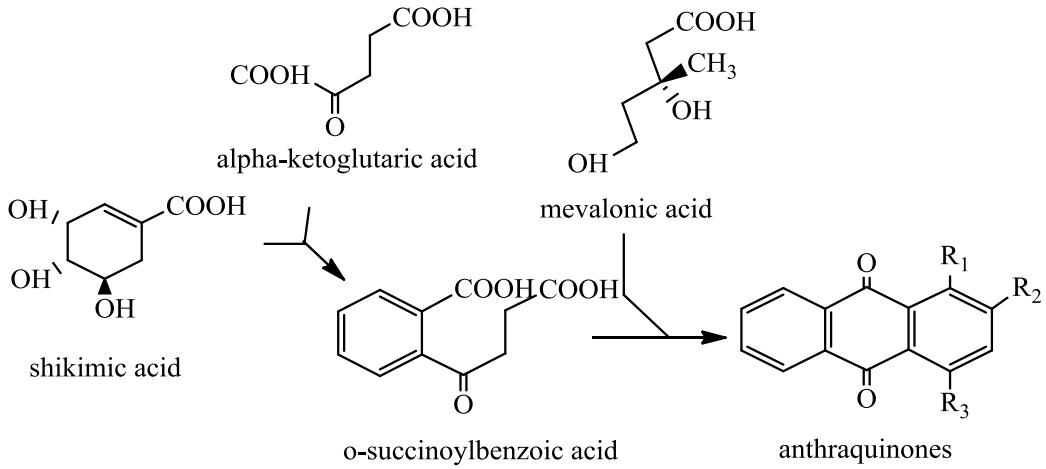

Schemes 3:

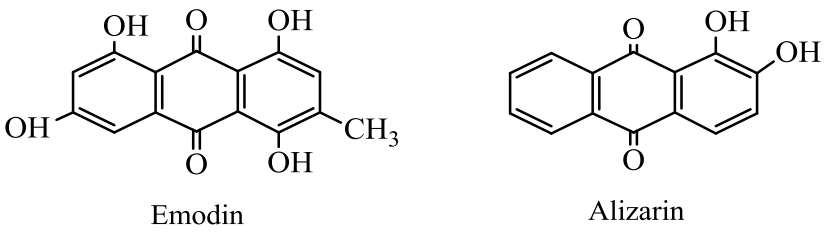

1.2.3 Extraction, purification and characterization of anthraquinones

Extraction is the first step in obtaining a phytoconstituent from a plant and, in this context, the choice of solvent is of prime importance to obtain a good yield (Chapter II). The anthraquinones can be isolated by sequential extraction with solvents of increasing polarity.[20] The different extract solutions can be further purified by a liquid-liquid partitioning step. As a first extraction step, a non-polar solvent can be used such as ether, benzene, chloroform,

dichloromethane, or ethyl acetate.[20,21] For free anthraquinones (deglycosylated or aglycones), less polar solvents are chosen, while for glycosylated anthraquinones, solvents with a higher polarity, such as methanol, ethanol, and water, are more appropriate.[15] The extraction can be performed at different temperatures with basic solutions such as sodium carbonate, sodium bicarbonate, or sodium hydroxide.[21] The techniques used for extraction are varied; however, maceration is the most used technique for the reduced forms, greater care must be taken in the extraction process to avoid their oxidation; the use of supercritical fluid is a good option in these cases.[22]

For isolation and purification of anthraquinones, chromatography techniques are usually used namely preparative thin-layer chromatography (PTLC), column chromatography, high-speed countercurrent chromatography (HSCCC), and flash chromatography.[22]

Recrystallization has also been used to purify the anthraquinones into a crystal by the physical transformation. The crystal is solid with an ordered internal arrangement of molecules, ions, or atoms.[23] Besides, The purified anthraquinones could be characterized by Mass spectrometry, UV–Visible (UV), Infrared spectroscopy (IR), and Nuclear Magnetic Resonance (NMR).[5,22]

1.2.4 Anthraquinones isolated from *Rubia tinctorum*

The main components of *R. tinctorum* are anthraquinones. Alizarin is the permanent red pigment in the plant *R. tinctorum* and the main anthraquinones interested in this work. In 1826 alizarin was the first isolated anthraquinones from *R. tinctorum* by Colin and Robiquet.[24] Subsequently, several other anthraquinones were isolated from *R. tinctorum*, namely purpurin, munjistin, rubiadin, pseudopurpurin, nordamnacanthal, lucidin, xanthopurpurin, and anthragallol.[25] The anthraquinones are also present as glycoside forms in *R. tinctorum*.[26] The main glycosylated anthraquinones accumulated in the roots is ruberythric acid (alizarin 2-β-D-primeveroside) that was isolated in crystalline form by Rochleder in 1851.[27] Nevertheless, lucidine 3-β-D-primeveroside, rubiadin (3-O-β-D-primrose), and galiosin (1-O-β-D-primveroside of pseudopurpurine) have also been identified in *R. tinctorum* roots.[28]

1.2.5 Pharmacological and technological applications of anthraquinones

Anthraquinones are attracting much attention due to their traditional, phytochemical, and pharmacological activities.[28] Besides to their known use as natural dyes, several biological activities have been described in the literature for these compounds, such as anticancer, anti-inflammatory, anti-arthritic, diuretic, phytoestrogen, anti-platelet, anti-fungal, anti-bacterial, anti-malarial, and antioxidant properties.[22,29] Anthraquinones, have laxative activity attributed to the presence of the hydroxyl group at the C-1 and C-8 positions of the anthraquinones ring.[30] Alizarin's main active anthraquinone of *R. tinctorum* has demonstrated several interesting biological properties that make it play an important role in recent research. Intensive investigations of its antioxidant activity indicate that it can be used as an osteotropic drug for the treatment of cancer cells, inhibitory effect on tumor cell growth, stimulation of cell proliferation as well as enhancement of malignant transformation.[31,32] Due to its ability to build complexes, alizarin can be used as a marker of stains for calcium deposits in tissues, and it can be applied in biochemical and clinical examinations.[31] Alizarin has been used for its chelating properties in the prevention of kidney stones.[33]

In addition to the numerous biological activities presented by anthraquinones, their applications in analytical chemistry are also notable, most often as strong chelating agents or as chromophores.[34] Anthraquinones have been used in photometry, fluorometry studies, redox reactions, and acid-base complexations.[15] Another interesting use of anthraquinones was achieved industrially. As pulping catalysts, they increase the yield of pulping processes by increasing the rate of delignification, and then performed in less time and at lower temperatures.[35] Anthraquinones also represent the second most important class of dyes, being behind the azo-dyes only for their lower tinctorial capacity and the greater difficulty of preparation. Anthraquinone dyes are composed of 9,10-anthraquinones that present electron-donor groups. According to the choice of these groups and the degree of substitution, a varied range of colors can be obtained.[36] This class of compounds is considered as a biopesticide with a high potential for use in nonlethal pest management and as an insecticide.[37]

1.3 Relevant chemical syntheses of Alizarin

Chemical modification of natural products is one of the most common approaches used in drug discovery, especially of anticancer agents.[38] Inserted in this class of compounds, alizarin was classified as an important chemical exponent of natural origin due to its ortho-dihydroxy structure.[32] There are many substituted alizarin that has been synthesized and studied for their pharmacological properties.[39] Among them a few are discussed in the following paragraphs.

A series of novel α-aminophosphonate derivatives containing an alizarin moiety was designed and synthesized as antitumor agents against several selected tumor cell lines (B, NCI-H460 (lung cancer cells), HepG 2 (liver cancer cell line), A549 (alveolar basal epithelial cancer cell line), MGC-803 (gastric cancer cell line), Hct-116 (colorectal cancer cell line), CNE (epithelioid cancer cell line), and Hela (Cervical cancer cell line)). The study showed that the target products could inhibit the proliferation of these selected tumor cell lines at moderate to high rates. Furthermore, compounds **1**, **2**, and **3** showed to induce apoptosis and involved G1 phase arrest by increasing the production of intracellular Ca^{2+} and reactive oxygen species (ROS) and affecting associated enzymes and genes in NCI-H460 cells.[39] Abbreviation: Nap, Naphthalene; F, Fluorine; Ph, α-amino-Phosphonate.

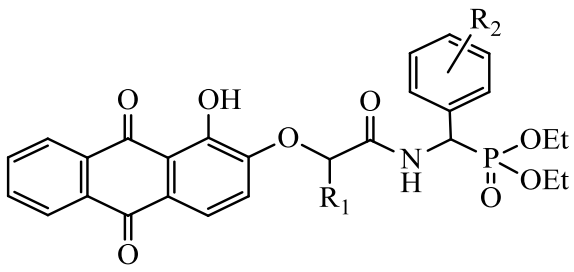

R_1= H R_2=4-Br
R_2=2-Br
R_2=2-OCH_3
R_2=4-OCH_3
R_2=3-OCH_3
R_2=2-F
R_2=4-F
R_2=2-Cl
R_2=Ph
R_2=3-CH_3
R_2=4-CH_3

R_1= CH_3 R_2=4-Br
R_2=2-Br
R_2=3-Cl
R_2=4-Cl
R_2=2-Cl
R_2=3-Cl
R_2=4-F
(1) R_2=2-F
R_2=3F
(2) R_2=2-OCH_3
R_2=3-OCH_3
R_2=4-OCH_3
R_2=Ph
(3) R_2=1-Nap
R_2=2-Nap
R_2=3-CH_3
R_2=4-CH_3

Other interesting anthraquinones derivatives were synthesis by Shizhen et al. (2013).[40] Two vanadium complexes with aromatic 1,2-dihydroxyanthra-quinone have been synthesized. Compound **4** showed specifically higher inhibition (88.65%) against HCT-8 (Ileocecal adenocarcinoma cell line) than the clinical anticancer drug 5-fluorouracil (5-FU, 69.97%).

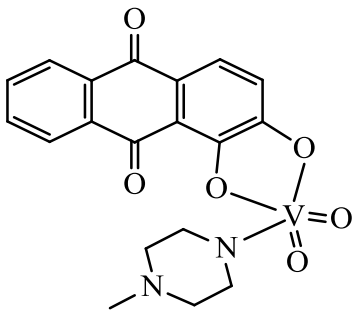

(4)

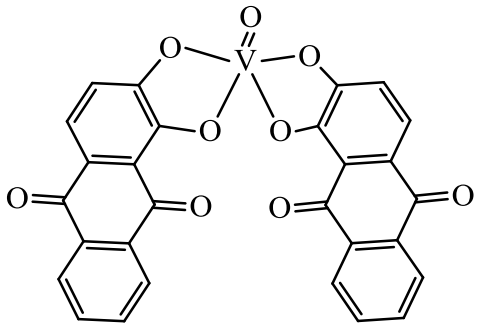

(5)

A series of novel hybrids of alizarin and diamide scaffold was synthesized by Guiyang Yao et al. (2014)[41] and tested in vitro against HepG-2, CNE, Hct-116, and MGC-803 cell lines. The results showed that all compounds exhibited a good inhibition effect with compounds **7b**, **7c**, **7d**, and **7e** demonstrated high cytotoxicity. Besides, their cytotoxicity was found to be better than alizarin. Particularly, compound **7c** revealed cytotoxic inhibition even better than 5-FU in nasopharyngeal carcinoma assay (CNE, IC50 = 9.08 μM). This compound derivative arrested cell cycle at the G1 phase, induced apoptosis and interacts with DNA.

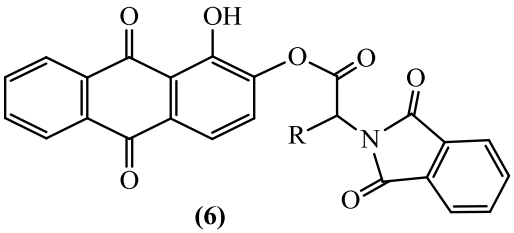

(6)

6b, 7b	$CH(CH_3)_2$		CH_3
6c, 7c	$CH(CH_3)CH_2CH_3$		CH_2Ph
6d, 7d	$CH_2CH(CH_3)_2$		CH_3
6e, 7e	CH_2CH_2SCH		CH_2Ph

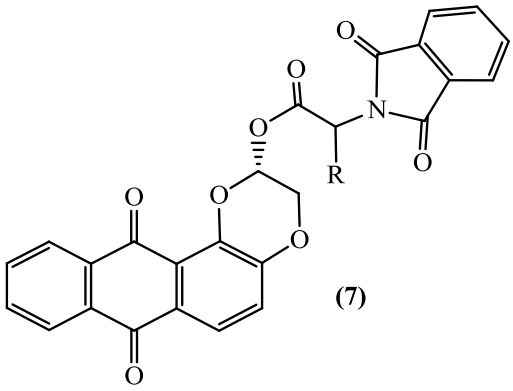

(7)

A series of novel alizarin and phosphoryl aminoacid scaffold were synthesized and their cytotoxic effect against MGC-803, HepG2, T24 (Urinary bladder cancer cell line), NCI-H460, and SK-OV-3 (Ovarian cancer cell line) cell lines was evaluated. All newly synthesized compounds exhibited relatively high cytotoxicity compared with alizarin and low cytotoxicity against the human normal liver cell line (HL-7702). Mainly, compound **9c** showed the best cytotoxicity against SK-OV-3 cells with IC50 = 7.09 μM by inducing cell apoptosis via regulation of Bcl-2 family members, activation of caspase-9 and caspase-3 as well as arresting cell cycle at the G2 phase.[42]

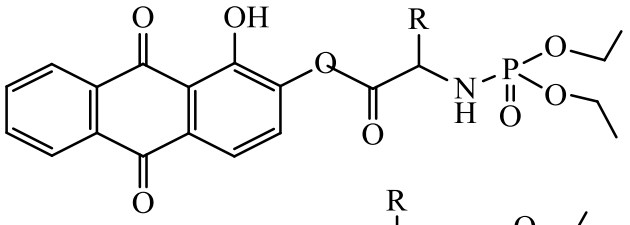

(8)

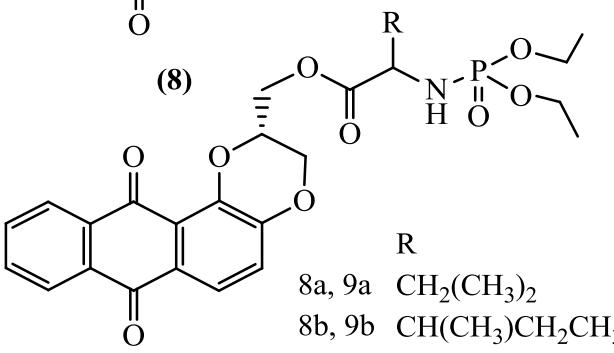

(9)

R	
8a, 9a	$CH_2(CH_3)_2$
8b, 9b	$CH(CH_3)CH_2CH_3$
8c, 9c	$CH_2CH_2CH(CH_3)_2$

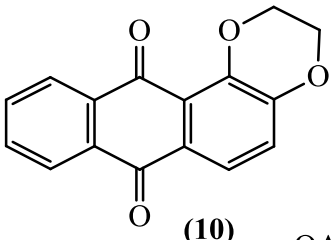

(10)

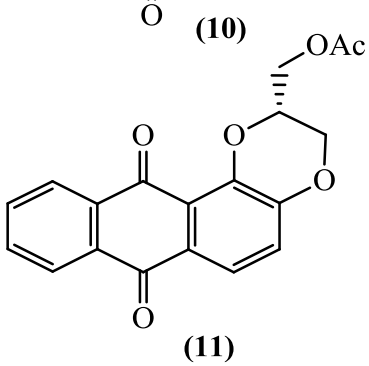

(11)

Eleven new 2-O-side-chain derivatives of alizarin were synthesized via esterification, substitution, hydrolysis, or elimination reactions. These new derivatives have different inhibiting activities against two tumor cells (HeLa and HCT-116), which may be associated with their DNA binding capacity. Compared with alizarin, most of the derivatives have significantly higher DNA binding affinity based on interaction with ct-DNA. In particular, compound **19** showed to exhibit the best cytotoxicity against HeLa cells with IC50 of 20 μM by inducing apoptosis cell death.[43]

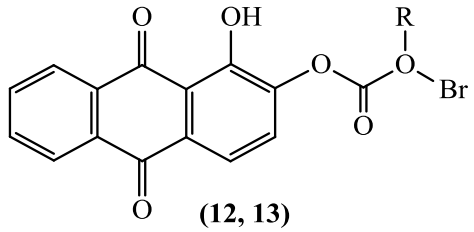

(12, 13)

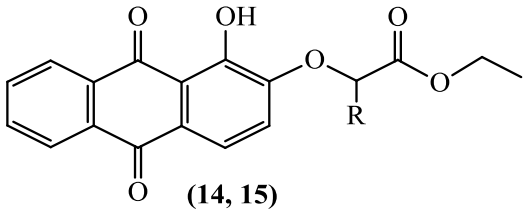

(14, 15)

12, 14, 16 R=H
13, 15, 17 R=CH_3
18 R=CH_2CH_2Br
19 R=$(CH_2)_3CH_2Br$
20 R=$(CH_2)_5CH_2Br$
21 R=$(CH_2)_7CH_2Br$
22 R=$(CH_2)_4CH{=}CH_2$

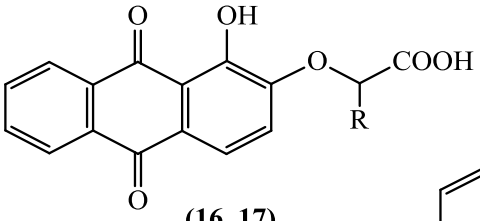

(16, 17)

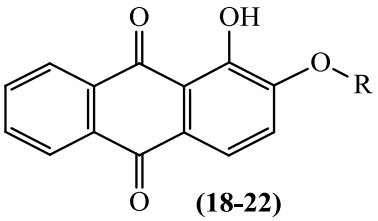

(18-22)

Seven alizarin derivatives were synthesized, and their antitumor activity was assessed against lymphocytic leukemia (P-388), epidermoid lewis lung carcinoma (LLC), sarcoma 37 (S-37), and cellosaurus sarcoma 180 (S-180) cell lines. All newly derivatives showed to exhibit antitumor activity with **25** was the most active compound concerning sarcoma S-180. Their effect was performed by forming heteroligand complexes with Ca-ATPase responsible for the active transport of calcium through cellular membranes, resulting in regulation on the tumor cell membranes.[44]

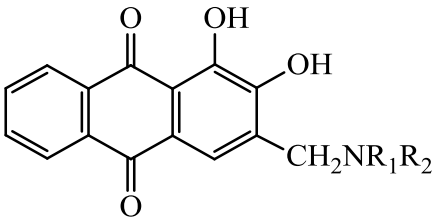

25
$R_1{=}R_2{=}CH_2CH_2OH$
$R_1{=}CH_3$ $R_2{=}CH_2CH_2OH$
$R_1{=}R_2{=}CH_2CH_2Cl$
$R_1{=}CH_3$ $R_2{=}CH_2CH_2Cl$
$R_1{=}R_2{=}$2-phthalimidoethyl
$R_1{=}R_2{=}CH_2CH_2NH_2$
$R_1{=}R_2{=}CH_2COOH$

Alizarin is also used as a chemicals platform to synthesize sustainable alternatives to current synthetic dyes by alkylation or esterification of hydroxyl groups.[45,46] Besides, several types of alizarin derivatives have also been reported as the chelating ligand.[40,47–50]

Considering the set activities of alizarin derivatives, it will be interesting to concentrate on synthesizing ligands with pyridine groups appended to an aromatic core of alizarin by ester linkers. This approach would open ways to use these derivatives in further syntheses as described by Kharlamova (2009),[51] and also as a ligand to prepare the transition metals complexes. The reaction of alizarin with a carbonyl chloride can form various compounds due to the presence of two hydroxyls group in alizarin. Thus two different mono and di-substituted compound could be synthesis; with mentioning that, the two hydroxyl groups have different reaction activities OH at position 2 is more reactive than OH at position 1.[52,43]

The addition of an organic molecule such as alizarin to pyridine is practically interesting for several reasons namely; the evaporation rates and toxicity will become low, along with the ability to biodegrade.[53] These properties make the complex useful for industrial or scientific applications such as catalysts, materials, and drugs. Alizarin pyridine derivatives may play a significant role in many biological systems since pyridine rings prevalent in natural systems and non-natural molecules with physiological activity.[54] Moreover, both alizarin and pyridine derivatives are known to possess an array of biological activities chiefly anticancer properties.[40,55] Pyridine derivatives were known to act as anticancer agents by inhibiting the activity of VEGFR-2 a vascular endothelial growth factor receptor, responsible to stimulate endothelial cell mitogenesis and cell migration.[55] Thus, anthraquinones exhibit anti-proliferative activity through interaction with DNA and inhibition of topoisomerase II activity.[56] A combination of the anti-proliferative and anti-migration agent may be used as a more aggressive form of therapy. Moreover, these ligands should have interesting optical properties since pyridine is a main electron-acceptor group, due to its great electron affinity.[57] Moreover, the combination of alizarin electron-donor and a pyridine electron-acceptor could give bipolar host materials.

Therefore, in this chapter, three alizarin derivatives para-, meta-, and ortho -substitution ligands were synthesized. To our knowledge, there is no previous study involving the incorporation of the pyridine moiety into alizarin. The molecular electrostatic potential (MEP), natural bond orbital (NBO), frontier molecular orbitals (FMOs) of the title compounds were also performed by the B3LYP/ method.

2. Materials and Methods

2.1 Chemicals and instruments

All chemicals used throughout the research were purchased from Aldrich, and used without further purification. THF was distilled over sodium (Na). Melting points were determined using an electrothermal melting point apparatus. NMR spectra were recorded at 298 K on Bruker AV300, Bruker AV400 or Bruker AV500 spectrometers in deuterated solvents and the residual solvent peak was used as the internal reference. Infrared spectra were recorded on PerkinElmer-Spectrum Two FT-IR Spectrometer UATR (4000-400 cm^{-1}). Mass spectrometry was recorded on micrOTOF II. All the chemical shifts (δ) are given in parts per million (ppm).

2.2 Preparation of *Rubia tinctorum* extracts

R. tinctorum roots were collected from the regions of Beni Mellal, Morocco (32°20′21.998″ N; 6°21′38.999″ W) in March of 2017. The roots were washed with running water, shade-dried (15 days) and milled into granulometry lower than 2 mm prior to extraction. The process of extraction was adapted from Akhtar et al. (2006)[58] with some modification. Adequate mass (15 g) of *R. tinctorum* roots is treated into 300 ml of ethanol and extracted in a Soxhlet apparatus for 6 hours. The solvent was evaporated until dryness under vacuum on rotavapor.

2.3 Crystallisation

Rubia tinctorum roots extract (1.12 g) was dissolved into 100 ml of glacial acetic acid using sonication. The mixture was then left in a freezer for 3 days. The resulting liquor was decanted and several orange-brown crystals residing at the bottom of the flask which were collected carefully using vacuum filtration (150 mg). The resulting pure compound was analyzed by ^{1}H and ^{13}C NMR spectroscopy in DMSO and the result as follow:

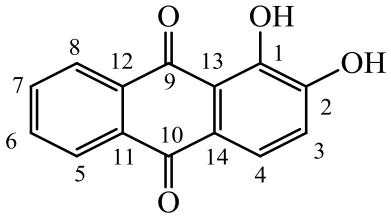

^{1}H (500 MHz): δ = 12.62 (s, 1H, OH1), 10.89 (s, 1H, OH2), 8.29 (dd, J_1= 2, J_2=8Hz), 8.17 (dd, J_1= 2, J_2=8Hz), 7.94 (m, 2H), 7.67 (d, J=8Hz), 7.24 (d, J=8Hz), and ^{13}C NMR (125 MHz): δ = 189.3, 181.1, 153.2, 151.2, 135.6, 134.5, 134.0, 133.3, 127.2, 127.0, 124.2, 121.6, 121.3, 116.7; Formula: $C_{14}H_8O_4$, Anal. calc.: C, 70.00; H, 3.36; found: C, 69.94%; H, 3.28%. From these results, we confirm the successful extraction of alizarin from the roots part of *R. tinctorum* with high purity.

2.4 Synthesis of ligands 1–3

2.4.1 Preparation of para-1 and meta-substitution ligands 2

At room temperature, 0.5g (2mmol) of alizarin in 15ml of dry pyridine was added under argon 1g (5.6 mmol) of the commercially available hydrochloride salt of isonicotinoyl or nicotinoyl chloride. The mixture was heated to 100 °C for 24h. The solvent was removed and the crude product was washed twice with $CHCl_3/H_2O$ (v/v). The organic phase was collected, dried over $MgSO_4$ and evaporated to dryness. The remaining solid was purified by flash column chromatography on SiO_2 ($CHCl_3$). The pure para (**1**) and meta-substituted ligands (**2**) were obtained as a yellow powder in ca. 72% and 57% yield, respectively.

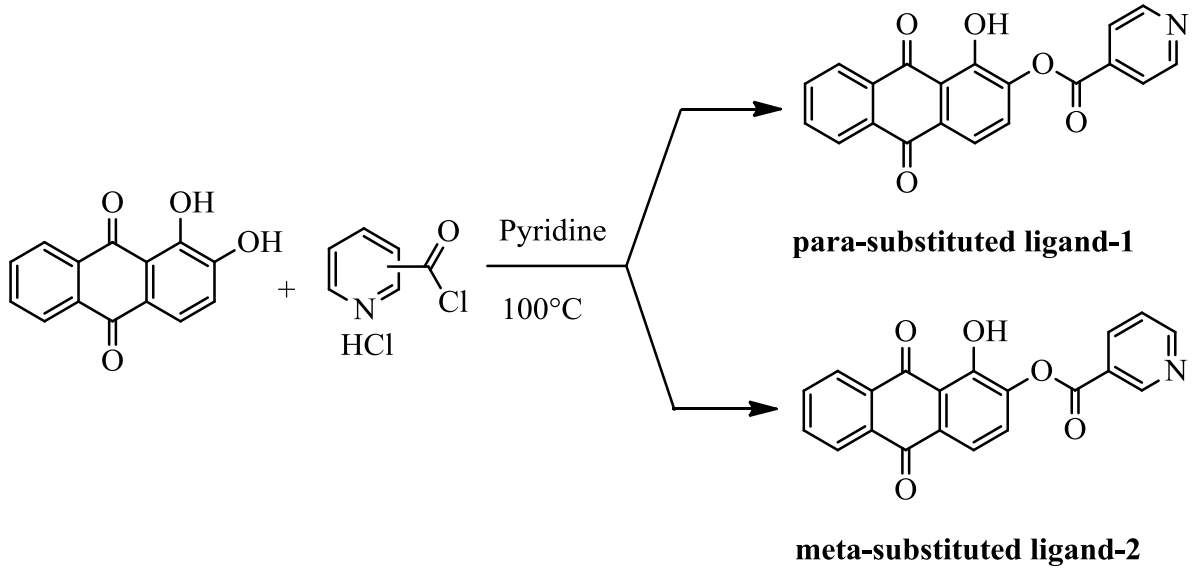

Figure 3: Reaction scheme for the synthesis of the para and meta-substituted ligands **1** and **2**.

2.4.2 Preparation of ortho-substitution ligand 3

At room temperature, 0.5g (2mmol) of alizarin in 60 ml of dry CH_2Cl_2 was added under argon 1g (5.6 mmol) of the commercially available 2-pyridinecarbonyl chloride hydrochloride. After 15 min of agitation, 5ml of dry Et_3N was added to the mixture. The reaction mixture was agitated at room temperature for two days. The solvent was removed and the crude product was washed twice with $CHCl_3/H_2O$ (v/v). The organic phase was collected, dried over $MgSO_4$, and evaporated to dryness. The remaining solid was purified by flash column chromatography on SiO_2 ($CHCl_3$) and then washed twice with MeOH and a small amount of acetone, which affording pure isomer ortho-substituted ligand (**3**) as a yellow solid in 42%.

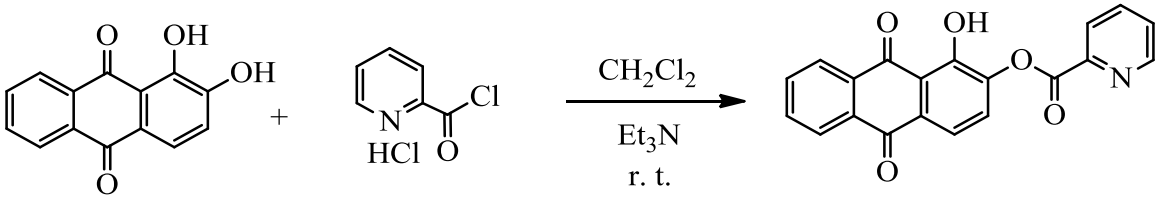

Figure 4: Reaction scheme for the synthesis of the ortho-substituted ligand **3**. Abbreviation: r.t, room temperature; Et_3N, trimethylamine, dichloromethane, CH_2Cl_2.

2.5 Quantum chemical calculations

Density functional theory (DFT) has proved to be useful for understanding the electronic structures of synthetic compounds. The full molecular geometry optimization of the compound was performed through the Gaussian 09 W program and GaussView molecular visualization software package[59] on a personal computer, based on density functional theory DFT, using Beck's three parameters hybrid exchange functional, with 6-311G (d, p) basis sets and Lee-Yang-Parr correlation functional (B3LYP). The optimized structure of each compound has been used to calculate the Molecular Electrostatic Potential (MEP) was determined to investigate the charge distribution on all compounds.

3. Results and Discussion

The design of the organic ligands **1**–**3** is based on the alizarin group, bearing a pyridine moiety as a coordinating site in which the junction between the two parts is effected by an ester group. The main difference between the three ligands is the position of the connection of the ester group to the pyridyl group (position 2 (-para), 3 (-meta), or 4 (-ortho)). Thus ligand could be referred to as positional isomers. All three components (alizarin moiety, pyridine, and OC=O group) of **1**, **2**, and **3** ligands are rigid units with some rotational flexibility around the ester junction.

The ligand **1** (yellow powder) was achieved in pyridine at 100°C under argon in the presence of the commercially available isonicotinoyl chloride hydrochloride and alizarin in 72% yield. Although, the second ligand **2** (yellow powder) was attained using the same protocol, with nicotinoyl chloride hydrochloride and alizarin in 57 %. Therefore, under the same conditions, we could not isolate ligand **3**, anything less a change in reaction conditions allowed us to prepare this ligand with a 42% yield. Indeed, the synthesis of ligand **3** (yellow powder) was carried out at room temperature in dichloromethane (CH_2Cl_2), trimethylamine

(Et_3N), 2-Pyridinecarbonyl chloride hydrochloride, and alizarin. All ligands are readily dissolved in polar solvents and melted in the range of 194–230°C and their structure was identified by FT-IR, ^{1}H NMR, and ^{13}C NMR spectroscopy.

3.1 Nuclear Magnetic Resonance spectra (^{1}H-NMR and ^{13}C-NMR)

Nuclear magnetic resonance spectra are an indispensable tool for the structure elucidation of anthraquinones it allows the deduction of nature and the number of substituents because all the substituents will give rise to signals with a characteristic chemical shift.[22] The ^{1}H and ^{13}C-NMR results of the three ligand series as follows:

para-substitution ligand 1:

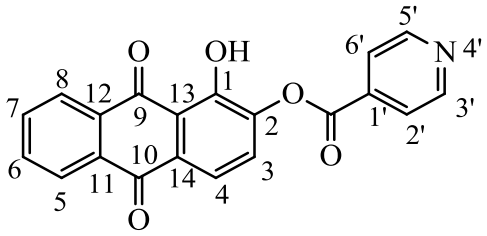

Yellow; mp 230°C; ESI-MS$^+$, 346.07; ^{1}H NMR (500MHz, $CDCl_3$): δ = 7.59 (d, J=8 Hz, 1H), 7.63, (m, 2H, H3), 7.92 (d, J=8 Hz, 2H, H4), 8.04 (d, J=6 Hz, 2H, H2′,6′), 8.31 (m, 2H, H5,8), 8.88 (d, J=6 Hz, 1H, H3′,5′), 12.80 (s, 1H, OH1), and ^{13}C NMR (125 MHz, $CDCl_3$): δ = 188.8 (C9), 181.6 (C10), 162.6 (CO), 154.2, 150.9, 143.9, 135.8, 135.1, 134.3, 133.6. 133.0, 131.3, 129.3, 127.6, 127.1, 123.4, 119.6, 117.6; Formula: $C_{20}H_{11}NO_5$, Anal. calc.: C, 69.57%; H, 3.21%; N, 4.06%; found: C, 69.56%; H, 3.22%, N, 4.03%.

Meta-substitution ligand 2:

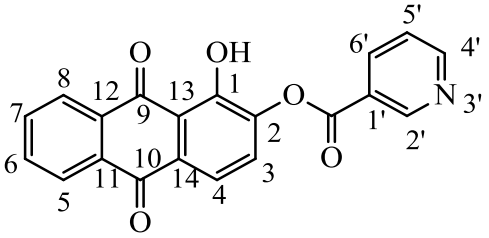

Yellow; mp 194°C; ESI-MS$^+$, 346.07; ^{1}H NMR (500MHz, CDCl3)): δ =7.59 (dd, J1 = 4.5 Hz, J2 = 8 Hz, 1H, H5′), 7.64 (d, J = 8 Hz), 7.83 (m, 2H), 7.94 (m, 2H), 8.32 (m, 3H), 8.88 (d,J= 4.5 Hz, 1H), 12.82 (s, 1H), and ^{13}CNMR (125MHz,CDCl3): δ = 188.8, 181.6, 162.5, 154.4, 150.3, 146.6, 144.5, 137.3, 135.0, 134.2, 133.6. 133.1, 131.1, 129.6, 127.8, 127.6, 127.0, 126.2, 119.6, 117.5; Formula: $C_{20}H_{11}NO_5$, Anal. calc.: C, 69.57%; H, 3.21%; N, 4.06%; found: C, 69.53%; H, 3.26%, N, 4.07%.

Ortho-substitution ligand 3:

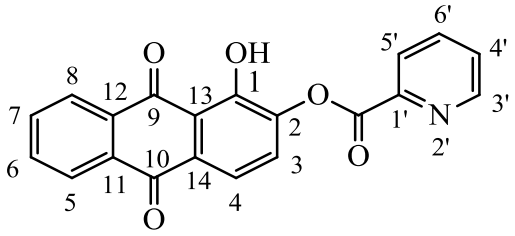

Yellow; mp 223 °C; ESI-MS$^+$, 346.07; ^{1}H NMR (500MHz, $CDCl_3$): δ =7.50 (m, 1H), 7.63 (d, J = 8 Hz), 7.84 (m, 2H), 7.94 (d, J = 8 Hz, 1H), 8.33 (m, 2H), 8.51 (m, 1H), 8.89 (dd, J1=3 Hz J2=6.5 Hz, 1H), 9.45 (d, J=2 Hz, 1H), 12.82 (s, 1H), and ^{13}C NMR (125 MHz, $CDCl_3$): δ = 188.8 (C9), 181.6 (C10), 162.7 (CO), 154.4 (C1), 153.4, 151.6 (C2), 144.0, 137.9, 135.1, 134.3, 133.6. 133.0, 131.1, 129.5, 127.6, 127.1, 124.7, 123.6, 119.6 (C3), 117.5; Formula: $C_{20}H_{11}NO_5$, Anal. calc: C, 69.57%; H, 3.21%; N, 4.06%; found: C, 69.60%; H, 3.25%, N, 4.04%.

3.2 Infrared (IR) spectroscopy

Fourier transform infrared (FTIR) spectroscopy is a rapid, economical, easy, and non-destructive technique that is a form of vibrational spectroscopy that plays several absorption peaks, which are used to investigate the presence of certain functional groups in a molecule.[68] The structure of the series ligands **1**–**3** was confirmed also by FTIR measurement.

The C=O is formed by the Pπ-Pπ bonding between carbon and oxygen atoms. Carbonyl (C=O) group stretching vibration is expected to appear in the region of 1680–1715 cm^{-1}.[69] In this study, the carbonyl group ν(C=O) stretching vibration appears at 1592.03 cm^{-1} as a strong band and 1741.95cm^{-1} as a weak band in FT-IR. The bands at 1586.29 cm^{-1}, 1562.04 cm^{-1}, and 1589.31 cm^{-1} for compounds **1**–**3**, respectively, were assigned to the presence of the C=C aromatic. Hydrogen-bonding is alters the frequencies of the stretching and bending vibration. The O–H stretching bands move to lower frequencies usually with increased intensity and band broadening in the hydrogen-bonded species. Hydrogen bonding if present in a five or six-member ring system that would reduce the O-H stretching band to a 3200–3550 cm^{-1} region.[70] In the present study, for the three ligands **1**–**3**, the stretching vibration of the hydroxyl group is observed at 3092.45, 3087.81, and 3088.74 cm^{-1}, respectively in the FT-IR spectrum. The C-N stretching vibration is always mixed with other bands and regularly assigned in the region 1382–1266 cm^{-1}.[62] Accordingly, in our present study, the values at 1355.02–1211.37, 1357.87–1266.77, and 1398.41–1266.24 cm^{-1} detected for meta, para, and ortho-substituted ligands (**1**–**3**), respectively in FT-Raman spectra are assigned to C-N stretching vibration.

A DFT study has conducted to investigate how to influence the position of substitution of the pyridine rings system on the valence electronic structure of ligands synthesis.

3.3 Density Functional Theory (DFT)

3.3.1 The equilibrium geometry optimization

The first task for the computational work is to determine the optimized geometry of the title ligands. The equilibrium geometry optimization of the ligands **1**–**3** was obtained using

the (DFT/B3LYP) method with the 6-311G+ (d, p) basis set. The optimized structures are listed in Figure 5.

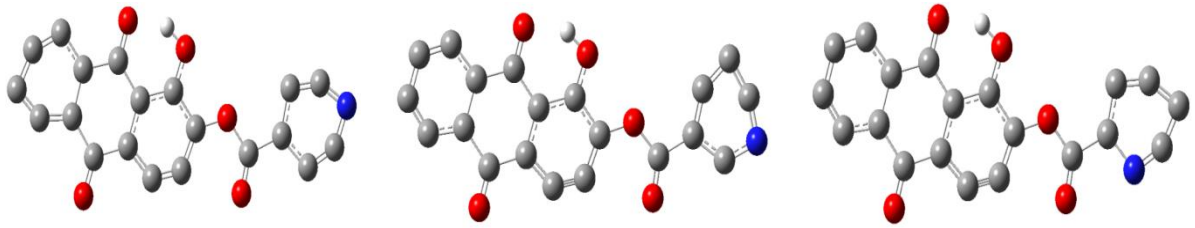

para-substituted ligands **1** meta-substituted ligands **2** ortho-substituted ligand **3**

Figure 5: Optimized structures of the para-, meta-, and ortho-substitution ligands **1**–**3**.

3.3.2 HOMO and LUMO energy

The atomic orbital compositions of the frontier molecule orbital are sketched in Fig 6. Different positions of the nitrogen group on the phenyl ring cause certain changes in frontier molecular orbital energies. The overall analysis of HOMO and LUMO energy values of the three ligands revealed that the EHOMO varied from -0.2522 eV to -0.2651 eV and ELUMO from -0.1450 eV to -0.1735 eV. The HOMO was mainly delocalized on the oxygen atom, phenyl ring, and the ester group for all series ligand. The greatest contributions to the HOMO were from the carbon-substituted aromatic ring containing the hydroxyl group (OH), carbonyl group (O9 and O10), and an ester group. On the other hand, LUMO was the main delocalized on the pyridyl group and oxygen atom of the ester group for para-substituted ligand (1) and ortho-substituted ligand (3) and alizarin moiety with CO of ester group contributed to LUMO for the meta-substituted ligand.

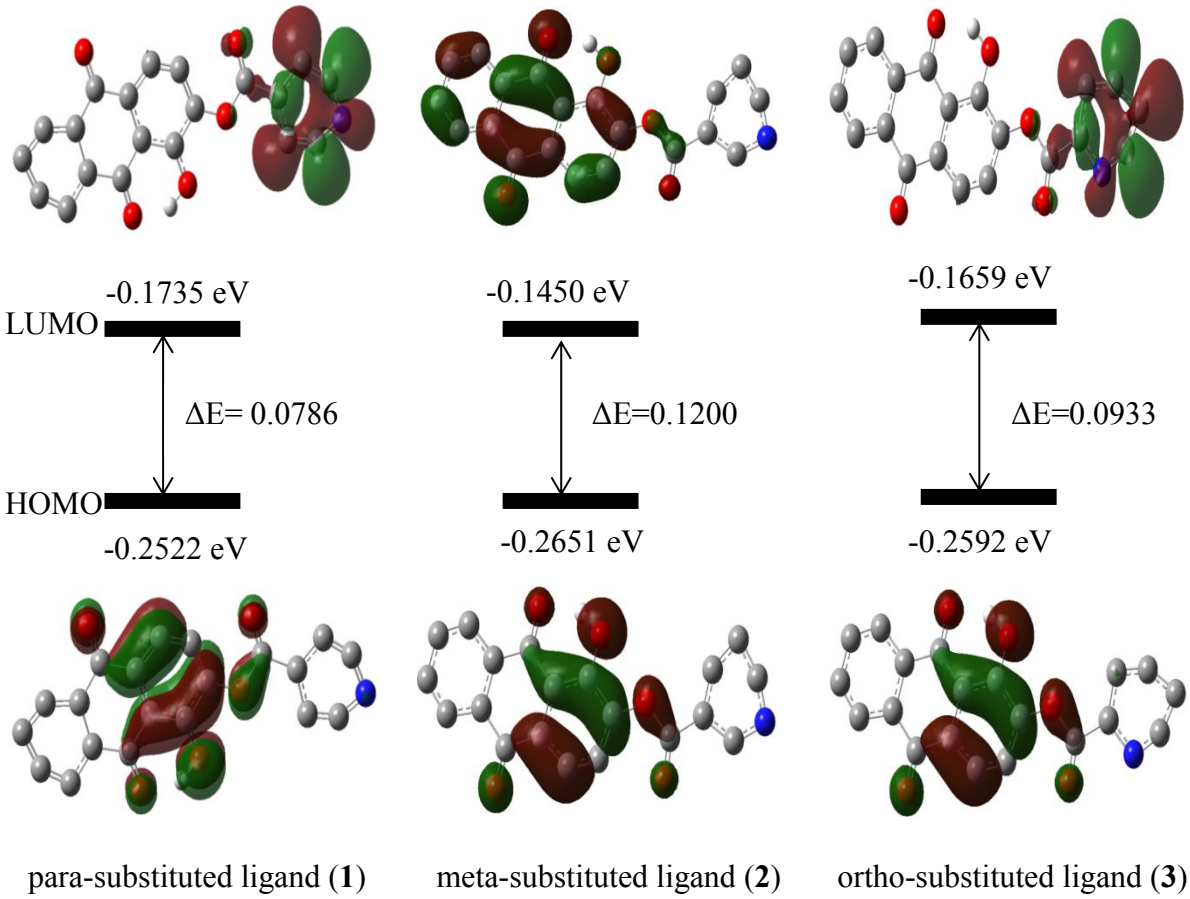

para-substituted ligand (**1**) meta-substituted ligand (**2**) ortho-substituted ligand (**3**)

Figure 6: The HOMO and LUMO coefficient distribution of para-, meta-, and ortho-substitution ligands **1**–**3** by B3LYP/6-311G+ (d, p).

3.3.3 Chemical reactivity

The reactivity indexes are another alternative approach for understanding the capacity of a species to accept or donate an electron. In Table 1, were report the static global properties, namely, electrophilic chemical potential (μ), chemical hardness (η), chemical softness (σ), electronegativity(χ), and global electrophilicity (ω) of ligands **1**–**3**.

- **Energy gap**

The energy gap of the one-electron excitation from HOMO to LUMO for meta-, para-, and ortho-substitution ligands were calculated about 0.1200, 0.0933, and 0.0786 eV, respectively (Table 1). This large HOMO-LUMO gap is an indication of good stability and a high chemical hardness for meta-substituted ligand (2). Para- (1) and ortho-substituted ligands (3) are considered as softer and have an excellent chemical reactivity. For all systems, 3D-plots of HOMO and LUMO were shown in Figure 6.

- **Hardness/softness**

Table 1 contains the computed chemical hardness values for all ligands **1**–**3**. The hardness is related to the stability of a molecule, for instance, if a molecule is very "hard", so that is very stable. It measures the resistance of a compound to changes in the electron density distribution or to electron charge transfer. Considering the results in Table 1 the highest

values of hardness, 0.0600 electronvolts (eV), belong to meta-substituted ligand (2) followed by para-substituted ligand (1) (0.0466 eV) and the least negative hardness value belongs to ortho-substituted ligand (3), with the amount of 0.0393eV. The calculated results for the molecule's hardness can justify the good stability for the meta-substituted ligand (2).

- **Electronegativity**

The electronic chemical potential is defined as the negative electronegativity of a molecule. The smaller the electronic chemical potential value (μ), the more stable is the compound. Table 1 lists the calculated electronic chemical potential values for the three studied ligands **1**–**3**. The trend in the electronic chemical potential for the three ligands is a para-substituted ligand (1) > ortho-substituted ligand (3) > meta-substituted ligand (2). The greater the electronic chemical potential, the less stable or more reactive is the ligand. Therefore, para-substituted ligand (1) (-0.2128 eV) is the most reactive, and meta-substituted ligand (2) (-0.2050 eV) is the least reactive among the three ligands.

- **Electrophilicity**

The electrophilicity values for ligand series **1**–**3**, are presented in Table 1. In a chemical process, it measures the capacity of a species to accept electrons and therefore measures the stabilization in energy after a system accepts additional electronic charges. Among these compounds, the meta-substituted ligand (2) has the lowest ω value (0.3502 eV), suggesting that is the strongest electrophile although, para- and ortho-substituted ligands found to be the strongest nucleophile. The electrophilic order can be considered as: meta-substituted ligand (2) > ortho-substituted ligand (3) > para-substituted ligand (1)

- **Dipole moment**

The dipole moment, which is the first derivative of energy, concerning an applied electric field is a measure of asymmetry in the molecular change distribution.[71] The dipole moment was calculated for the series ligand **1**–**3** at the B3LYP/6-311G (d, p) level of theory which follows the trend: ligand (2) > ortho-substituted ligand (3) > para-substituted ligand (1). Meta-substituted ligand (2) and ortho-substituted ligand (3) show the highest values (2.8353 and 2.6611 Debye, respectively) which could form more efficient secondary interactions with receptor compared to para-substituted ligand (1) (Table 1). An elevated level of dipole moment enhances the hydrogen bond formation, nonbonding interaction, binding affinity, and polar nature of a molecule.

Table 1: Quantum chemical parameters of the selected compounds with DFT at B3LYP/6-311G+ (d, p) basis set.

Comp. No.	1	2	3
E HOMO (eV)	-0.2522	-0.2651	-0.2592
E LUMO (eV)	-0.1735	-0.1450	-0.1659
(ΔE) Energy gap (eV)	0.0786	0.1200	0.0933
(I) Ionization energy (eV)	0.2522	0.2651	0.2592
(A) Electron affinity (eV)	0.1735	0.1450	0.1659
(η) Global hardness (eV)	0.0393	0.0600	0.0466
(σ) Global softness (eV^{-1})	25.4323	16.6611	21.4592
(μ) Chemical potential	-0.2128	-0.2050	-0. 2125
(χ) Electronegativity	0.2128	0.2050	0.2125
(ω) Global Electrophilicity	0.5761	0.3502	0.4845
Dipole moment (D)	1.8862	2.8353	2.6611

A= –ELUMO, I= –EHOMO, η=1/2(ELUMO-EHOMO), μ=1/2(EHOMO+ELUMO), ω= $\mu^2/2\eta$, σ= 1/2η.

3.3.4 Molecular electrostatic potential (MEP) maps

MEP for title ligands is calculated by the B3LYP/6-311G+ (d, p) level as shown in Fig 7. The color codes of these maps are in the range between -4.665 to 4.665 a.u., -4.100 to 4.100 a.u., and -4.574 to 4.574 a.u. correspond to ortho-substituted ligand (3), meta-substituted ligand (2), and para-substituted ligand (1), respectively. As can be seen from Fig 7, the red region has been localized on the vicinity of an oxygen atom from the carbonyl group (O9, O10), and the OH-substituted phenyl ring of alizarin moiety as well as the carbonyl group (O) of the ester group, can be considered as the electrophilic reactivity center while, the positive region is located near the nitrogen atom, ester and the phenyl groups for all isomers that will be the reactive sites for nucleophilic attack. In this respect, the ligands **1**–**3** are useful to both bonds metallically and the blue region that does not correspond to the intermolecular interactions

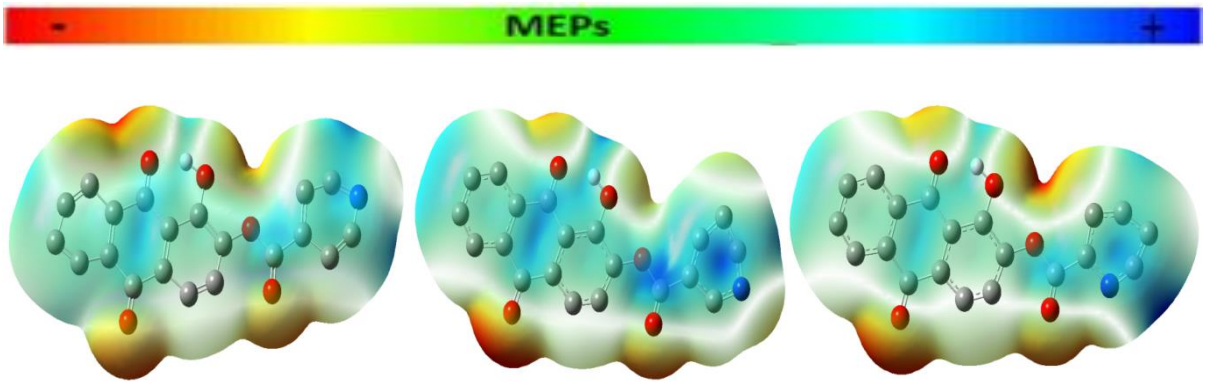

para-substituted ligand **1** meta-substituted ligand **2** ortho-substituted ligand **3**

Figure 7: Molecular electrostatic potential map calculated using B3LYP/6-311G+ (d, p) level.

4. Conclusions

In this work, alizarin was extracted and purified from *R. tinctorum* to be esterified by pyridine moiety. This approach yielded three alizarin derivatives of pyridinecarboxylic acid that were successively synthesized and characterized using various spectroscopic methods and elemental analysis. Electronic properties of investigated molecules were studied using the calculated energy of HOMO and LUMO orbitals, HOMO–LUMO energy gap (Egap), and chemical reactivity. All vertical excitation energies were computed using B3LYP/6-311G+ (d, p) optimized ground-state geometries. In this study, para-substituted ligand (1) shows the lowest energy gap (0.0786 eV) and the highest chemical softness (25.4323 eV) values which may contribute to the higher chemical reactivity than others. Besides, the meta-substitution ligand is least chemically reactive having the highest energy gap among the four ligands. The MEP map confirms the existence of intermolecular interactions. The three new compounds could be considered reactive core that gives scope for further studies and applications in pharmaceutical and optical materials.

5. References

(1) Simpson, M. Plant Systematics - 3rd Edition; **2010**.
(2) Verma, A.; Kumar, B.; Alam, P.; Singh, V.; Gupta, S. K. Int. J. Pharm. Sci. Res. **2016**.
(3) Deshkar, N.; Tilloo, S.; Pande, V. Pharmacogn. Rev. **2008**, 2 (3), 124–134.
(4) De Santis, D.; Moresi, M. Ind. Crops Prod. **2007**, 26 (2), 151–162.
(5) Flora, O. K. **2011**.
(6) Figue-Henric, É. **1980**.
(7) Baghalian, K.; Maghsodi, M.; Naghavi, M. R. Ind. Crops Prod. **2010**, 31 (3), 557–562.
(8) Henderson, R. L.; Rayner, C. M.; Blackburn, R. S. Phytochemistry **2013**, 95, 105–108.
(9) Bellakhdar, J. Le Maghreb à Travers Ses Plantes. **2018**, p 323.
(10) Lajkó, E.; Bányai, P.; Zámbó, Z.; Kursinszki, L.; Szőke, É.; Kőhidai, L. Cancer Cell Int. **2015**, 15 (1), 1–15.
(11) Some Traditional Herbal Medicines, Some Mycotoxins, Naphthalene and Styrene.; **2002**; Vol. 82.
(12) Sharifzadeh, M.; Ebadi, N.; Manayi, A.; Kamalinejad, M.; Rezaeizadeh, H.; Mirabzadeh, M.; Bonakdar Yazdi, B.; Khanavi, M. J. Med. Plants **2014**, 13 (51), 62–70.
(13) Rima Ghafari; Mouslemanie, N.; Nayal, R. Int. J. Pharm. Sci. Res. **2018**, 9 (October), 5–10.
(14) Bellakhdar, J. 1992.
(15) Diaz-Muñoz, G.; Miranda, I. L.; Sartori, S. K.; de Rezende, D. C.; Diaz, M. A. N. Stud. Nat. Prod. Chem. **2018**, 58, 313–338.
(16) Duval, J.; Pecher, V.; Poujol, M.; Lesellier, E. Ind. Crops Prod. **2016**, 94, 812–833.
(17) Reddy, N. R. R.; Mehta, R. H.; Soni, P. H.; Makasana, J.; Gajbhiye, N. A.; Ponnuchamy, M.; Kumar, J. PLoS One **2015**, 10 (6), 2–32.
(18) Alhakmani, F.; Khan, S. A.; Ahmad, A. Asian Pac. J. Trop. Biomed. **2014**, 4 (Suppl 2), S656–S660.
(19) Chien, S. C.; Wu, Y. C.; Chen, Z. W.; Yang, W. C. Evidence-based Complement. Altern. Med. **2015**, 2015.
(20) Frohwein, Y. Z.; Dafni, Z.; Friedman, M.; Matele, R. I. Agric. Biol. Chem. **1973**, 37 (3), 679–680.
(21) Atta-ur-Rahman. Studies in Natural Products Chemistry (Part G); **2003**; Vol. 26.
(22) Derksen, G. C. H.; Van Beek, T. A. Stud. Nat. Prod. Chem. **2002**, 26, 629–684.
(23) Yu, L.; Reutzel-Edens, S. M. Encycl. Food Sci. Nutr. **2003**, 34, 1697–1702.
(24) Colin, J.-J.; Robiquet, P.-J. Annales de Chimie et de Physique. **1827**, pp 225–253.
(25) K., O. **1980**; Vol. 39.

(26) Cuoco, G. Etude Chimique et Caractérisation de Principes Colorants Historiquement Employés Dans l' Impression Des Indiennes., **2012**.
(27) Richte, D. 379. Anthraquiutone Colouring Matters : Ruberythric Acid. J. Chem. Soc. **1936**, 1701.
(28) Derksen, G. C. H. Red , Redder, MADDER Analysis and Isolation of Anthraquinones from Madder Roots (Rubia Tinctorum), **2001**.
(29) Bajpai, V. K.; Alam, B.; Quan, K. T.; Choi, H.; An, H.; Ju, M.; Lee, S.; Huh, Y. S.; Han, Y.; Na, M. MC Complement. Altern. Med. **2018**, 18 (200), 2–7.
(30) C. M. O. S.; E.P.Schenkel; Gosman, G.; Mello, J. C. P.; Mentz, L. A.; Petrovick, P. R. Farmacognosia: Da Planta Ao Medicamento, Editora Da UFSC, Florianó polis; **2007**.
(31) Ami, A.; Stanojevi, M.; Markovi, Z. Org. Biomol. Chem. **2018**, 16 (11), 1890–1902.
(32) Syed, M. M.; Doshi, P. J.; Kulkarni, M. V.; Dhavale, D. D.; Kadam, N. S.; Kate, S. L.; Doshi, J. B.; Sharma, N.; Uppuladinne, M.; Sonavane, U. Taylor & Francis, **2019**; Vol. 37.
(33) Bartnik, M.; Facey, P. C. Glycosides; Elsevier Inc., 2017.
(34) Diaz, A. N.. Talanta **1991**, 38 (6), 571–588. (35) Hart, P. W.; Rudie, A. W. Anthraquinone-a Review of the Rise and Fall of a Pulping Catalyst. Tappi Journal. **2014**, pp 23–31.
(36) Kim, E. mi; Choi, J. hong. Fibers Polym. **2013**, 14 (12), 2054–2060.
(37) Deliberto, S. T.; Werner, S. J.; Collins, F.; Deliberto, S. T.; Services, W.; Wildlife, N.; Collins, F. Pest Manag. Sci. **2016**, 72 (10), 1813–1825.
(38) Pan, S. Y.; Zhou, S. F.; Gao, S. H.; Yu, Z. L.; Zhang, S. F.; Tang, M. K.; Sun, J. N.; Ma, D. L.; Han, Y. F.; Fong, W. F. Evidence-based Complement. Altern. Med. **2013**, 1–25.
(39) Ye, M.-Y.; Yao, G.-Y.; Pan, Y.-M.; Liao, Z.-X.; Zhang, Y.; Wang, H.-S. Eur. J. Med. Chem. **2014**, 83, 116–128.
(40) Du, S.; Feng, J.; Lu, X.; Wang, G. Dalt. Trans. **2013**, 42 (26), 9699–9705.
(41) Morgan, L. R.; Thangaraj, K.; LeBlanc, B.; Rodgers, A.; Wolford, L. T.; Hooper, C. L.; Fan, D.; Jursic, B. S. J. Med. Chem. **2003**, 46 (21), 4552–4563.
(42) Huang, R.; Jin, L.; Yao, G.; Dai, W.; Huang, X.; Liao, Z.-X.; Wang, H. Med. Chem. Res. **2017**, 26 (10), 2363–2374.
(43) Yao, G.; Ye, M.; Dai, W.; Pan, Y.; Ouyang, X.; Wang, H. Chem. Nat. Compd. **2014**, 50 (2), 242–246.
(44) Rozin, Y. A.; Tat'yanenko, L. V.; Buryndina, E. I.; Barybin, A. S.; Popova, V. G. Pharm. Chem.]ournal **1997**, 30 (8), 520–522.
(45) Fabbri, D.; Chiavari, G.; Ling, H. J. Anal. Appl. Pyrolysis **2000**, 56 (2), 167–178.
(46) Drivas, I.; Blackburn, R. S.; Rayner, C. M. Dye. Pigment. **2011**, 88 (1), 7–17.
(47) Churchill, M. R.; Keil, K. M.; Bright, F. V.; Pandey, S.; Baker, G. A.; Keister, J. B. Inorg. Chem. **2000**, 39 (25), 5807–5816.
(48) Schwab, P. F. H.; Diegoli, S.; Biancardo, M.; Bignozzi, C. A. Inorg. Chem. **2003**, 42 (21), 6613–6615.
(49) Soares, S. M.; Lemos, S. S.; Sales, M. J. A.; Back, D. F.; Lang, E. S. Polyhedron **2009**, 28 (17), 3811–3815.
(50) Mo, M.; Zhang, B.; Du, S. Z.; Lu, X. M.; Wang, G.; Fen, J. Mo- W. Inorg. Chem. **2013**, 52 (16), 9470–9478.
(51) Kharlamova, T. V. Chem. Nat. Compd. **2009**, 45 (5), 629–633.
(52) Lapini, A.; Fabbrizzi, P.; Piccardo, M.; Di Donato, M.; Lascialfari, L.; Foggi, P.; Cicchi, S.; Biczysko, M.; Carnimeo, I.; Santoro, F. Phys. Chem. Chem. Phys. **2014**, 16 (21), 10059–10074.
(53) Lu, X.-B. In Carbon Dioxide and Organometallics; 2015; pp 40–41.
(54) Arévalo, R.; Espinal-Viguri, M.; Huertos, M. A.; Pérez, J.; Riera, L. Elsevier Inc., 2016; Vol. 65.
(55) El-Naggar, M.; Almahli, H.; Ibrahim, H. S.; Eldehna, W. M.; Abdel-Aziz, H. A. Molecules. **2018**, 23 (6), 1459.
(56) Al-otaibi, J. S.; Gogary, T. M. EL. J. Mol. Struct. **2017**, 1130, 799–809.
(57) Su, S. J.; Sasabe, H.; Takeda, T.; Kido, J. Chem. Mater. **2008**, 20 (5), 1691–1693.
(58) Akhtar, M. S.; Ali, M.; Madhurima; Mir, S. R.; Singh, O. Indian J. Chem. - Sect. B Org. Med. Chem. **2006**, 45 (8), 1945–1950.

(59) Vektariene, A.; Vektaris, G.; Svoboda, J. Arkivoc **2009**, 7, 311–329.
(60) Osman, O. I. Int. J. Mol. Sci. **2017**, 18 (2), 239.
(61) Godarzi, M.; Ahmadi, R.; Ghiasi, R.; Yousefi, M. Int. J. Nano Dimens. **2018**, 0 (0), 62–68.
(62) Hellal, A.; Chafaa, S.; Chafai, N. J. Mol. Struct. **2016**, 1103, 110–124.
(63) Hoque, M. J.; Ahsan, A.; Hossain, B. J. Sci. Tech. Res. **2018**, 5 (4), 7360–7365.
(64) Parr, R. G.; Pearson, R. G. J. Am. Chem. **1983**, 105 (26), 7512–7516.
(65) Sawant, A. B.; Gill, C. H.; Nirwan, R. S. Indian J. Pure Appl. Phys. **2012**, 50 (1), 38–44.
(66) Chattaraj, P. K.; Maiti, B. J. AM. Chem. SOC **2003**, 125 (11), 2705–2710.
(67) Tokatlı, A.; Özen, E.; Ucun, F.; Bahc, S. Acta Part A Mol. and Biomolecular Spectrosc. **2011**, 78 (3), 1201–1211.
(68) Peak, D. Fourier Transform Infrared Spectroscopic Methods of Soil Analysis; Elsevier Inc., **2013**.
(69) Bharanidharan, S.; Saleem, H.; Subashchandrabose, S.; Suresh, M.; N, R. B. Arch. Chem. Res. **2017**, 1 (2:7), 1–14.
(70) Varsanyi, G. Vibrational Spectra of Benzene Derivatives; **1969**. https://doi.org/10.1016/b978-0-12-714950-9.x5001-7.
(71) Haghdadi, M.; Kenary, F. S.; Basra, H. G. Org. Chem. an indian J. **2014**, 10 (9), 371–376.

Chapter VII

Crystal structure and Hirshfeld surface analysis of 3,4-dihydro-2H-anthra[1,2b][1,4]dioxepine-8,13-dione

Abstract

The syntheses and characterization of two new alizarin derivatives functionalized with 1,3-dibromo-propane are described (4 and 5). The structure of the title compound (4), C17H12O4 was characterized using X-ray crystallography. The dihedral angle between the mean plane of the anthraquinone ring system (r.m.s. deviation = 0.039 Å) and the dioxepine ring is 16.29 (8)º. In the crystal, the molecules are linked by C—H···O hydrogen bonds, forming sheets lying parallel to the ab plane. The sheets are connected through π– π and C=O··· π interactions to generate a three-dimensional supramolecular network. Hirshfeld surface analysis was used to investigate intermolecular interactions in the solid-state: the most important contributions are from H···H (43.0%), H···O/O···H (27%), H···C/C···H (13.8%), and C···C (12.4%) contacts.

1. Introduction

Rubia tinctorum L. (*R. tinctorum*) belongs to the Rubiaceae family and is commonly referred as Madder. This species is widely distributed in southern and southeastern Europe, in the Mediterranean area (e.g, Morocco), and in central Asia.[1] It has been used since ancient times for its antibacterial, antifungal, and anti-inflammatory activities.[2] Apart from its pharmacological value, this plant has also been used as natural food colorants and for dyeing textiles.[3] Its reddish roots (madder roots) contain various secondary metabolites, mainly hydroxyanthraquinones.[1] 1,2-Dihydroxyanthraquinone is one of the most common natural hydroxyanthraquinone and supposed to be the main component of *R. tinctorum*.

The development of novel natural compounds and their synthetic derivatives with better biological behavior virtue have significantly gained bioorganic chemists' interest in the hope of creating new and better medicinal agents. In Chapter VI, we have demonstrated that alizarin derivatives are very useful scaffolds for the synthesis of a variety of pharmaceutical compounds.[4–11] Besides, the color of alizarin-based compounds can be modified by the type and position of the substituents attached to the anthraquinone nucleus.[12,13] 1,2-chelate, polyhydroxyanthraquinones can display as a redox agent, acting as semiquinone(-) or catecholate(2-) due to their similarity to biological active catechols and quinoids, [14] and due to their unexpected behavior,[15] which can lead to unusual properties of their complexes. Several types of alizarin derivatives have also been reported as a chelating ligand.[9,16–19]

1,5-dioxa (**30**) and its derivatives are an important class of heterocyclic molecules given their associated pharmaceutical activity. Several 3-substituted aminomethyl-3-hydroxy-l,5-benzodioxepins (**31**) have been shown to possess interesting bronchial dilator activity, while various 3,3-disubstituted 1,5-benzodioxepin derivatives (**32**) were recognized as analgesics, antiarrythmics, and sedatives.[20] Thus, it will be interesting to fuse a dioxipin ring on the hydroxyl group of alizarin scaffolds.

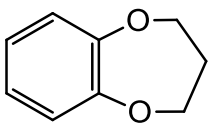

(30)

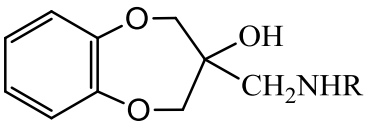

(31)

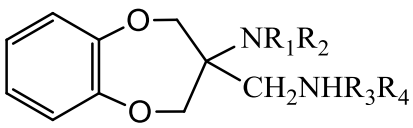

(32)

Our continuing interest in the synthesis of bioactive alizarin derivatives led us in this chapter to focus our attention on the synthesis new ligands functionalized with 1,3-dibromo-propane for exploring their biological mode of action or to be used as a platform to further syntheses. The synthesis ligands were characterized using ^{1}H and ^{13}C NMR spectroscopy. One of the ligands was obtained as crystal, and its structure was established by X-ray analysis with further analysis of its Hirshfeld surface.

2. Materials and Methods

2.1 Chemicals and instruments

All chemicals used throughout the research were purchased from Aldrich, and used without further purification. Data collection: APEX2;[21] cell refinement: SAINT;[21] data reduction: SAINT;[21] program(s) used to solve structure: SHELXT2014/5;[22] program(s) use to refine structure: SHELXL2018/3;[23] molecular graphics: ORTEP-3 for Windows[24] and DIAMOND[25] software used to prepare material for publication: PLATON[26] and publCIF.[27]

2.2 Extraction, purification, and characterization of alizarin from *Rubia tinctorum*

R. tinctorum roots were collected from the regions of Beni Mellal. The roots were washed, shade-dried (15 days) and milled into granulometry lower than 2 mm prior to extraction. Adequate mass (15 g) of *R. tinctorum* roots is treated into 300 ml of ethanol and extracted in a Soxhlet apparatus for 6 hours. The solvent was evaporated until dryness under vacuum on rotavapor. The residue (1.12 g) was dissolved into glacial acetic acid (100 ml) then left in a freezer for 3 days. The resulting liquor was decanted and several orange-brown crystals residing at the bottom of the flask which were collected carefully using vacuum filtration (150 mg). The resulting pure compound was analyzed by ^{1}H and ^{13}C NMR spectroscopy in DMSO (Chapter VI).

2.3 Synthesis of ligand 4

Under argon, alizarin (0.5g 2mmol) was treated with 1,3-dibromopropane (0.42 g, 2 mmol) in dimethylformamide (30 ml) and in the presence of hydrous potassium carbonate (1g 7.2 mmol) with stirring and heated at 120°C for 24 hours. The reaction mixture was evaporated in vacuum to dryness and the resulting crude product was acidified with 12N hydrochloric acid and extracted with chloroform (3x30 mL) then chromatographed on a silica gel column with dichloromethane/petroleum ether (1/1) as a solvent, yielded 200 mg, (35%) of compound **4** as a yellow compound.

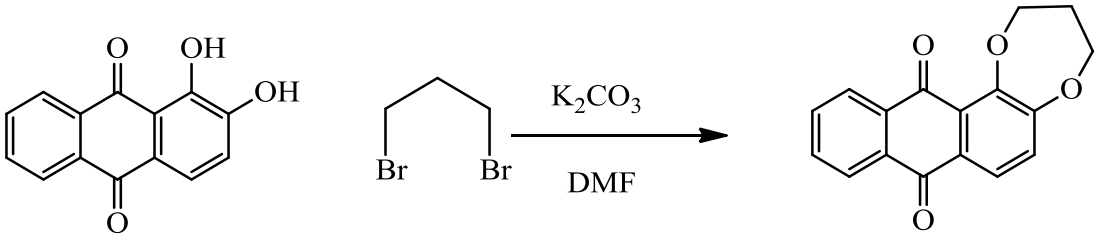

Figure 1: Reaction scheme for the synthesis of the title compound. Abbreviation: K_2CO_3, hydrous potassium carbonate; DMF, dimethylformamide.

3. Results and Discussion

The ligand **4** (yellow powder) was achieved with the presence of the commercially available 1,3-dibromopropane and alizarin in 35% yield, respectively. The structure of the ligands was identified by ^{1}H NMR and ^{13}C NMR spectroscopy.

3.1 Nuclear Magnetic Resonance spectra (^{1}H-NMR and ^{13}C-NMR)

- **Analytical data**

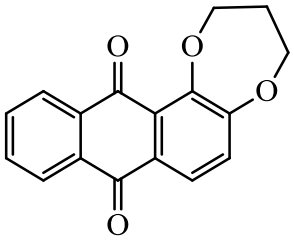

^{1}H NMR ($CDCl_3$, 500 MHz): δ [ppm]: 8.21 (m, 2H), 7.95 (d, J = 8.5 Hz, 1H), 7.72 (m, 2H), 7.26 (d, J = 8.5 Hz, 1H), 4.48 (t, J = 6 Hz, 2H), 4.43 (t, J = 6 Hz, 2H), 2.34 (qt, J = 6 Hz, 2H); ^{13}C NMR ($CDCl_3$, 126 MHz): δ [ppm]: 182.9, 182.5, 157.3, 151.3, 135.2, 133.9, 133.4, 132.6, 129.6, 127.1, 126.5, 126.0, 125.9, 123.3, 70.5, 70.2, 30.0. Anal. Calcd. for $C_{17}H_{12}O_4$: C, 72.85%; H, 4.32%; Found: C, 72.82%; H, 4.29%.

The crystal of the title compound (yellow needles) was obtained by slow evaporation of a solution of dichloromethane/petroleum ether (1:1) and analyzed by X-ray crystallography to determine its atomic and molecular structure.

3.2 Structural commentary of the title compound

The ligand 4 crystallizes in space group $P2_1/n$ with one molecule in the asymmetric unit: it consists of three fused six-membered rings and one seven-membered ring as shown in Fig 2. The fused-ring system is close to planar with an r.m.s. deviation for all non-hydrogen atoms of 0.039 Aº (the dihedral angle between the aromatic rings of the anthraquinone unit and the central ring range from 1.5 to 1.9º). The dioxepine ring is inclined to the mean plane of the anthraquinone ring system by 16.29 (8)º. A puckering analysis of the seven-membered ring yielded the parameters $q2$ = 0.896 (2) Å, $\varphi 2$ = 113.50 (12)º, $q3$ =0.358 (2) Å, and $\varphi 3$ = 217.8 (3)º. These metrics indicate that the ring adopts a screw boat conformation. The C—O and C O bond lengths lie within the ranges 1.355 (2) –1.457 (2) Å and 1.216 (2) –1.226 (2) Å, respectively, confirming their single and double-bond character.

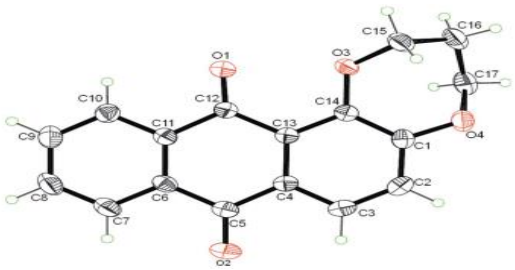

Figure 2: The molecular structure of the title compound with displacement ellipsoids drawn at the 50% probability level.

3.3 Supramolecular features

In the extended structure of compound, C15—H15B···O1 hydrogen bonds form inversion dimers with an $R^2_2(14)$ ring motif. Adjacent dimers are linked by C15—H15A···O3 contacts, thereby generating corrugated chains of molecules (Fig 3a). AC17—H17B···O2 hydrogen bond links the chains together (Table 1, Fig 3b and 3c), forming sheets propagating in the ab plane. These sheets are supported by extensive π–π contacts between adjacent rings, with centroid-to-centroid distances Cg1···Cg2 = 3.599 (2) and Cg2···Cg3 = 3.683 (2) Å[Cg1, Cg2 and Cg3 are the centroids of the rings C1–C4/C13–C14, C4–C6/C11–C13 and C6–C11, respectively] and weak C12=O1···π [oxygen–centroid distance = 3.734 (2) Å] interactions (Fig 4), linking the slabs to form a three-dimensional supramolecular network.

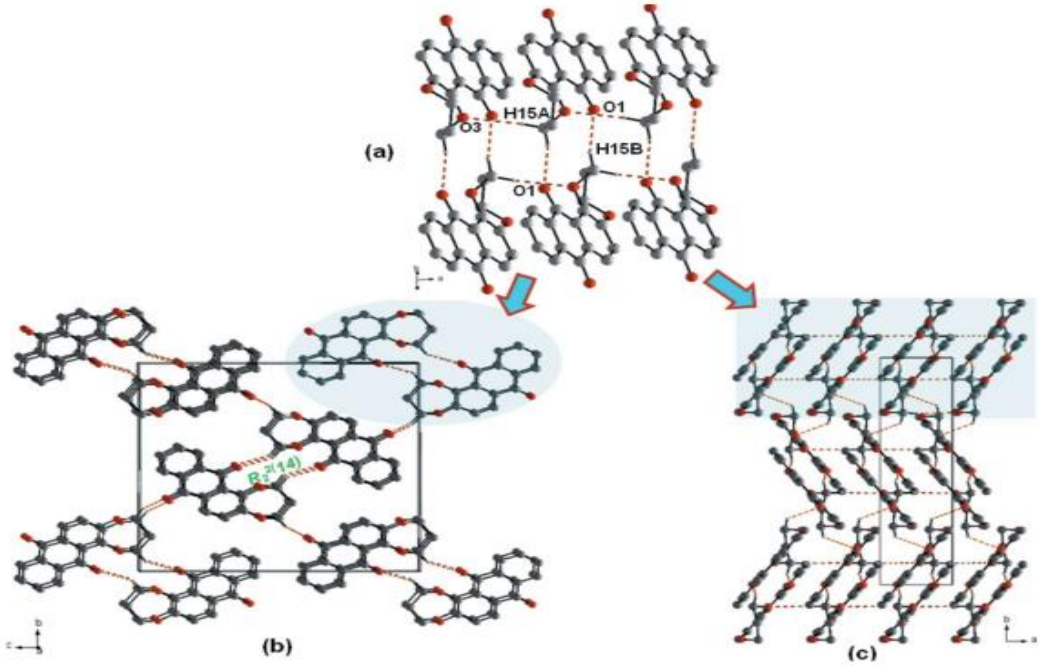

Figure 3: Inversion dimers with $R^2_2(14)$ ring motifs; (b) and (c) packing diagrams of the title compound, viewed along the a and b axes, respectively. Dotted lines indicate C—H···O hydrogen bonds.

Table 1: Hydrogen-bond geometry (Å, º).

D—H···A	D—H	H···A	D···A	D—H···A
C15—H15B…O1^{i}	0.99	2.43	3.248(2)	139
C15—H15A…O3^{ii}	0.99	2.48	3.248(3)	171
C17—H17A…O4^{iii}	0.99	2.59	3.580(3)	174

Symmetry codes: (i) -x; -y +1; -z +1; (ii) x +1; y; z; (iii) x -1; y; z.

3.4 Database survey

A search in the Cambridge Structural Database (CSD, Version 5.40, updated to February 2020; Groom et al., 2016)[27] revealed 55 alizarin-ring motifs incorporated in more complex molecules or bearing functional groups. These include several compounds with a different

substituent in place of the dioxepine in the title compound, viz. 1-hydroxy-2-methoxy-6-methyl (BOTXUE; Ismail et al., 2009),[28] 1,2-dimethoxy (ref code: KIBHUZ; Kar et al., 2007)[29] and 3-hydroxy-1,2-dimethoxy (BOVVEO; Xu et al., 2009).[30] In these compounds, the anthraquinone ring system is almost planar, the dihedral angle between the benzene rings for BOTXUE, KIBHUZ and BOVVEO being 3.49, 2.83 and 1.12º, respectively. The methoxy groups in position 1 (C14) in KIBHUZ and BOVVEO are almost perpendicular to the anthraquinone ring plane. The other compound belongs to the same class of alizarins with different substituents.

3.5 Hirshfeld surface analysis

The nature of the intermolecular interactions in title compound have been examined with *CrystalExplorer17.5*,[31] using Hirshfeld surface analysis[32] mapped over d norm, with a fixed color scale of -0.1779 to 1.3612 a.u (see Fig S1a in the supporting information) and two-dimensional fingerprint plots.[33] The intense red spots on the surface are due to the C—H···O hydrogen bonds (Fig 5). Fig S2 (supporting information) shows the molecular electrostatic potential surface generated using TONTO with a STO-3G basis set in the range -0.050 to 0.050 a.u. within the Hartree–Fock level of theory. Molecular sites evidenced in red correspond to positive potential energy and in blue to negative potential energy.[34] As illustrated in Fig 5, the overall fingerprint plot for title compound and those delineated into H···H, H···O/O···H, C···H/H···C and C···C show characteristic pseudo-symmetric wings in the d_e and d_i diagonal axes. The most important interaction is H···H, contributing 43% to the overall crystal packing, which is reflected in Fig 5b as widely scattered points of high density due to the large hydrogen content of the molecule, with small split tips at $d_e \approx d_i$ 1.2 Å. The contribution from the O···H/H···O contacts (27%) [note that the O···H interactions make a larger contribution (14.6%) than the H···O interactions (12.4%)], corresponding to C—H···O interactions, is represented by a pair of sharp spikes characteristic of a strong hydrogen-bond interaction, $d_e+d_i \approx 2.35$Å (Fig 6c). The significant contribution from C···H/H···C contacts (13.8%) to the Hirshfeld surface of title compound reflect the short C···H/H···C contacts, and the distribution of points has characteristic wings, Fig 5d, with $d_e+d_i \approx 2.55$ Å. The distribution of points in the $d_e=d_i \approx 1.75$ Å range in the fingerprint plot delineated into C···C contacts indicates the existence of weak–stacking interactions between the central anthracene ring and the C6–C11 and C1–C4/C13–C14 rings (Fig 5b and 6e). Aromatic–interactions are indicated by adjacent red and blue triangles in the shape-index map (Fig S1b) and also by the lattice region around these rings in the Hirshfeld surfaces mapped over curvedness in Fig S1c. The contribution of 3.2% from C···O/O···C contacts is due to the presence of short interatomic C =O···π contacts, and is apparent as the pair of parabolic tips at $d_e + d_i \approx 3.2$ Å in Fig 5f.

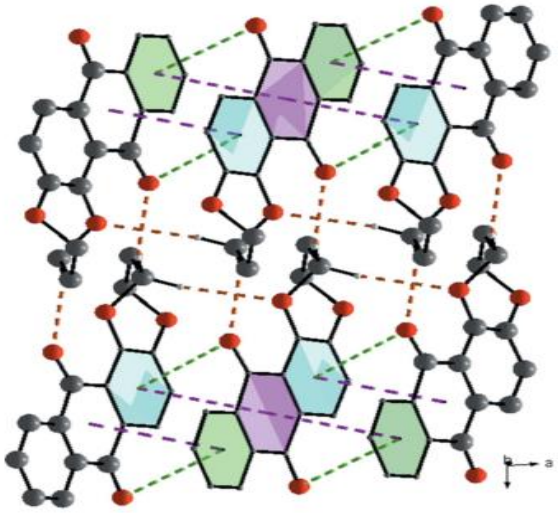

Figure 4: Partial crystal packing for (I) showing the C—H···O hydrogen bonds and the offset π –π (purple) and C=O···π (green) interactions between inversion-related molecules.

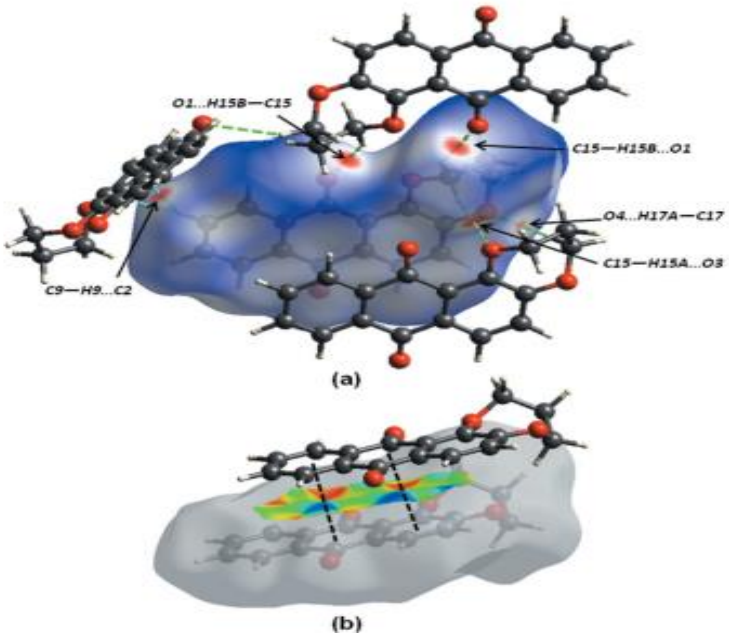

Figure 5: Views of the Hirshfeld surface for (I) mapped over (a) d norm showing the C—H···O contacts as green dashed lines and short C···H/H···C contacts as cyan dashed lines; and (b) shape-index highlighting the stacking (black lines).

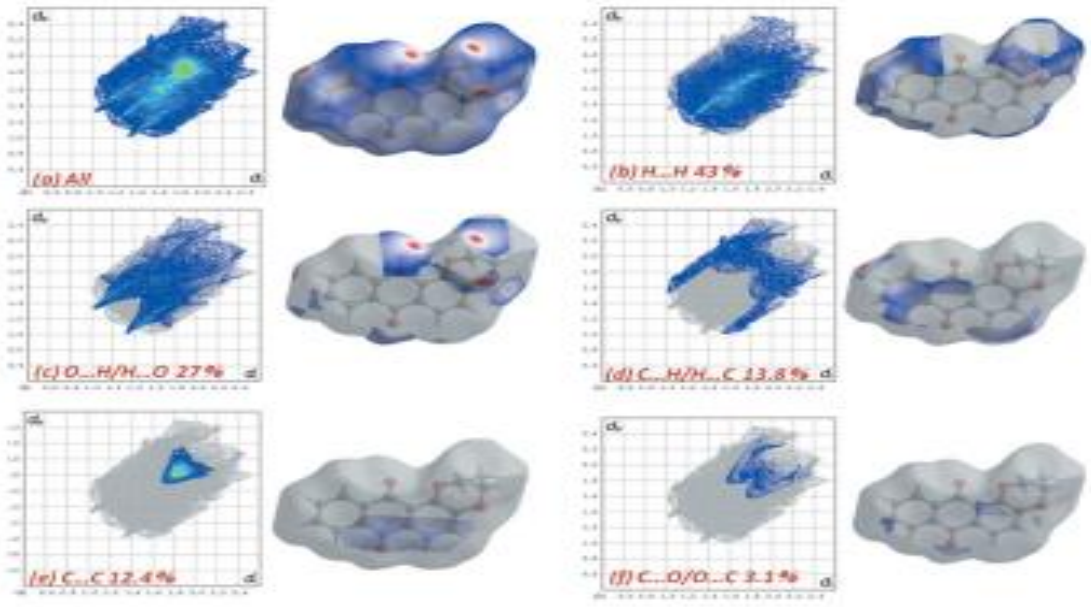

Figure 6: The full two-dimensional fingerprint plots for (I) showing (a) all interactions, and delineated into (b) H···H, (c) H···O/O···H, (d) H···C/C···H, (e) C···C and (f) O···C/C···O interactions.

3.6 Refinement

Crystal data, data collection and structure refinement details are summarized in Table 2. H atoms were placed in calculated positions and refined in the riding model: C—H = 0.95–0.99 Å with U iso (H) = 1.2U eq (C). The reflection (011), affected by the beam-stop, was removed during refinement.

Table 2: Experimental details.

Chemical formula	$C_{17}H_{12}O_4$
Formula weight	280.27 g/mol
Temperature	173(2) K
Wavelength	0.71073 Å
Crystal size	0.100 x 0.100 x 0.120 mm
Crystal system	monoclinic
Space group	$P2_1/n$
Unit cell dimensions	a = 4.2951(2) Å α = 90°
	b = 16.7714(9) Å β = 95.941(2)°
	c = 18.0537(11) Å γ = 90°
Volume	1293.51(12) $Å^3$
Z	4
Density (calculated)	1.439 g/cm^3
Absorption coefficient	0.103 mm^{-1}
F(000)	584

Theta range for data collection	2.43 to 29.49°
Index ranges	-5<=h<=4, -23<=k<=23, -24<=l<=25
Reflections collected	19692
Independent reflections	3436 [R(int) = 0.0435]
Max. and min. transmission	0.9900 and 0.9880
Structure solution technique	direct methods
Structure solution program	SHELXS-97 (Sheldrick 2008)
Refinement method	Full-matrix least-squares on F^2
Refinement program	SHELXL-2014 (Sheldrick 2014)
Function minimized	$\Sigma\ w(F_o^2 - F_c^2)^2$
Data / restraints / parameters	3436 / 0 / 190
Goodness-of-fit on F^2	1.017
Final R indices	2309 data; R1 = 0.0551, wR2 = 0.1339 $I>2\sigma(I)$ all data R1 = 0.0896, wR2 = 0.1558
Weighting scheme	$w=1/[\sigma^2(F_o^2)+(0.0623P)^2+0.8429P]$ where $P=(F_o^2+2F_c^2)/3$
Largest diff. peak and hole	0.415 and -0.319 eÅ^{-3}
R.M.S. deviation from mean	0.050 eÅ^{-3}

3.7 Supporting information

Geometry. All esds (except the esd in the dihedral angle between two l.s. planes) are estimated using the full covariance matrix. The cell esds are taken into account individually in the estimation of esds in distances, angles and torsion angles; correlations between esds in cell parameters are only used when they are defined by crystal symmetry. An approximate (isotropic) treatment of cell esds is used for estimating esds involving l.s. planes.

3.7.1 Fractional atomic coordinates and isotropic or equivalent isotropic displacement parameters (Å^2)

	x	y	z	Uiso*
O1	−0.2635 (5)	0.49906 (10)	0.64736 (8)	0.0546 (5)
O2	0.1717 (4)	0.34277 (9)	0.89646 (7)	0.0449 (4)
O3	0.0471 (3)	0.40325 (8)	0.56747 (6)	0.0293 (3)
O4	0.4204 (4)	0.25897 (8)	0.56830 (7)	0.0356 (3)
C1	0.3367 (5)	0.29496 (11)	0.63141 (10)	0.0274 (4)
C2	0.4523 (5)	0.26018 (11)	0.69817 (11)	0.0321 (4)
H2	0.590316	0.215932	0.697909	0.038*
C3	0.3704 (5)	0.28874 (11)	0.76486 (10)	0.0302 (4)
H3	0.451085	0.264092	0.810209	0.036*
C4	0.1701 (4)	0.35347 (10)	0.76600 (9)	0.0244 (4)
C5	0.0822 (5)	0.37964 (11)	0.83960 (10)	0.0285 (4)
C6	0.1143 (5)	0.45162 (10)	0.84226 (9)	0.0269 (4)

C7	0.1904 (5)	0.47948 (12)	0.91105 (10)	0.0351 (5)
H7	−0.121046	0.451264	0.955331	0.042*
C8	−0.3662 (6)	0.54788 (13)	0.91472 (11)	0.0407 (5)
H8	−0.413992	0.567394	0.961621	0.049*
C9	−0.4731 (5)	0.58819 (12)	0.85004 (11)	0.0377 (5)
H9	−0.595642	0.635045	0.852781	0.045*
C10	−0.4023 (5)	0.56056 (11)	0.78134 (11)	0.0308 (4)
H10	−0.478159	0.588130	0.737151	0.037*
C11	−0.2198 (4)	0.49227 (10)	0.77718 (9)	0.0248 (4)
C12	−0.1467 (5)	0.46397 (10)	0.70231 (9)	0.0271 (4)
C13	0.0595 (4)	0.39292 (10)	0.69919 (9)	0.0227 (4)
C14	0.1495 (4)	0.36425 (10)	0.63107 (9)	0.0238 (4)
C15	0.2543 (5)	0.40456 (12)	0.50847 (10)	0.0331 (4)
H15A	0.474823	0.405280	0.530766	0.040*
H15B	0.216063	0.453607	0.478396	0.040*
C16	0.1997 (6)	0.33217 (13)	0.45871 (11)	0.0389 (5)
H16A	0.001584	0.338786	0.426047	0.047*
H16B	0.372274	0.327239	0.426649	0.047*
C17	0.1829 (6)	0.25735 (13)	0.50493 (11)	0.0384 (5)
H17A	−0.026930	0.253140	0.522692	0.046*
	0.214839	0.210027	0.473818	0.046*

3.7.2 Atomic displacement parameters (Å^2)

	U^{11}	U^{22}	U^{33}	U^{12}	U^{13}	U^{23}
O1	0.0835 (14)	0.0550 (10)	0.0254 (7)	0.0370 (9)	0.0062 (8)	0.0053 (6)
O2	0.0590 (12)	0.0499 (9)	0.0257 (7)	0.0106 (8)	0.0036 (7)	0.0110 (6)
O3	0.0301 (8)	0.0378 (7)	0.0201 (6)	0.0062 (6)	0.0009 (5)	0.0009 (5)
O4	0.0345 (9)	0.0386 (8)	0.0346 (7)	0.0062 (6)	0.0078 (6)	−0.0075 (6)
C1	0.0248 (10)	0.0272 (9)	0.0307 (9)	−0.0022 (7)	0.0053 (7)	−0.0040 (7)
C2	0.0296 (11)	0.0267 (9)	0.0394 (10)	0.0036 (7)	0.0010 (8)	0.0015 (7)
C3	0.0297 (11)	0.0283 (9)	0.0313 (9)	0.0005 (7)	−0.0030 (8)	0.0054 (7)
C4	0.0245 (10)	0.0230 (8)	0.0252 (8)	−0.0033 (7)	0.0002 (7)	0.0022 (6)
C5	0.0314 (11)	0.0298 (9)	0.0237 (8)	−0.0042 (7)	0.0002 (7)	0.0022 (7)
C6	0.0309 (11)	0.0278 (8)	0.0220 (8)	−0.0070 (7)	0.0025 (7)	−0.0014 (6)
C7	0.0445 (14)	0.0376 (10)	0.0238 (9)	−0.0053 (9)	0.0064 (8)	−0.0010 (7)
C8	0.0538 (16)	0.0407 (11)	0.0295 (10)	−0.0035 (10)	0.0143 (9)	−0.0078 (8)
C9	0.0429 (14)	0.0317 (10)	0.0402 (11)	0.0007 (9)	0.0126 (9)	−0.0054 (8)
C10	0.0342 (12)	0.0264 (9)	0.0322 (9)	−0.0008 (7)	0.0054 (8)	−0.0002 (7)
C11	0.0274 (10)	0.0233 (8)	0.0239 (8)	−0.0051 (7)	0.0027 (7)	−0.0011 (6)
C12	0.0304 (11)	0.0274 (9)	0.0234 (8)	0.0015 (7)	0.0015 (7)	0.0006 (6)
C13	0.0233 (10)	0.0213 (8)	0.0231 (8)	−0.0039 (6)	0.0010 (6)	0.0006 (6)
C14	0.0218 (10)	0.0255 (8)	0.0236 (8)	−0.0033 (7)	0.0005 (7)	−0.0003 (6)
C15	0.0353 (12)	0.0407 (11)	0.0246 (9)	0.0246 (9)	0.0002 (8)	0.0014 (7)
C16	0.0396 (14)	0.0525 (12)	0.0256 (9)	0.0027 (10)	0.0080 (8)	−0.0079 (8)
C17	0.0376 (13)	0.0428 (11)	0.0357 (10)	−0.0027 (9)	0.0078 (9)	−0.0145 (8)

3.7.3 Geometric parameters (Å, º)

O1—C12	1.216 (2)	C7—H7	0.9500
O2—C5	1.226 (2)	C8—C9	1.386 (3)
O3—C14	1.355 (2)	C8—H8	0.9500
O3—C15	1.457 (2)	C9—C10	1.387 (3)
O4—C1	1.370 (2)	C9—H9	0.9500
O4—C17	1.452 (3)	C10—C11	1.394 (3)
C1—C2	1.384 (3)	C10—H10	0.9500
C1—C14	1.413 (3)	C11—C12	1.496 (2)
C2—C3	1.375 (3)	C12—C13	1.489 (2)
C2—H2	0.9500	C13—C14	1.411 (2)
C3—C4	1.387 (3)	C15—C16	1.514 (3)
C3—H3	0.9500	C15—H15A	0.9900
C4—C13	1.414 (2)	C15—H15B	0.9900
C4—C5	1.485 (2)	C16—C17	1.513 (3)
C5—C6	1.477 (3)	C16—H16A	0.9900
C6—C11	1.393 (2)	C16—H16B	0.9900
C6—C7	1.397 (2)	C17—H17A	0.9900
C7—C8	1.379 (3)	C17—H17B	0.9900
C14—O3—C15	117.23 (15)	C11—C10—H10	120.0
C1—O4—C17	116.12 (16)	C6—C11—C10	119.49 (16)
O4—C1—C2	115.92 (17)	C6—C11—C12	121.76 (16)
O4—C1—C14	123.85 (16)	C10—C11—C12	118.75 (15)
C2—C1—C14	120.22 (16)	O1—C12—C13	123.57 (16)
C3—C2—C1	120.95 (18)	O1—C12—C11	118.43 (17)
C3—C2—H2	119.5	C13—C12—C11	117.99 (14)
C1—C2—H2	119.5	C14—C13—C4	119.06 (16)
C2—C3—C4	120.08 (17	C14—C13—C12	121.55 (15)
C2—C3—H3	120.0	C4—C13—C12	119.39 (15)
C4—C3—H3	120.0	O3—C14—C13	118.68 (15)
C3—C4—C13	120.52 (16)	O3—C14—C1	122.38 (15)
C3—C4—C5	117.40 (15)	C13—C14—C1	118.92 (15)
C13—C4—C5	122.07 (16)	O3—C15—C16	110.66 (16)
O2—C5—C6	121.06 (17)	O3—C15—H15A	109.5
O2—C5—C4	120.92 (18)	C16—C15—H15A	109.5
C6—C5—C4	118.02 (15)	O3—C15—H15B	109.5
C11—C6—C7	120.04 (18)	C16—C15—H15B	109.5
C11—C6—C5	120.65 (16)	H15A—C15—H15B	108.1
C7—C6—C5	119.31 (16)	C17—C16—C15	110.55 (16)
C8—C7—C6	120.04 (18)	C17—C16—H16A	109.5
C8—C7—H7	120.0	C15—C16—H16A	109.5
C6—C7—H7	120.0	C17—C16—H16B	109.5
C7—C8—C9	120.06 (18)	C15—C16—H16B	109.5
C7—C8—H8	120.0	H16A—C16—H16B	H16A—C16—H16B
C9—C8—H8	120.0	O4—C17—C16 (18)	110.46 (18)
C8—C9—C10	120.42 (19)	O4—C17—H17A	109.6
C8—C9—H9	119.8	C16—C17—H17A	109.6
C10—C9—H9	119.8	O4—C17—H17B	109.6

C9—C10—C11	119.94 (18)	C16—C17—H17B	109.6
C9—C10—H10	120.0	H17A—C17—H17B	108.1

4. Conclusions

The alizarin scaffold reacts with 1,3-dibromo-propane providing two functional 1,2-propylenedioxyanthraquinone systems. The ligands could easily be purified with the help of a silica gel column with dichloromethane/petroleum ether. The crystal and molecular structure of ligand **4** has been determined from single-crystal X-ray diffraction data. It crystallizes in the monoclinic space group $P2_1/n$, with a = 4.2951(2) Å, b = 16.7714(9) Å, c = 18.0537(11) Å =, α = 90°, β = 95.941(2)°, γ=90°, and Dcalc = 1.439 g/cm^3 for Z = 4. The crystal structure studies show the existence of intermolecular H···H (43.0%), H···O/O···H (27%), H···C/C···H (13.8%), and C···C (12.4%) bonding.

5. References

(1) Nakanishi, F.; Nagasawa, Y.; Kabaya, Y.; Sekimoto, H.; Shimomura, K. Plant Physiol. Biochem. **2005**, 43 (10–11), 921–928.
(2) Lajkó, E.; Bányai, P.; Zámbó, Z.; Kursinszki, L.; Szőke, É.; Kőhidai, L. Cancer Cell Int. **2015**, 15 (1), 1–15.
(3) Berrie, B. H. Proc. Natl. Acad. Sci. **2009**, 106 (36), 15095–15096.
(4) Chang, P., Lee, K.H., Shingu, T., Hirayama, T., Hall, I. H., Huang, H. C. J. Nat. Prod. **1981**, 45 (2), 206–210.
(5) Huang, S.; Yeh, S.; Hong, C. J. natu **1995**, 58 (9), 1365–1371.
(6) Morgan, L. R.; Thangaraj, K.; LeBlanc, B.; Rodgers, A.; Wolford, L. T.; Hooper, C. L.; Fan, D.; Jursic, B. S. J. Med. Chem. **2003**, 46 (21), 4552–4563.
(7) Kharlamova, T. V. Chem. Nat. Compd. **2009**, 45 (5), 629–633.
(8) Esposito, F.; Kharlamova, T.; Distinto, S.; Zinzula, L.; Cheng, Y. C.; Dutschman, G.; Floris, G.; Markt, P.; Corona, A.; Tramontano, E. FEBS J. **2011**, 278 (9), 1444–1457.
(9) Du, S.; Feng, J.; Lu, X.; Wang, G. Dalt. Trans. **2013**, 42 (26), 9699–9705.
(10) Guiyang, Y.; Weilong, D.; Heng-shan, W.; Ye, M.; Huang, R.; Pan, Y.; Liao, Z.-X. Med. Chem. Res. **2014**, 23 (12), 5031–5042.
(11) Ye, M.-Y.; Yao, G.-Y.; Pan, Y.-M.; Liao, Z.-X.; Zhang, Y.; Wang, H.-S. Eur. J. Med. Chem. **2014**, 83, 116–128.
(12) Fabbri, D.; Chiavari, G.; Ling, H. J. Anal. Appl. Pyrolysis **2000**, 56 (2), 167–178.
(13) Drivas, I.; Blackburn, R. S.; Rayner, C. M. Dye. Pigment. **2011**, 88 (1), 7–17.
(14) Pierpont, C. G.; Buchanan, R. M. Coord. Chem. Rev. **1981**, 38 (1), 45–87.
(15) Ward, M. D.; McCleverty, J. A. J. Chem. Soc. Dalt. Trans. **2002**, No. 3, 275–288.
(16) Churchill, M. R.; Keil, K. M.; Bright, F. V.; Pandey, S.; Baker, G. A.; Keister, J. B. Inorg. Chem. **2000**, 39 (25), 5807–5816.
(17) Schwab, P. F. H.; Diegoli, S.; Biancardo, M.; Bignozzi, C. A. Inorg. Chem. **2003**, 42 (21), 6613–6615.
(18) Soares, S. M.; Lemos, S. S.; Sales, M. J. A.; Back, D. F.; Lang, E. S. Polyhedron **2009**, 28 (17), 3811–3815.
(19) Mo, M.; Zhang, B.; Du, S. Z.; Lu, X. M.; Wang, G.; Fen, J. Mo- W. Inorg. Chem. **2013**, 52 (16), 9470–9478.
(20) Steel, P. J.; Fitchett, C. M. Aust. J. Chem. **2013**, 66 (4), 443–451.
(21) Bruker (2012). APEX2, SAINT and SADABS. Bruker AXS Inc., Madison, Wisconsin, USA.

(22) Sheldrick, G. M. (2015a). Acta Cryst. A71, 3–8.
(23) Sheldrick, G. M. (2015b). Acta Cryst. C71, 3–8.
(24) Farrugia, L. J. (2012). J. Appl. Cryst. 45, 849–854.
(25) Brandenburg, K. (2012). DIAMOND. Crystal Impact GbR, Bonn, Germany.
(26) Spek, A. L. (2020). Acta Cryst. E76, 1–11.
(27) Westrip, S. P. (2010). J. Appl. Cryst. 43, 920–925.
(28) Groom, C. R., Bruno, I. J., Lightfoot, M. P. & Ward, S. C. (2016). Acta Cryst. B72, 171–179.
(29) Ismail, N. H., Osman, C. P., Ahmad, R., Awang, K. & Ng, S. W. (2009). Acta Cryst. E65, o1435.
(30) Kar, P., Suresh, M., Krishna Kumar, D., Amilan Jose, D., Ganguly, B. & Das, A. (2007). Polyhedron, 26, 1317–1322.
(31) Xu, Y.-J., Yang, X.-X. & Zhao, H.-B. (2009). Acta Cryst. E65, o1524.
(32) Turner, M. J., MacKinnon, J. J., Wolff, S. K., Grimwood, D. J., Spackman, P. R., Jayatilaka.
(33) Spackman, M. A. & Jayatilaka, D. (2009). CrystEngComm, 11, 19–32.
(34) McKinnon, J. J., Jayatilaka, D. & Spackman, M. A. (2007). Chem. Commun. pp. 3814–3816.
(35) Spackman, M. A., McKinnon, J. J. & Jayatilaka, D. (2008). CrystEngComm, 10, 377–388.

Part D

Chapter VIII

Concluding remarks and future perspectives

1. Concluding remarks

In the introduction of this thesis (**Part A, Chapter I**), the importance of research, to valorized up-grade, the vast range of plant species in Morocco was highlighted. It has also emphasized the importance of studying the chemical composition of *Z. lotus*, exploiting it as sources of valuable compounds, as well to use a known structure bioactive compounds of *R. tinctorum* as scarfford for semi-synthesis. The wild *Z. lotus* and *R. tinctorum* have gained increasing attention in the last decade in the Mediterranean countries (e.g. Morocco). A vast search in literature highlighted that this plant species could be considered as a rich source of bioactive compounds eliciting many beneficial effects on human health **(Part A, Chapter II and Part B, Chapter V)**. The extraction and identification of triterpenic acids and phenolic compounds from *Z. lotus* as well as the structural modification of anthraquinone scarfford extracted from *R. tinctorum* would be an additional valorization pathway of these wild species given the diversity of biological activities reported for these families.

In the first part of the experimental work developed in this thesis (**Part B, Chapter III**), the dichloromethane extract from four morphological parts of *Z. lotus* was studied by GC-MS. In this extract, it was possible to identify and quantify 123 compounds in this species of the genus Zizyphus, with emphasis on the high number of saturated and unsaturated fatty acids, diacids, hydroxyfatty acids alcohols, fatty acid ethyl/methyl, long-chain aliphatic alcohol /aldehydes, and aromatic compounds, monoglycerides, tocopherols, sterols, triterpenic acids, and other minor compounds. Some of the compounds detected in the extract and reported here, as far as it was possible to verify, was the first time that they were identified in this genre. In what concerns the terpenic composition, 4 pentacyclic triterpenes were indicated as wild *Z. lotus* components, for the first time: lupeol, oleanolic acid, betulinic acid, and ursolic acid. Pentacyclic triterpenes are the most abundant lipophilic compounds found in root barks (10230 mg/kg dw), mainly represented by betulinic acid (9838 mg/kg dw). Fatty acids were the most common lipophilic components of leaves and seeds, reaching a maximum of 1470 mg/kg dw in leaves.

The phenolic composition of *Z. lotus* was subsequently studied by high-performance liquid chromatography-ultraviolet detection-mass spectrometry (**Part B, Chapter IV**). The findings of this chapter indicated that 78 phenolic compounds were identified in seeds, pulp leaves, and root barks, 69 of them referenced for the first time as constituents of wild *Z. lotus*. Root barks and leaves exhibited the highest total concentration of the identified phenolic compounds, accounting for 6321 and 5904 mg/kg dw, respectively. Flavonoids were the predominant phenolic compounds in root barks, accounting for 7635 mg/kg dw, mainly constituted by flavan-3-nols (7579 mg/kg dw), such as (epi)catechin, (epi)gallocatechin dimer (epi)gallocatechin, (epi)catechin-O-hexoside and (epi)catechin-O-(rutinosyl-rhamnoside)-O-hexoside. Leaves and pulp contained the highest amounts of flavonols, accounting for 5055 and 2129 mg/kg dw, respectively, represented by quercetin-3-O-rhamnosyl(6-O-hexoside) (1757 and 1069 mg/kg dw, respectively). Seeds revealed the highest flavone content (360 mg/kg dw), mainly represented by apigenin derivatives. Therefore, dihydrochalcones and flavanones were only found in the leaves (269 and 17 mg/kg dw, respectively). Besides, the leaves contained the highest amounts of phenolic acids, accounting for 277 mg/kg dw.

Lipophilic and phenolic-rich extracts, derived from wild *Z. Lotus* were screened in terms of their biological activities such as antioxidant, antibacterial, and antitumor activities (**Chapter V**). The antioxidant activity of wild *Z. lotus* phenolic-rich extracts was tested through the DPPH and ABTS scavenging effect as well as through ferric reducing power (FRAP). Phenolic-rich extracts of root barks and leaves were the most active in neutralizing DPPH (IC50 values of 5.97 and 9.68 µg/mL, respectively) and ABTS (IC50 values of 69.16 and 56.12 µg/mL, respectively) free radicals. Once more, root barks shows higher ferric reducing power compared to other fractions. Moreover, the correlation of antioxidant activities and phenolic-rich extracts of wild *Z. lotus* suggested as a possible product to be used in the food industry, as an alternative to synthetic antioxidants.

The antitumor activity of wild *Z. lotus* was screened in terms of the in vitro inhibitory action upon the cellular viability of MDA-MB-231, MCF-7, and HepG2 cell lines. Root barks lipophilic extract presented more inhibitory action (IC50 values of 6.01, 18.78, and 23.27 µg/mL, respectively) on the MDA-MB-231, MCF-7, and HepG2 cell growth, compared to the lipophilic leaves extract (IC50 values of 85.87, 59.27, and 67.34 µg/mL, respectively). Lipophilic seeds and pulp extracts are less potent against cells line (IC50 > 100 µg/mL). HepG2 cell was sensitive to phenolic-rich extract of root barks (IC50 = 79.45 µg/mL) than to other fractions. The pure betA, representative of the main compound identified in root barks lipophilic extract, also prevented the cell proliferation of MDA-MB-231 (IC50 = 22.67µM). Considering the high concentration of betA (9838 mg/kg dw), this triterpenic acid may be mostly implicated in the suppressive effect of root barks lipophilic extract. MDA-MB-231 cells were exposed, for 48h, to the respective IC50 concentrations of root barks lipophilic extract to understand their ability in modeling cellular responses, and consequently important potentially signaling pathways for the cellular viability decrease. The results indicated that root barks lipophilic extract arrest MDA-MB-231 cells via cell migration arrest, blocking the cell cycle at the G2 phase, and inducing apoptosis, and demonstrated that the root barks treatment acted through downregulating PI3K/Akt signaling molecules.

The antibacterial activities of lipophilic and phenolic-rich extracts, derived from wild *Z. lotus*, were evaluated against four bacterial strains namely: Gram-negative *E. coli* and Gram-positive MSSA, *S. epidermidis*, and MRSA. Lipophilic and phenolic-rich extracts of pulp and seeds, in the range 8-2048 µg/mL, were not efficient in preventing the growth of strains used contrarily to *S. epidermidis* which was susceptible to lipophilic seeds extract (MIC = 1024 µg/mL). However, the phenolic-rich extract of root barks was effective to suppress the MRSA growth (MIC = 1024 µg/mL). Besides, leaves lipophilic extract also inhibited the *E. coli* growth (MIC = 1024 µg/mL). These data revealed the potential of wild *Z. lotus* extracts to be investigated in the scope of antibacterial therapeutics.

Chapter VI (**Part C**) deals with the extraction and purification of anthraquinone dye alizarin from the roots of *R. tinctorium*. The alizarin scaffolds have been used to develop a new chemical and medicinal agent. Three alizarin derivative, para-substitution ligand **1**, meta-substitution ligand **2**, and ortho-substitution ligand **3** were synthesized and characterized. The bioactivities of the current isomer were investigated using DFT study.

The result showed that para-substitution ligand (1) had a higher chemical reactivity than others. Besides, all compounds could be as an electrophilic and nucleophilic reactivity center.

In **Chapter VII** (**Part C**) 1,2-propylenedioxyanthraquinone derivatives **4** and **5** (yield 35 and 9.5%, respectively) were syntheses by the reaction of alizarin and 1,3-dibromo-propane. The physical and chemical structure-property of the ligand **4** was found by single-crystal X-ray diffraction data. It crystallizes in the monoclinic space group $P2_1/n$, with a =4.2951(2) Å, b = 16.7714(9) Å, c = 18.0537(11) Å, α= 90°, β= 95.941(2)°, γ = 90°and Dcalc =1.439 g/cm^3 for Z = 4. Hirshfeld surface analysis was also used to investigate intermolecular interactions in the solid-state: the most important contributions are from H···H (43.0%), H···O/O···H (27%), H···C/C···H (13.8%), and C···C (12.4%) contacts.

2. Future perspectives

The purpose of this thesis consisted of the valorization of two plant species endemic in the region of Beni Mellal, Morocco, either by a chemical characterization survey of sequential extracts and the evaluation of some biological activities in the case of *Z. lotus* or by the use of alizarin; the main bioactive compound of *R. tinctorum* as a platform to the synthesis of new bioactive derivatives.

However, there are still some issues that need to be tackled:

(i) to perform the bioactivity-guided fractionation of lipophilic and phenolic-containing extracts, to clarify the main responsible for the studied biological activities;

(ii) to prepare wild *Z. lotus* bioactive-enriched fractions, by using environmentally friendly techniques, such as ultrasound-assisted extraction, microwave heating, super- or subcritical fluids supercritical fluid extraction and membrane filtration technology;

(iii) to investigate the hypothesis of an interaction between betulinic acid and other compound(s)/enriched-fractions of root barks lipophilic extract, regarding the antiproliferative action upon TNBC MDA-MB-231 cells;

(iv) to explore the chemical and biological properties of alizarin derivatives, as well as their interactions with metal ions.

Appendix

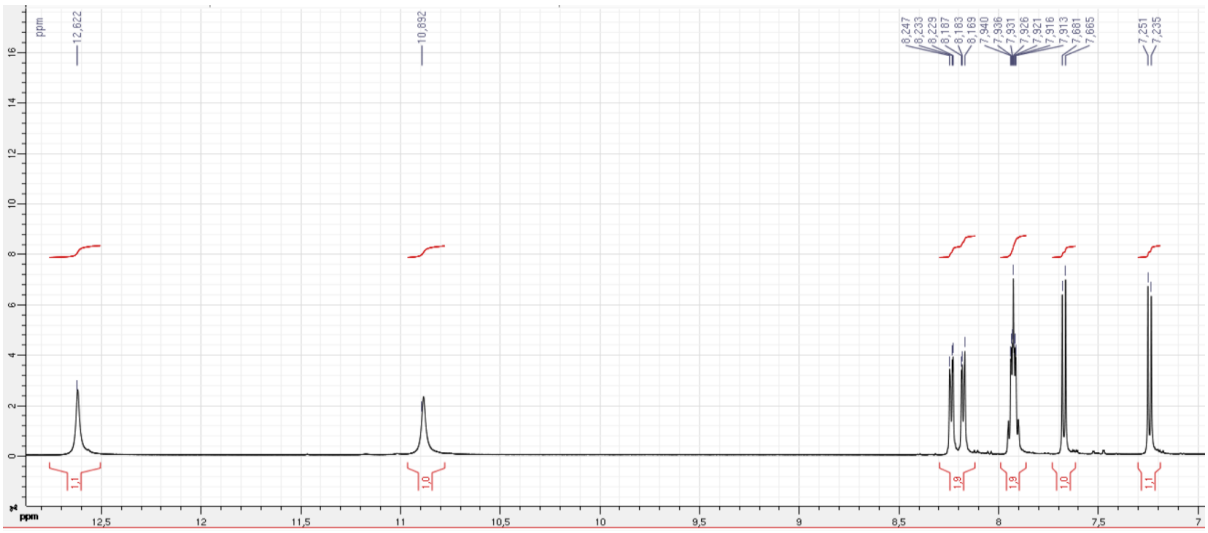

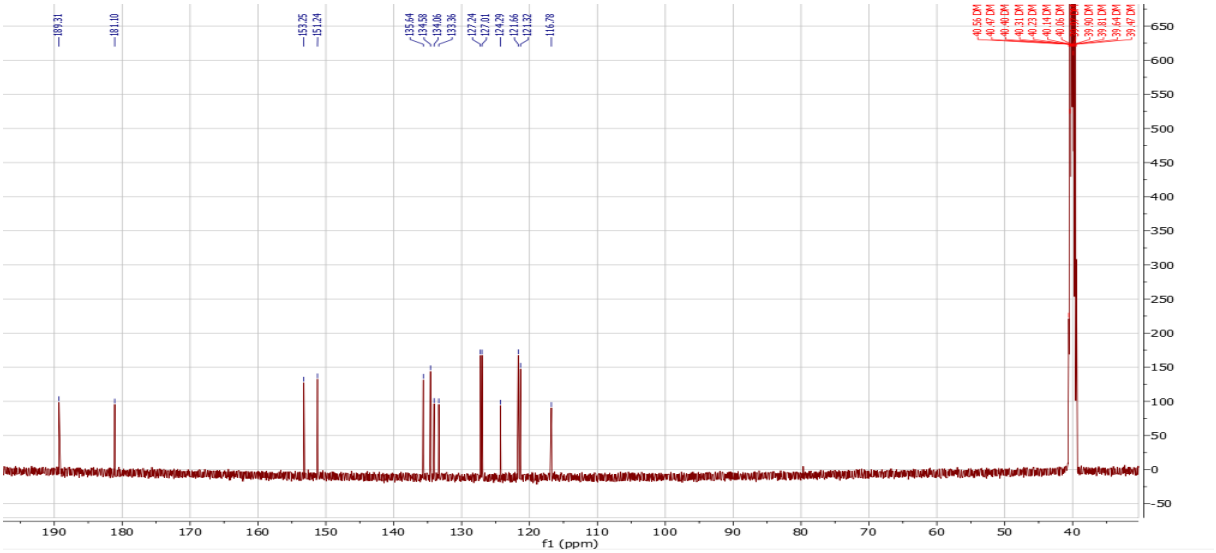

^{1}H and ^{13}C NMR spectra of Alizarin

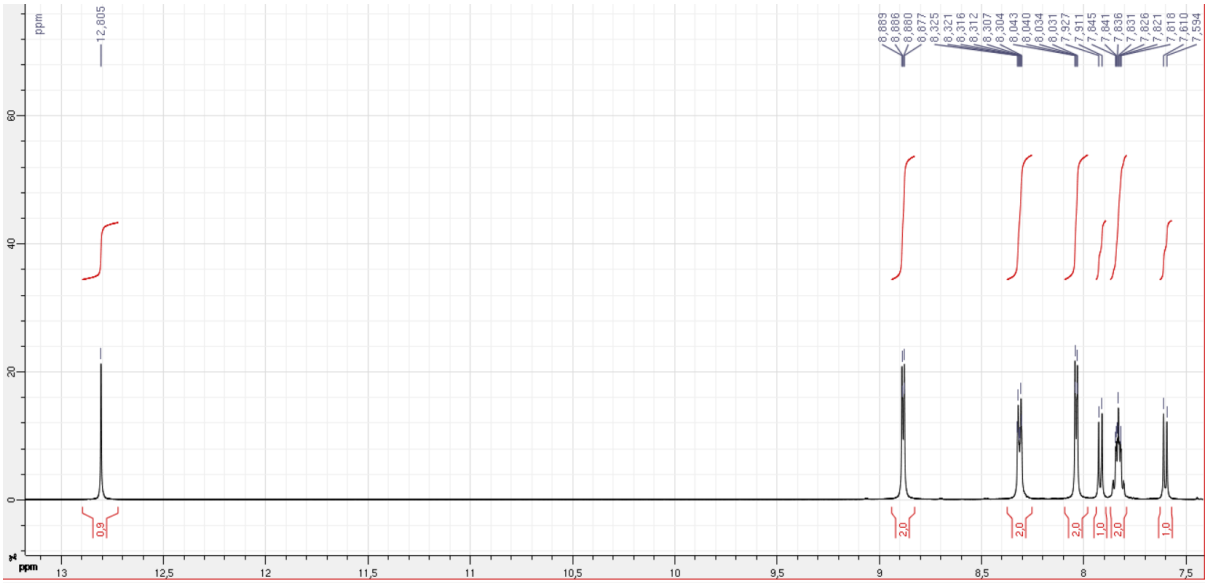

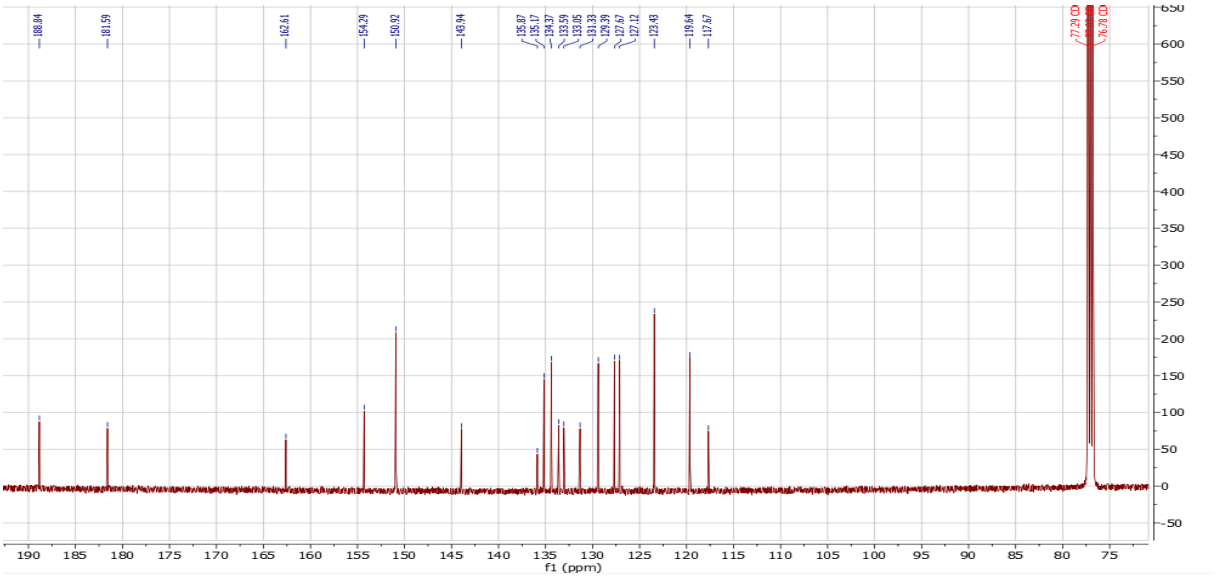

^{1}H and ^{13}C NMR spectra of para-substitution ligand **1**

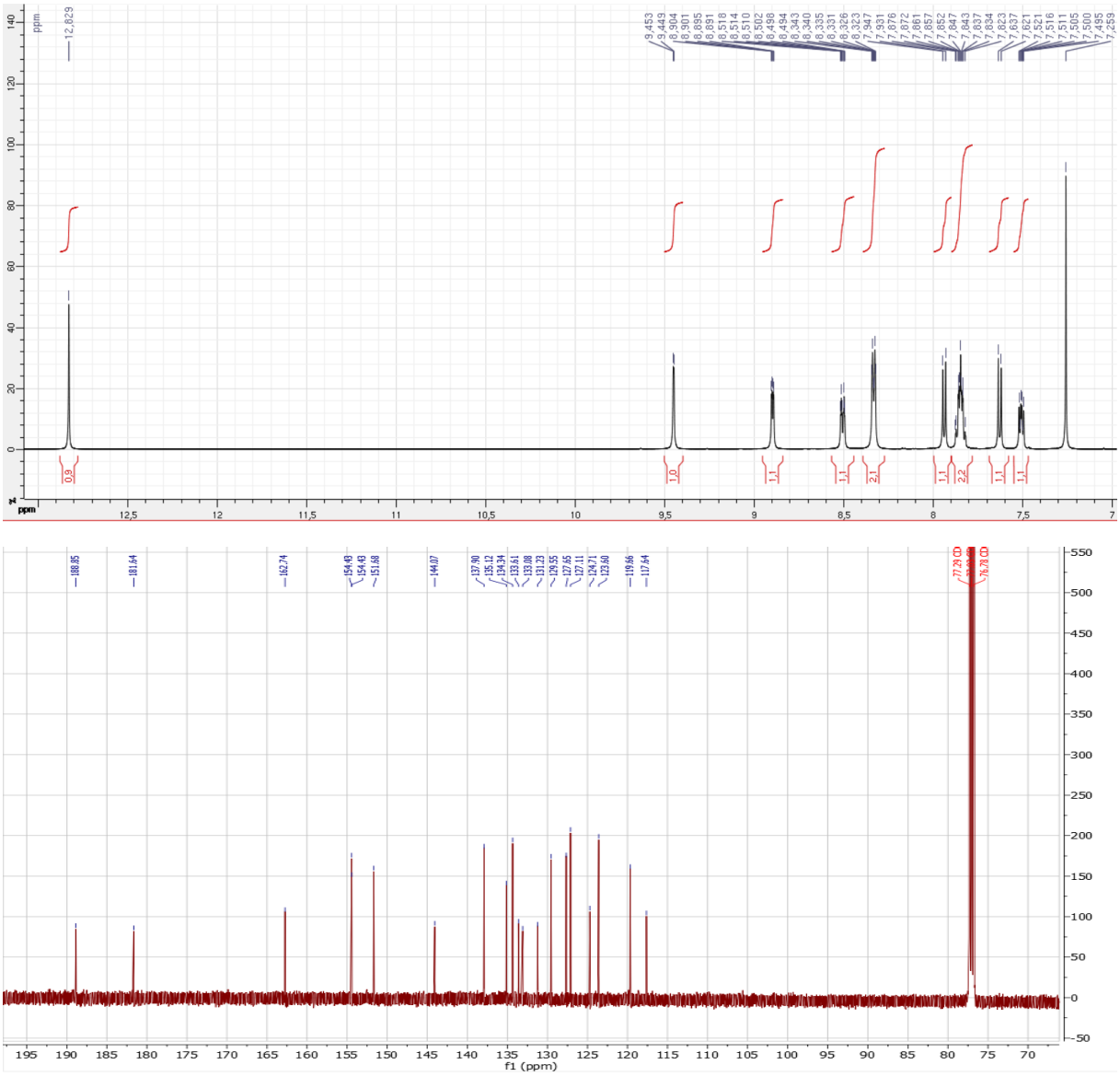

^{1}H and ^{13}C NMR spectra of meta-substitution ligand **2**

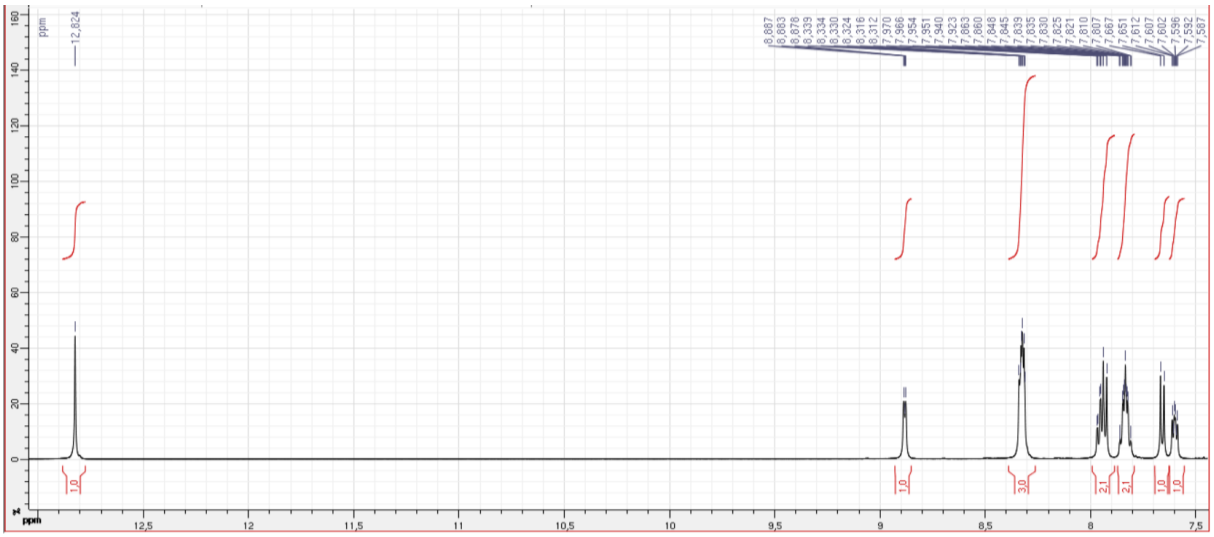

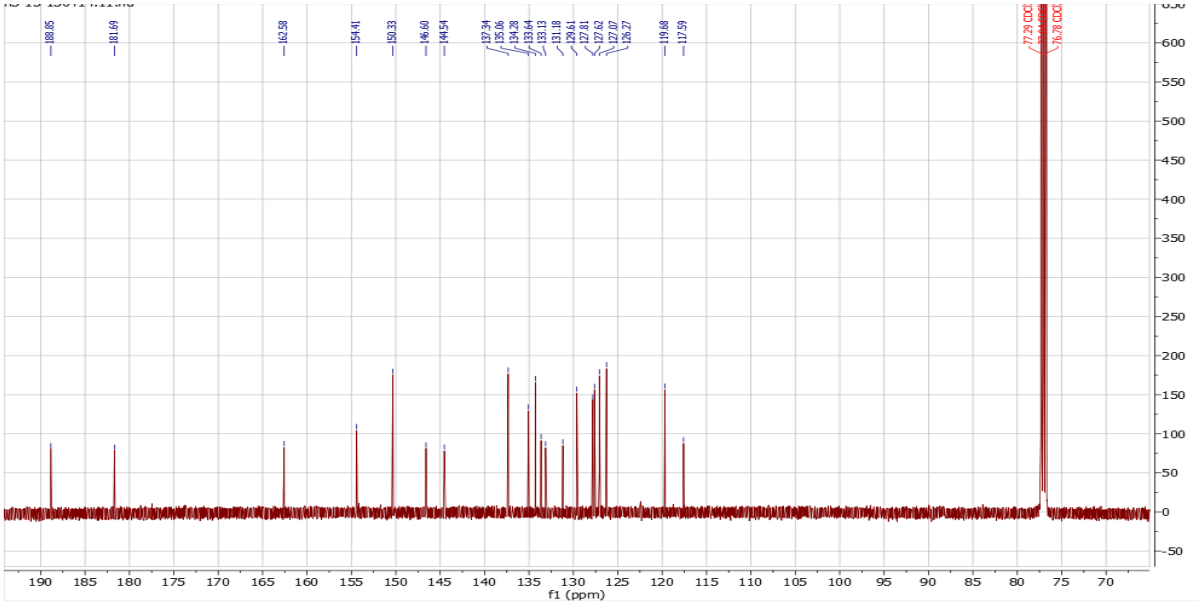

^{1}H and ^{13}C NMR spectra of ortho-substitution ligand **3**

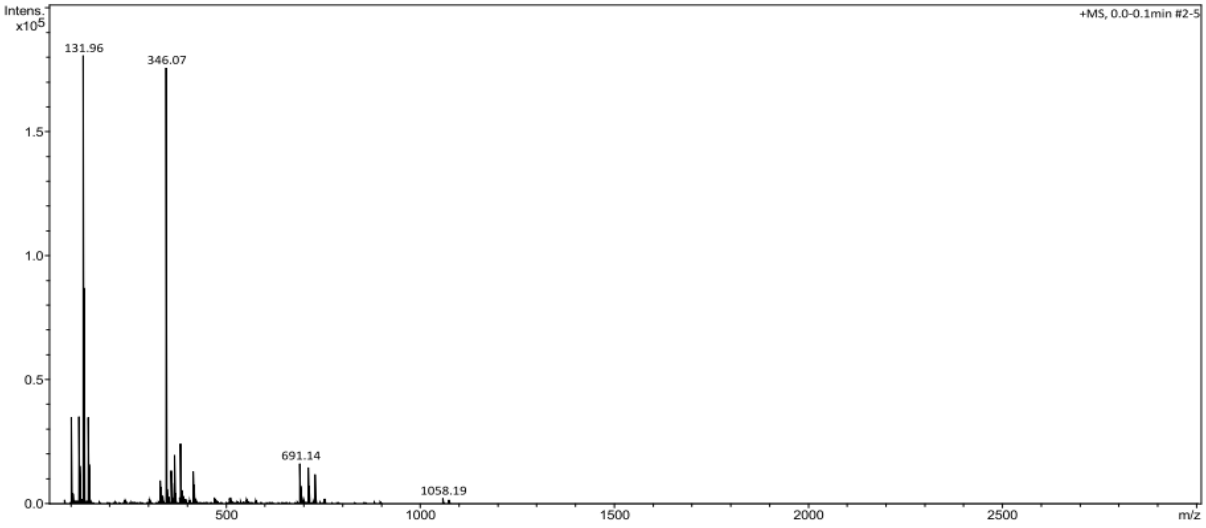

ESI-MS spectrometry of para-substitution ligand **1**

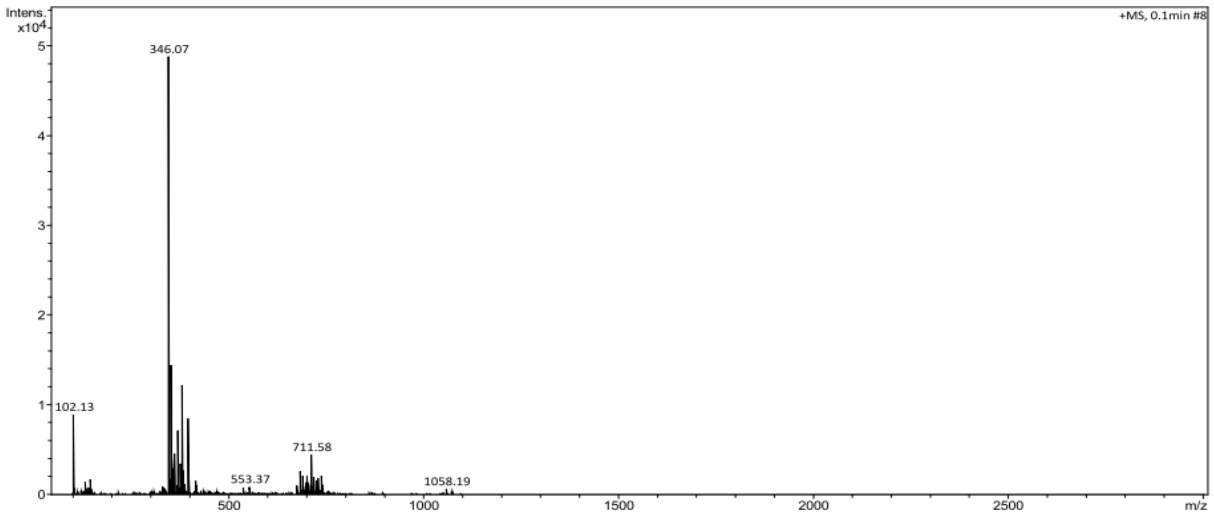

ESI-MS spectrometry of meta-substitution ligand **2**

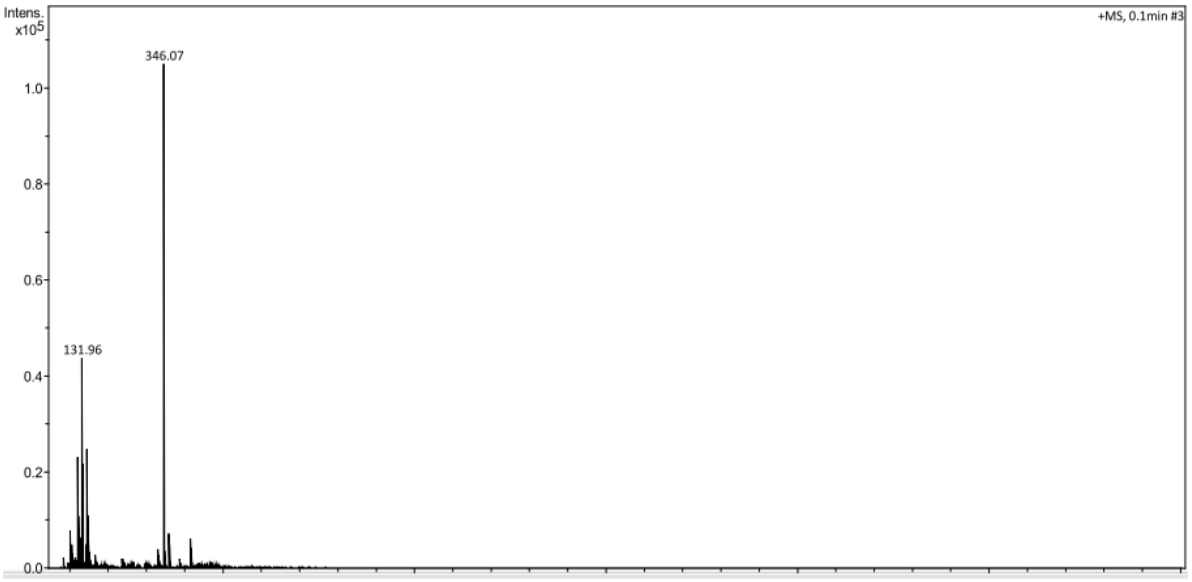

ESI-MS spectrometry of ortho-substitution ligand **3**

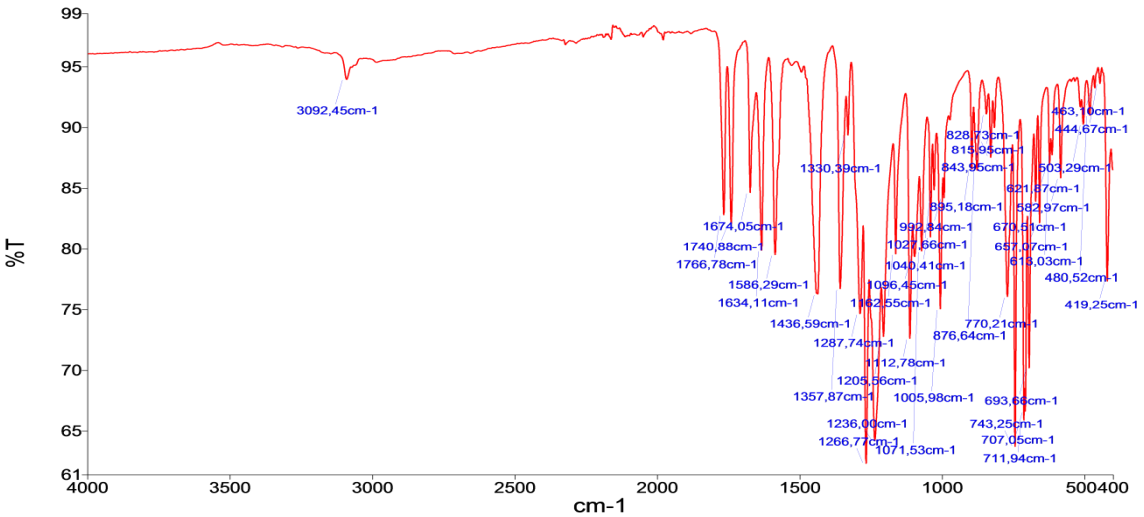

FT-IR of para-substitution ligand **1**

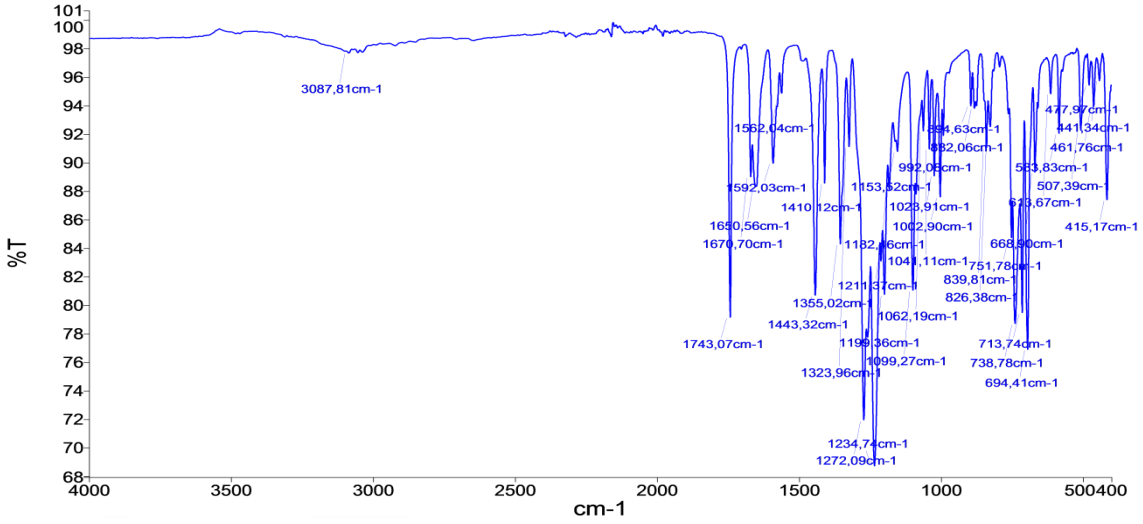

FT-IR of meta-substitution ligand **2**

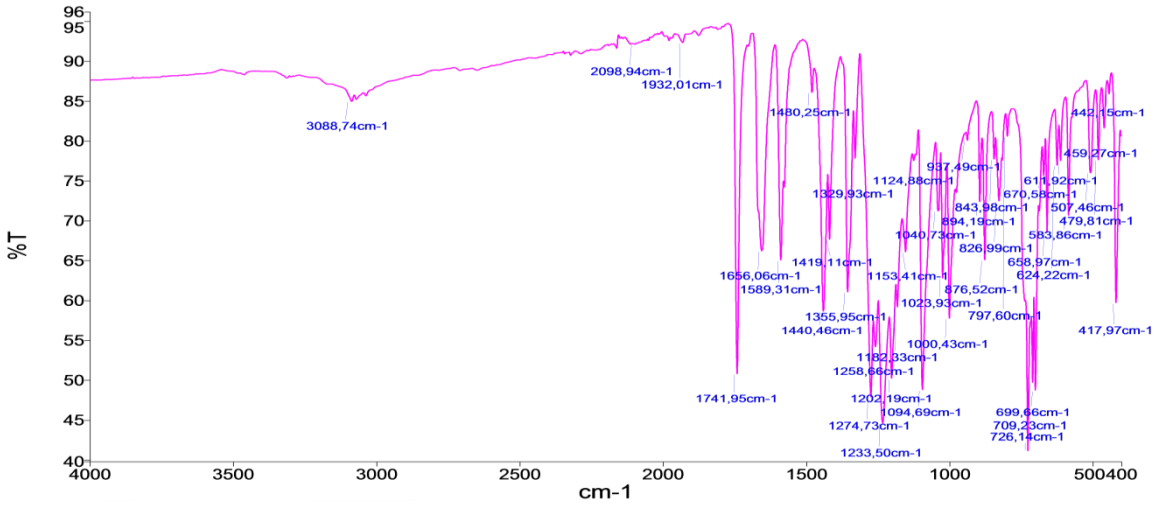

FT-IR of ortho-substitution ligand **3**

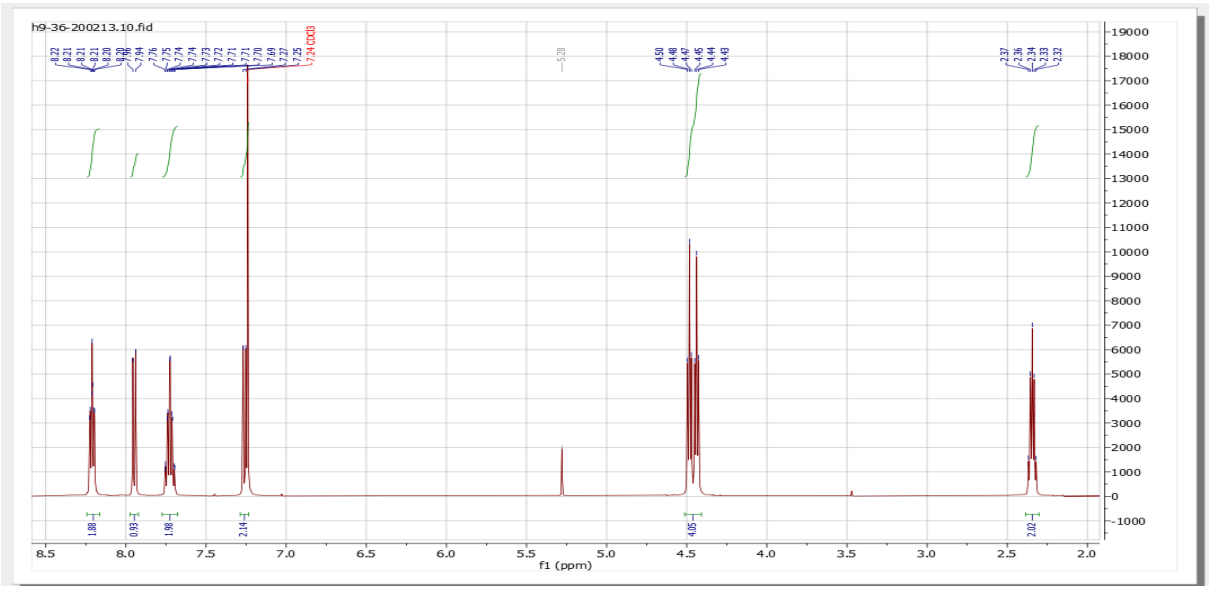

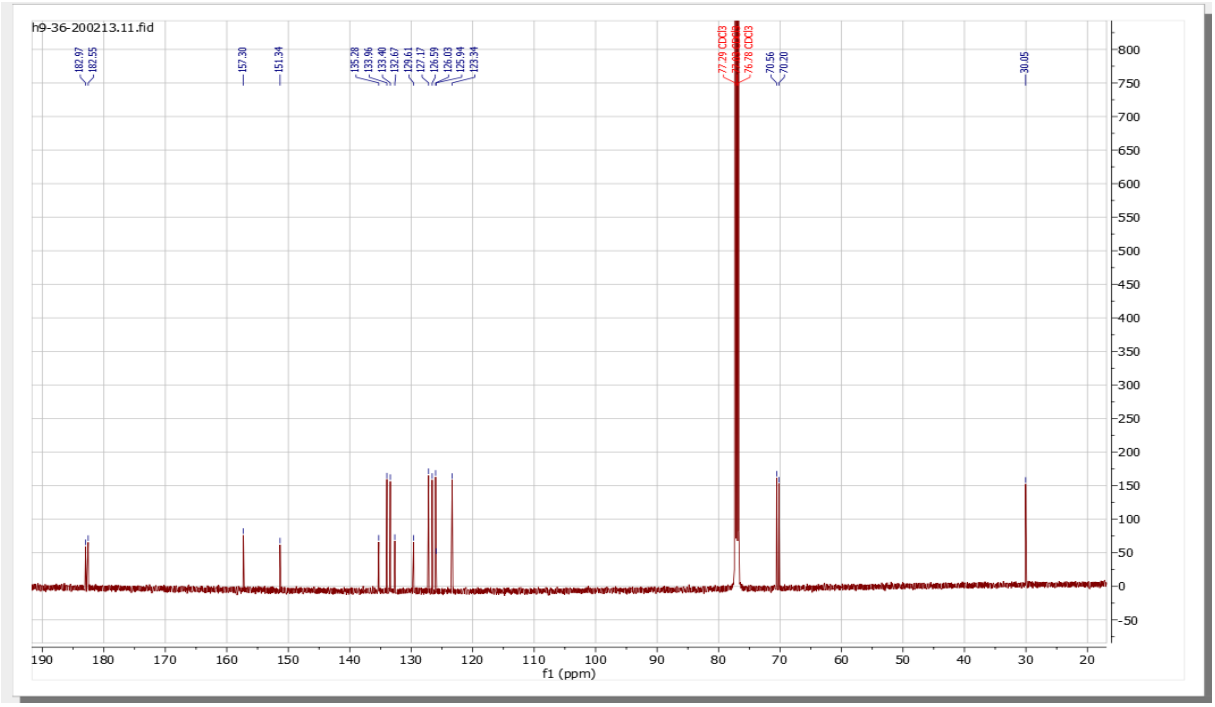

^{1}H NMR and ^{13}C NMR spectra of ligand **4**